ISSN 0514 – 8790

AKADEMIE DER WISSENSCHAFTEN DER DDR
Forschungsbereich Geo- und Kosmoswissenschaften
ZENTRALINSTITUT FÜR PHYSIK DER ERDE

Veröffentlichungen des Zentralinstituts für Physik der Erde
Nr. 78

Symposium of Digital Data Acquisition and Processing in Seismology GDR Reinhardsbrunn, March 14th – 19th, 1983

Proceedings
compiled by
Ch. TEUPSER

Editor: The Director of the Central Institute for Physics of the Earth

Als Manuskript gedruckt Potsdam 1983

F 402/83

Contents

Preface

The Symposium of Digital Data Acquisition and Processing in Seismology was hold in Reinhardsbrunn GDR from 14 till 19 March 1983. It was organized by the Central Institute for Physics of the Earth of the Academy of Sciences of the GDR and sponsored by the Commission of the Academies of Sciences of the Socialist Countries for Planetary Geophysics (KAPG) and the European Seismological Commission (ESC).

The scientific programme included the following topics:

- Instrumentation:
  broad-band seismographs, digital data acquisition, teletransmission, storages
- Real-time processing:
  signal detection and discrimination, seismogram transformation wave group recognition, data collection
- off-line processing of seismic records:
  spectral analysis of body and surface waves, seismogram parametrization and bulletin, focal localization, data exchange.

The symposium continued the sequence of meetings held in the last years concerning the problems of seismological instrumentation and data processing in many European countries. The main task was the presentation of the actual state of the application of digital techniques in seismology and the discussion of problems arising from their use in the international co-operation of seismologists.

It was a great pleasure of the organizing committee to receive a number of representative foreign participants. 35 papers were red at the symposium. The full text or a summary is printed in this volume. Additionally, it contains 4 announced papers which were not red but kindly submitted to the editor. In the contents these papers are marked by an asterisk. The papers are alphabetically arranged with respect to the first author. If he did not read the paper the lecturer is underlined.

The volume was compiled by Dr. habil. Christian Teupser assisted by Dr. Roswitha Heinrich in preparing the papers and by Christa-Maria Dietl in writing the typescript.

H. Stiller
President
European Seismological Commission

H. Kautzleben
Director
Central Institute for Physics of the Earth

DOI: https://doi.org/10.2312/zipe.1983.078

Experience with Extended Operation of a Telemetered Digital Array Station: Consequences for Data Handling, Network Design and Signal Identification

by

H. AICHELE[1)]

Summary

Two independent systems for recording continuous digital seismic data are in operation at the GRF-observatory. A digital broad-band system with a dynamic range of 132 dB has been in operation since 1976. A complete array of this instrumentation with 13 stations comprising 19 instruments has operated since March 1980. A SRO-station with the seismometer in a 116 m deep borehole has operated since 1978 at the site of the three component station A1. This seismometer transmits data to the recording center at the observatory. Our experience with these systems allows us to give results concerning the reliability of the technical equipment as well as the data transmission facilities. The off-line processing of the broad-band array data clearly indicates possibilities for improving epicenter determinations and source identification. Further developments are recommended on the basis of this experience. These developments should be discussed within the European Seismological Commission's Subcommission on Data Acquisition and its appropriate Working Groups.

1. The GRF recording system for teleseismic observation

The development of a new seismic recording system at the GRF-observatory was started during 1972. The aim was to overcome some disadvantages of conventional instrumentation which included recording of short- and long-period signals with different instruments and limited dynamic range due to analog recording systems. It was intended to improve such an instrumentation not only at a single station but within an array. So data telemetry was also part of the development.

The best instrumental response for teleseismic observation purposes is a flat response proportional to velocity from 0.05 Hz to 5 Hz. Twenty Hz was chosen as the sampling rate for digitized data, and the upper frequency limit is due to the system's antialiasing filter (Figure 1). The digitized data are written in a 16 bit word with a gain-ranging system. Twelve bits, including a sign bit, represent the measured value corresponding to a resolution of 66 dB. The remaining 4 bits are used to indicate the amplification level so that the system now operates with a dynamic range of 132 dB.

A three component station started its continuous operation as a first testing device in 1975, already with data transmission on commercial telephone lines. After a thorough theoretical investigation of the best array configuration within given conditions (geological structure, expense, noise suppression and so on) the array installation started. The first subarray (A) started its continuous operation in 1976. In 1978 the Sprengnether High Performance Seismometer S-5100 was replaced by the newly

1) Seismologisches Zentralobservatorium, D-8520 Erlangen, Krankenhausstr. 1-3

DOI: https://doi.org/10.2312/zipe.1983.078

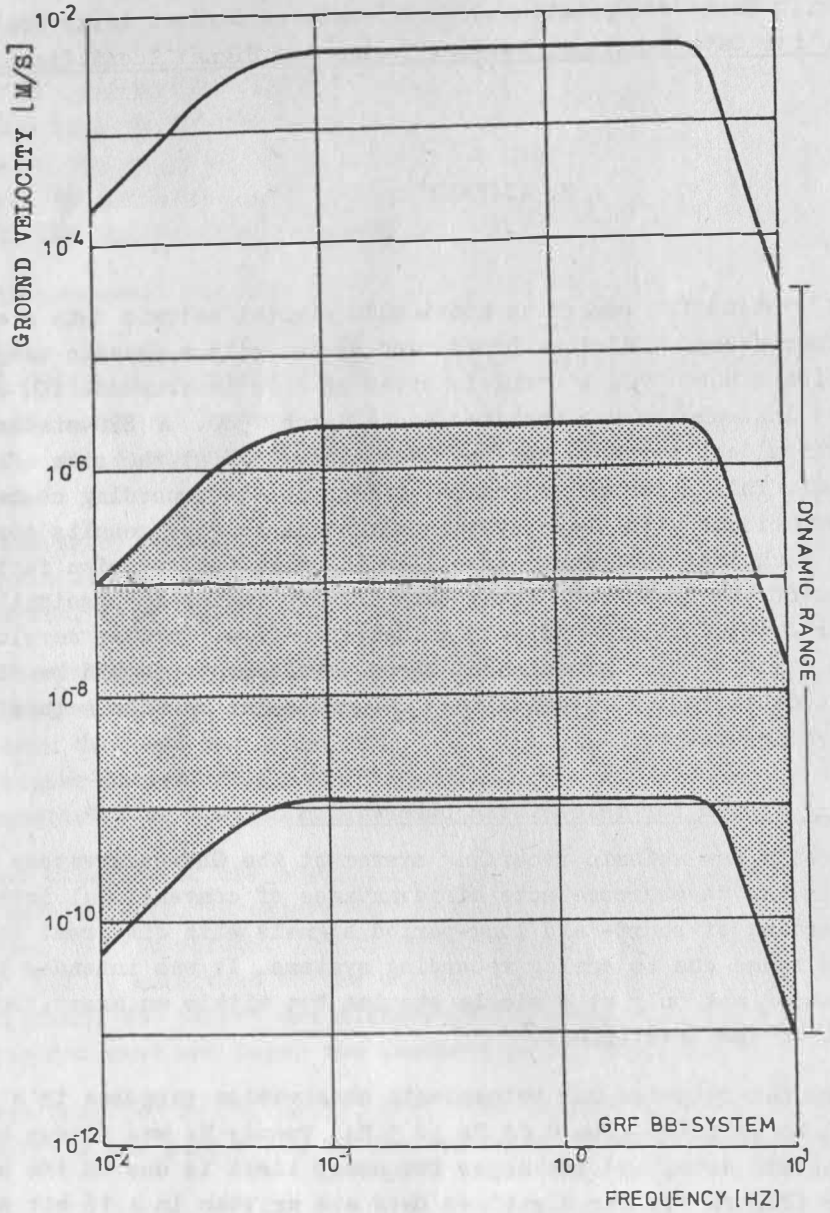

Fig. 1. Velocity response characteristic, dynamic range, and resolution (shaded area) of the GRF broad-band system

developed, thoroughly sealed, leaf-spring feedback seismograph system STS-1V and STS-1H (WIELANDT and STRECKEISEN, 1982). The second subarray (B) became operational during 1978 and the dynamic range was increased from 120 dB to 132 dB. In the same year a 116-m borehole was drilled and independently from the array a SRO system was installed and started continuous recording (PETERSON et al., 1976). The installation of the array comprising three three-component stations at the subarray centers A1, B1, and C1 as well as 10 vertical stations was completed in March 1980. The array has operated with continuous data recording since the time (Figure 2) (HARJES and HENGER, 1973; HARJES, 1973; HARJES, 1975; HARJES and SEIDL, 1978; SEIDL and KIND, 1982).

DOI: https://doi.org/10.2312/zipe.1983.078

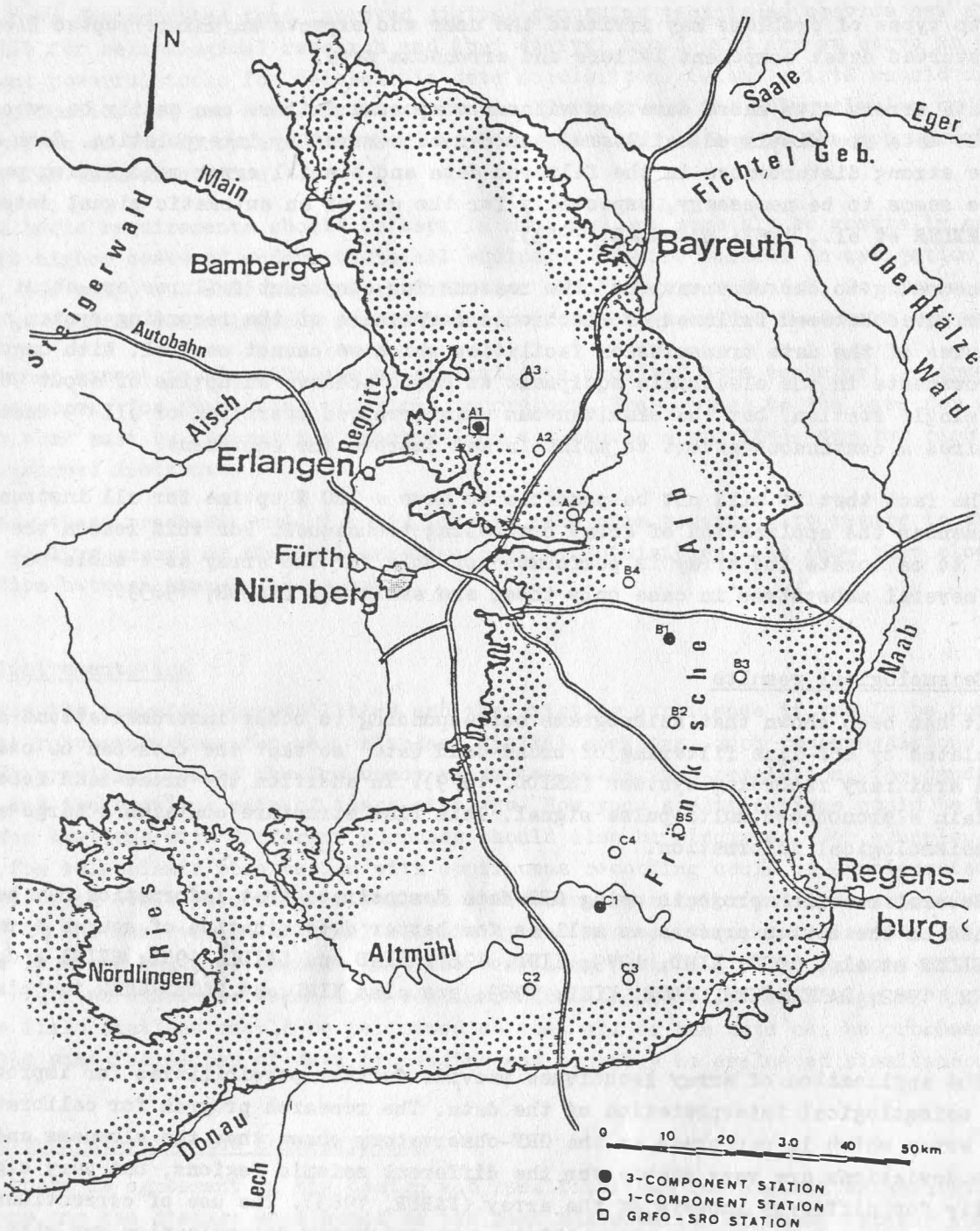

Fig. 2. Location of GRF-array stations

DOI: https://doi.org/10.2312/zipe.1983.078

2. Experience with continuous operation

Two types of problems may irritate the user who expects an uninterrupted flow of undisturbed data: component failure and erroneous data.

Data errors with short duration without component failure can easily be recognized if the data are displayed unfiltered and can be removed by interpolation. Such errors cause strong disturbances in the filtered data and special error recognition procedures seems to be necessary, especially for the use of an automatic signal detector (STAMMLER et al., 1983; STAMMLER, 1983).

According to our observations, the reasons for component failures are about equally distributed between failures of electronic components of the recording system and failures of the data transmission facilities which we cannot control. With ongoing improvements in the electronic equipment we could achieve an uptime of about 90 % for the single station, but the simultaneous uninterrupted operation of all 19 instruments requires a continuous effort to maintain and improve the equipment.

The fact that it will not be possible to have a 100 % uptime for all instruments influences the application of array processing techniques. For this reason the procedure to calibrate the array is performed not only for the array as a whole but also for several subsystems in case only those are available (FABER, 1983).

3. Seismological results

It has been shown that seismograms corresponding to other instrumentations can be simulated by off-line filtering of broad-band data so that the data can be compared with arbitrary recording systems (SEIDL, 1979). In addition the broad-band recordings contain a pronounced multi-pulse signal. This fine structure contains a large amount of seismological information.

Several research projects using GRF data demonstrate that information may be obtained on the source process as well as for better determination of source parameters (MUELLER et al., 1978; KIND, 1979; KIND, 1981; KIND and SEIDL, 1982; SEIDL and BERCKHEMER, 1982; RADEMACHER, ODOM, KIND, 1983; see also KIND and RADEMACHER in this volume).

The application of array techniques provide further possibilities for improving the seismological interpretation of the data. The research program for calibrating the array which is performed at the GRF-observatory shows that the slowness and azimuth deviations are very stable for the different seismic regions, but vary significantly for different subsets of the array (FABER, 1983). The use of corrections derived from calibration results will improve epicenter determination and with improved beam forming possibilities the gap between the detection threshold and the identification threshold can be decreased. Also the variations of the calibration anomalies within the array may give indications of structural anomalies under the array or along the ray paths.

DOI: https://doi.org/10.2312/zipe.1983.078

4. Consequences from new developments

We have demonstrated that improved digital recording techniques provide new possibilities for seismological research and that digital broad-band arrays serve as one of the most powerful tools for teleseismic data acquisition. Seismologists should discuss the implications of new developments at an early stage and the Subcommission on Data Acquisition of the European Seismological Commission may be one of the appropriate bodies for this discussion.

Two basic requirements should be kept in mind and can probably be generally accepted. The higher costs of modern technical equipment require careful investigation of where, how many, and what kind of installation should be recommended, to insure that the best use for seismological research purposes is obtained and funds are not wasted.

Another aspect is that the use of digital data requires more technical equipment than necessary for processing classical recordings. Free access to the data for research work must be assured for everyone and not become a privilege for few rich and well equipped institutes.

Under these preconditions, I would like to make some remarks with regard to the three working groups of the Subcommission on Data Acquisition, and show that close cooperation between them is necessary.

4.1. Instrumentation

Given the technical possibilities and the existing experience it should be possible to make recommendations for new, standard digital stations. Such recommendations should include specification of the frequency characteristics, the resolution, the dynamic range and the sampling rate of these stations. How such specifications could be modified for stations with different purposes should also be discussed. For example, stations for teleseismic observation with continuous recording could be complemented by stations with event recording as well as by eventually simpler and less expensive stations for the observation of local seismicity and microearthquakes. Also the extention of the observed range of signals into the very long periods (100 s) by some well located stations should be taken into consideration. And finally the design of digital mobile field stations should be performed so that all of the data can be processed with the same facilities of data processing and probably be evaluated simultaneously.

4.2. Standardization and normalization

If there is agreement on the design and specifications for digital seismological stations one can discuss what would be the best distribution of such stations for seismological research requirements within the area of interest of the European Seismological Commission. The design of such an optimized network of permanent recording stations should also recognize the role of array stations and take into account the already existing stations. Furthermore, the lowest magnitude earthquakes of interest and how many stations are needed for a reliable source estimation of such earthquakes should be determined.

DOI: https://doi.org/10.2312/zipe.1983.078

Another question is, how could a basic network best be complemented by the additional equipment that I mentioned above. These questions should be discussed by the working group in close co-operation with the EMSC data center. In addition to the network design, site selection criteria for a proper presite survey method should be developed, to make sure that new installations can be properly calibrated and that high reliability and homogeneity of the results can be achieved.

4.3. Data collection and processing

The future work and the possible recommendations of this working group can be performed only in very close co-operation with the other working groups as well as in close co-operation with the data centers especially the EMSC. Four aspects for this work shall be discussed further: data processing, data handling, data exchange, and data storage.

As it is undesirable that research with digital data become a privilege for few people, the technical expenditures necessary for processing the data should be kept at a minimum level. This can be achieved through standardization. Even if some minimum requirements of data processing facilities must be fulfilled to make proper use of the data, the hardware will be less important in the future than the software. Therefore, it should be one task of further recommendations to assure that an easier exchange of programs and algorithms will be possible so that the results which were obtained with the same data at different processing facilities can easily be compared.

It is important to assure that everyone can access all data from all stations easily. The data of the systems SRO, ASRO, HGLP and DWWSSN are collected together as network-day-tapes as well as event-network-tapes. But if all existing stations were to record their data digitally, no data center could handle these data.

The especially valuable data of digital recording arrays cannot be included in the routine data stream because of the huge amount of data. On the other hand if every seismologist would be forced to collect the data for his research work from each single station this would be a step backward and could form a serious obstacle for the use of digital data. Even though we are still at the beginning of this discussion we should find appropriate methods to handle the data and keep them easily accessible.

As shown in the previous section, the data exchange would be facilitated if a central institution were able to collect and distribute all available data, but it also should be possible to exchange data between stations. Every user should be able to process the data of other recording systems without being forced to do to much preprocessing work to adapt the data to his processing facilities. For this reason at the ESC meeting in Leeds the working group presented a proposal for a standard data format for the data exchange. This proposal should be discussed further so that we can modify it if necessary and come to a recommendation of such an exchange format.

An important question resulting from the development of digital recording systems is the question of permanent storage of continuous data recording. Due to the large amount of data gathered with digital recording some seismologists have come to the conclusion that permanent storage of continuous recordings is no longer possible or even necessary. According to the extensive discussion of this problem at the special

DOI: https://doi.org/10.2312/zipe.1983.078

symposium on European Digital Seismic Networks at the meeting of the European Seismological Commission at Budapest 1980 (AICHELE, 1980; DAHLMAN, 1980) we cannot abandon the requirement of permanent storage of all data at least for some properly selected stations. Even if it's not possible at the moment to store the data permanently it has been shown at this meeting that new irreversible storage media with very high density which are to be developed will enable us to store continuous data records permanently in the future.

I would like to thank R. E. Habermann for reading the manuscript and his helpful assistance.

References

AICHELE, H. — Some remarks on the question of data retention for seismological observatories. Paper presented at the 17th General Assembly of the European Seismological Commission. Budapest 21-29 August 1980

DAHLMAN, O. — Selection criteria for data retention. Paper presented at the 17th General Assembly of the European Seismological Commission. Budapest 21-29 August 1980

FABER, S. — GRF-Array-Kalibrierung. Paper presented at the 43. meeting of the German Geophysical Society. Aachen 22.3.-25.3.1983

HARJES, H.-P.; HENGER, M. — Array-seismology. Zeitschr. f. Geophys. (1973), 865-905

HARJES, H.-P. — Zur Erfassung, Bearbeitung und Interpretation seismischer Daten. Geol. Jb. E1, Hannover (1973), 63-74

HARJES, H.-P. — Wide-band seismic recordings at the Graefenberg (GRF)-station. Exploitation of seismograph networks (ed. K.G. Beauchamp) Noordhoff, Leiden (1975), 205-218

HARJES, H.-P.; SEIDL, D. — Digital recording and analysis of broadband seismic data of the Graefenberg (GRF) Array. J. Geophys. 44 (1978), 511-523

KIND, R. — Observations of sPn from Swabian Alb earthquakes at the GRF Array. J. Geophys. 45 (1979), 337-340

KIND, R. — Length of rupture from the Swabian Alb event on 3 September 1978 derived from the Pn duration at GRF. Geol. Jahrb. E21 (1981), 13-25

KIND, R.; SEIDL, D. — Analysis of broadband seismograms from the Chile-Peru Area. Bull. Seis. Soc. Am. 72 (1982), 2131-2145

MUELLER, G.; BONJER, K.-P.; STOECKL, D.; ENESCU, D. — The Romanian earthquake of March 4, 1977. I. Rupture process inferred from fault-plane solution and multiple-event analysis. J. Geophys. 44 (1978), 203-218

PETERSON, J.; BUTLER, H.M.; HOLCOMB, L.G.; HUTT, C.R. — The seismic research observatory. Bull. Seis. Soc. Am. 66 (1976), 2049-2068

RADEMACHER, H.; ODOM, R.I.; KIND, R. — The Upper Mantle structure under South-East Europe. Derived from GRF broadband records of Greek earthquakes. J. Geophys. 52 (1983), 7-13

DOI: https://doi.org/10.2312/zipe.1983.078

SEIDL, D. — The simulation problem for broad-band seismograms. J. Geophys. 48 (1979), 84-93

SEIDL, D.; BERCKHEMER, H. — Determination of source moment and radiated seismic energy from broadband recordings. Physics of the Earth and Planetary Interior 30 (1982), 209-213

SEIDL, D.; KIND, R. — Das instrumentelle und seismologische Konzept des Graefenberg Array. Geol. Jahrb. E 23 (1982), 207-220

STAMMLER, W. — Design of matched filters and related frequency selective filters for the detection of teleseismic events. IEEE Trans. Geoscience Electron. GE-21 (1983) 2, 20

STAMMLER, W.; KIND, R.; AICHELE, H. — Automatic on-line detection of weak earthquakes at the Graefenberg-Array. Paper presented at the Second European Signal Processing Conference (in press)

WIELANDT, E.; STRECKEISEN, G. — The leaf-spring seismometer. Design and performance. Bull. Seis. Soc. Am. 72 (1982), 2346-2367

A Set of Optimum Response Curves of Instruments According to Dynamic Range of Recorders

by

Z.I. ARANOVICH [1)]

The paper is concerned with generalized amplitude-frequency relationships for basic body and surface waves in parametric dependence upon magnitude and epicentral distance for two types of earthquakes - near and distant, the first type being Δ = 20 - 100 km, M = 0.5 - 8, and the second type Δ = 20° - 100°, M = 4 - 8.5. These relationships have served as the basis for constructing sets of optimum response curves of seismic instruments applied to near and distant earthquakes. Pass-bands of the response curves have been considered in two alternatives: in relation to displacement and in relation to velocity. In doing so, consideration has been given to dynamic ranges of recorders 40, 60, 80 and 120 dB. The performed analysis has shown an obvious advantage of response curves of velocigraph type, which number in the set was two-three times less than that in case of a displacement type. A number of recommendations on using such sets of response curves in seismological practice is made.

published as: Арановіч, З.И. Наборы оптимальных амплитудно-частотных характеристик сейсмометрической аппаратуры в зависимости от динамического диапазона регистрации. Сейсмические приборы, Москва 15 1982

[1)] Institute of Physics of the Earth, USSR, Moskow D-242, B. Gruzinskaya 10

DOI: https://doi.org/10.2312/zipe.1983.078

Многоканальный цифровой измерительный комплекс для регистрации сейсмологической информации в широких динамическом и частотном диапазонах

З.И. АРАНОВИЧ, С.А. НЕГРЕБЕЦКИЙ, О.А. СЕРОВА, Г.Д. ЧЕИШВИЛИ, И.Ф. ЛОМТАТИДЗЕ, А.К. АЛШИБАЯ, А.Л. КОФНЕР, Ю.В. СТЕПАНЕЦ [1)]

Summary

At the basis of the calculation carried out for the dynamic and frequency range of the seismic signals recorded in wide range of epicentral distances and energy classes and also taking into account errors of the digital devices the structure and the technical characteristics of the universal digital measuring complex MIK were chosen (conversion in the form of a floating point, use of pre-event memory and energy level gradient trigger algorithm in the narrow frequency window). Work for developing of prototypes of MIK and their experimental test in conditions of real recording were carried out. The main structural sketches of MIK, its technical characteristics and its functional possibilities of work with different recorders, transmitters and preprocessors are enclosed.

В настоящее время не вызывает сомнения то, что аппаратура для регистрации сигналов от землетрясений в широких диапазонах энергетических классов и эпицентральных расстояний должна безусловно быть многоканальной и цифровой, обладать измерительной шкалой в виде с плавающей запятой, иметь достаточный буфер памяти для обеспечения режима ждущей регистрации без пропуска первых вступлений, самостоятельно обнаруживать, с достаточной степенью надежности, эти первые вступления, включать регистраторы для записи обнаруженных сигналов или выводить информацию в каналы радиотелеметрии. Такая аппаратура должна обладать также внутренней службой времени, устройством для автоматического контроля как сейсмометрических каналов, так и всего цифрового тракта.

В ИФЗ АН СССР в последнее время выполнен ряд работ (АРАНОВИЧ, 1982; АРАНОВИЧ и др., 1980; АРАНОВИЧ и др., 1979) где на модельных сигналах и реальных записях землетрясений проведены расчеты, дающие количественную оценку требований к таким параметрам сейсмологической измерительной аппаратуры как необходимый динамический диапазон регистрации возможных амплитуд сигналов и необходимые для этого частотные характеристики сейсмометрических каналов, а также требования к распределению точности кодирования сейсмических сигналов для обеспечения оптимального режима регистрации сейсмологической информации.

[1)] Институт Физики Земли АН СССР, Москва Д-242, Грузинская 10

DOI: https://doi.org/10.2312/zipe.1983.078

В таблице № I даны возможные значения погрешностей спектров регистрируемых сейсмических сигналов, ширина полосы этих спектров, при минимуме значения относительных погрешностей для каждого спектра, и значения погрешностей на заданной в 2,5 декады частотной полосе в зависимости от максимальной амплитуды эквивалентных смещений почвы (динамического диапазона) поступающих в пункт регистрации сейсмических сигналов. Имеется ввиду, что сигналы регистрируются цифровой аппаратурой с динамическим диапазоном I20 дБ в виде с плавающей запятой. Расчеты проводились для сигналов эквивалентных первым вступлением прямых продольных волн землетрясений, которые могут регистрироваться в ближней зоне. Приведенные в таблице данные убедительно показывают преимущества способа цифрового преобразования сейсмических сигналов в виде с плавающей запятой, который обеспечивает регистрацию землетрясений в большом диапазоне энергетических классов при минимуме вносимых погрешностей в широкой полосе частот. Так, например, даже для сигналов попавших лишь в небольшую часть (40 дБ) от общего динамического диапазона аппаратуры в I20 дБ, ширина регистрируемого спектра с погрешностью I,5 % составляет I,28 декады, а на высокочастотной границе спектра такого сигнала при заданной ширине в 2,5 декады, погрешность возрастает только ло 30 %.

Выполненные расчеты позволили заложить в разрабатываемую аппаратуру такие основные параметры как число каналов, подключаемых к измерительному комплексу, соответствующие для них частоты дискретизации и необходимую шкалу преобразования аналоговых сигналов в цифровую форму, обеспечивающую необходимый динамический диапазон и требуемое распределение точности цифрового преобразования в этом диапазоне. Структура основного измерительного узла данного комплекса, то есть управляемого масштабного усилителя, обеспечивающего последующее аналого-цифровое преобразование в виде с плавающей запятой и основные алгоритмы работы этого блока были опробованы в ИФЗ АН СССР (НЕГРЕБЕЦКИЙ и др., I980) на начальном этапе разработки данного многоканального цифрового измерительного комплекса (МИК).

Разработка МИК проводилась совместно специалистами ИФЗ АН СССР и Специального конструкторского бюро научного приборостроения АН ГССР.

На рис. I показана блок-схема аппаратуры МИК, которая дает общее представление о структуре этого комплекса и взаимодействии, входящих в его состав, основных блоков.

Аналоговые сигналы с комплекта электронных сейсмометрических каналов (АРАНОВИЧ и др., I982) в виде напряжения поступают на дифференциальные входы модуля коммутатора каналов (КК) - аналогового мультикомплексора, который, по заложенной в него программе, поочередно подключает двух проводные линии от сейсмометрических каналов, к модулю измерительного усилителя. Дифференциальные входы мультиплексора и измерительного усилителя позволяют подавлять синфазные помехи, возникающие при работе МИКа с электронными сейсмометрами через длинные кабельные линии.

Модуль измерительного усилителя (ИУ) состоит из усилителя с автоматическим переключением четырех значений его коэффициента передачи (256, I6,I и I/I6) и аналого-цифрового преобразователя (АЦП). С выхода ИУ цифровая информация в двоичном коде (I0 разрядом мантиссы, знак и два разряда порядка) поступает в буфер памяти. Использование в ИУ, по сравнению с (НЕГРЕБЕЦКИЙ и др., I980), коэффициентов кратных 2^4, позволяет при вводе информации с МИК в ЭВМ избежать дополнительного преобразования.

DOI: https://doi.org/10.2312/zipe.1983.078

Таблица № I Возможные значения погрешностей спектров сейсмических сигналов, записанных цифровой аппаратурой с динамическим диапазоном I20 дБ в виде с плавающей запятой

Максимальная эквивалентная амплитуда смещений почвы МКМ	$I0^3$	$I0^2$	I0	I	0,I	0,0I
Динамический диапазон регистрируемых сигналов	I20	I00	80	60	40	20
Ширина спектров, зарегистрированных сигналов в декадах и значения относительных погрешностей в этой полосе (в %%)	I,75	I,6	I,45	I,37	I,28	I,2
	$I,5.I0^{-4}$	$2.I0^{-3}$	$I,5.I0^{-2}$	0,I5	I,5	20
Погрешность в %% на высокочастотной границе спектра шириной в 2,5 декады	$I0^{-2}$	$5.I0^{-2}$	0,2	2	30	500

СТРУКТУРНАЯ СХЕМА

МИК

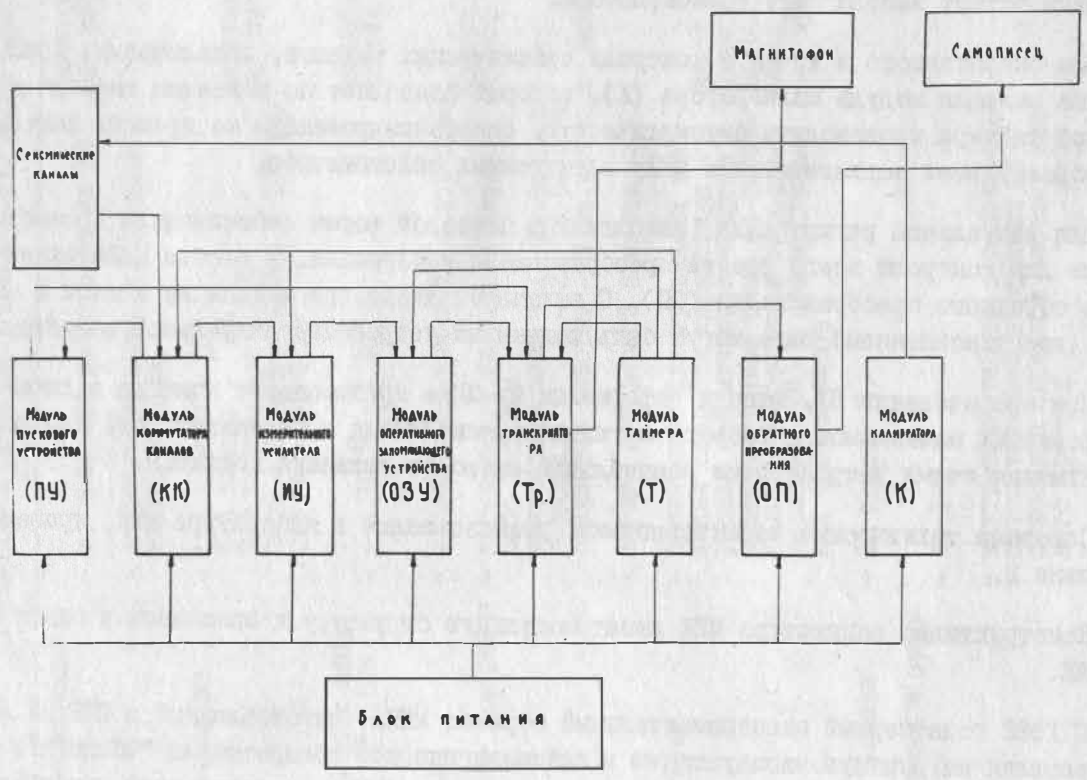

Рис. I. Общая структурная блок-схема аппаратуры МИК

DOI: https://doi.org/10.2312/zipe.1983.078

Модуль оперативного запоминающего устройства (ОЗУ) представляет собой буфер памяти емкостью 32 Кслов, где происходит непрерывное занесение цифровой информации от первой ячейки до последней, после чего цикл повторяется и т. д.

Модуль транскриптора (Тр) осуществляет формирование выводимых из МИК цифровых массивов информации, состоящих из I6-ти разрядных двоичных слов. Этот модуль формирует также этикетку выводимых массивов, состоящую из кода номера данной станции, номера суток и кода текущего времени (часы, минуты) на момент включения вывода информации из МИКа. Команда "Старт вывода" информации из транскриптора вырабатывается пусковым устройством в МИКе или задается в виде кода от внешних устройств (например микро ЭВМ). Прекращение вывода информации ("стоп вывода") происходит по заданному времени от внутреннего таймера МИКа или также от кодовой команды внешнего устройства.

Модуль таймера (Т), помимо функций внутренней службы времени в МИКе, вырабатывает необходимые импульсные сигналы управляющие работой всех блоков этой аппаратуры.

Схемы модуль пускового устройства (ПУ) непрерывно анализируют сигналы, поступающие с двух вертикальных компонент электронных сейсмометрических каналов (короткопериодного и среднепериодного) и, при превышении одной из пяти заданных в ПУ скоростей нарастания уровня сейсмической энергии в узком частотном окне, настроенном на максимум спектра прямых продольных волн (соответственно близких и удаленных) землетрясений, вырабатывают команды "старт вывода" для транскриптора.

Для оперативного и точного контроля сейсмических каналов, подключаемых к МИКу, в его состав включен модуль калибратора (К), который позволяет по командам внешних устройств или от таймера производить автоматическую, синхронизированную по времени импульсную калибровку всех подключенных к МИКу злектронных сейсмометров.

Для визуальной регистрации, выводимых в цифровой форме сейсмических процессов, а также для контроля всего тракта преобразования информации, в состав МИКа включен модуль обратного преобразования (ОП). С выхода ОП любые при канала из девяти в аналоговом (восстановленном) виде могут быть поданы на устройства визуальной регистрации.

При срабатывании ПУ, выводу информации из МИКа предшествует команда включения лентопротяжных механизмов цифрового магнитного накопителя и переписца, что необходимо для достижения этими устройствами номинальной скорости движения носителя.

Основные технические характеристики, реализованные в аппаратуре МИК, приведены в таблице 2.

Конструктивно аппаратура МИК имеет модульную структуру и выполнена в одном крейте КАМАК.

С I982 года первый экспериментальный образец МИКа, изготовленный в СКБ НП АН ГССР, установлен на опытную эксплуатацию в сейсмологической обсерватории "Тбилиси". В настоящее время ведется подготовка к запуску в производство партии этих приборов, в ходе которой предусматривается замена элементной базы в отдельных модулях МИКа с целью уменьшения потребляемой им мощности до 4 ÷ 5 ВА.

DOI: https://doi.org/10.2312/zipe.1983.078

Таблица № 2 Основные технические характеристики аппаратуры МИК

Число подключаемых аналоговых каналов	– 9, возможно расширение дл I8
Входные цепи	– дифференциальные, парафазные входы, I00КОМ,
Частоты дискретизации (поканально)	– I-3 каналы – I00 Гц 4-6 каналы – I0 Гц 7-9 каналы – I Гц либо с I по N – канал – I00 Гц где N – от I до 9
Диапазон измеряемых входных напряжений (В) (по каждому каналу)	– $\pm$ 4.I0^{-6} ÷ $\pm$ I0
Способ измерения	– с плавающей запятой (4 порядка)
Результат одного измерения	– шестнадцати разрядное слово либо 2 байта мантисса и знак – II дв.разрядов порядок – 2 дв.разряда служебная информ. – 3 дв.разряда
Режим работы	– ждущий с буферной памятью
Алгоритм включения	– превышение фиксированных изменений скорости нарастания уровня сейсмической энергии в узком частотном окне по вертикальным компонентам коротко-периодн. (КП) и среднепериодных (СП) каналов
Объем буферной памяти	– 32 Кслов
Временная задержка в буфере по КП-каналам	– до I00 с
Служба времени	– внутренний таймер с воможностью автоматической коррекции от приемника сигналов системы единого времени
Регистрируемая временная информация	– непрерывная разметка выводимых массивов (час, минута, секунда), начальная этикетка – код часов минут, № суток, № станции
Длительность выводимых массивов	– при срабатывании от КП-каналов – 5 мин. при срабатывании от СП-каналов – 25 мин.
Контроль сейсмометрических каналов	– автоматическая, синхронизированная импульсная, калибровка всех каналов.
Контроль за работой цифрового тракта	– полное обратное преобразование, с выводом любых трех каналов на визуальную регистрацию
Внешнее управление	– 4 команды: старт вывода, стоп вывода, импульсная калибровка, резервная команда
Вывод информации и ввод команд	– в стандарте ТТЛ
Диапазон рабочих температур	– + 5 ÷ + 45°С
Электропитание	– постоянный ток, 24 В, не более 30 ВА

DOI: https://doi.org/10.2312/zipe.1983.078

Первые образцы аппаратуры МИК, изготовленные опытным производством СКБ НП ГССР, комплектуются электронным сейсмометрическим каналом и цифровыми ленточными магнитными накопителями, выпускаемыми Особым конструкторским бюро ИФЗ АН СССР, и серийными трехканальными переписцами.

На рис. 2 приведены построенные графопостроителем ЭВМ начальные участки записей трех близких землетрясений (в, г, д), зарегистрированных аппаратурой МИК в ждущем режиме, отклик короткопериодного электронного сейсмометрического канала (временная характеристика) (а), полученная методом импульсной калибровки при работе МИК'а в условиях реальной регистрации, и предшествующий этому отклику отрезок записи микросейсмического фона помех (б). Полученные прямым расчетом спектров таких откликов амплитудно-частотные характеристики (АЧХ) этих каналов дают возможность сразу построить их АЧХ во всем диапазоне частот (периодов) таких каналов (АРАНОВИЧ и др., 1981), что возможно только при использовании цифрового преобразования в виде с плавающей запятой.

В настоящее время в ИФЗ АН СССР ведется подготовка экспериментального опробования работы МИК'а в соединении с микро-ЭВМ типа "Электроника-60" и накопителем типа ИЗОТ-5003 болгарского производства. Такой комплекс обеспечит регистрацию и предварительную экспресс-обработку сейсмологической информации в реальном масштабе времени. Планируется также проведение экспериментов совместно с Венгерской Академией наук по передаче информации с МИК'а по каналам цифровой радиотелеметрии. Это позволит опробовать работу МИК'а в режиме выносного измерительного терминала, уже в системе сбора сейсмологической информации с нескольких таких станции.

Литература

АРАНОВИЧ, З.И. — Наборы оптимальных амплитудно-частотных характеристик сейсмометрической аппаратуры в зависимости от динамического диапазона регистрации. Сейсмические приборы, Москва 15 (1982)

АРАНОВИЧ, З.И., МЕЛАМУД, А.Я., НЕГРЕБЕЦКИЙ, С.А., ТРАПЕЗНИКОВ, Н.А., КУШНИР, Г.С. — Анализ некоторых характеристик сейсмологической информации и метрологические требования к системе регистрации. Сейсмические приборы, Москва 13 (1980), 89-99

АРАНОВИЧ, З.И., МЕЛАМУД, А.Я., НЕГРЕБЕЦКИЙ, С.А. — Некоторые вопросы точности сейсмометрической регистрирующей аппаратуры. Сейсмические приборы, Москва 12 (1979)

НЕГРЕБЕЦКИЙ, С.А., ТУРЕЦКИЙ, И.М. — Устройство для обеспечения формата "плавающая запятая" в цифровых сейсмических регистрирующих системах. Сейсмические приборы, Москва 13 (1980), 122-126

АРАНОВИЧ, З.И., ТРАПЕЗНИКОВ, Н.Л. — Построение широкополосных сейсмометрических каналов на базе серийных сейсмоприемников. Сейсмические приборы, Москва 15 (1982)

АРАНОВИЧ, З.И., МЕЛАМУД, А.Я., НЕГРЕБЕЦКИЙ, С.А. — Импульсная калибровка сейсмометрических каналов с большим динамическим диапазонам. Физика Земли, 12 (1981)

DOI: https://doi.org/10.2312/zipe.1983.078

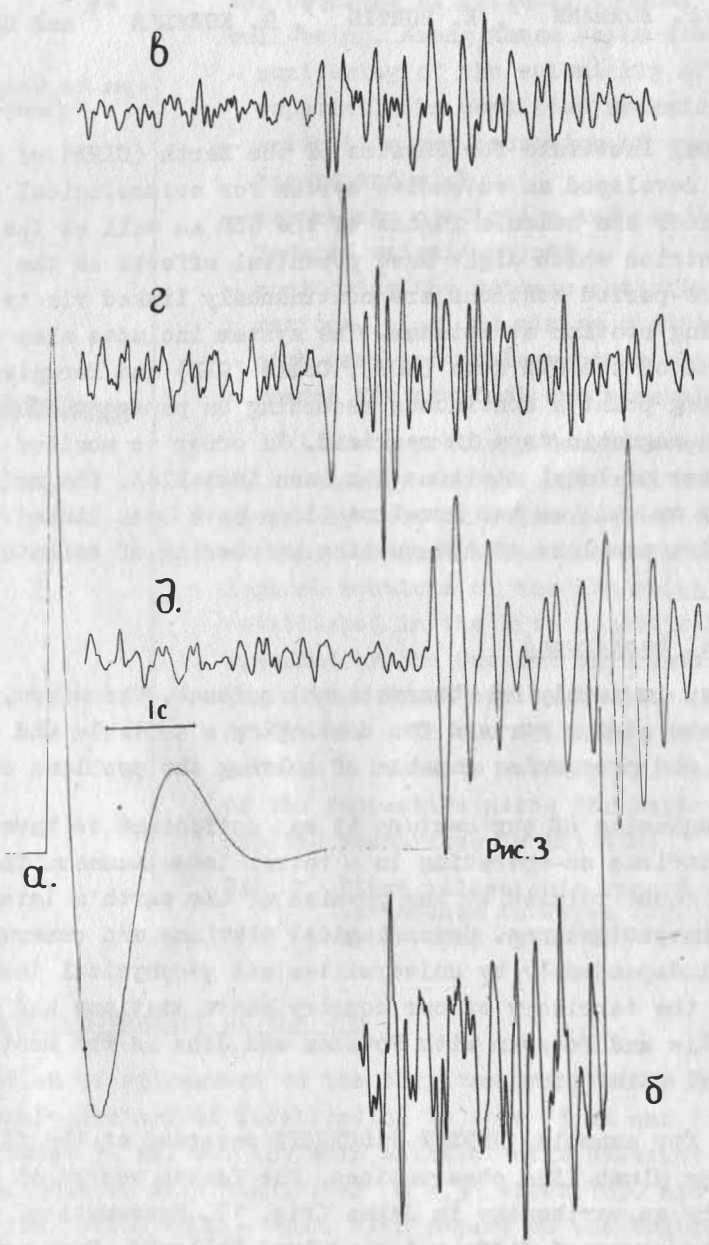

Рис.3

Рис. 2. Примеры записей, полученных на аппаратуре МИК:
а) отклик сейсмометрического канала на импульсную калибровку,
б) микросейсмический фон помех, предшествующий первому вступлению такого отклика,
в), г), д) начальные участки трех близких землетрясений

DOI: https://doi.org/10.2312/zipe.1983.078

The System for Acquisition and Processing Seismological Data in the GDR

by

P. BORMANN [1], E. HURTIG [1], G. KOWALLE [1] and Ch. TEUPSER [2]

Summary

The Central Institute for Physics of the Earth (CIPE) of the Academy of Sciences of the GDR has developed an extensive system for seismological data acquisition with a view to monitor the seismic regime of the GDR as well as the seismic activity of neighbouring countries which might have potential effects on the territory of the GDR. As of now six short-period stations are continuously linked via telephone lines with the central recording station at Potsdam. The system includes also the seismological first rate stations of the GDR Moxa (MOX), Collm (CLL) and Berggießhübel (BRG). At the central recording point a continuous recording on paper and an event-triggered digital recording on magnetic tape is realized. In order to monitor local seismicity at special sites a number of local stations has been installed. The main seismological station of CIPE in Moxa as well as two local stations have been linked with a computer at Jena in order to solve problems of the on-line processing of seismic data.

1. Historical background

Seismology is mainly an observational science. Therefore, it is no wonder that seismologists have always strived for developing a suitable and efficient system of data acquisition and processing capable of solving the problems of interest.

At the beginning of our century it was sufficient to have a widely scattered system of single stations co-operating in a rather loose manner. The problems to be solved were mainly those related to the physics of the earth's interior and to principal structural investigations. Seismological stations and observatories were installed in most cases independently by universities and geophysical institutions. This was also the case on the territory of our country where stations had been established at Jena, Leipzig, Halle and Potsdam with Potsdam and Jena as the most historical places from a seismological point of view.

In 1889, for example, REBEUR-PASCHWITZ recorded at the first time teleseismic events during plumb line observations. The famous record at Potsdam of April 17, 1889, was caused by an earthquake in Japan (Fig. 1). Systematical trials of recording seismic events by means of different pendulums followed. Much activity was concentrated on the improvement of seismic instrumentation. At Potsdam a continuously working seismological station was established.

In Jena the first seismograph - an optically recording REBEUR-EHLERT pendulum with a magnification of 4000 - was installed in 1900 in a cellar of the Physical Institute of the Jena University. In 1923 the former "Reichsanstalt für Erdbebenforschung" was founded at Jena with O. HECKER and subsequently A. SIEBERG as their first directors.

[1] Central Institute for Physics of the Earth of the Academy of Sciences of the GDR, DDR-1500 Potsdam, Telegrafenberg

[2] Central Institute for Physics of the Earth of the Academy of Sciences of the GDR, DDR-69 Jena, Burgweg 11

DOI: https://doi.org/10.2312/zipe.1983.078

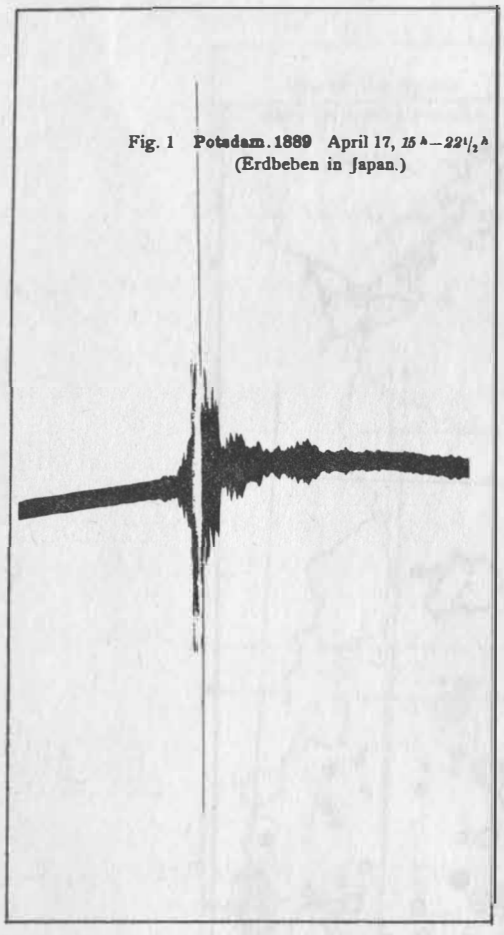

Nowadays seismology has a steadily growing relevance for the solution of fundamental problems of national economy and social well-being. Among these tasks are:

- monitoring of the seismicity of the world especially in populated seismic regions,
- estimation and reduction of earthquake hazard and risk,
- earthquake prediction and prediction of induced seismic events,
- monitoring the seismic activity in special regions, e. g. in mining districts, near high dams and nuclear power plants,
- search for new fuel and mineral resources.

All these problems demand a new strategy in seismology and new national and/or regional systems of seismological data acquisition. The centralized network of seismological stations of the GDR which has been established in the late seventieth and is operated by the Central Institute for Physics of the Earth of the Academy of Sciences of the GDR - in the following called CIPE network - tries to satisfy at least parts of the respective needs for basic and applied researches in the GDR.

Fig. 1. First teléseismic record of an earthquake in Japan (April 17, 1889) at Potsdam by REBEUR-PASCHWITZ)

2. Seismicity and seismic hazard potential of the GDR

Fig. 2 shows the distribution of epicenters on the territory of the GDR for the time period 1500 - 1899. The general accuracy of localization is some 15 km and for events marked with dotted circles around 30 km. For the main seismic activ district of the GDR, the Vogtland region, only earthquakes with magnitudes $M > 3$ after 1850 are depicted. Fig. 3 shows seismicity for the period 1900 - 1980. With regard to the Vogtland region only events with $M > 3.6$ are shown. The accuracy of epicenter localization has increased and is in general around 10 km. New types of seismic events are connected with mining activities (hatched circles).

The main seismic areas within Europe influence the seismic hazard potential of the GDR. Intensities up to 3.5 have been observed on our territory in connection with stronger earthquakes in the Swabian Alb (FRG), Austria, and Northern Italy (Friuli earthquake). The latter event caused perceptible ground motions up to the Baltic Sea Coast. Thus, our task is the detailed comprehensive monitoring and precise localization and description of all natural as well as man-made induced seismic events down to $M \approx 2$ on our territory but also of stronger regional events in Central Europa.

DOI: https://doi.org/10.2312/zipe.1983.078

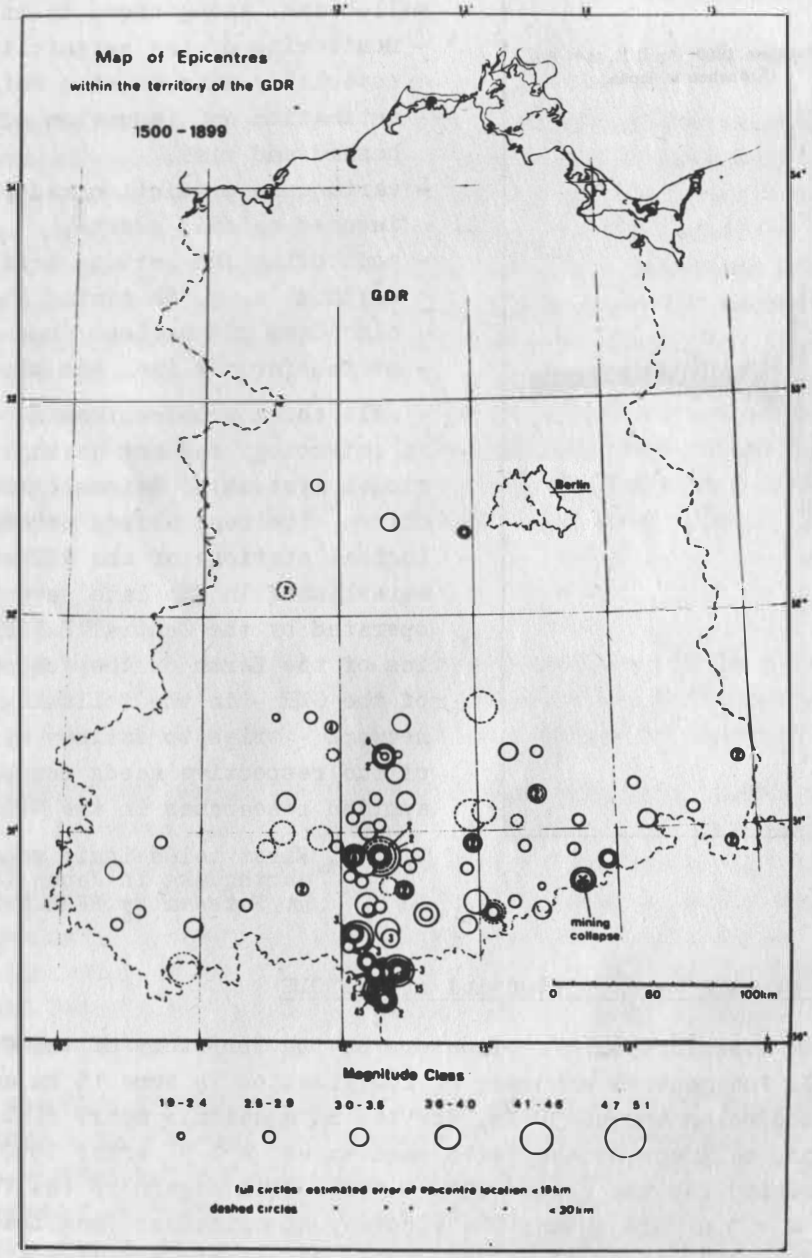

Fig. 2. Epicenter distribution for events on the territory of the GDR for the period 1500 - 1899

DOI: https://doi.org/10.2312/zipe.1983.078

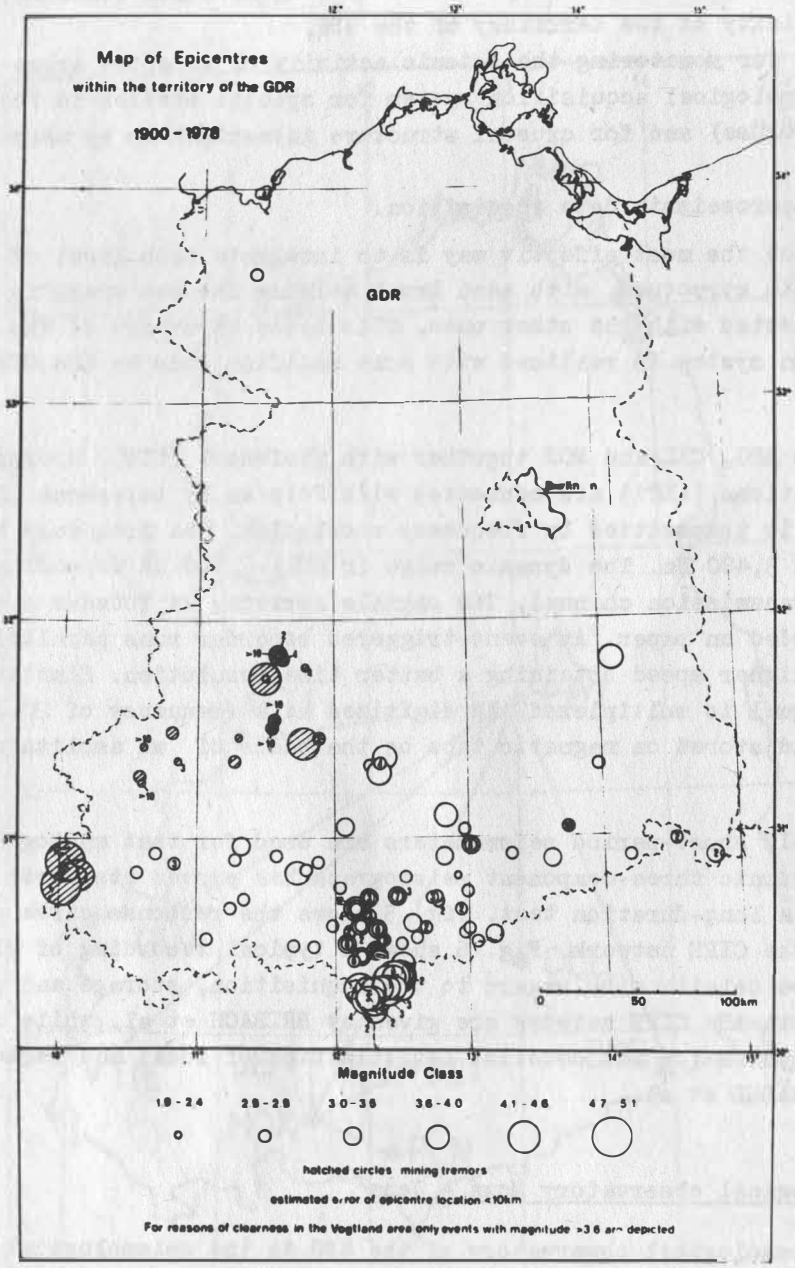

Fig. 3. Epicenter distribution for events on the territory of the GDR for the period 1900 - 1980. Matched circles mark events in mining regions

3. The CIPE network

In order to solve the above mentioned problems a comprehensive system of seismological data acquisition was needed. This system comprises different components or subsystems:

- first order seismological stations incorporated into the international system of data acquisition and exchange (e. g. MOX, BRG, CLL[1])

[1] The seismological station Collmberg (CLL), which co-operates within the CIPE network, belongs to the Karl-Marx-University Leipzig

DOI: https://doi.org/10.2312/zipe.1983.078

- regional seismological station system for solving national problems, mainly for studying the seismicity of the territory of the GDR,
- local systems for monitoring the seismic activity of selected areas and objects,
- a mobile seismological acquisition system for special studies in focal regions (aftershock studies) and for crustal structure investigation by means of explosion seismology,
- a system of macroseismic data acquisition.

In our experience the most effectiv way is to integrate each level of data acquisition into a hierarchic structure, with each level solving its own specific problems but being interconnected with the other ones. This basic structure of the seismological data acquisition system is realized with some modifications by the CIPE network (Fig. 4).

The stations BRG, CLL and MOX together with Tiefenort (TIE), Großwechsungen (GWS) and Altmark-stations (ALT1) are connected with Potsdam by telephone lines. The seismometer signal is transmitted by frequency modulation. The frequency band used lies between 300 and 3,400 Hz. The dynamic range is 80 ... 100 dB depending on the noise level of the transmission channel. The signals arriving at Potsdam are then demodulated and recorded on paper. An event-triggered recorder runs parallel to that paper recorder at a higher speed obtaining a better time resolution. Simultaneously, the demodulated signal is multiplexed and digitized at a frequency of 20 Hz. The events are selected and stored on magnetic tape on the basis of an amplitude threshold criterion.

SM-3 or VSJ-II short-period seismometers are used for that analog data transmission. The EDS 1 electronic three-component seismograph has proved its worth as a long-period seismometer in a long-duration test. Fig. 5 shows the response curve of the instruments used in the CIPE network. Fig. 6 shows a typical recording of all instruments at Potsdam. More details with regard to the acquisition, storage and processing of seismic data with the CIPE network are given by BRIBACH et al. while results achieved by using this system for the detailed investigation of local and regional events are discussed by GRÄSSL et al.

4. The seismological observatory Moxa - Jena

The main seismological observatory of the GDR is the seismological station Moxa of CIPE. On January 1st, 1964, this station started to work and was officially included into the world-wide data exchange. During the first years the main instruments of the station were electromagnetic seismographs. Most of them has been developed at our institute and been manufactured in our workshop. The frequency responses of the instruments are shown in Fig. 7. For all characteristics of type A, B, and C, which have been standardized amongst socialist countries, a complete set of three components is at our disposal. Furthermore, one vertical seismograph works in the frequency range of 4 to 20 cps with a magnification of 300,000 and a second one with a characteristic adapted to the inverse noise spectrum and with a peak magnification of 100,000 at 1 s. These two instruments make it possible to detect weak signals and to distinguish between nearby blasts and remote events. The analogue equipment of the station Moxa is full in operation since many years and delivers data to the international centres.

DOI: https://doi.org/10.2312/zipe.1983.078

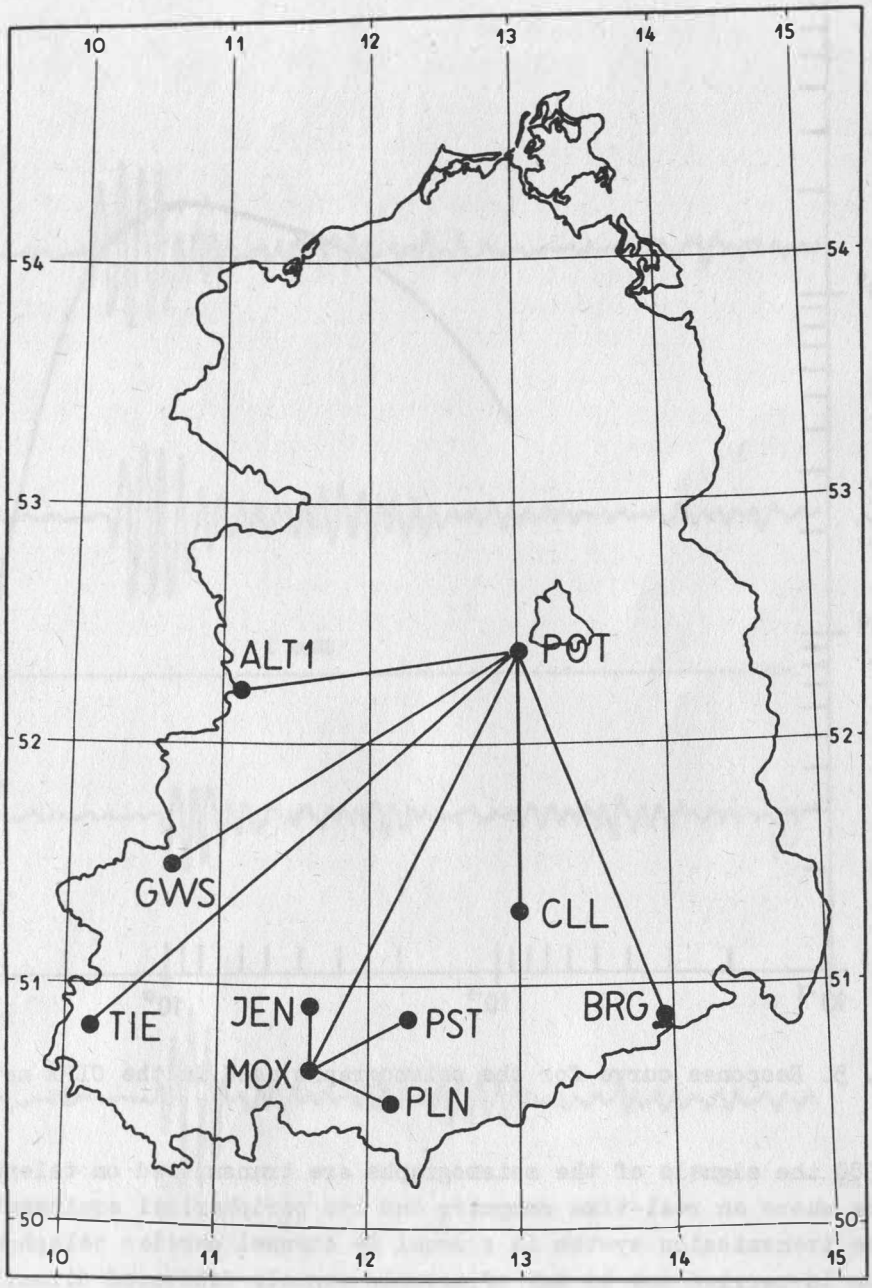

Fig. 4. The seismological CIPE network. Seismic signals are telemetered from the seismic stations to the recording center at Potsdam (POT) by telephone lines. The stations are: ALT1 - Altmark 1, GWS - Großwechsungen, TIE - Tiefenort, MOX - Moxa, PST - Posterstein, PLN - Plauen, CLL - Collm and BRG - Berggießhübel

DOI: https://doi.org/10.2312/zipe.1983.078

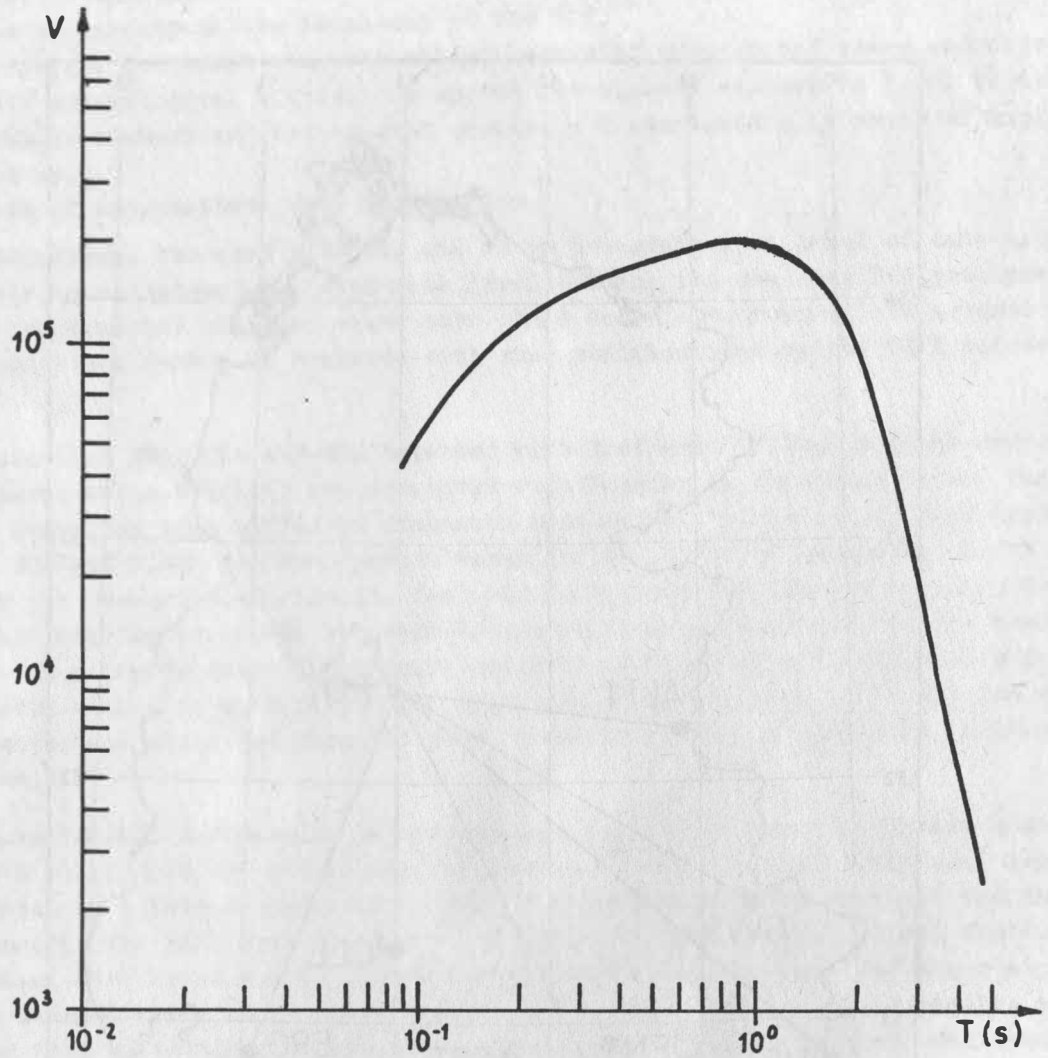

Fig. 5. Response curve for the seismographs used in the CIPE network

Since 1980 the signals of the seismographs are transmitted on telephone lines from Moxa to Jena where an real-time computer and its peripherical equipment have been installed. The transmission system is a usual 24 channel carrier telephone system. The transmission is carried out by way of seismic signals delivered directly by electronic seismographs or after amplifying and conversion of the signals of electromagnetic seismograph. Detailed informations on the seismographs and their response curves are given in a seperate paper by TEUPSER. The responses are similar to the above mentioned analogue ones which has proved very suitable. Besides seismic signals some non-seismic data like temperature, air pressure, and wind velocity can be transmitted by a carrier-current telegraph system. It will be put in operation very soon in order to monitor the functions of the seismographs, to detect non-seismic signals, and to identify noise.

DOI: https://doi.org/10.2312/zipe.1983.078

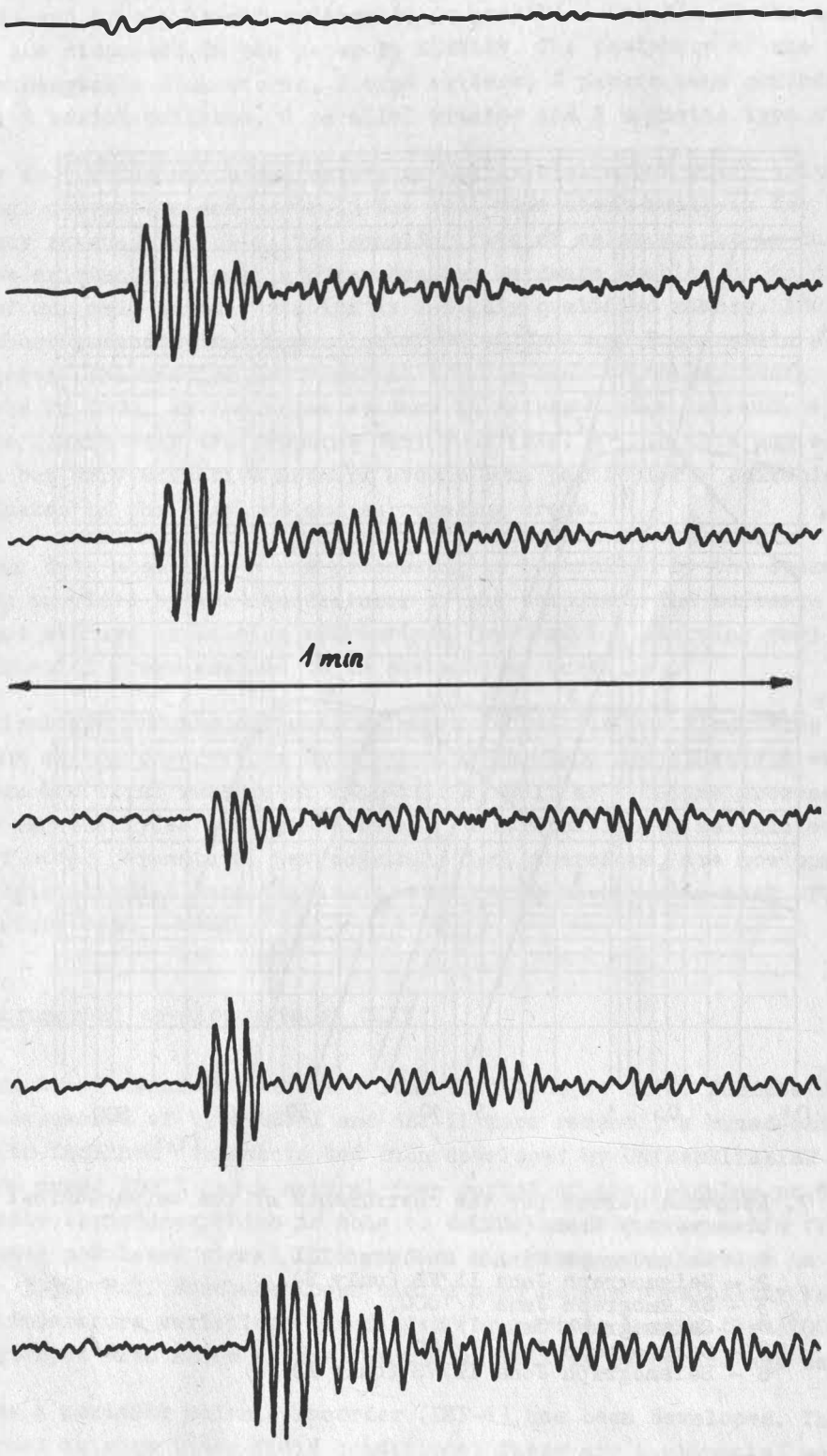

Fig. 6. Record of an event in Oregon (41.6 N, 120.1 W) of April, 14, 1983, at the recording center at Potsdam (epicentral distance D = 81°). Beginning from the top there are shown the traces of ALT 1, GWS, TIE, MOX, CLL and BRG

DOI: https://doi.org/10.2312/zipe.1983.078

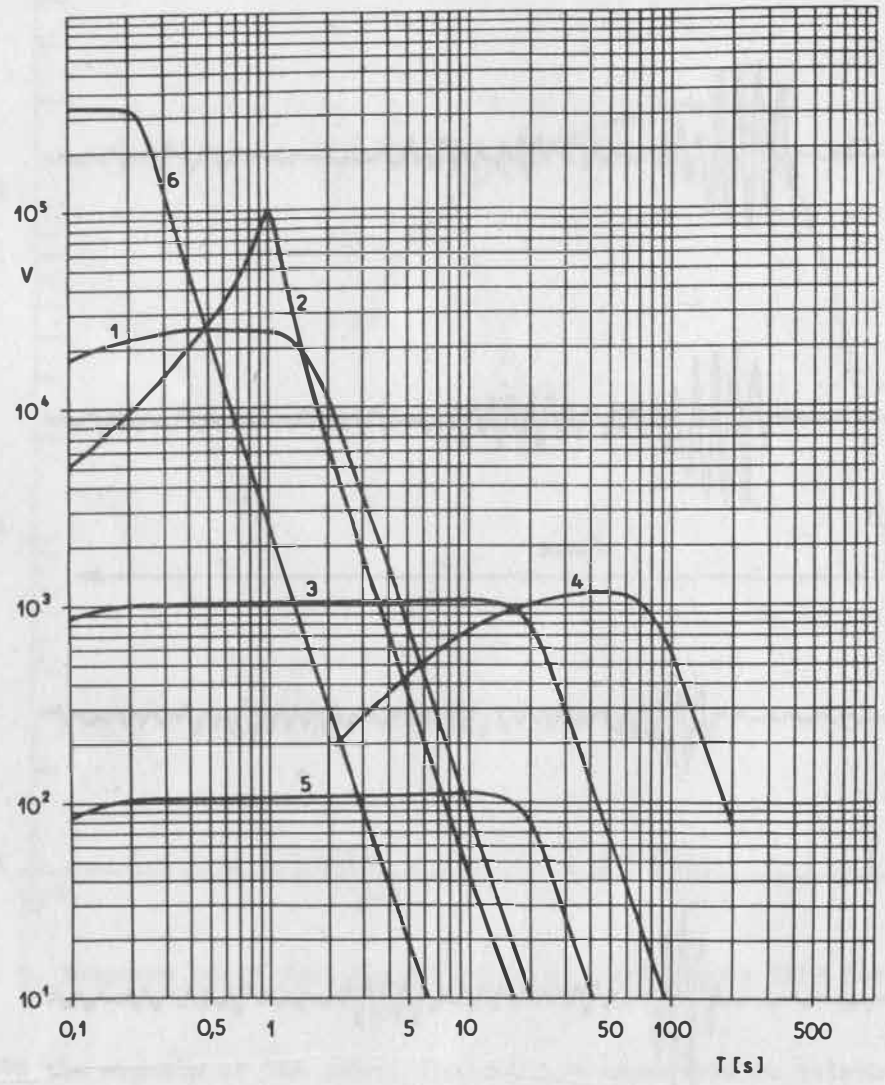

Fig. 7. Response curves for the instruments of the seismological observatory Moxa (MOX).

1 - Seismograph Kirnos Modified III,
2 - Seismograph Jena II/NB (only Z),
3 - Seismograph Jena I/1000,
4 - Seismograph Jena I/L,
5 - Seismograph Jena I/100,
6 - Seismograph Jena II/VS (only Z)

DOI: https://doi.org/10.2312/zipe.1983.078

The computer used is an on-line computer PRS 4000 of VEB ROBOTRON. The word size is 16 bit, double and triple length arithmetic is possible. Details of the sampling and data read-in are discussed in the paper by KÜHNERT. The periphery of the computer consists of 3 exchangeable disk stores, 2 type writers, 2 papers tape punches, 2 paper tape readers, 2 serial printers, 1 parallel printer and 2 magnetic type stores.

The timing is carried out by an extern quartz crystal clock which triggers the analogue-to-digital converters and controls the real-time clock built-in the computer. The timing accuracy reached is 0.1 s. The sampling rate of seismographs is currently 20 samples/s. The existence of such a comprehensive hardware enables us to process the information of our main seismic station in a highly qualified manner. Additionally the data of two short-period seismographs installed at Jena and Posterstein are linked with the computer. The station Posterstein is quite near to the epicenter of the well-known earthquake of 1872. As the noise at Jena is rather high an seismograph of the Station Plauen will be linked with the computer very soon (Fig. 4). In this way we will have at hand a little but very effective network around Moxa particularly suitable for localization earthquakes in the Vogtland and surrounding areas.

The on-line data acquisition and processing is controlled by the operating system which has been provided by the manufacturer of the computer. The software for data acquisition and storage containing subroutines for read-in, starting real-time operation and application programes had to be designed by ourselves.

After commissioning of the computer we began to realize the first step of automatic data processing at the observatory Moxa - Jena. BURGHARDT and NEUNHÖFER will deal with in their papers the first results of real-time as well as off-line processing procedures applied especially to the detection and identification of seismic events and determination of other parameters. New possibilities, therefore, are now opened up in carrying out seismological investigations, which will be the main task of the computer at our observatory Jena - Moxa.

5. Recent instrumental developments at CIPE

The development of seismometers has a long tradition at CIPE. Besides the short- and long-period instruments of type SSJ-I and SSJ-II more recently a broad-band triaxial seismograph with inclined components has been developed by UNTERREITMEIER and TEUPSER. This seismograph named EDS 1 has a natural free period of the pendulum of 5 s to 15 s. It has a capacity transducer, which is able to detect mass displacements from 10 nm to 1 mm. A frequency modulated signal is formed on the basis of a carrier in the telephone band (300 Hz - 3,300 Hz). Feedback loops can be used as one possibility to reduce the influence of temperature variations and drifts for periods larger than 1000 s. The instrument is equipped with motor drives for the correction of period and zero-position.

At CIPE also a portable seismic recorder (DKR-1) has been developed. The recorder DKR-1 is designed to work under field conditions. There are 4 channels, mostly used for registration of 3 seismic traces and time information. The information will be stored in digital form on magnetic tape cassettes with a sampling rate of 70 Hz. The DKR-1 is equipped with an event detector, buffer, a control unit and a programmable

DOI: https://doi.org/10.2312/zipe.1983.078

switching mechanism. Time information is taken from a radio receiver built-in. The stored information can be played back by a special unit in analogue or digital form.

The digital output is realized on standard magnetic tape, the analogue one on paper tape. By means of a standard interface it is also possible to have a direct computer input. The recorder DKR-1 is useable for different purposes:

- explosion seismology
- temporary seismotectonic networks for studying local seismicity and aftershocks
- investigation of local noise conditions etc.

Fig. 8 shows an aftershock registration by DKR-1 of the Monte-Negro-Earthquake, April 15, 1979. A special expedition of the CIPE was carried out to study the aftershocks of this earthquake. The results have been published in detail in the expedition report by G. HURTIG and NEUNHÖFER.

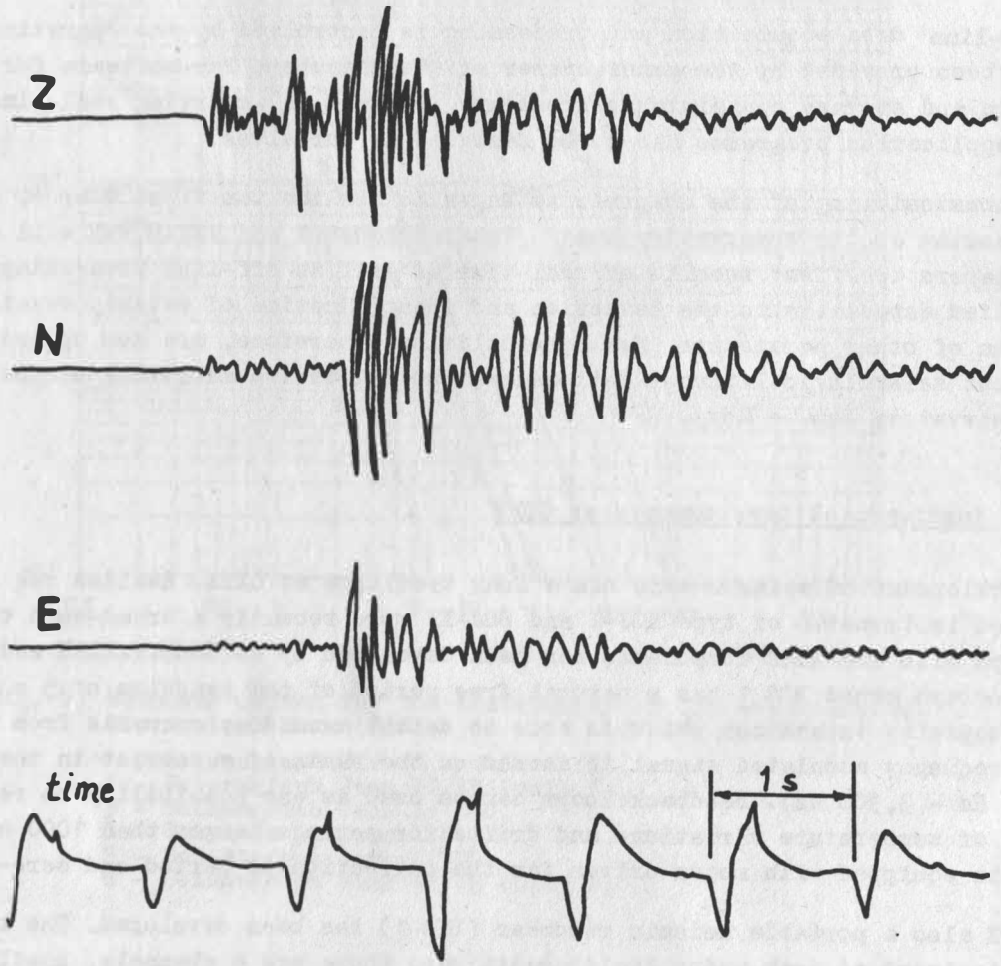

Fig. 8. Record of an aftershock (2.6.1979; 23:17 GMT) of the Monte-Negro-Earthquake, April 15, 1979 by the DKR-1 (recording station: Petrovac)

DOI: https://doi.org/10.2312/zipe.1983.078

6. Conclusions

1. The experience of operating the CIPE network over some years showes clearly the efficiency for monitoring global, regional, and local seismicity. Having all seismic traces on one record the determination of onset time is easily to manage localization with the P-arrival time at several stations and/or the P-S time differences is possible and easily to manage.
2. Digital recording of seismic signals of the stations of the CIPE network enables to investigate regional and local events in more detail. To solve these problems in real time a PRS 4000 computer was installed at Jena. The seismic signals of MOX and local stations are linked to the computer.
3. The development of seismometers and seismic recording equipment is continued at CIPE. In recent years the electronic broad-band seismograph EDS 1 and the portable seismic recorder DKR-1 have been developed. This new equipment enables to improve the quality of seismological data acquisition at the seismological observatories and during seismic field experiments.

7. References

BURGHARDT, P.T. — Real-time detection of seismic signals. (1983), this volume

GRÄSSL, S.; GROSSER, H.; KUHNT, W. — Spectral processing of local seismic events. (1983), this volume

GRÜNTHAL, G. — Zur Seismizität des Territoriums der DDR. Gerl. Beitr. Geophys. 90 (1981), 202-211

HURTIG, E.; NEUNHÖFER, H. — Seismologische Expedition des ZIPE der AdW der DDR in das Herdgebiet des Erdbebens vom 15. April 1979 in Montenegro (SFR Jugoslavien), Potsdam (1980)

HURTIG, E., et al. — Das seismologische Stationsnetz der DDR. Gerl. Beitr. Geophys. 89 (1980), 205-209

KLINGE, K.D. — Acquisition and storage of digital seismic data at the seismological observatory Moxa/Jena. (1983), this volume

KÜHNERT, S. — Experience with a remote seismic data transmission and interface system. (1983), this volume

NEUNHÖFER, H. — Identification of seismic events by computer. (1983), this volume

TEUPSER, CH. — High sensitive electromagnetic seismographs with extinct galvanometer reaction and sensitivity control. PAGEOPH 73 (1969), 120-128

TEUPSER, CH. — The seismological station Moxa. Veröff. d. Zentralinst. f. Physik der Erde 31 (1975), 577-584

TEUPSER, CH. — Instrumentation and calibration of the digital processing system Moxa - Jena (1983), this volume

TEUPSER, CH.; HURTIG, E. — The seismological data acquisition system in the GDR. Proc. of the 17th Assembly of the ESC Budapest, (1980),191-194

DOI: https://doi.org/10.2312/zipe.1983.078

TEUPSER, CH.;
KLINGE, K.-D.
Die seismologische Datenerfassungsanlage Moxa - Jena.
Gerl. Beitr. Geophys. 90 (1981) 6, 507-513

UNTERREITMEIER, E.;
TEUPSER, CH.;
BUDER, H.
Der elektronische Seismograph EDS 1.
Gerl. Beitr. Geophys. 87 (1978) 6, 441-454

Acquisition, Storage, and Processing of Seismic Data with the CIPE Network

by

J. BRIBACH, W. STRAUCH and H. GÜNZEL [1)]

Summary

The frequency-modulated signals of short-period vertical seismometers from 6 stations are transmitted to the recording and processing centre in Potsdam. The central recording unit digitizes (84 dB, 20 sps), buffers, and stores the data on audiocassette as well as computer compatible tapes using event triggering techniques. While the audiocassette tape recorder is used for immediate replay at suitably selected amplification levels and for analogue filtering the computer compatible tapes are stored for later digital off-line processing. Exact timing is guaranteed by time signals from the time service department of CIPE. High magnification (200 k) direct paper recordings at normal (60 mms^{-1}) and higher speeds are used for the first evaluation of seismic data (phase identification, localization, magnitude estimation). The digital data are processed off-line by a desk computer or for more sophisticated calculations by a large EC 1040 computer. False alarm records are erased by operator control. The data are formated and descriptive informations such as origin time, epicentre co-ordinates, distortion of channels are added. A software package is available for standard processing in routine and further research work.

1. Development

Up to 1977 the main seismological observatories of the GDR, Berggießhübel (BRG), Collm (CLL) and Moxa (MOX), managed their data exchange (reports of evaluations) by teletype or by sending photographic records on request to scientists in the GDR or for international exchange. The well known Potsdam station lost its sensitivity due to increasing industrial noise and could not keep up with the stations in southern GDR founded on solid rock far away from big cities or industrial centres.

Starting in 1978 Potsdam has got a new importance as the recording and evaluation centre of the GDR seismological network controlled by the Central Institute of Physics of the Earth (CIPE). In spring 1978 telephone lines from CLL, BRG, and MOX has been switched to Potsdam. These lines allow a frequency modulated transmission in the range from 300 to 3400 Hz.

1) Central Institute for Physics of the Earth of the Academy of Sciences of the GDR
DDR-1500 Potsdam, Telegrafenberg

DOI: https://doi.org/10.2312/zipe.1983.078

At first every line was tested for one or two months by transmitting the signal of a high quality frequency generator. Considering the transmission of one signal only the test gaves a dynamic range between 80 and 90 dB per line. But the test also showed the necessity of switch out detection.

2. The CIPE network

Currently the signals of six seismic stations are transmitted to Potsdam. The measuring points are situated in the south and the southwest of the GDR (s. BORMANN et al., this volume Fig. 4).

2.1. Equipment of the stations

At every station operates a short-period vertical seismometer VSJ-II with a standardized response characteristic proportional to ground displacement within the range from 0.2 to 1.6 s. The filtered signals are frequency modulated by a voltage-frequency converter working after the voltage integrating principle. The level of conversion depends on the noise of the used telephone line. Generally this level is chosen so that the demodulated signal of 1 nm is about 5 times higher than the transmission noise.

2.2. Potsdam centre

In Potsdam recording unit the received carrier is first checked for failures. Short pulses within the carrier generate trigger stop for 5 s to minimize false alarms. An failure longer than 5 s switches off the demodulating unit to avoid damage of the direct recording devise. The demodulated signal is split up for several functions as direct recording, buffered direct recording, and digital recording.

The demodulated signals of the outside stations are side-by-side registered on a six channel direct writing oscillograph. The magnification (flat of the response curve) of the ground motion is 200,000. Another device records the signals of Potsdam station itself with its short- and long-period seismometers (Fig. 1).

If the seismic signal of one station exceeds 50 nm (for periods less than 1 s) a trigger pulse is set. To avoid false triggering the used analogue criteria demands the arrival of positive and negative exceeding within a time window from 0.05 to 0.5 s. Outside of this window a failure is detected switching-off the equivalent channel of the direct recorder. A correct trigger pulse starts buffered digital and additional direct recording for about four minutes. If one more station triggers within one minute, the registration runs until it is stopped by an operator. In this way registrations of different length are produced for weak and for strong events.

After passing a 5 Hz low-pass filter the six demodulated signals of the outside stations and the short-period Potsdam signal are multiplexed and digitized with a sampling rate of 20 Hz. The digital word consists of 14 bit mantissa, 1 bit sign and of 1 bit time code signal. This gives a dynamic range of 84 dB or 12 μm in steps of 0.73 nm. The digitized signal is delayed by a hardware memory for one minute to get weak first onsets, too.

DOI: https://doi.org/10.2312/zipe.1983.078

After triggering the digital information is stored by an audio cassette recorder. This record is used as backup and for quick analogue direct recording on several levels and speeds especially if the continuous direct record is off-scale. Also simple analogue filtering of the output of the cassette recorder can be used. Triggering also starts a byte-serial recording on half inch computer tape using the bytewise mode of an incremental working computer tape recorder. At last the buffered digital signal is converted back in its analogue form and registered by faster recording speed if triggering occures. This recorder can also work as replay unit in connection with the audio cassette recorder.

3. Data storage and processing

The collected data are off-line processed on a ROBOTRON EC 1040 computer with disk and tape units, printers, a plotter, and a terminal communication system.

False alarm records or records which are wrong due to irregularities of the recording unit have to be deleted. Then time information is decoded to estimate the start time of the record. This start time and other informations describing the record (source parameters as preliminary determined by the CIPE net; parameters necessary for the data processing) are put together as head information block.

The digital records of every event are stored as one dataset on magnetic tape. The head information blocks are also stored separately to have a catalogue which contains the basic informations about all events stored in digital form. The data format for the head and the digital records is described by KLINGE and GÜNZEL (1983). As soon as more complete or better data about the seismic events are available the head informations can be changed in a simple way.

Search routines are available to select records which are interesting for users from several points of view. For the scientific work the software package of the EC 1040 with a lot of standard routines as well as specially developed programs are used. The programs can run in batch processing or interactive at the terminal using the time sharing option (TSO) of the computer.

4. Routine processing of the seismic records

The basic material for the daily processing of the seismic records are the visible records. The evaluation is concentrated on the localization of local and regional seismic events. The arrival times of the first and if possible of secondary P and S waves are measured and put in the desk computer to find the best solution for the focus in an interactive process. For local and regional events a search routine combined with a damped Geiger-algorithm is used to guarantee high stability of the solutions. The depth is fixed to zero. Due to the weakness of the most events and the low density of the station network often only the minimum number of 3 stations has recorded an event. Therefore, the experience of the operator plays an important role to get reliable results.

Teleseismic events are also localized to get fast preliminary informations about the global seismic activity. The localization program for this case is mainly based on

DOI: https://doi.org/10.2312/zipe.1983.078

THE GDR SEISMOLOGICAL STATION NETWORK

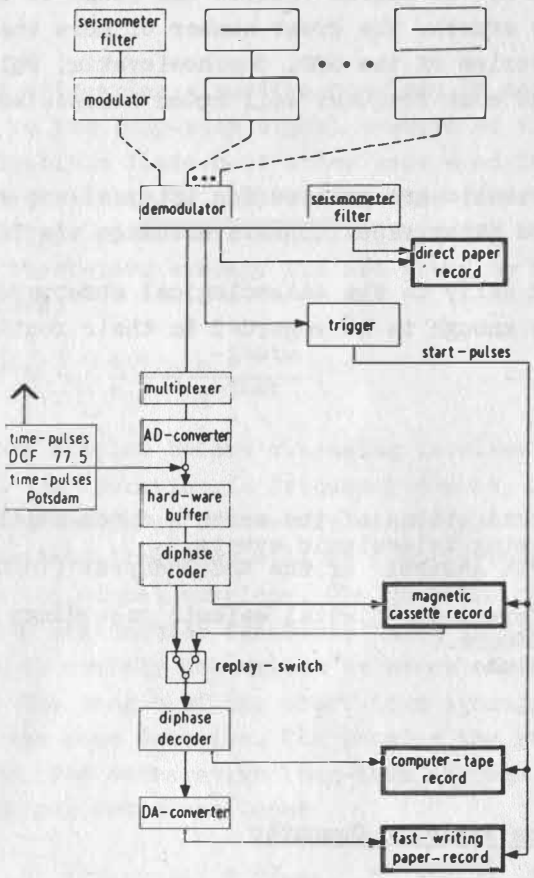

OBSERVATORIES
SP-vertical signal, 0.2 .....1.6 sec flat

TELEPHONE LINES
FM-signal 300..... 3400 Hz
dynamic range 80....90 dB

CENTRAL REGISTERING STATION POTSDAM

paper-record
6 channels side-by-side, 60 mm/min

trigger
amplitude-test, displacement ≥ 50 nm

analog-to-digital-converter
14 bits dual plus sign, 16th bit for time pulses

buffer
parallel delay of 60 sec

cassette recorder
digital serial information,
2500 bit per sec

computer-tape recorder
800 bpi-computer-tape postprocessing
by a R 40-computer

fast-writing paper-record
switchable 2.5 or 5 mm/sec

Fig. 1. Configuration of the processing centre Potsdam

DOI: https://doi.org/10.2312/zipe.1983.078

the estimation of azimuth and slowness of P or PKP waves recorded by the network. Azimuth and distance (from the slowness) give the epicentre co-ordinates with satisfactory accuracy for preliminary purposes. Systematical deviations were investigated by BORMANN and WYLEGALLA (1980) and can be considered to refine the results. Secondary onsets as PP, S or the different core phases are used if available to get a higher distance accuracy.

The weak natural seismicity at the GDR territory is unfortunately strongly hided by an increasing number of artificial events as quarry blasts or mining explosions. Recently about 10 to 20 of such events are recorded mostly on daytime. Localization and the comparison of the seismograms with a set of master records was found to be the only practicable method to identify these events. The great number of more than 100 possible artificial sources at the territories of the GDR, Czechoslovakia, Poland and FRG makes this way useful only for the most frequent well known sources and the problem is not yet completely solved.

The interpretations and localization results are printed for internal use and the most important informations are punched on paper tape for data exchange via Telex.

The preliminary locations are reported daily to the seismological observatories in the GDR, Czechoslovakia and Poland, early enough to be regarded in their routine seismogram evaluations.

References

BORMANN, P.; WYLEGALLA, K.	Structural investigations of the earth's upper mantle by means of localizing teleseismic events. Proc. of the 17th Assembly of the ESC Budapest (1980)
KLINGE, K.-D.; GÜNZEL, H.	Standard tape format for digital seismic recordings with the CIPE station network. (1983), this volume

Seismic Data from Field to Computer

by

J. BRIBACH, A. SCHULZE, J. WOLTER [1)]

Summary

In the paper the mobile digital seismic recording system DKR-1 is demonstrated. The main parts of this system are discussed in detail. Additionally the possibilities of converting the recorded data into a computer compatible format are shown. To complete the survey several computer processed (i. e. filtered) seismic events recorded by means of the DKR-1 are considered.

1) Central Institute of Physics of the Earth of the Academy of Sciences of the GDR, DDR-1500 Potsdam, Telegrafenberg

DOI: https://doi.org/10.2312/zipe.1983.078

Real-Time Detection of Seismic Signals

by

P.T. BURGHARDT [1)]

Summary

The real-time event detector in the Jena monitoring system is represented. Is properties are discussed in the frequency domain. The results and especially the efficiency of the automatic detection are summarized.

The event triggering algorithm consists of measuring the ratio of the short-term signal average to the long-term signal average of the absolute values. We prefer this simple detection algorithm instead of other ones used in microearthquake processing. Then, the variety of signals can be greater for this detection algorithm than for those only applied on a special type of seismic signals (STEWART, 1977; ALLEN, 1978). The frequency properties of the short-term average STA are given by the known transfer function (m number of averaged values)

$$(1) \quad H(e^{j\omega\Delta t}) = \frac{1}{m}\,\frac{1 - e^{-j\omega\Delta t m}}{1 - e^{-j\omega\Delta t}} .$$

Rectifying the samples before averaging involves a nonlinear filter operation. In order to interpret the operation in frequency domain, a truncated sine wave is considered. Its spectrum is concentrated in the vicinity of $\omega = \omega_0$, the frequency of sine wave. After rectification this frequency will be roughly doubled. The short-term average approximately follows the signal envelope. The envelope of a rectified high-frequency sine train approaches the rectangular function, which is the transfer function of the averager. The envelope is exactly determined by means of the HILBERT transform of the signal in time domain. The length of the short-term average filter is matched to a rectangular function of the same duration. The shorter the rectangular signal the greater must be its amplitude. The comparative long-term average LTA is a recursion filter with the short-term filter output as input

$$(2) \quad v_{n\Delta t_2} = r v_{(n-1)\Delta t_2} + c y_{n\Delta t_2} = c(y_{n\Delta t_2} + r y_{(n-1)\Delta t_2} + \cdots + r^{n-1} y_{\Delta t_2}) ,$$

$$r + c = 1 .$$

$y_{n\Delta t_2}$ is the current short-term average output, $v_{(n-1)\Delta t_2}$ is the last recursive long-term average output. The transfer function of the recursion filter (2) is given by:

$$(3) \quad V(z) = \frac{c}{1 - rz^{-1}}\, Y(z) .$$

It is not necessary to compute the ratio in intervals of data sampling rate $\Delta t = 0.05$ s. As the amplitude of the transfer function of the short-term averager is zero for $f = 1/T \cdot n$, $n = 1,2,\ldots$ (T is the length of average interval) the sampling rate for computing the long-term average will be T, too (Fig. 1).

---

1) Central Institute for Physics of the Earth of the Academy of Sciences of the GDR, DDR-69 Jena, Burgweg 11

DOI: https://doi.org/10.2312/zipe.1983.078

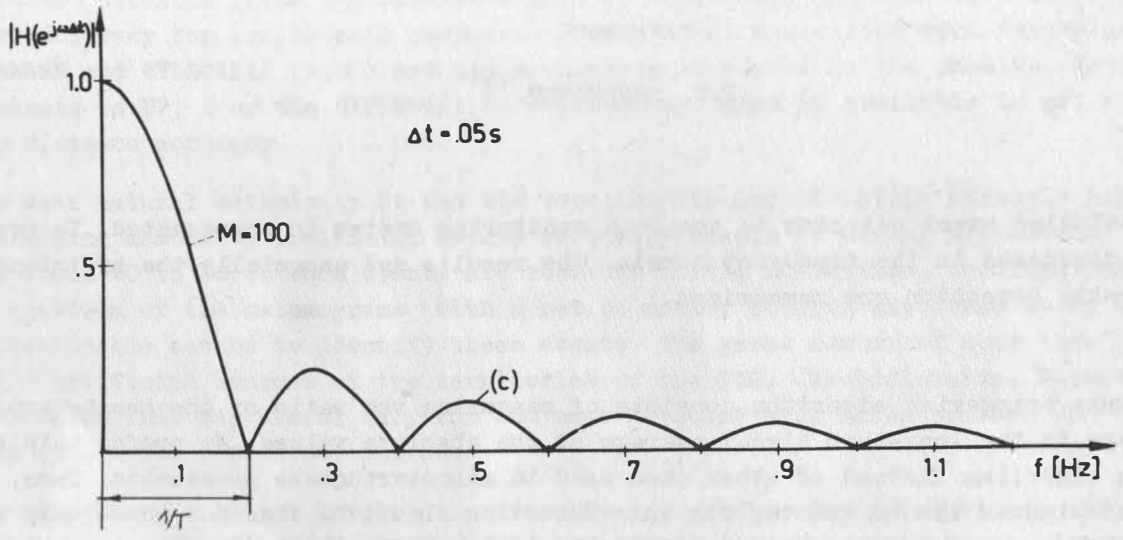

Fig. 1. Frequency response of the short-term average

The transfer function of (3) is a comb for $f = 2/T \cdot n$, $n = 0. \pm 1, \cdots$, but at these frequency points the short-term average has zeros and, therefore, the resulting transfer function of both averages shows no repetitions for $0 \leq f \leq 1/2\Delta t$. The long-term recursive average is for noise and during a long signal approximately constant and, hence, the frequency properties are determined by rectifying and the short-term average. We choose the summation window length of the short-term average as 5 s, the sampling-rate for the short-term average and the ratio is 1 s. The summation window length of the long-term average is 16 times the window length of the short-term average.

The detection threshold is the mean value plus a multiple of the standard deviation of independently determined quotients KRT = STA/LTA calculated from subsequent not overlapping time window . The variance of noise can be expressed by the variance of the quotient, if LTA is long enough compared with STA and the mean of STA is nearly constant for the length of LTA. The formula notation y and v is changed to STA, LTA in order to emphazise the measured quantity. The detector influences the very tail of the KRT distribution function. After the central limit theorem the density function approaches from a unsymmetrical one of the absolute values to a density function of the Gaussian shape. But as a test has shown that for the summation length of 100 data samples corresponding to 5 s the density function is not yet of Gaussian type. A possibility for determining the threshold is the computation of the likelihood ratio in the following optimum criteria:

$$(4) \quad l(KRT) = \frac{f(KRT/s)}{f(KRT/0)} > \frac{P_0}{P_1};$$

f(KRT/s), f(KRT/0) are the conditional probability density functions of KRT in the two cases of signal present or signal absent, respectively.

P_0, P_1 are the overall probabilities of the signal and noise event. The random variable KRT is declared as the maximum of the ratio measured by a multiple of the standard deviation. The inequality (4) involving the likelihood ratio minimizes the probability of error for the two cases: the signal may be missed though it is present or the

DOI: https://doi.org/10.2312/zipe.1983.078

noise may be mistaken for signal though the signal is not present (false alarm). Fig.2 shows an example.

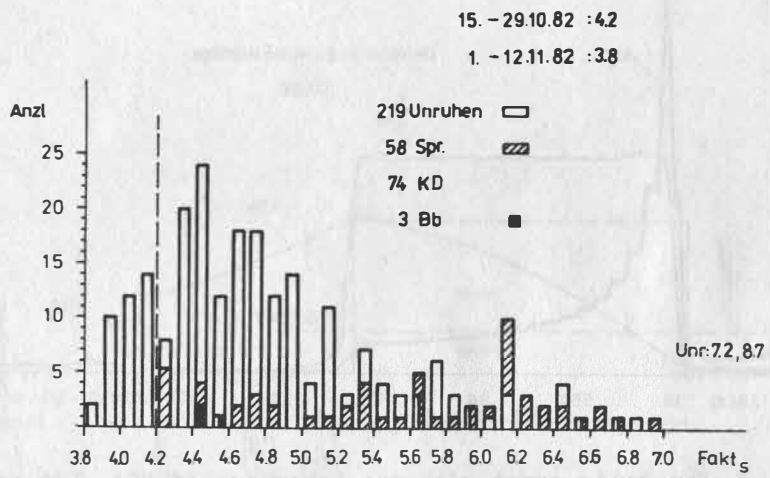

Fig. 2. Conditional probability density functions of the maximum KRT measured by multiples of standard deviation

The optimum criteria is fulfilled the first time for the threshold parameter $d_i = 5.6$ in Fig. 2. It is noteworthy that this threshold value is valid to some extent for a certain microseismic level. If the filter for noise suppression is changed d_i varies, too. In our application the threshold is set below the optimal one. That means the false alarm rate will be greater, but most signals will be detected. The detected event is identified by a program which compares the amplitudes and the periods of the noise and of the beginning of the event.

This identification reliably decides whether or not a signal is present. The standard deviation of the ratio KRT is computed for non overlapping time windows of 10 minutes. The quickly varying noise fluctuations of human and traffic disturbances are not compensated by the standard deviation of the ratio KRT. Slow fluctuations of the noise level cause an increase or decrease of threshold. With the long-term average LTA as recursive filter (2) one can approximate the dispersion of the ratio:

$$(5) \quad \sigma^2_{KRT} \approx \frac{\sigma^2_{STA}}{\overline{STA}^2} \left(\frac{1 - r}{1 + r} + 2r - 1\right), \qquad r = 15/16 .$$

The bar indicates averaging. The dispersion of KRT is approximately inverse to the so-called noise stability on the right-hand side of (5) (STEINERT et al., 1975).

A consequence of (5) is that the offset has to be removed because for a steadily increasing average the dispersion and, thus, the threshold will be very small. You noticed that we did not use the ratio for determining a threshold at all. The use of the short-term average is sufficient. The ratio is useful to define a definite beginning of the signal and to approximate subsequent onsets of the wavetrain.
The short-term average as an approximation of the envelope of the signal will be used to determine roughly its end. As the long-term average slowly decreases after an event, it has to be reset so that other following events may not overshadow the previous one. With a fixed long-term average the ratio is a scaled short-term average.

DOI: https://doi.org/10.2312/zipe.1983.078

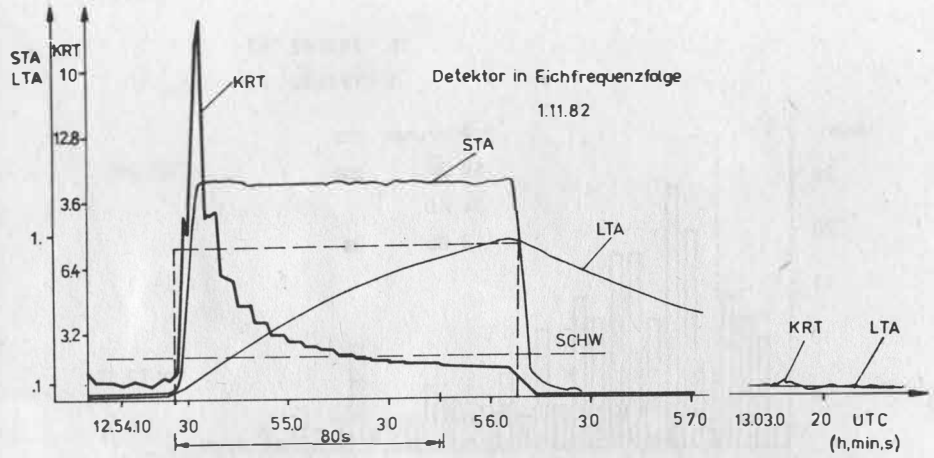

Fig. 3. Synthetic event with the behaviour of STA, LTA and KRT

Fig. 3 and Fig. 4 show an synthetic and real event with the computed short-term and long-term averages during the event. An event is considered to be finished, when within a time window of 20 s no STA trigger occured. The last trigger defines the end. For timing the onset we go back from the triggering time. When the difference of successive ratios STA/LTA falls below a threshold or changes the sign, the onset is declared (Fig. 5). When the event is not be masked by noise, an accuracy of better than $\pm$ 2 s is attainable.

The detector computes the following parameters: the maximum of the ratio, the number of triggers as compared with the duration of the event, the ratio of the beginning to the duration of the event, the threshold, the maximum KRT measured by standard deviation, and the LTA before event characterizing the noise level. For a certain duration of the event the signal will be automatically stored on disk. After the beginning of the signal the program for event identification is called and under fixed conditions the event is automatically stored on magnet tape. The detector provides the relation between the data segments and the event so that the human operator may find the data for further processing. The program system for detecting is divided in two segments of 3,5 K and 1 K of memory. Every segment needs about a few hundred ms for executing. The detector program operates with time cycle of 20 s.

References

ALLEN, R.V. — Automatic earthquake recognition and timing from single traces. Bull. Seis. Soc. Am. 68 (1978) 5, 1521-1532

STEINERT, O.; HUSEBYE, E.S.; GJOYSTDAL, H. — Noise variance fluctuations and earthquake detectability. J. Geophys. 41 (1975), 289-302

STEWART, S.W. — Real time detection and location of local seismic events in Central California. Bull. Seis. Soc. Am. 67 (1977), 443-452

DOI: https://doi.org/10.2312/zipe.1983.078

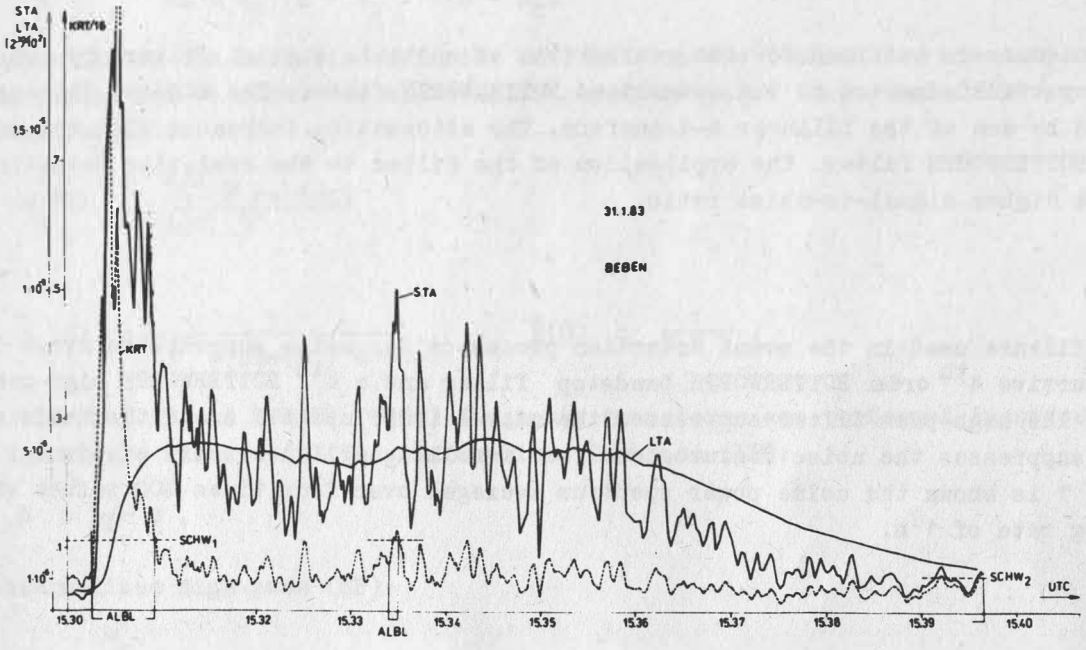

Fig. 4. Behaviour of STA, LTA and KRT within a real event

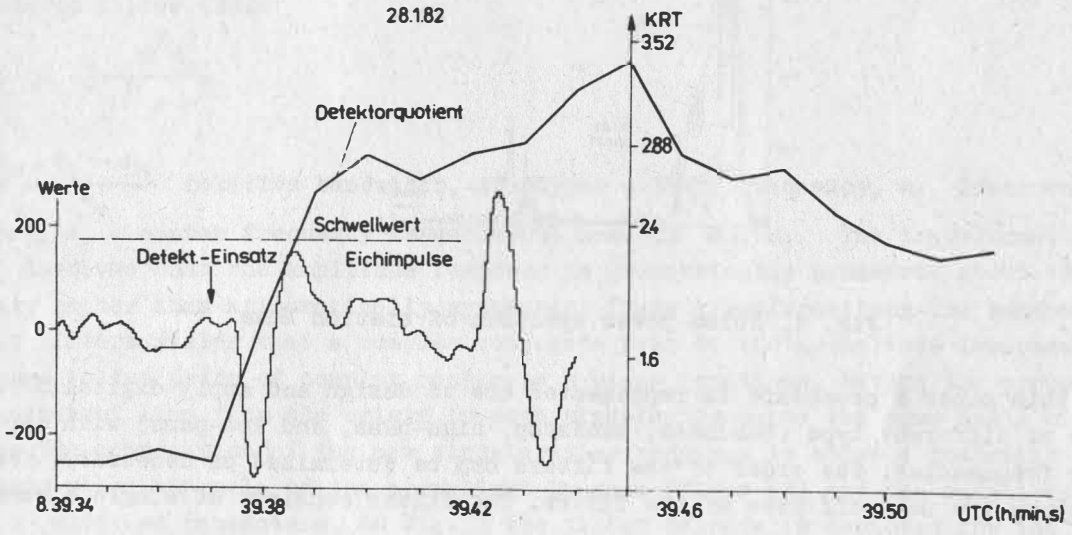

Fig. 5. Onset determination by detector

DOI: https://doi.org/10.2312/zipe.1983.078

Realization of Digital Filters

by

P. T. Burghardt [1)]

Summary

A procedure is outlined for the realization of suitable digital filters by applying frequency transformation to the normalized BUTTERWORTH filter. The digital filters are designed by use of the bilinear z-transform. The attenuation increases with the order of the BUTTERWORTH filter. The application of the filter to the real-time detection yields a higher signal-to-noise ratio.

The filters used in the event detection processor for noise suppression are a digital recursive 4^{th} order BUTTERWORTH bandstop filter and a 4^{th} BUTTERWORTH high-pass filter. The high-pass filter suppresses the microseismic up to 1 s and the bandstop filter suppresses the noise disturbances from a rolling mill near Moxa station.
In Fig. 1 is shown the noise power spectrum averaged over four times 400 values with a sampling rate of 1 s.

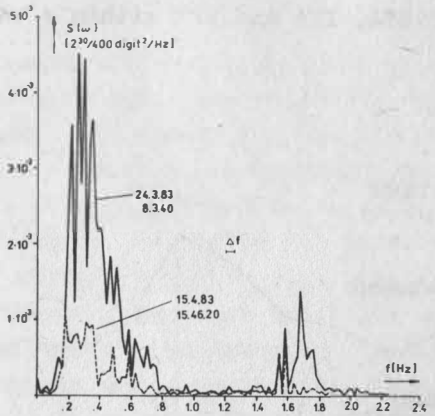

Fig. 1. Noise power spectrum of station Moxa

In this paper a procedure is represented how to design and apply digital BUTTERWORTH filter of different type (bandpass, bandstop, high-pass, and low-pass) with certain corner frequencies. The order of the filters can be determined of necessity. The order determines the roll-off rate of the filter. The filter consists of single elements

1) Central Institute for Physics of the Earth of the Academy of Sciences of the GDR, DDR-69 Jena, Burgweg 11

DOI: https://doi.org/10.2312/zipe.1983.078

which are connected to a filter cascade. The computation of the elements is simple and can be performed by a pocket or table computer. We begin with the normalized n-order low-pass BUTTERWORTH filter. This filter has its corner frequency for $\Omega = 1$. Its transfer function in the LAPLACE transform domain is

$$(1) \quad H_n(S) = \frac{1}{(S - S_1)(S - S_2)\ldots(S - S_n)} .$$

All poles lie on the unit circle in the left half on the S-plane and are complex conjugate pairs. Now we summarize the complex conjugate pairs that single filters with real coefficients arise

$$H_n(S) = \prod_{i=1}^{n/2} \tilde{H}_i(S)\hat{H}(S)$$

with

$$(2) \quad \tilde{H}_i(S) = \frac{1}{S^2 - 2\mathrm{Re}\{S_i\} + 1} , \qquad \hat{H}(S) = \frac{1}{S + 1} .$$

After BLINCHIKOFF and ZVEREV (1976) frequency transforms are performed in order to get from the single filters (2) the denormalized low-pass (LP):

$$(3) \quad S = \frac{1}{\omega_c} s ,$$

the denormalized high-pass (HP):

$$(4) \quad S = \frac{\omega_c}{s} ,$$

ω_c: cut-off frequency; the bandpass filter (BP):

$$(5) \quad S = \frac{1}{\gamma} \left(\frac{s^2 + \omega_o^2}{s^2 \omega_o}\right) ,$$

the bandstop filter (BS):

$$(6) \quad S = \frac{1}{\gamma} \frac{s^2 \omega_o^2}{s^2 + \omega_o^2}$$

with $\gamma = \frac{\omega_2 - \omega_1}{\omega_o}$ relative bandwidth, ω_2 upper cut-off frequency, ω_1 lower cut-off frequency, ω_o = center frequency is geometric mean of ω_2, ω_1. The transformation (5) and (6) involves that the amplitude response is geometrically symmetric about the center frequency rather than arithmetically symmetric. These transformations for bandpass and bandstop filters yields that a complex conjugate pair of the normalized low-pass filter transforms to two pairs of complex conjugate s-plane locations, having the property that a straight line from the origin to each singularity makes the same angle with the $j\omega$-axis. The computation of the new singularities requires to solve a quadratic equation, into which the pole of the normalized low-pass filter (2) and the relative bandwidth γ enter as parameters. In Fig. 2 the filter cascade is depicted for the order n. In order to use the filter for digital time series we have to transform the analog filters from the s-plane to the z-plane. There are a lot of design techniques. However, non-band-limited functions such as high-pass and bandstop functions may be transformed by use of the bilinear z-transform:

DOI: https://doi.org/10.2312/zipe.1983.078

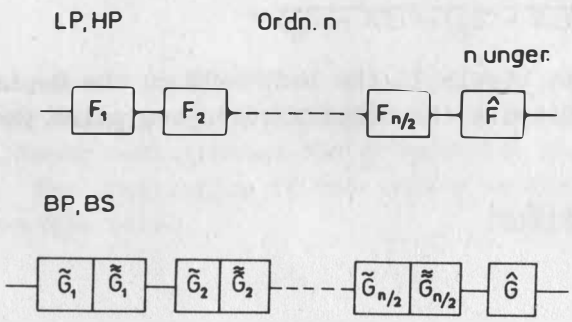

Fig. 2. Filter cascade of the order n

$$(7) \quad s = \frac{2}{\Delta t} \frac{1 - z^{-1}}{1 + z^{-1}}$$

Δt: sample rate. This transformation eliminates the foldover problem by mapping the left half of s-plane into the interior of the unit circle in the z-plane. However, this transformation contains the disadvantage of nonlinear warping of the frequency scale. For frequencies $f > \frac{1}{2} f_N$ (f_N NYQUIST frequency) this frequency warping may be intolerable. One can compensate the warping by prewarping the analog filter design to ensure the shifting back of critical frequencies by applying the transformation. After applying the frequency transform and the bilinear z-transform we obtain e. g. for a bandpass filter instead of (2)

$$(8) \quad G_{BP}(z) = \frac{d^2(1 - z^{-2})}{c_2 z^{-2} + c_1 z^{-1} + 1}$$

as one of the single digital filters. The parameters are determined by the analog bandpass filter ones and by the sampling rate. Besides the filter parameters we compute the filter response of the unit impulse serie 1,0,0,... . This procedure is equivalent to the polynom division of the rational function in z. The filter response represents the coefficients of the appropriate nonrecursive filter. The length of filter response determines that intervall after the filter transfer function is full effective. The higher the order n the longer the filter response.

A procedure for computing the amplitude response from the filter coefficients belongs to the simple programs in FORTRAN language for digital filter design. Out experience in filter application with the process-control type computer showed that for corner or center frequencies less than one tenth of f_N the coefficients of the recursive filter are different for the last digit.

Fig. 3 shows the filter response of a low-pass filter with a corner frequency of 1 Hz for f_N = 1,4,10,20 Hz. In such cases where one cannot meet all requirements of accuracy you can enlarge the increment of the sampling rate after antialiasing filtering by a high-pass.

DOI: https://doi.org/10.2312/zipe.1983.078

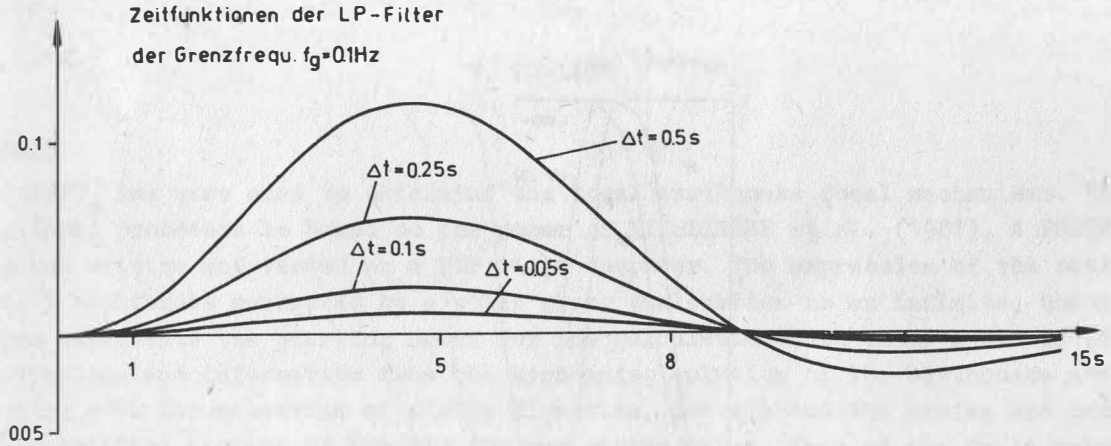

Fig. 3. Filter response of low-pass filter f_c = 0.1 Hz

We carry out the filtering with the process-control type computer PRS 4000 with douple precision word of 32 bit satisfying the necessary accuracy of recursion filtering. For filtering of one value with one single filter of the cascade the computer needs .5 ms, that means 1 % of sampling rate of Δt = 0.05 s. The program memory is not essentially enlarged by increasing the order of filter. All the elementary filters of the cascade are realized by the same subroutine.

The long-period part of the noise spectrum gives a lot of data amplitude fluctuation. The dispersion of the ratio STA/LTA is large. In order reduce the false alarm rate the threshold is set at a higher level. Subsequently, short impuls trains of burstings are neglected. If we suppressed the long-period range by a high-bass filter, the noise stability would be better and the false alarm rate would reduced. On the other hand the non stationary disturbances of rolling mills are set off on a large scale. We have to suppress widely the noise of the rolling mills. The center frequency of the higher noise spectrum can be delayed for a few hundredth cps. According to the level of the long-period range we use two high-pass filters with cut-off frequencies 0.67 Hz and 0.86 Hz, respectively. The bandstop filters are delayed from 1.25 - 2.22 Hz to 1.46 - 2.73 Hz (Fig. 4).

In Fig. 5 is depicted a small event. The detector can find it after filtering with the high-pass and bandstop filter pair, because the SNR is enlarged (Fig. 5). With a few exceptions the detector recognizes all events, which are discovered by a human operator. The prize payed is a great false alarm rate. After filtering the onset can be more exactly determined. After filtering we have a output delay of 1 s. Therefore, it is necessary to filter the output time series with same filters having a negative phase response. That means the inverse filtered time series have to be filtered once more.

References

BLINCHIKOFF, H.J.; ZVEREV, A.I. Filtering in the time and frequency domains. New York (1976)

DOI: https://doi.org/10.2312/zipe.1983.078

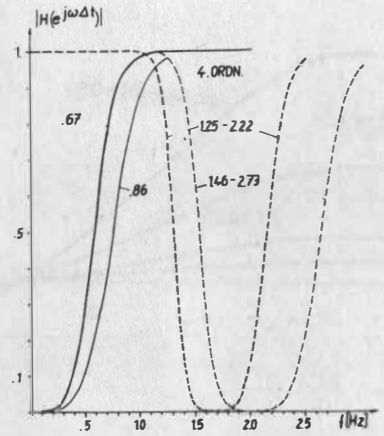

Fig. 4. Bandstop and high-pass for noise suppression

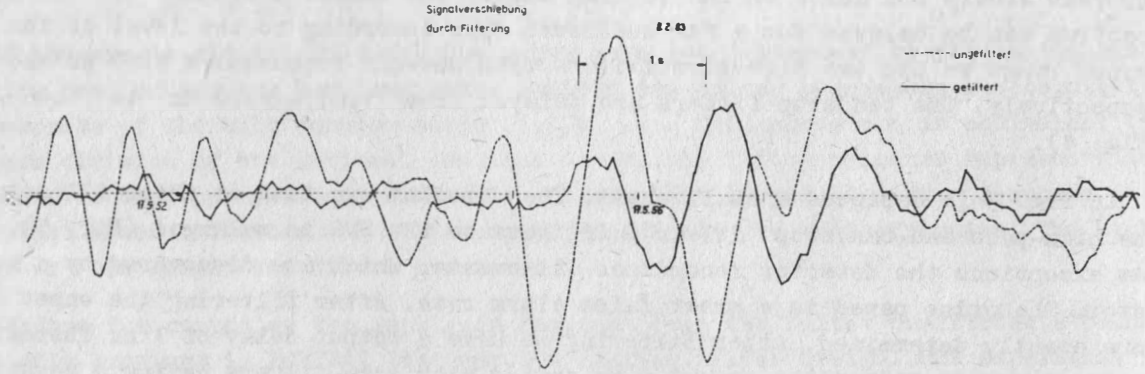

Fig. 5. The filtered event in relation to the unfiltered one

DOI: https://doi.org/10.2312/zipe.1983.078

Focal Mechanisms Inferred from Local SV to P Amplitude Ratios

by

V. BURLACU [1)]

Summary

$(SV/P)_z$ data were used to determine the local earthquake focal mechanisms. The computational procedure is based on the paper of KISSLINGER et al. (1981). A FORTRAN program was written and tested on a PDP 11/34 computer. The expression of the ratio of SV to P amplitudes generated by a point shear dislocation in an infinite, homogeneous medium represents the starting point for the calculations. As input a set of $(SV/P)_z$ observations and information from the hypocenter solution of the earthquake are used. Starting with the selection of a slip direction, the dip and the strike are determined by the smallest scatter of the dip for any strike value. Each of the fault parameters are then adjusted by an iterative least-squares adjustment.

1. Introduction

The knowledge of the focal mechanism for small normal and intermediate earthquakes using a local network with only a few seismic stations is essential for local and regional tectonic studies. The small number of stations implies the use besides the first motion signs of the P and S wave amplitude information.

The observed quantity is the ratio of maximum SV and P wave peak-to-peak amplitude $(SV/P)_z$ within the first three half-cycles recorded on the vertical component which is compared with the calculated ratio in order to obtain the focal mechanism. The ratio offers the advantage of being independent of the calibration and instrument response and also, for small epicentral distances, of the magnitude (KISSLINGER, 1980).

If the focal parameters are free to vary arbitrarily, the mechanism solution may be not well-constrained for a set of amplitude ratio data because of the strongly non-linear dependence of $(SV/P)_z$ with these parameters. Based on first-motion polarities and knowledge of the regional tectonics it is possible to impose some constraints on the starting solution.

2. Theoretical background

It was shown (LINDH et al., 1978) that, for a known velocity structure, the body wave amplitudes for a given azimuth and epicentral distance is determined by the focal mechanism of the earthquake. Starting from the dislocation theory (VVEDENSKAYA, 1956) the ratio of the far-field body wave amplitudes generated by a point shear dislocation in an elastic, infinit, and homogeneous medium can be computed. The co-ordinate systems x, y, z and $\bar{x}, \bar{y}, \bar{z}$ related to the fault plane (Fig. 1) are expressed:

---

1) Central Institute of Physics, Center of Earth Physics and Seismology, P.O. Box MG-2, Bucharest-Măgurele, Romania

DOI: https://doi.org/10.2312/zipe.1983.078

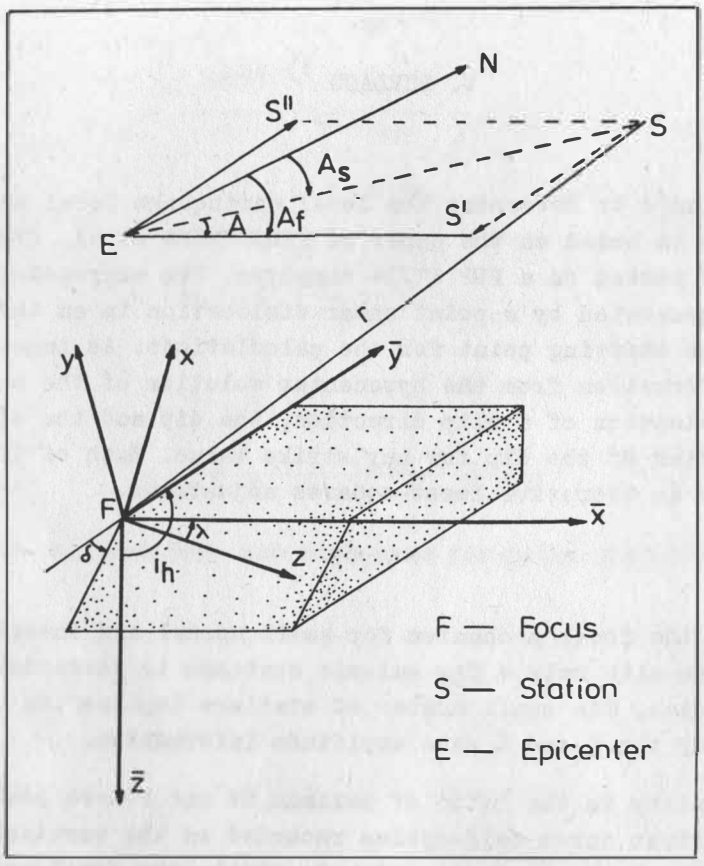

Fig. 1. The co-ordinate systems related to the fault plane

(1) $\bar{x} = r \sin i_h \cos A$, $\bar{y} = r \sin i_h$, $\bar{z} = r \cos i_h$,

$x = -\bar{x} \sin\lambda + \bar{y} \cos\delta \cos\lambda + \bar{z} \cos\lambda \sin\delta$, $y = -\bar{y} \sin\delta + \bar{z} \cos\delta$,

$z = \bar{x} \cos\lambda + \bar{y} \cos\delta \sin\lambda + \bar{z} \sin\lambda \sin\delta$.

The ratio of the body-wave amplitudes leaving the focus depends on the angles δ, λ and A (KISSLINGER, 1982):

(2) $(SV/P)_o = (V_P/V_S)^3 (1 - B/2D) \cot i_h$

where:

$B = (\cot\delta - \tan\delta) \sin\lambda \tan i_h \sin A + 2\sin\lambda + \csc\delta \cos\lambda \tan i_h \cos A$,

$D = \cos\lambda \cos A \sin i_h (-\sin i_h \sin A \sec\delta + \cos i_h \csc\delta)$

$+ \sin\lambda \sin i_h \cos i_h \sin A (\cot\delta - \tan\delta) + \sin\lambda (\cos^2 i_h - \sin^2 i_h \sin^2 A)$

with: δ = dip of the fault, λ = direction of slip measured in the fault plane from the strike, A = azimuth to the station measured from the fault strike, i_h = take-off angle of the ray to the station, V_P, V_S = P and S wave velocities.

DOI: https://doi.org/10.2312/zipe.1983.078

The $(SV/P)_o$ ratio must be propagate to the free surface. The $(SV/P)_z$ ratio is obtained by correcting $(SV/P)_o$ from the layered structure effect:

$$(3) \quad (SV/P)_z = (SV/P)_o \, W_{SV}/W_P$$

where W_{SV} and W_P are the transmission coefficients. For Poisson's ratio of 0.25 the W_{SV}/W_P correction is shown in Fig. 2. It can be seen that for incident angles up to 30° the correction is important and must be used. For incident angles between 30° and 37°, near the critical angle for SV to P conversion by reflection, the correction changes very rapidly so stations within this range should be excluded. For incident angles from 37° to 80° the correction is approximately 1 and can be neglect.

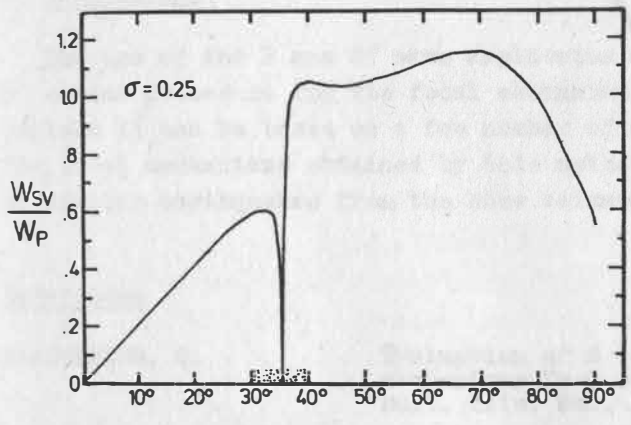

Fig. 2.
Factor to convert the ratio of the amplitudes of incident SV to incident P into the ratio of the amplitudes of the vertical components (after KISSLINGER et al., 1981)

3. Computation and results

For the practical computation a FORTRAN program was written and tested on a PDP 11/34 computer. The program use as input the hypocenter solution of an earthquake and a set of $(SV/P)_z$ ratios observed at N seismic stations. As velocity recordings were used, amplitudes were corrected. The displacement response curve is shown in Fig. 3.

Optionally the computational procedure can start in two ways. First, if there are enough independent information, a starting slip value can be used. Second, if the independent information are missing, the program chooses as starting slip values from 0° to 180° in small steps in order to identify all plausible starting solutions.

From the equation (2) it can be seen that for assumed slip and strike values there are, generally, two dip values which yield the observed amplitude ratios. The pairs of dip values differ from station to station but for good input data there are strike values for which there are closing dip values.

Using a set of strikes and based on the scattered dip values the program selects the strike for which the scatter of the mean dip is minimum. This strike, the corresponding mean dip, and the selected slip represent the starting solution to which an iterative least-squares adjustment is applied.

DOI: https://doi.org/10.2312/zipe.1983.078

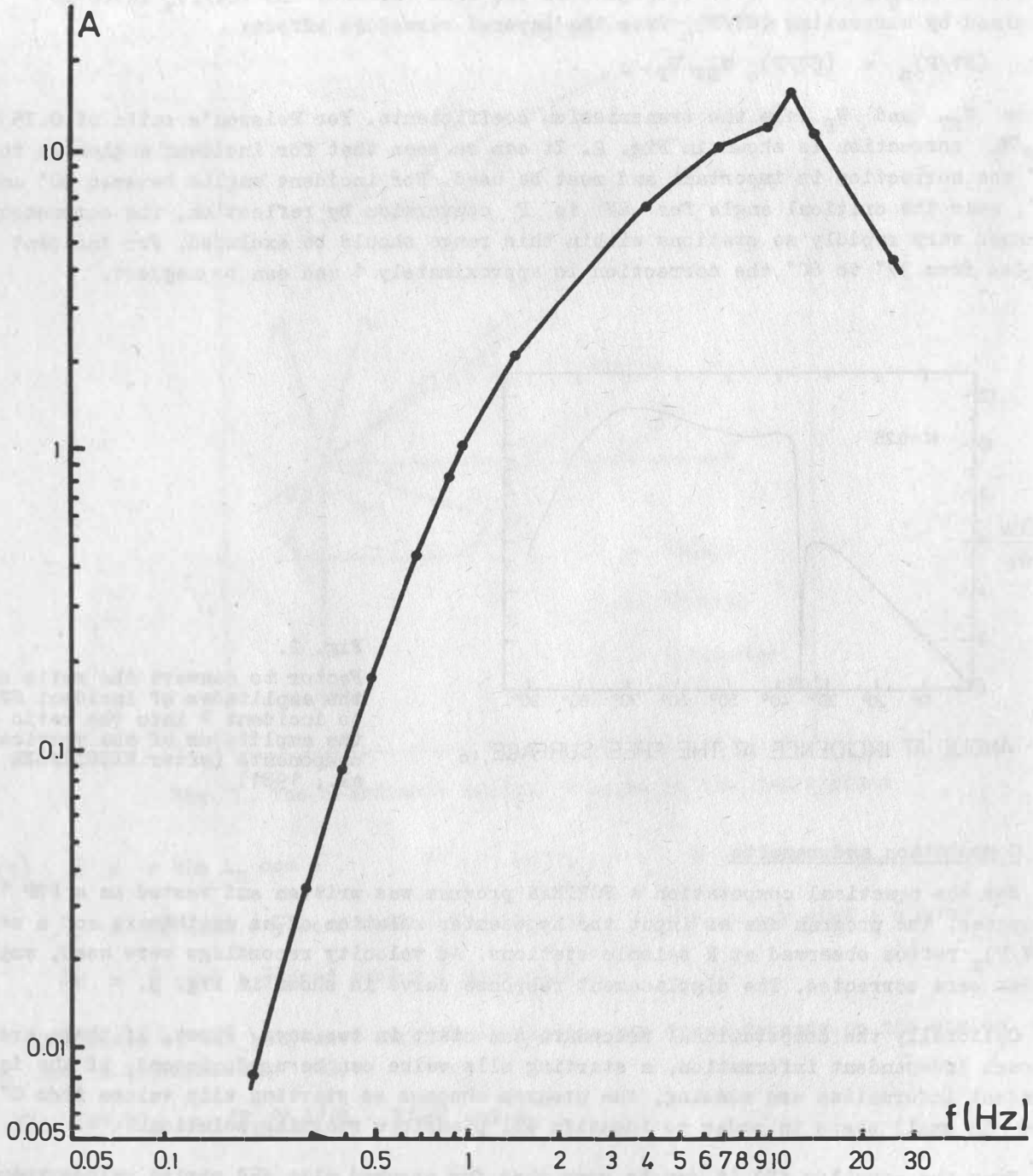

Fig. 3. Displacement response curve

The procedure was tested and then was applied to a set of 6 earthquakes. The computational procedure was used in the two ways with fixed starting slip direction and with varying slip direction. In Table 1 are listed the two conjugate planes for each earthquake only for the case of varying starting slip direction. The results are in good agreement with the known focal mechanisms of similar earthquakes from the same seismic zones.

DOI: https://doi.org/10.2312/zipe.1983.078

Table 1. Focal mechanism determinations

Date	M_S	h(km)	Plane 1 Dip	Plane 1 Slip	Plane 1 Strike	Plane 2 Dip	Plane 2 Slip	Plane 2 Strike
22.01.1982	1.3	86.9	24°	18°	12°	83°	113°	265°
24.02.1982	2.4	150.2	14°	126°	312°	79°	82°	95°
05.05.1982	2.6	150.4	35°	118°	163°	60°	72°	310°
24.05.1982	2.1	126.7	32°	128°	311°	65°	69°	88°
05.06.1982	1.6	1.5	88°	2°	80°	88°	178°	350°
19.06.1982	2.4	17.5	65°	10°	91°	81°	155°	357°

4. Conclusions

The use of the P and SV wave amplitudes recorded at local seismic stations provide a useful procedure for the focal mechanism determination. This procedure has the advantage it can be based on a few number of stations with good azimuthal distribution. The focal mechanisms obtained by this method are in good agreement with known results of similar earthquakes from the same seismic zones.

References

KISSLINGER, C. — Evaluation of S to P amplitude ratios for determining focal mechanisms from regional network observations. Bull. Seis. Soc. Am. 70 (1980), 999-1014

KISSLINGER, C.; BOWMAN, J.R.; KOCH, K. — Procedures for computing focal mechanisms from local $(SV/P)_z$ data. Bull. Seis. Soc. Am. 71 (1981), 1719-1729

KISSLINGER, C. — Errata. Bull. Seis. Soc. Am. 72 (1982), 344

LINDH, A.; FUIS, G.; MANTIS, C. — Seismic amplitude measurements suggest foreshocks have different focal mechanisms than aftershocks. Science 201 (1978)

VVEDENSKAYA, A.V. — Determination of the displacement field of earthquakes by the use of dislocation theory. Izvest. Acad. Nauk S.S.S.R., Ser. Geofiz. 3 (1956)

DOI: https://doi.org/10.2312/zipe.1983.078

Telemetric Equipment for Measuring the Seismic Waves Propagation Velocity

by

P. DANEV [1)]

It is well known that the velocity variations of the P and S seismic waves propagation can be used for an eventual earthquake prediction. The difficulty in determining these variations proceeds from the necessity to localize with a very great precision the epicentre of each earthquake used as well as to record a great number of earthquakes in the investigated regions. These difficulties are avoided if big industrial blasts are used. Their location is known with a great precision and the seismic waves arrivals generated by them in principle are well recorded by the seismic equipment at distances up to 100 - 120 km.

In the Geophysical Institute of the Bulgarian Academy of Sciences a special equipment has been developed for measuring the absolute time of big industrial blasts in a telemetric way. If the absolute time as well as the times of the different arrivals in the seismic stations are known, the velocity measurement is not hard.

The equipment consists of two parts - a portable equipment set and an equipment in the central seismic station. The portable set (Fig.1) is installed in the region of the blast approximately at 50 m distance. It contains a seismometer, VCO, low consumption

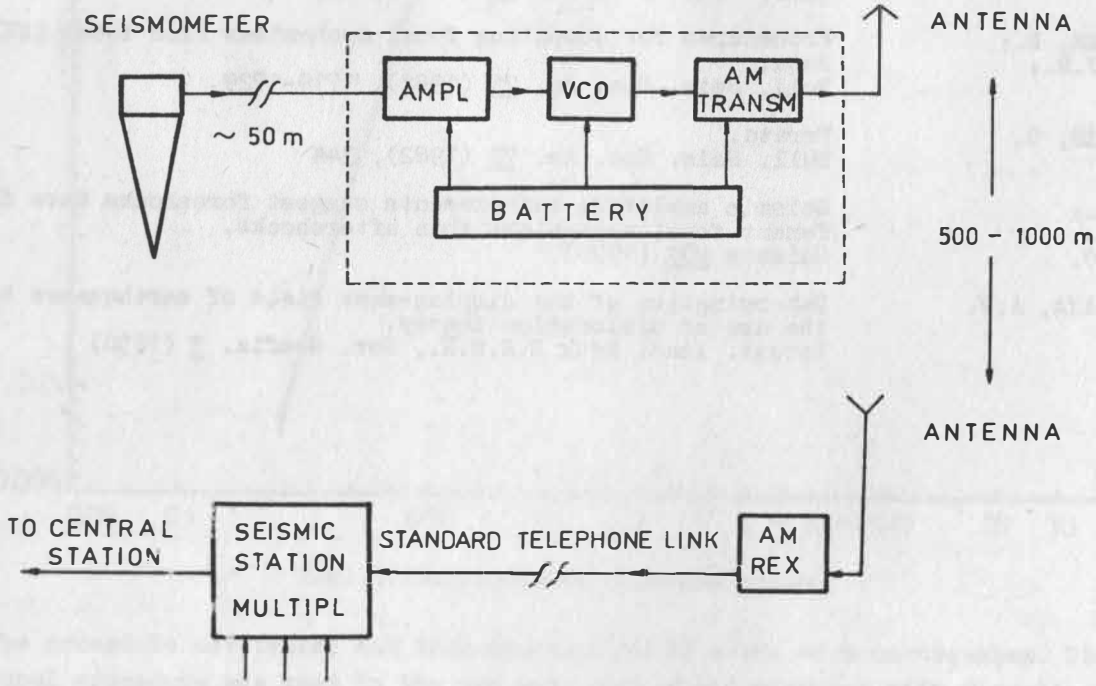

Fig. 1. Portable equipment

1) Institute of Geophysics. Acad. G. Bonchev Str., Bl. 13, 1113 Sofia, Bulgaria

DOI: https://doi.org/10.2312/zipe.1983.078

AM transmitter and battery supply. It is switched on about 30 min before the blast. At a distance of 1000 - 1500 m from the transmitter the receiver is installed, whose signal is transmitted by the ordinary telephone set to the nearest seismic station. Here the signal is multiplexed with the other signals of the seismic station and telemetrically reaches the central seismic station.

The equipment in the central station (Fig. 2) consists of a filter and a discriminator with a signal device which indicates that the portable set is switched on. The signal from the place of the blast can be recorded on a taperecorder and then reproduced as an analog seismogram with different velocity. Besides, the signal after the discriminator is digitized and is applied to five inputs of the computer event detector. The arriving signals from the whole telemetric system are simultaneously applied. The computer fixes the times of the different arrivals with a precision 0.01 s. Further on, the seismic waves propagation velocity is computed by a special routine.

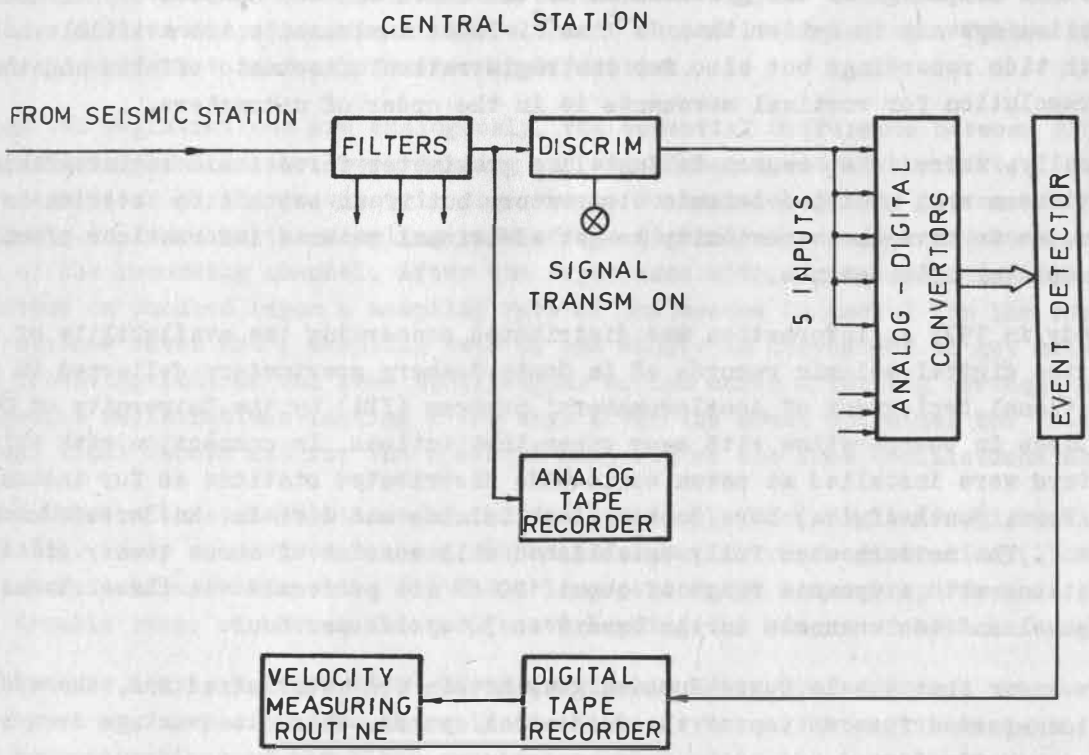

Fig. 2. Central station equipment

DOI: https://doi.org/10.2312/zipe.1983.078

Possibilities to Use Modern Earth Tide Gravimeters for Registrations of Seismic Effects and Related Phenomena

by

H.-J. DITTFELD [1)]

Summary

Modern earth tide gravimeters are also acting as seismographs of large dynamic range if the unfiltered electrical output is recorded. Especially the digital recording equipments of the earth tide stations are available for the registration of free oscillations of the earth and other phenomena. An example is given for the use of Askania gravimeters with registrations on special channels for the different purposes.

Tidal gravimeters are constructed for the continuous measurements of the variations of the vertical component of the gravitation of the earth and the sensitivity of modern tidal registration systems is better than 10^{-8} ms^{-2}. These instruments are available not only for earth tide recordings but also for the registration of seismic effects and the expected resolution for vertical movements is in the order of nanometers.

Naturally, there is no reason to install a gravimeter for seismic registrations if there exists a well equipped seismic observatory but if an earth tide station is erected anywhere, so we have the opportunity to get additional seismic informations practically without special seismographs.

Already in 1977 an information was distributed concerning the availability of the very long-period digital seismic records of La Coste-Romberg gravimeters collected in the 'International Deployment of Accelerometers' program (IDA) by the University of California at San Diego in co-operation with many other institutions. In connection with this project gravimeters were installed at seven world-wide distributed stations as for instance in the USA, in Peru, South Africa, Nova Scotia, Cook Islands and Garm in the Soviet Union (Tadshikistan). The network when fully established will consist of about twenty stations. Registrations with a dynamic range of about 120 dB are performed via three channels: The tide channel and two channels in the band 1 to 30 cycles per hour.

It is known that the La Coste-Romberg gravimeters are astatisized and, therefore, have a very long-period free motion of the mechanical system. This disadvantage does not exist for Askaniagravimeters.

In the gravimetric observatory Potsdam of the Central Institute for Physics of the Earth tidal registrations have been performed with this type since 1957. The Askania GS 11 and 12 type gravimeters originally have been equipped with differential photoelements and inner galvanometers needed for measurements under field conditions. The electrical output with a comparable low gain was connected in parallel to the inner galvanometer. As investigated by WIRTH (1965) this system was strong damped because of the qualities of the electric circuit and, therefore, usuable for tidal registrations only.

1) Central Institute for Physics of the Earth of the Academy of Sciences of the GDR, DDR-1500 Potsdam, Telegrafenberg

DOI: https://doi.org/10.2312/zipe.1983.078

After the development of electronic amplifiers of high quality the GS 11 and GS 12 type gravimeters have been used for tidal registrations with electric recorders and to get a higher gain the inner galvanometer was disconnected during registrations under the conditions in the observatory. Therefore, the inner damping was avoided and the electric output became usuable for seismic registrations, too.

The mechanical system of the gravimeter consists of springs bearing a mass of about one hundred gramms. It is not astatisized and its period amounts between one and one and a half second. After amplification it is possible to measure vertical movements of the mass in the order of 0.5 nm. So the gravimeter acts like a seismograph of very large dynamic range and the output may be splitted up by filtering via special channels for short-period seismic registrations, for measurements of the free oscillations of the earth and tidal registrations, respectively. - A description was given of an equipment consisting of gravimeter, amplifier, filters and recording units by DITTFELD (1979).

Nowadays the GS 11/GS 12 type gravimeters in their original form are no more sufficient for modern tidal measurements and the new types GS 15 and GS 25, respectively, are used for these purposes. But their mechanical system is nearly the same and all the suggestions concerning the use for seismic measurements may be accepted for the modern types, too. Additionally the gain of the electric output is higher by a factor of thousend and we do not need any further amplification.

Almost the registrations are analogously. The essential difference between tidal and seismic registrations is the lower damping and the higher speed of the latter. As the tidal registration at the gravimetric observatory Potsdam is already performed digitally we have only to increase the sampling rate of the digital measurement and to change the damping of the recording channel. After the experience with digital registrations of the GS 15 output on punched tapes a sampling rate of one second is useful for the registration of surface waves and a sampling rate of one minute is convenient to get material for the investigations of the free oscillations of the earth after big earthquakes. These special registrations lasting a few days after the event contained the data for the normal tidal record and for the spectral analysis of the free oscillations as well.

To demonstrate the possibilities of this equipment plots of digital registrations are shown in Fig. 1. By comparison between the seismic gravimetric registration (2) in Fig.2 and the records of a short-period (1) and a long-period (3) seismograph becomes apparent how the dynamic range of the gravimeter is overlapping the ranges of both seismographs.

As there are nearly hundred GS 11/GS 12 gravimeters distributed around the world and the new types are very expensive there is in the last years a strong trend in the direction to reconstructions of the older gravimeters that means the installation of a capacitive sensor instead of the old photoelectric transduces inside the gravimeter. Every reconstruction includes the possibility to get a separated seismic output. Reconstructions were performed by BONATZ/FRG (more than 30 gravimeters since 1973), by ROGATNEV/Moscow, by MENTES/Sopron and at the gravimetric observatory Potsdam. Especially the version elaborated at the Moscow Institute of Physics of the Earth may be of interest because except of the modernisation of the transducer the gravimeter is equipped with four channels of the electric output for different geophysical purposes. Therefore, the whole system is named capacitive seismogravimeter. Similar four channel registrating systems are developed in the same way also for strain meters and for the OSTROVSKY

DOI: https://doi.org/10.2312/zipe.1983.078

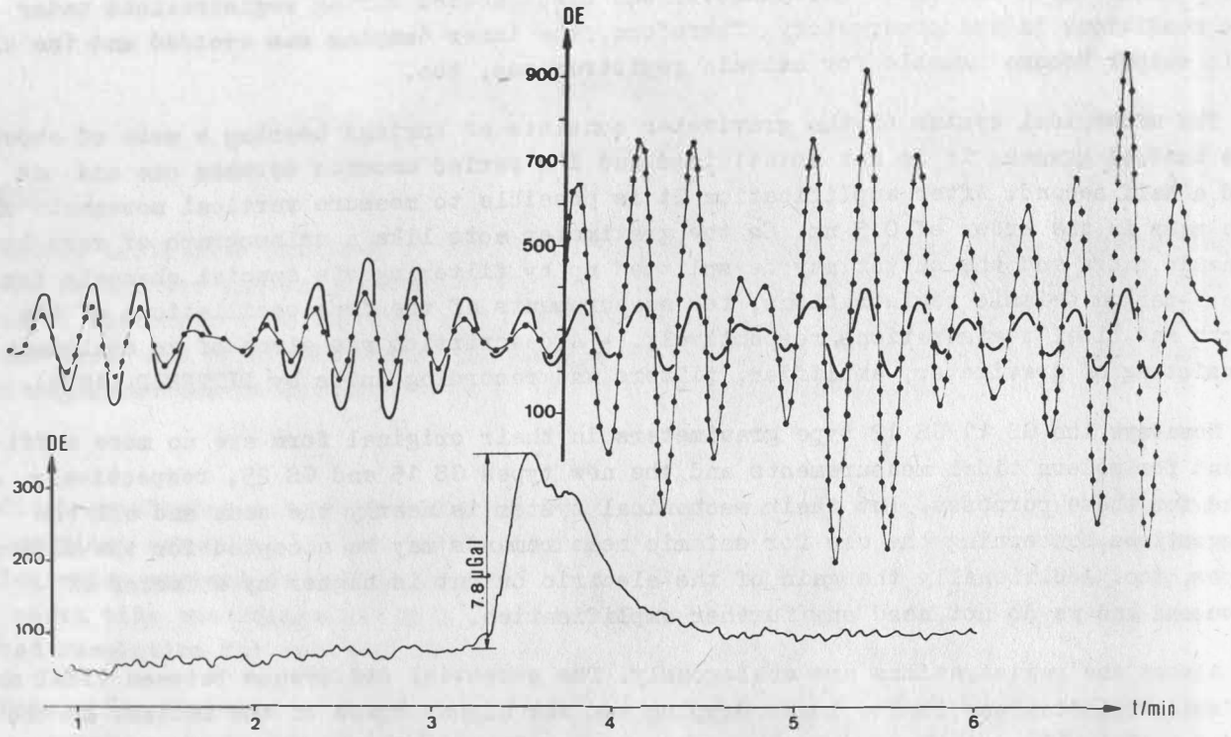

Fig. 1. Plots of digital registrations of Askania gravimeters
Upper curves: Surface waves after earthquake with different amplifications
Lower curve: Artificial event (passing of a lorry), DE - signal in digits

clinometers. The following properties of seismogravimeters on the base of Askania gravimeters may be mentioned:

- The parameters of the initial sensor are very stable because of the usual hermetisation and thermostatisation of the gravimeter. - Here we have to keep in mind that the seismic phenomena are only a noise for gravimetric measurements but on the other hand the tidal effect is a very small oscillation of the zero position for the seismic registrations.
- The maximum resolution of the mechanical system in connection with the capacitive transducer may be about 10^{-11} m.
- With different channels - for instance for periods from 10 to 100 s and 0.1 µm resolution as well as of 3 µm resolution between 10 and 1000 s, respectively, and also with a special channel for registrations of the free oscillations between 200 and 5000 s, respectively, with a sensitivity of 0.2 nm s^{-2} (ROGATNEV, 1982) - the seismogravimeter may be used as a complex geophysical measuring station without any other measuring devices.
- The sampling of the different outputs is very easy because the signals are amplified and the amplitudes are sufficient for the use of digital voltmeters and also for applications of different systems of data transmission.

DOI: https://doi.org/10.2312/zipe.1983.078

Supposing the reconstruction of older Askania gravimeters will be not in every case succesful because for instance the hermetisation, the thermostatisation or the compensations of air pressure and temperature effects will be not sufficient. Then, the gravimeter is not exact enough for tidal measurements. But it is in every case a seismograph of very large dynamic range and it may be used for measurements of non-tidal effects. Calibrations of the sensitivity against ground movements are possible by intercomparison with seismographs with known parameters or by the aid of a vibrating platform. The latter method was used by TOBYAS and DIVIS (1980) for a normal GS 12 gravimeter. They got a static magnification of the vertical ground motions of about 870 without amplifier and the inner galvanometer was connected. Disconnecting the galvanometer and passing over to the capacitive transducer one can expect magnifications of nearly a million with a maximum sensitivity for oscillations with a period of a few seconds.

Finally it shall be pointed out that we did not propose to replace gravimeters for seismographs but the existing instruments may be helpful in the network of the seismic stations and their multiple use is favourable for a further concentration of the observations which are needed for geophysical investigations.

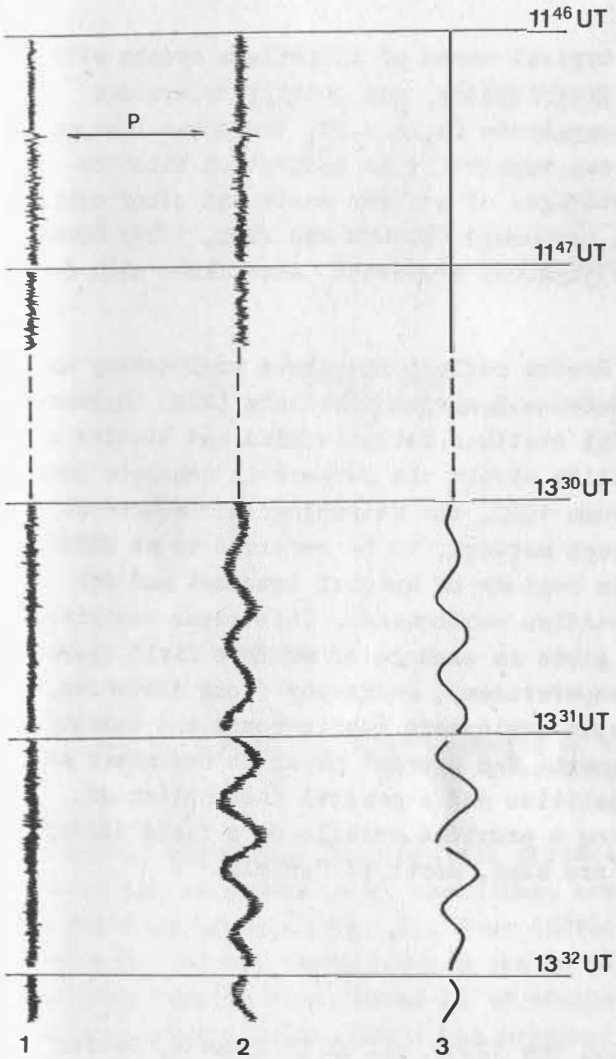

References

BONATZ, M.
Gezeitenregistrierungen mit einem auf kapazitiven Abgriff umgerüsteten Gravimeter GS12.
Mitt. Inst. Theor. Geod. Nr. 22, Bonn (1973)

DITTFELD, H.-J.
Ein Gezeitengravimeter als seismisches Instrument.
Gerl. Beitr. Geophys. 88 (1979) 3, 219

TOBYAS, V.; DIVIS, K.
Sensitivity of the GS12 gravimeter to vibrations.
Stud. geophys. et geod. 24 (1980), 333

VOLKOV, V.A.; JORDANOV, N.D.; ROGATNEV, I.I.
Predvaritelnije resultaty nabljudenii v Obninske jomkostnym seismogravimetrom.
CAPG, Subprojekt 14.3, Symposium über die Vervollkommnung von Gezeitenbeobachtungen mit Gravimetern, Potsdam (1982)

WIRTH, H.
Gekoppelte Systeme bei geophysikalischen Meßgeräten.
Arb. geod. Inst. Nr. 7 Potsdam (1965)

Fig. 2.

Comparison between an unfiltered gravimetric registration and seismograph records

1 - short-period seismograph
2 - gravimeter
3 - long-period seismograph

DOI: https://doi.org/10.2312/zipe.1983.078

The Uppsala Mobile Seismograph Network, MOSEN

by

T. van ECK and O. KULHÁNEK [1)]

Summary

Since summer 1982, a mobile seismograph station network is kept fully prepared at the Seismological Dept., Uppsala for rapid deployment in aftershock surveys. Currently, the field equipment consists of four hybrid seismograph stations for both analogue and digital recording which also can operate as eight independent stations. Preference has been given to products which facilitate quick field installation and large recording capacity. The complete instrumentation includes a microcomputer, situated in the department, for off-line interpretation and recution of data. Several examples of field experiments will be given.

1. Introduction

Earthquakes in the Baltic Shield represent typical cases of intraplate events with sporadic occurrence rather diffuse epicentral distribution and poorely understood tectonic origin. In spite of their rather low magnitude ($m_b \leq 4.5$), there has been an increasing interest in earthquakes from the area, especially in connection with construction of nuclear power plants, long-term storages of nuclear waste and other critical facilities. Several studies have also been performed (BUNGUM and FYEN, 1979; SLUNGA, 1981 and KULHÁNEK et al., 1983) to investigate physical processes associated with foci of earthquakes in the Baltic Shield.

Recent instrumentation investments made in Sweden reflect the above engineering and research interests. Since 1980, the National Defense Research Institute (FOA) in Stockholm operates a network consisting of 17 digital stations for detection and studies of microearthquakes in southern Sweden. Detectability within the network is complete down to approximately magnitude 1 events. Since autumn 1982, the Seismological Department, Uppsala University, operates a mobile seismograph network, to be referred to as MOSEN. The network is designed for detailed studies in regions of special interest and for surveys of microaftershocks to "major" Fennoscandian earthquakes. This paper describes the network, its capacity and limitations and gives an example of MOSEN's field operation. Logistical problems, the climate (low temperatures), geography (long distances, low population), large storage capacity and rapid deployment requirements and economy frame severely constrained the choice of equipment. The present paper is organized as follows. In section 2 and 3 we present technicalities and a general description of equipment, which meets our requirements. Section 4 provides details on a field survey carried out in 1982 around the Dannemora iron ore mine, north of Uppsala.

---

1) Seismological Department, Uppsala University, Box 12019, S-750 12 Uppsala, Sweden

DOI: https://doi.org/10.2312/zipe.1983.078

2. Field equipment

After thorough consideration, we have chosen a hybrid network with 5 analog and 4 digital recording stations (Fig. 1). Analog stations are used for visual inspection and direct field interpretation whereas for signal analysis, high-quality digital data are employed.

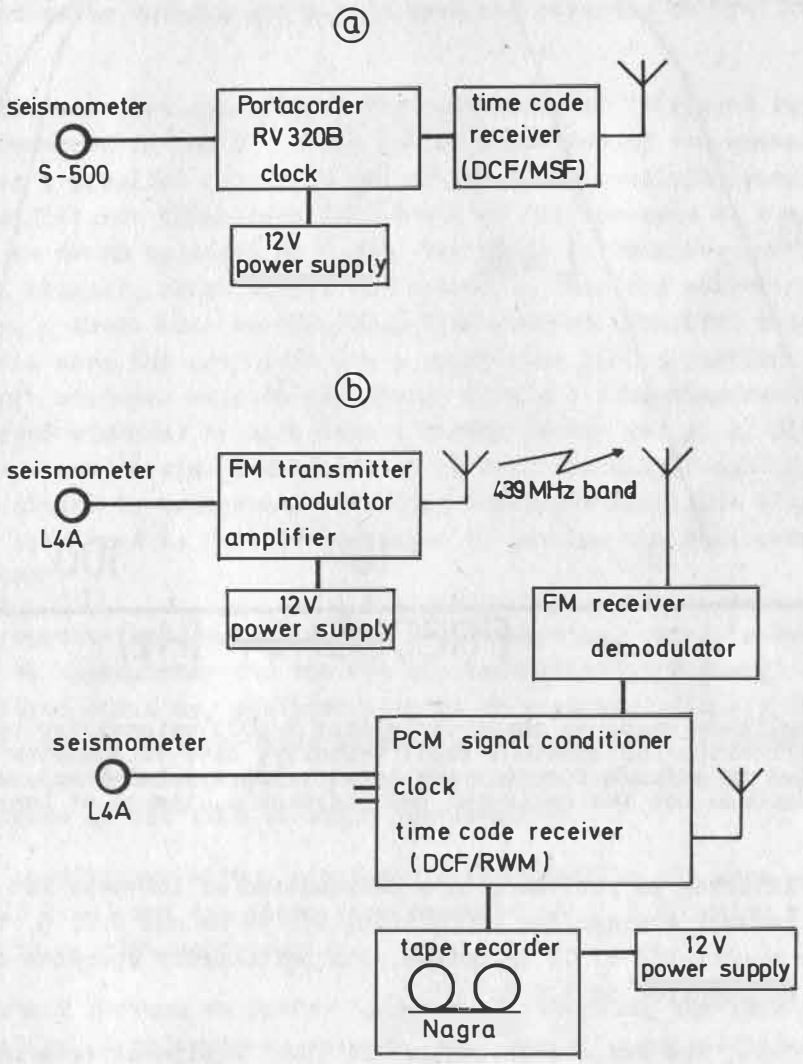

Fig. 1. Major elements of the field equipment:
a) analog recording set; b) digital recording set

Analog recorders, four Geotech portacorders RV 320 B and one RV 320, with alternatively ink or smoked paper recording, are equipped with 1 Hz, S-500 seismometers, coupled as velocity sensors (Fig. 2). Four different recording speeds (1, 2, 4, and 8 mm/s) are available and the amplification can be varied from 42 to 96 dB in 6 dB increments. The internal quartz clock proved to be stable in constant temperature environments. Nevertheless, we record an additional external time signal (DCF-77.5 kHz or MSF-60 kHz) either continuously or at the beginning and end of each record sheet when the paper is changed.

DOI: https://doi.org/10.2312/zipe.1983.078

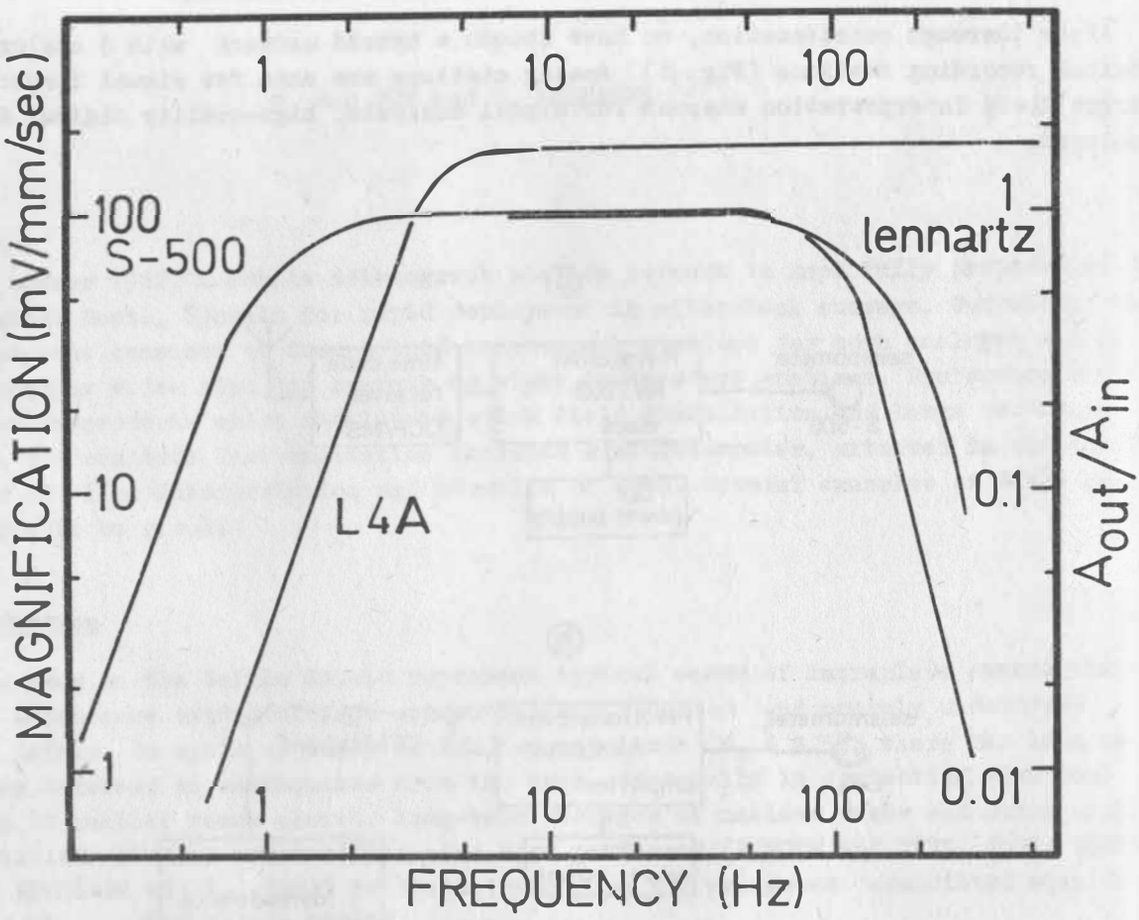

Fig. 2. Amplitude response characteristics: S-500) seismometer relative magnification for constant input velocity; LA4) seismometer magnification in mV/mm/s for constant input velocity; Lennartz) relative response for the recording and playback equipment of Lennartz

A band-pass filtering is performed by a combination of low-pass and high-pass filters with selectable cut-off frequencies of 5, 12.5, 25, 50 Hz and 0.2, 5, 10 Hz, respectively. Filters have a roll-off of 12 dB/octave. The portacorder operates on a 12 V battery and has a power consumption of 1.2 W.

Digital recorders, the Pulse Code Modulation (PCM) equipment from Lennartz, operate in low temperatures and offer a large tape-storage capacity, two of our decisive requirements with respect to above objectives. Operation in low temperatures, down to -35 °C, has been tested in northern Sweden. The storage capacity of a commonly used 2400 feet, 1/4" tape, is 19.2 Mbytes or 8.5 hours of recording time of 2 channels with 111 Hz sampling frequency. Digital recording is performed by means of 2 Hz Mark L4A seismometers, coupled to digital recorders. All our Mark L4A seismometers have been tested on a shaking table in the frequency range from 5-250 Hz and in general fulfill the specification provided by the manufacturer (Fig. 2). Analog voltage outputs of the L4A seismometers are recorded by high- and low-gain channels, differing by recommended 30 or 36 dB in magnification and digitized into 12 bit samples. In that way, we obtain

DOI: https://doi.org/10.2312/zipe.1983.078

a dynamic range of 102 or 108 dB which, due to the low internal amplifier noise, can be fully disposed. The system is equipped with antialiasing filters with adjustable cut-off frequencies of 20, 40, 80 and 160 Hz and with a roll-off of 36 dB/octave. They are of Bessel type and have linear phase characteristics. Digitizing rates are optional from 37 to 1333 Hz, depending upon the number of channels multiplexed (max 8 channels) and the tape recording speed (2.38, 4.75, 9.5 or 19 cm/s). The internal clock of the digital recorder makes advantage of automatic calibration, employing an external time signal (DCF-77.5 kHz or RWM-9.996/20.696 MHz). The internal and external times together with the amplified seismometer outputs are multiplexed and recorded on 1/4" tapes, using the Miller code.

The digital equipment provides options for continuous or triggered recording. The latter is often preferred in the field due to the reduction of the amount of data. The trigger operates on a parallel output of one of the eight available channels (selectable). This output may be filtered (high-pass 0.2, 5 and 10 Hz, low-pass 4, 8 and 16 Hz) and amplified (from 0 to 60 dB in steps of 6 dB). Two kinds of triggers are possible. Firstly, an amplitude-level trigger, which starts the recording when the selected level has been exceeded. Secondly, a Short-Time-Average/Long-Time-Average (STA/LTA) trigger, which starts the recording when the energy within a short-time record portion (STA defined for 0.5-, 1- or 2-second windows) exceeds the energy within a long-time record portion (LTA defined for 60-second windows) by more than a chosen factor (e. g. 2, 2.5 or 3). A delay memory provides a pre-event-time record of 1.6 to 26.2 seconds preceding the trigger instant. Once the system is triggered, recording continues until the STA/LTA ratio falls below the trigger level and is further prolonged by setting the post-event-time (optional from 5 to 80 seconds).

Three stations operate independently. The fourth station, which is furnished with amplifiers and an FM transmitter (in the 439 MHz band with 0.5 W power) is recorded by any of the other three stations, equipped with an FM receiver. Signals from two different stations, recorded on one tape, provide certain advantages when discriminating seismic onsets against man-made disturbances. On the other hand, telemetering restricts the location sites because of the line-of-sight requirements.

The PCM signal conditioner with a clock and a receiver(Fig. 1) uses approximately 4 W (12 V DC or 220 V AC) and the Nagra tape recorder about 5 W during recording, i. e. when triggered or in continuous operation.

For microaftershock surveys we prefer independent recording stations as described above. The alternative, a telemetered network, will not only put additional constraints on the recording sites, but will also take a longer time to install.

3. Laboratory equipment

Playback of digital data can be done in the field by making use of a tape recorder, PCM decoder, D/A converter and Watanabe WR 3101 chart recorder. At the department, an HP-1000 L/5, a 16-bit microcomputer with pheripherals, facilitates handling of the digital (Fig. 3). The main objective of the system is to store interesting data on 1/2", 9 track tapes (in European Seismic Standard Tape Format - ESSTF) after visual inspection and to perform routine analysis of the selected signals, including filtering and FFT. So far, about 50 % of the necessary software has been implemented.

DOI: https://doi.org/10.2312/zipe.1983.078

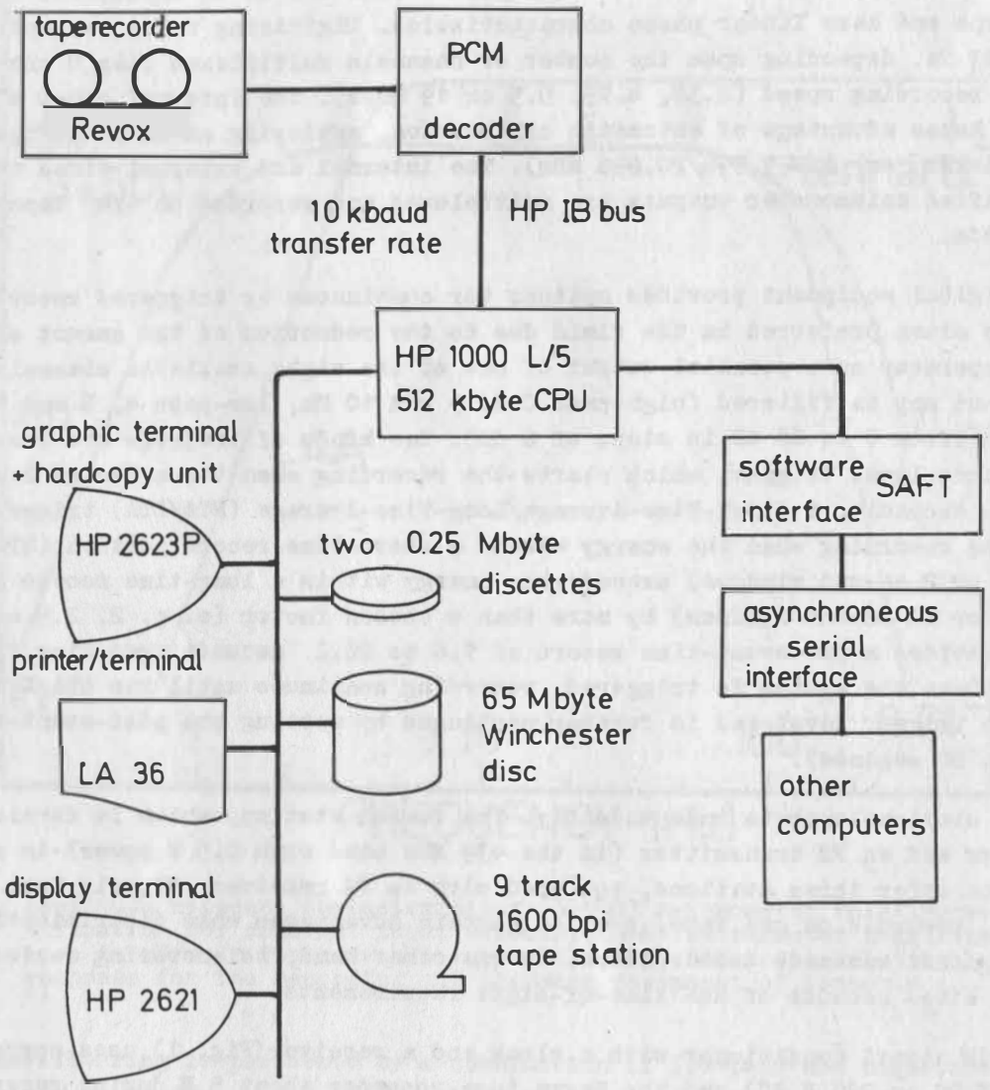

Fig. 3. Major elements of the laboratory equipment

The microcomputer receives data from a microprocessor controlled PMC decoder through an HP Interface Bus (HP-IB), an IEEE Standard 488-1978 implementation, at a rate of 10 kbaud (kbit/s) and stores data on a Winchester disc or on a 1/2", 9 track tape for further processing. The data transmission is limited due to the low CPU speed of the current HP-1000 L/5. The complete software package will include programs for producing lists of trigger times and event searching on 1/4" tapes via the Revox recorder.

Data stored on the disc or on a 1/2" tape can be displayed on the graphic terminal and/or copied by the hardcopy unit. The graphics program includes options such as changing the time resolution, magnification and reduction and reading of P- and S-wave arrival.

DOI: https://doi.org/10.2312/zipe.1983.078

4. Field experiment

In June 1982, MOSEN has been tested during a two-week field experiment around the active Dannemora iron ore mine, 40 km north of Uppsala, by recording and locating production explosions in the mine. A nine-station temporary network was deployed around the mine and recorded about 100 mine explosions, more than 50 rockbursts/bumps, and about 40 teleseismic events during a 14-day survey period. Station sites and location of explosions used are shown in Fig. 4. The mining authorities provided exact location and approximate origin time of the explosions, detonated a depths of 350 - 400 meters.

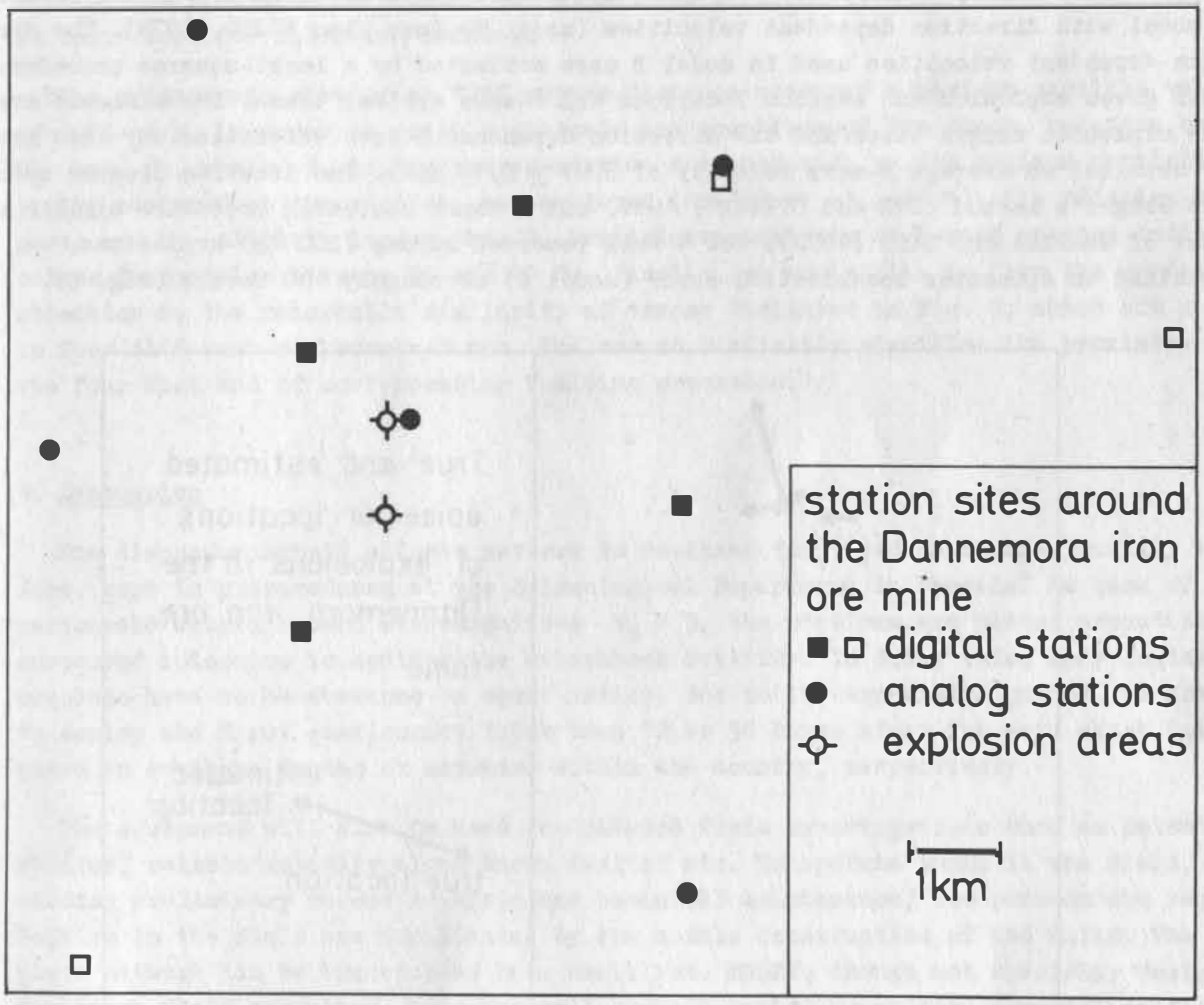

Fig. 4. Station sites around the Dannemora iron ore mine, together with explosion locations. Open squares indicate digital stations operating only for a short time

DOI: https://doi.org/10.2312/zipe.1983.078

4.1. Time-reading errors

In order to estimate the accuracy of arrival-time readings, three experienced analysts measured indepently a number of P-wave arrival times. For analog records, with recording speed of 8 mm/s, a standard time-reading error of 0.16 mm or 20 ms was found. For digital records, with a sampling of 222 Hz, played back on a high-speed chart recorder (50 mm/s), a standard time-reading error of 4 ms was found.

4.2. Localization errors

At this writing, detailed velocity structure in and around the mine is unknown to us. Lacking any better approximation, two different P-wave velocity models have been used for source localization. Firstly, a homogeneous half-space model (model A) and secondly a model with direction dependent velocities (model B) (see also KIJKO, 1975). The direction dependent velocities used in model B were estimated by a least-squares procedure with given explosion and station locations and P-wave arrival times. The unknowns are the explosion origin times and the direction dependent P-wave velocities. By this method we obtained an average P-wave velocity of 6.07 $\pm$ 0.17 km/s. The location program uses the Geiger's method (LEE and STEWART, 1981) and a depth searching procedure similar to that of SHAPIRA and BÅTH (1977). For 9 well recorded strong (200 kg) explosions, we obtained an epicenter-localization error (model A) of roughly 100 meters (Fig. 5).

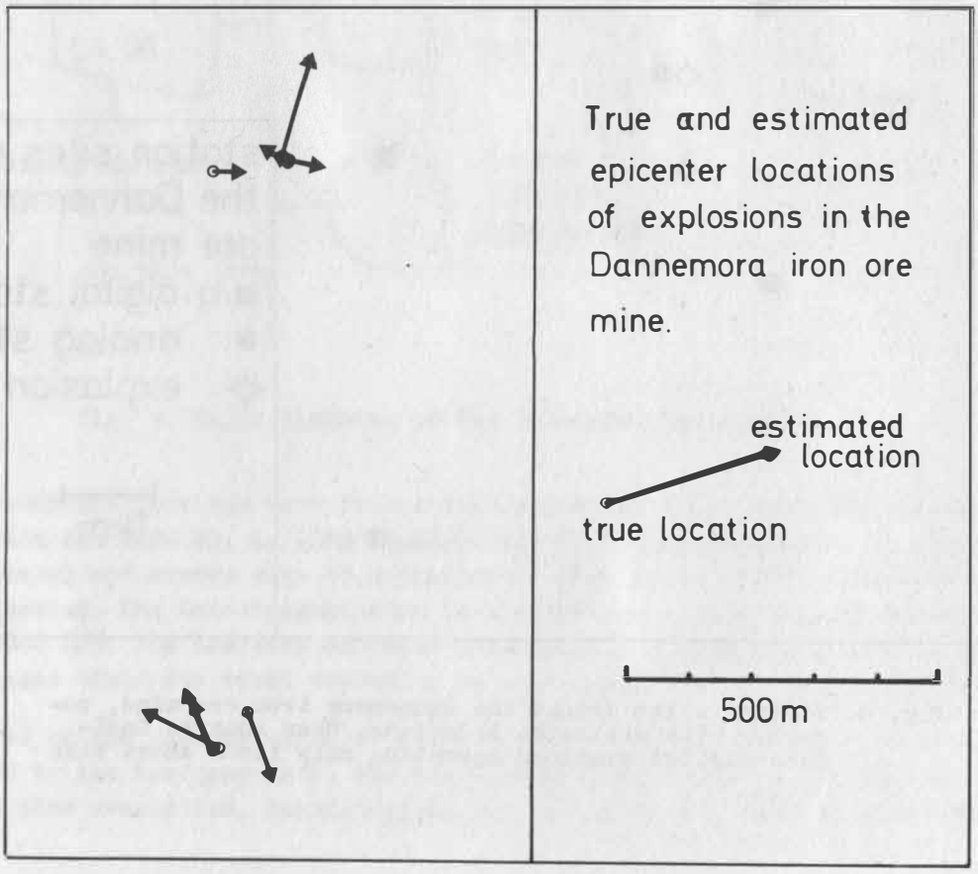

Fig. 5. Mislocation of explosions detonated at the two active mining sites

DOI: https://doi.org/10.2312/zipe.1983.078

The localization errors obtained with model B were slightly less. Obviously, such an accuracy is good enough to distinguish between the two main explosion sites (Fig. 4). Focal-depth estimates, as expected (see SHAPIRA and BÅTH, 1977), were quite large. The depth search has been restricted to the depth interval between 0 and 700 meters.

4.3. Rockburst observations

During the field experiment, we observed a number of rockbursts and/or bumps (see COOK, 1976 for terminology). Figure 6a shows a record of a rockburst, felt by the local population. The shock was followed by a number of bumps from nearly the same location. In total, at least 13 of similar bumps, within a time window of 38 hours, have been identified. Although the rockburst occured close to one of the main explosion sites, no slides, new fractures or similar phenomena have been observed by miners when they resumed their work the following morning.

The seismograph station at 1200 meters distance measured a maximum particle velocity of 0.15 mm/s. In order to roughly estimate the magnitude of the shock, relation between M_L and Rv, where R is the source-station distance and v the maximum particle velocity measured at the station, was employed (McGARR et al., 1981). The relation suggests an M_L slightly larger than 0. Preliminary analysis of P-wave spectra indicates corner frequencies between 20 and 40 Hz. Finally, we would like to draw the readers attention to the remarkable similarity of traces displayed in Fig. 6, which are due to four different rockbursts/bumps. The record similarity signifies the proximity of the four foci and of corresponding faulting processes.

5. Discussion

The discussed hybrid seismic network is designed for rapid deployment and is, therefore, kept in preparedness at the Seismological Department in Uppsala. In case of an earthquake within Sweden with magnitude $M_L > 3$, the stations are placed around the suspected epicentre to monitor the aftershock activity. In doing this, many logistical problems have to be overcome on short notice. Due to the experience gained, we are able to deploy the first station not later than 12 or 36 hours after the main shock taking place in southern Sweden or anywhere within the country, respectively.

The equipment will also be used for planned field investigations such as seismicity studies, seismic activity along known faults, etc. To operate MOSEN in the field, including preliminary record analysis and technical maintenance, two persons are required. Repairs in the field are facilitated by the module construction of the units. The complete network can be transported in a small van. MOSEN, though not specially designed for rough field campaigns, operates well even in rather tough environmental conditions with high humidity and low temperature.

Acknowledgements

We wish to thank our colleagues Conny Holmqvist, Norris John and Klaus Meyer for their help in the field work and Dannemora mine authorities for providing explosion data and permission to use some of the mine facilities. K.D. Lennartz of Lennartz Electronics GmbH assisted significantly by introducing us the digital equipment.

DOI: https://doi.org/10.2312/zipe.1983.078

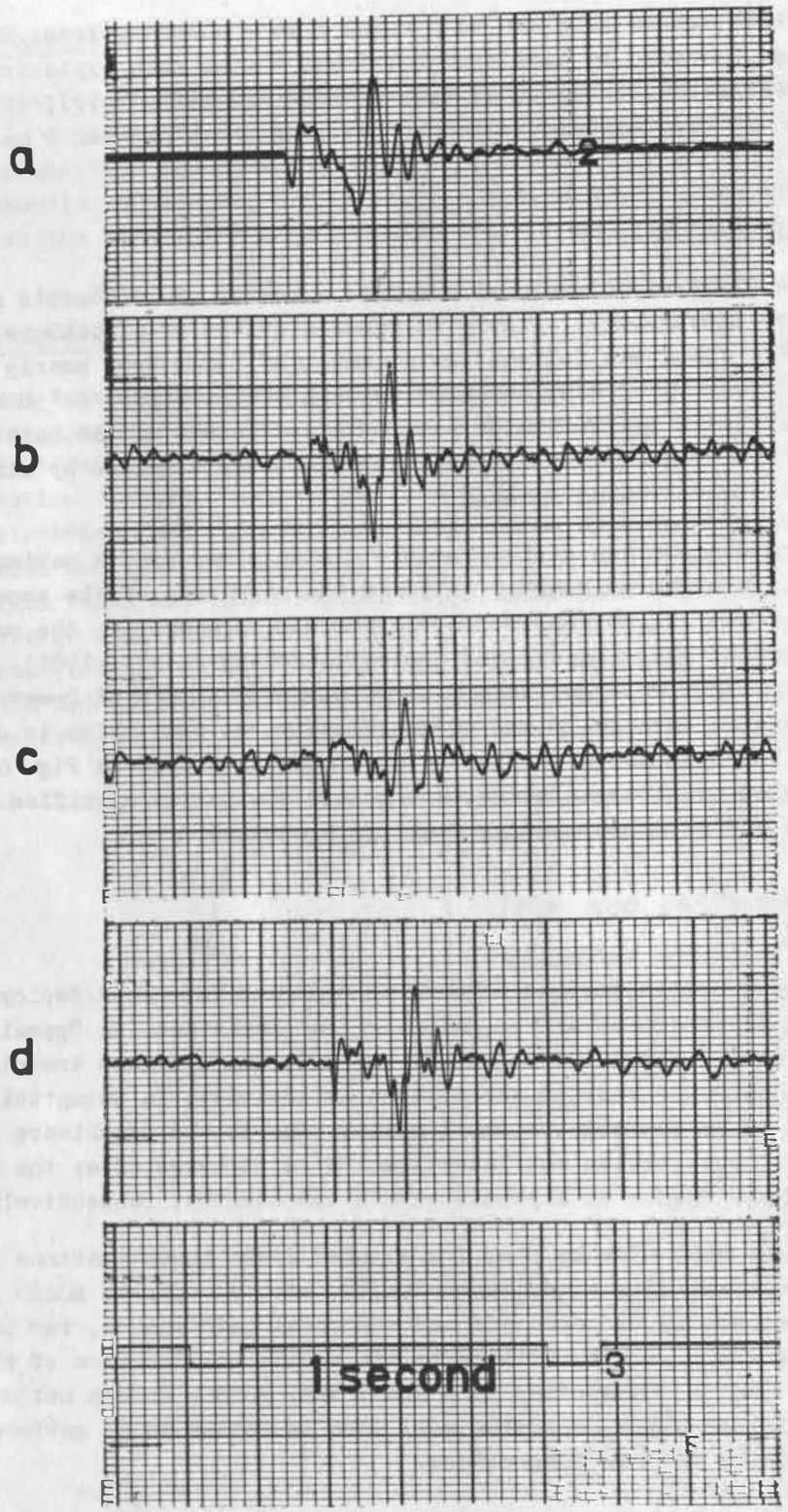

Fig. 6. Rockburst and bumps recorded by a vertical-component L4A seismometer at a hypocentral distance of about 1200 meters. On June 29, 1982, at 00 44 local time, a strong rockburst (a) took place in the Dannemora mine. The shock was felt and followed by a series of bumps delayed by: b) 15 minutes c) 19 minutes and d) 156 minutes. Magnification of traces relates as 1, 320, 320, and 320

DOI: https://doi.org/10.2312/zipe.1983.078

References

BUNGUM, H.; FYEN, J. — Hypocentral distribution, focal mechanisms tectonic implications of Fennoscandian earthquakes 1954 - 1978. Geologiska Föreningens i Stockholms Förhandlingar 101 (1979), 261-271

COOK, N.G.W. — Seismicity associated with mining. Eng. Geol. 10 (1976) 2-4, 99-122

KIJKO, A. — Methods for determining positions of very near earthquakes. Mat. i Prace Instytuty Geofiz. (Publs. Inst. Geophys. Pol. Ac. Sci.) 84 (1975), 121 pp.

KULHÁNEK, O.; van ECK, T.; JOHN, N.; MEYER, K.; WAHLSTRÖM, R. — Spectra of the earthquake sequence February-March, 1981, in south-central Sweden. Tectonophysics 93 (1983), 337-350

LEE, W.H.K.; STEWART, S.W. — Principles and applications of microearthquake networks. Academic Press (1981), 293 pp

McGARR, A.; GREEN, R.W.E.; SPOTTISWOODE, S.M. — Strong ground motion of mine tremors: Some implications for near-source ground motion parameters. Bull. Seis. Soc. Am. 71 (1981), 295-319

SHAPIRA, A.; BÄTH, M. — Short distance hypocenter location in layered media. Seismological Institute Uppsala, (1977) Report 2-77, 24 pp

SLUNGA, R. — Fault mechanisms of Fennoscandian earthquakes and regional crustal stresses. Geologiska Föreningens i Stockholms Förhandlingar 103 (1981) 27-31

Spectral Processing of Local Seismic Events

by

S. GRÄSSL, H. GROSSER and W. KUHNT [1)]

Summary

The paper deals with spectral processing of small earthquakes and microearthquakes in the magnitude range from $M_L = -1 \ldots 4$. The main objective is to investigate the source parameters of those local events using the well-known elastic dislocation theory. In this way it may be possible to bridge the gap between regional seismology and laboratory crack investigations. Besides the pure detection problem for small local events, the main presupposition for detailed source mechanism investigations is a broad-frequency range of the seismometers (usually microearthquakes show predominant spectral content between 1 and 100 Hz in dependence of the magnitude). Conventional short-period seismic instruments are not very suitable because of their restricted frequency-response.

1) Central Institute for Physics of the Earth of the Academy of Sciences of the GDR, DDR-1500 Potsdam, Telegrafenberg

DOI: https://doi.org/10.2312/zipe.1983.078

From the point of view of spectral dislocation theory certain seismological constraints are discussed in relation to the capabilities of the recording systems used in the calculations. Generally it is very difficult to interpret the seismograms of such local events because of the interaction of the source mechanism with the seismically inhomogeneous earth's crust. The spectral interpretation provides informations about source parameters (fault dimensions, slip direction, stress drop, seismic moment). As a basic result there are not principal differences between the spectral properties of the different events. The problem of source intensivity estimation by means of different magnitudes is discussed in some details. It is shown that the magnitude of local events e. g. local magnitude, duration magnitude av. is not very convenient for the description of the energy release of local seismic events. Some of the reasons are discussed (e. g. source type and source orientation, structural inhomogeneities in the earth's crust). The local scaling of seismic source parameters is necessary to give comparable information about local events.

1. Introduction and method

Central Europe represents a region of rather low natural seismicity. Earthquake with a magnitude greater than 4 in the territory of the GDR during the last years are very seldom. Some of these local earthquakes are felt up to distances of 15 - 20 km and macroseismic data of these main shocks have been studied in detail. Central Europe and the GDR especially belong to those regions of the world most intensively studied by detailed tectonical investigations. The dynamical interpretation of such local earthquakes is of important significance for the investigation of the recent tectonical stress pattern.

The dynamical investigation of local earthquakes is a rather difficult attempt because of

1. the fast amplitude decay of the main crustal phases with increasing source - receiver distance due to the large absorption and scattering of seismic waves in the lithosphere. Generally seismic records of good quality can be expected only from few very near seismological stations. Considering the CIPE network (BORMANN, 1983) it is possible to say that in the mean only 3-5 seismological stations give satisfactory records of local events. In many cases it is difficult to identify clear wave phases and the directions of the first wave onsets, respectively, which are the basis for the calculation of the fault plane solution;
2. the earth's crust in Central Europe possesses a very complex structure with lateral and vertical heterogeneities. Therefore, the seismograms recorded at the seismological stations of the GDR are characterized by a strong interaction of the source mechanism and wave propagation effects. Due to this high variability it is difficult to eliminate the wave propagation influences from the recorded seismograms.

For comparison purposes regional scaling effects have to be taken into the account in every case.

Investigations of the source mechanism are well known from far field investigations of teleseismic events. For source studies using the record of local events this well developed theory can be applied. Usually these investigations make use of the displacement spectra observed at different distant stations. These spectra are often interpreted

DOI: https://doi.org/10.2312/zipe.1983.078

in terms of a source model proposed by MADARIAGA and BRUNE: The interpretation is reduced to the estimation of 3 significant parameters:

- The zero frequency level, which reflects the seismic moment as a measure of the strength of the event.
- The corner frequency is used to calculate the source dimensions, given a fixed geometry and rupture velocity, no fracture information is incorporated in this model except that the result of the rupture is the slip on the fault. This widely used procedure has a rather weak theoretical basis. It is known from the general theory of Fourier transformations that the length T of a transient time function is inversely proportional to the width f_o of the corresponding amplitude spectrum of the Fourier transform. The usual relationship $f_o \cdot T \approx$ const. is established mathematically. But the relation between the time duration and the source dimensions depends strongly on model although it yields often reasonably accurate estimates of the general trends only of the source dimensions. Moreover, the problem of the corner frequency concept is that very simple theories are used to interpret complex source data and the relation between corner frequency and signal duration may be much more complicated. Most natural seismic sources are complex multiple events not only in the global scale but also in the case of small local events. Asperities and barriers are significant in all scales and seismic pulses radiated from different segments of the fault superimpose more or less random by to give a complex signal. In such a case the corner frequency does not reflect the total duration of the elongated source process, it represents the mean length of the partial signals. Under these conditions erroneous source dimensions will be estimated. Generally source parameters represent average values over the entire source plane only.
- The high frequency properties of the seismic far field spectrum are properties of discontinuities of the seismic signals. Abrupt changes in fracture strength cause the dominating high frequency radiation. As it is reasonable to assume different discontinuities the high-frequency behaviour of the seismic far field spectrum is controlled by a complex overlapping of different single high frequency asymptotes.

2. Results

The objective of this paper is to show the application of Madariaga's source model to small local seismic events. In our study local events were investigated within two magnitude ranges: microearthquakes at very near distances with local magnitudes variing approximately from -1 ... 2 and local earthquakes with magnitudes in the range between 2 - 4. A typical example of the events within the second class is the earthquake on february 20, 1982 near the city of Leipzig. This event was recorded by nearly all seismological stations in the GDR. The microseismic magnitudes estimated of this event varied between 2.2 - 3.3. The macroseismic magnitude derived from the epicentral intensity was about 3.7 ± 0.2. These rather large difference indicates the high variability of the maximum amplitudes for different recording sites and limites the general use and the regional comparability of magnitudes. The reasons of this scatter are: propagation effects due to the heterogeneity of the earth's crust in the area under investigation and azimuthal amplitude differences due to the radiation pattern of the seismic source. The estimation of the fault plane solution of local events is thus an important procedure and at the same time a rather difficult attempt because of the small amplitudes of the

DOI: https://doi.org/10.2312/zipe.1983.078

first crustal wave onsets (P_g). Typical vertical sections through the crust indicate positive velocity jumps which are responsible for the main crustal phases. It is reasonable to assume both the P-wave train and the S-wave train consist of interfering signals with the same polarity. By calculation of mean phase spectra and by cross-correlation investigations it is thus possible to detect general polarity differences of π or 2π between the wave groups at different stations. By calibration of these relative polarity pattern using the most clear records of the nearest station it is possible to give the true pattern of the P-wave and S-wave polarities also in those cases when clear P-wave onsets are not visible. In Fig. 1 the fault-plane solution derived by this combined procedure mentioned above for the Leipzig event is shown. The discrimination between fault plane and auxiliary plane was made basing on geological assumptions. The NW-SE striking plane agrees rather well with the general trend of the tectonic lines in the region under investigation.

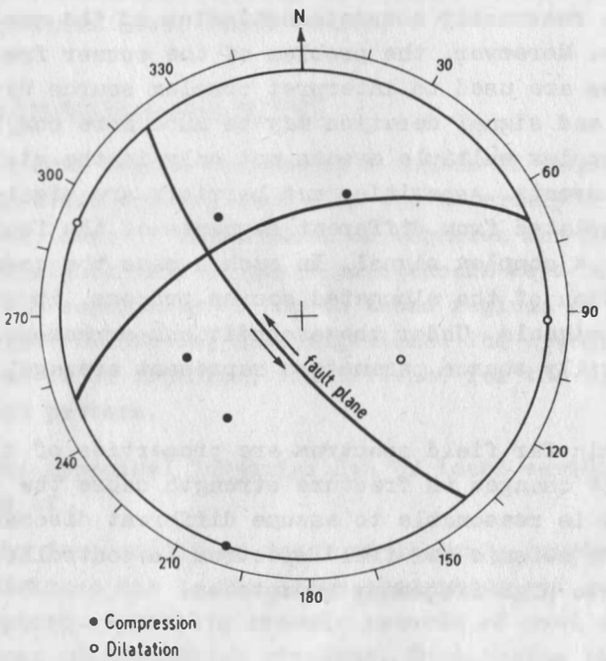

Fig. 1. Fault plane solution of the event no. 1

A serious problem in local earthquake investigations is the enlarged frequency range having to record for dynamical earthquake investigations. According to Madariaga's model the source radius is inversely proportional to the corner frequency. To estimate the corner frequency it is desirable to detect in a clear manner the high frequency asymptote. That means that for local event investigations frequencies in the order of 100 Hz must be detected. In Fig. 2 the P-wave spectrum of the Leipzig event recorded in a distance of about 65 km is shown. Corrections for attenuation along the wave propagation in the earth's crust and for the transfer function of the recording channel were carried out. The rather clear picture predicted from the theory of kinematical source models is visible: long-period level, corner frequency near 12 Hz for P-waves and 8 Hz for S-waves, the high-frequency decay is proportional to a power of - 1.8.

To get such high frequency information the digitization of the magnetic type records could be done with a high sampling rate only. In this case a sampling frequency of 714 Hz was used. In comparison the Fig. 3 and 4 show the corrected displacement spectra of P- and S-waves of the same event recorded by the standard seismological stations of the CIPE network. Because of the restricted frequency response information about the low frequency level could be derived only. The radiation pattern using the fault plan solution is corrected in Fig. 3 and 4.

DOI: https://doi.org/10.2312/zipe.1983.078

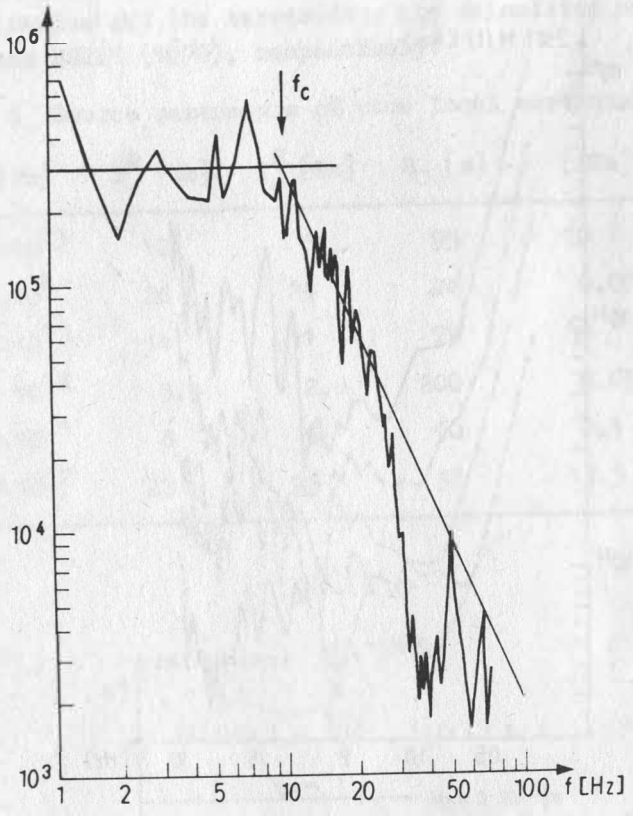

Fig. 2. P-wave broad-band spectrum of the event no. 1

Neglecting the frequency range lower than 1 Hz all displacement spectra only show the dc-level with some overcorrection of the absorption. The seismic moment is characterized by a large scatter of about one order comparing the records of the different stations. This scatter corresponds to the significant magnitude differences of more than unit stated above. Correction of the radiation pattern using the fault plane solution did not decrease this general scatter. Therefore, the causes of this scatter must be the crustal inhomogeneities in the region under investigation. The results indicate a stronger scatter of the seismic moment derived for P-waves than for S-waves.

The microearthquakes investigated in the second class are events in a brittle sediment. The source receiver distance is only some hundred meters. The Figures 5 and 6 show the corresponding displacement spectra for P-waves and for S-waves in comparison with the noise spectra at different recording sites. The zero frequency level, a corner frequency and a high frequency decay proportional to a power of about -2.8 are visible. The principal shape of the displacement spectra of the two groups of events is very similar. Note the significant larger scatter of the zero frequency level of P-waves with respect to the those of S-waves. The spectra are not corrected by the radiation pattern because of the limited number of stations and the seismic moment shows a similar scatter as in the former case.

DOI: https://doi.org/10.2312/zipe.1983.078

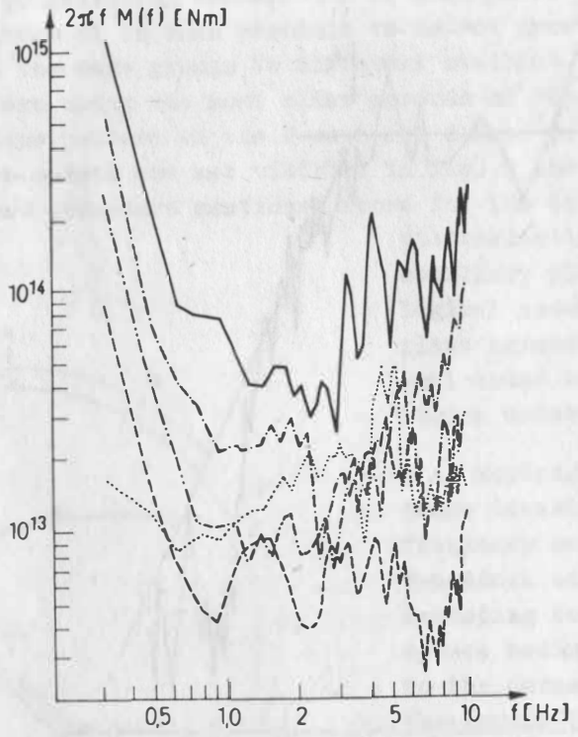

Fig. 3. P-wave spectra of the event no. 1

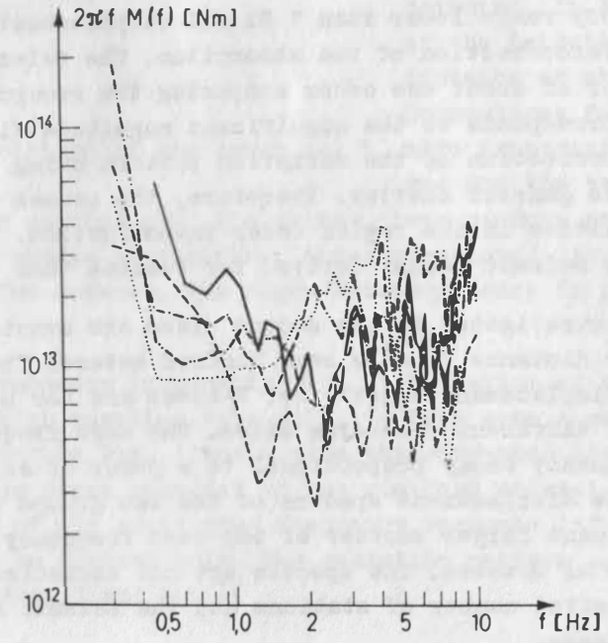

Fig. 4. S-wave spectra of the event no. 1

DOI: https://doi.org/10.2312/zipe.1983.078

In Tab. 1 the source parameters of all events investigated are shown for comparison. An important relation is the dependence of the seismic moment of the source radius (Fig. 7). The source radius and the stress drop are calculated after the formulas given by MADARIAGA (1976) and BRUNE (1970), respectively.

Tab. 1 Source parameters of some local earthquakes

No.	M_0 [Nm]	f_c^P [Hz]	f_c^S [Hz]	R_0 [m]	[MPa]	D_0 [mm]
1	$2 \cdot 10^{13}$	12	8	95	10	20
2	$2.2 \cdot 10^{9}$	26	24	24	0.07	0.1
3	$3 \cdot 10^{13}$	14	11	75	34	64
4	10^{12}	3.4	2.8	200	0.055	0.05
5	$1.7 \cdot 10^{11}$	8	6	90	0.1	0.04
6	$1.7 \cdot 10^{12}$	23	25	38	13.5	11

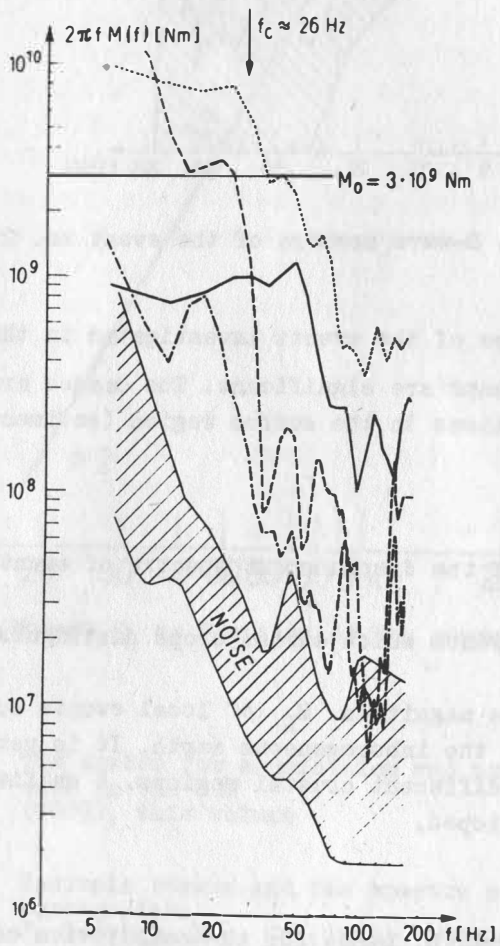

Fig. 5. P-wave spectra of the event no. 2

DOI: https://doi.org/10.2312/zipe.1983.078

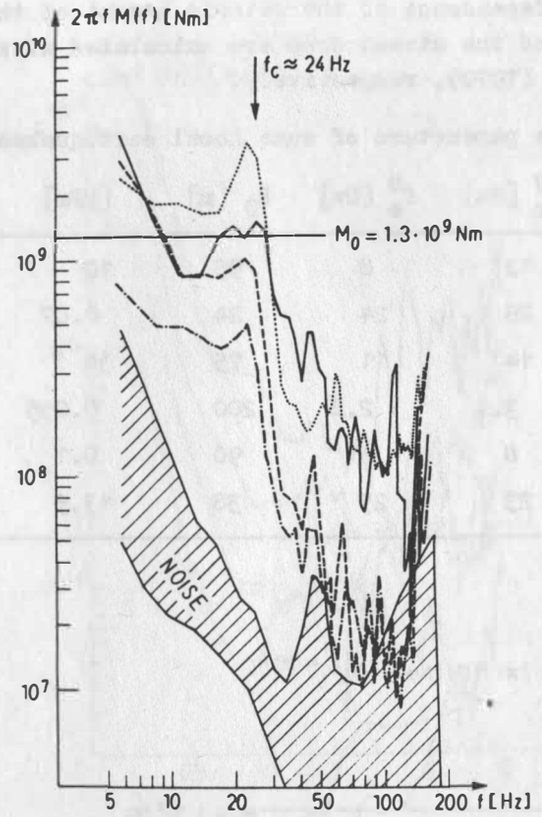

Fig. 6. S-wave spectra of the event no. 2

Comparing the stress-drops of the events investigated in this study principal differences between the two groups are significant. The causes are different fracture strengths and stress conditions in the source region (sediments, crystalline rocks) probably.

Some general conclusions:

- The principal behaviour of the displacement spectra of events within the two magnitude groups is very similar.
- There are two groups of events which stress drops distinguishing by more than two orders.
- The seismic moment and the magnitude M_L of local events scatter very strongly due to propagation effects in the inhomogeneous earth. It is very difficult to compare local events occuring in different crustal regions. A unified magnitude approach for local events must be developed.

Acknowledgement

The authors wish to thank Mrs. L. Lonse for the computation of the most numerical results.

DOI: https://doi.org/10.2312/zipe.1983.078

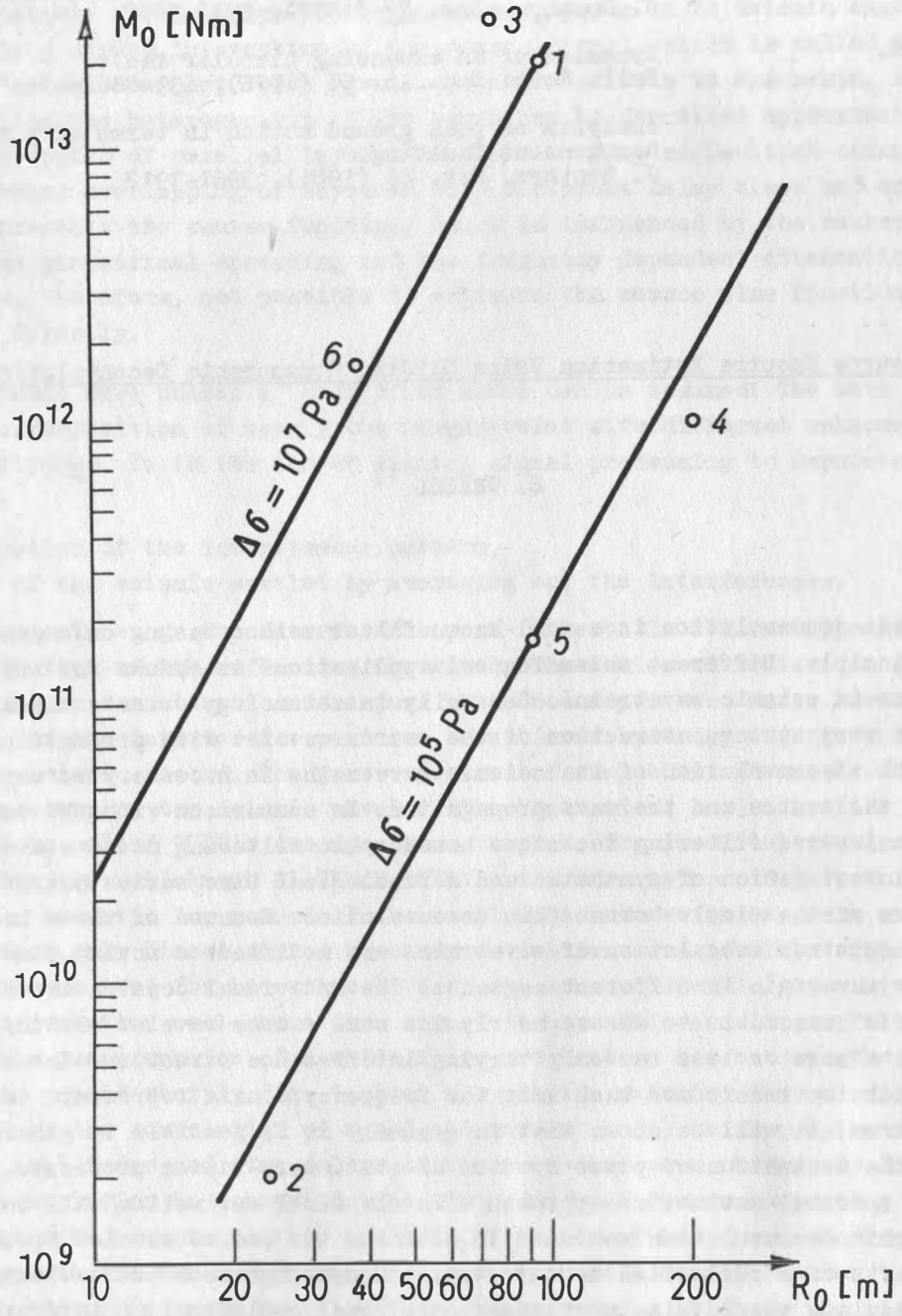

Fig. 7. Seismic Moment M_0 as function of the source radius R_0

References

BORMANN, P.; HURTIG, E.; KOWALLE, G.; TEUPSER, Ch. The system for acquisition and processing of seismological data in the GDR (1983), this volume

BRUNE, J.N. Tectonic stress and the spectra of seismic shear waves from earthquakes. J. Geophys. Res. 75 (1970), 4997-5009

DOI: https://doi.org/10.2312/zipe.1983.078

DAS, S.; AKI, K. — Fault planes with barriers: A versatile earthquake model. J. Geophys. Res. 82 (1977), 5648-5670

MADARIAGA, R. — Dynamics of an expanding circular fault. Bull. Seis. Soc. Am. 66 (1976), 639-666

McGARR, A. — Analysis of peak ground motion in terms of a model of inhomogeneous faulting. J. Geophys. Res. 86 (1981), 3961-3912

Source Spectra Estimation Using Sliding Homomorphic Deconvolution

by

S. GRÄSSL [1)]

Summary

Homomorphic deconvolution is a well-known filter method basing on a generalized superposition principle. Different seismological applications are known for the separation of interferences in seismic wavetrains. Generally in seismology seismic signals are characterized by a very strong interaction of the source wavelet with propagation effects in a layered earth. Deconvolution of the seismic wavetrains is necessary to separate the influences of the source and the wave propagation. In comparison with the conventional least square inverse filtering technique homomorphic filtering needs weaker preassumptions. The investigation of synthetic and seismological time series has shown the rather limited value of the simple homomorphic deconvolution. Because of these known difficulties the cepstrum calculation of wavetrains was modified: a moving time window divides the whole wavetrain in different segments. The individual cepstra are stored and stacked. It is reasonable to assume nearly the same source wavelet within the different segments but a more or less randomly varying interference structure. The stacked cepstrum which is transformed back into the frequency domain represents mainly the source spectrum. It will be shown that in generally it is possible to generalize these method for the estimation of power spectra of stationary random processes. Comparisons of this new spectral estimation approach with classical estimation will be demonstrated. The homomorphic deconvolution was used to estimate the source wavelet spectrum from different parts of a reflection seismic trace. Comparing these estimations it was possible to calculate the intrinsic attenuation of real geological media from reflection seismic records.

1) Central Institute for Physics of the Earth of the Academy of Sciences of the GDR. DDR-1500 Potsdam, Telegrafenberg

DOI: https://doi.org/10.2312/zipe.1983.078

Due to the seismic wave propagation in an inhomogeneous earth seismic signals are characterized by a strong interaction of the source signal, which is called in the following the "seismic wavelet" with wave propagation effects in the earth. As a very good approximation the heterogeneity of the earth can be described approximately in many cases by a system of parallel layers. Due to secondary reflections seismic signals represent a complex overlapping of wavelets with different delay times and amplitudes. The wavelet represents the source function, which is influenced by the rather well-known processes of the geometrical spreading and the frequency dependent attenuation mainly. Generally it is, therefore, not possible to estimate the source time function from a seismic record directly.

For many seismic wave phases a simplified model can be assumed: The wave packet consists of a superposition of nearly the same wavelet with different unknown time delays and amplitudes. It is the aim of digital signal processing to separate these two components:

- the identification of the interference pattern,
- the recovery of the seismic wavelet by averaging out the interferences.

In reflection seismic e. g. the interference part reflects in a first approximation the vertical distribution of the reflecting horizonts. The series of reflection coefficients can be considered as a realization of a pure white noise process. Under these conditions the elimination of the interference part can be achieved by computing the autocorrelation function of the seismic record. The power spectrum of the seismic trace is then identical to the power spectrum of the seismic wavelet. The theoretical basis for this procedure is given by the so called WOLD's decomposition theorem. The practical realization can be carried out using the well-known BLACKMAN-TUKEY estimation method. Detailed investigations of seismic acoustic log records indicate significant deviations from a white noise process, therefore, only biased source spectrum estimations are possible. Thus, an alternative procedure was used for the estimation of the source function given by the so-called homomorphic deconvolution well-known from signal theory. This non-linear filter method does not need the preassumption of a white noise process. To demonstrate the principle approach of this method shortly Fig. 1 shows a synthetic example: The seismic wavetrain was constructed by the convolution of a seismic wavelet $s(t)$ with a spike series $i(t)$ describing the amplitudes and time delays of the secondary wave phases. By Fourier transformation the convolution is converted into the product of the corresponding spectra. The complex logarithm transforms this product into a sum of the corresponding logarithmic spectra. To separate the two components by linear filters a second Fourier transformation transforms back these frequency functions into another space which is the time domain again. The transformed time function is called cepstrum.

Under rather simple restrictions it is possible to separate in the cepstral domain the two components $s(t)$ and $i(t)$. After inverting the procedure the two components connected in the wavetrain by convolution can be estimated separately. The practical application of this powerfull method to real seismological records is rather difficult because of two reasons:

1. The separation is possible only in the case of rather simple interference structures. The estimation of the time delay of the depth phases from the P-wave signals of underground nuclear explosions is a well-known application.
2. The beginning and the end of the wavetrain must be defined clearly.

DOI: https://doi.org/10.2312/zipe.1983.078

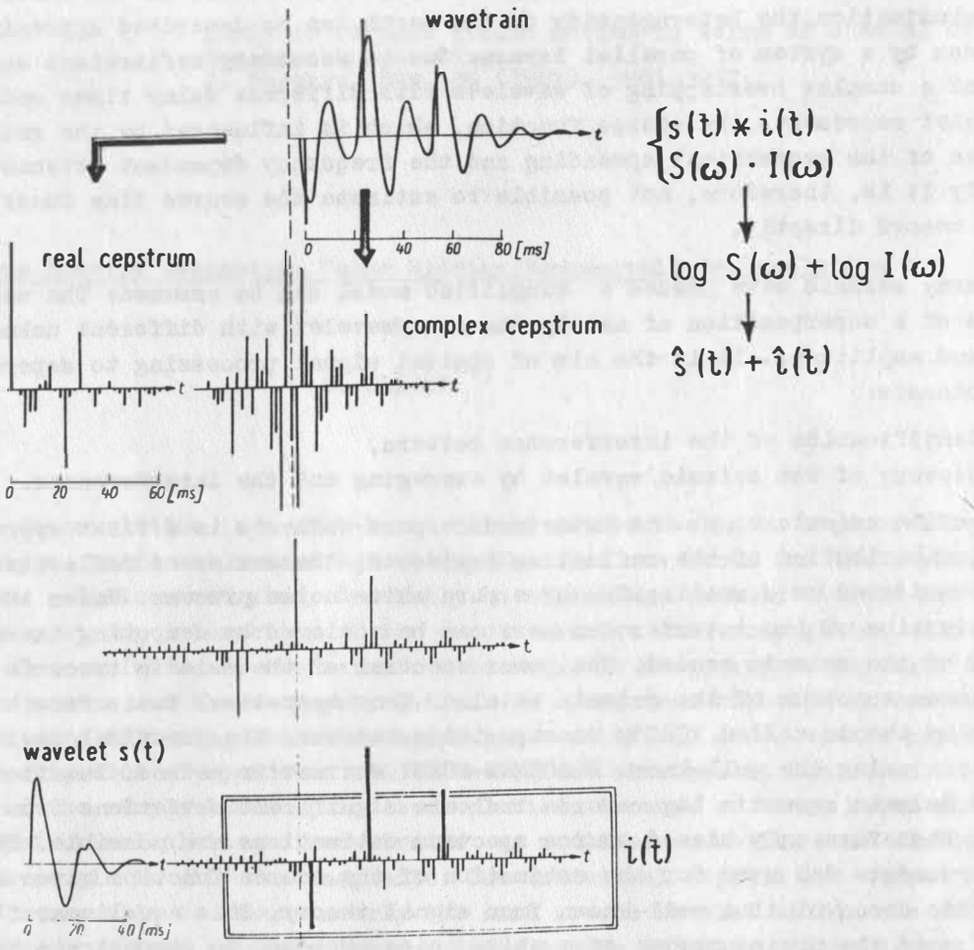

Fig. 1. Homomorphic deconvolution of a synthetic seismic wavetrain

Because of these restrictions the method was modified in the following manner: The investigated wavetrain is segmented using a time window of finite length. This window slides along the time series. The interference part and the wavelet are estimated for each position of the time window. As it is reasonable to assume the same signal and a more or less randomly varying interference structure for differing window positions, the interferences are cancelled out by stacking the different cepstra. The mean cepstrum represents as a good approximation the signal part of the wavetrain. The very frequent change from the time domain into the frequency domain and back in to the time domain can be carried out effectively only using the FFT-algorithm. For the investigation of the interference part the partial cepstra are stacked with time delays corresponding to the different time positions of the window.

To investigate the effectiveness of this method for the estimation of the signal spectrum a synthetic random linear process was investigated comparing the result with the spectrum calculated by means of the classical BLACKMAN-TUKEY estimation procedure (Fig. 2). This Figure demonstrates in a clear manner the advantages of this non-linear method.

DOI: https://doi.org/10.2312/zipe.1983.078

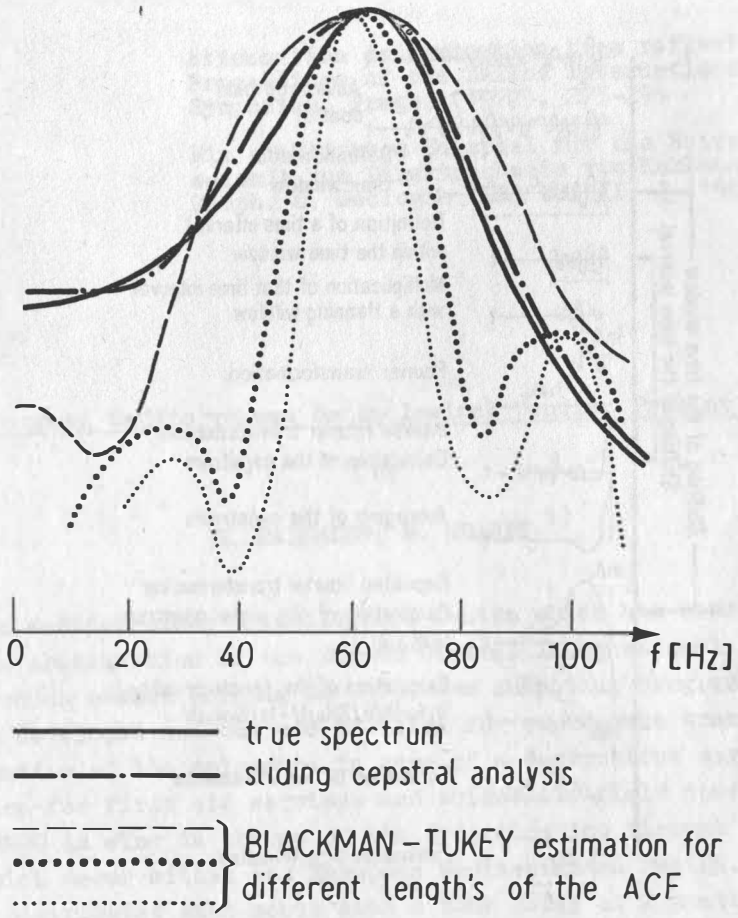

Fig. 2. Comparison of different spectral estimation methods for a finite realization of a linear process

Therefore, this method was used for the calculation of the intrinsic absorption from reflection seismic records by comparing the seismic wavelet spectra calculated from different parts of a reflection trace. In a rather good approximation the wavelet spectra correspond to the source spectra which are influenced by the depth-dependend attenuation. The spectral quotient yields the frequency dependent absorption in the corresponding depth interval. The flow diagram (Fig. 3) demonstrates once more the principle of the sliding homomorphic analysis. The program was tested using synthetic seismic traces competed with attenuation from real acoustic log data. In the next Fig. 4 the result of a practical application is shown. The motivation for these investigations was the statement proofed experimentally that hydrocarbons in the pores of sediments yield a significant higher absorption for P-waves. Therefore, the CDP-stacked seismic traces in the region of an oil deposit were investigated.

The cross section of the areal distribution of absorption for a profile crossing the oil deposit is shown. In the region of the deposits marked by crosses the higher absorption is remarkable.

DOI: https://doi.org/10.2312/zipe.1983.078

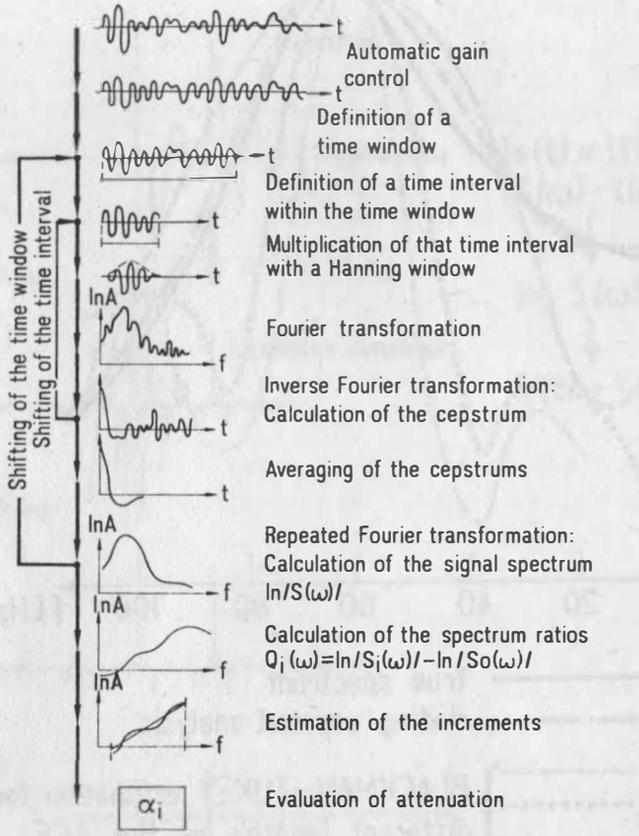

Fig. 3. Flow diagram for the estimation of the absorption from a reflection seismic trace (after DANCKWARDT et al., 1977)

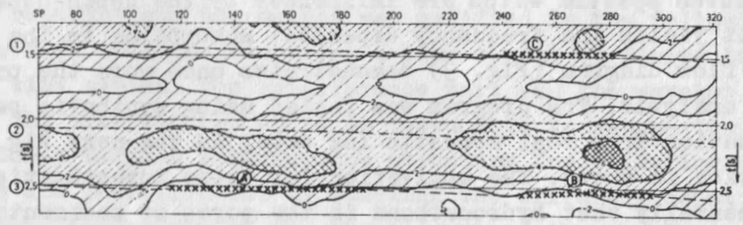

Fig. 4. Areal distribution of seismic attenuation along a profile crossing an oil deposite
xxxxxx oil deposite
isolines of attenuation (x4.10^{-6} s/m)
(after PATZER, PRÖHL, 1980)

DOI: https://doi.org/10.2312/zipe.1983.078

References

DANCKWARDT, E.; LEISSRING, B.; PATZER, U. — Attenuation determination from reflection seismic data. Proceedings of the XXIInd International Geophysical Symposium. Prague (1977), 275-294

PATZER, U.; PRÖHL, S. — Ein praktisches Beispiel für die Nutzung der Reflexionsseismik zum Direktnachweis von Kohlenwasserstoffen. Geoph. u. Geologie III, Bd. II, 2 (1980), 107-115

The European Mediterranean Seismological Centre, Present and Future

by

H. HAESSLER, M. GRANET [1)]

The European Mediterranean Seismological Centre which has been launched in 1976, January, is the continuation of the Bureau Central International de Séismologie located in Strasbourg which ceased working in 1975. New computing programs for earthquakes location have been developed and the use of Telex for rapid data transmission led to a rapid determination of the epicentre in case of a destructive earthquake. This is of great importance for first aid services and scientific field operation in an appropriate way. The EMSC is also in charge of the determination through a regular procedure of earthquakes which occur within the European Mediterranean region. These earthquakes locations are distributed each month with a time delay of 2 months. Considering the last 7 years, the input data (by telex, paper tape, bulletins ...) have considerably increased. In fact the number of earthquake determinations has been growing up from 581 in 1976 to 1420 in 1981. Due to this increase a new regular procedure is presently developed by the scientific and technic staff of the EMSC.

1) Institut de Physique du Globe, 5 Rue René Descartes, 67084 Strasbourg-Cedex, France

DOI: https://doi.org/10.2312/zipe.1983.078

Description of Data Acquisition and Data Processing Facilities at Seismological Telemetric Network in Hungary

by

L. HETÉSI [1)]

Summary

This paper deals with the Hungarian seismic station network, which will be reorganized in this and the next year. The first of these stations situated in Mátra Mountains has been in continuous operation since 1977 and uses analog recording by FM telemetry. The new seismic network consist of four outstations with the centre in Budapest. The digitized signals of vertical SP seismometers are transmitted by digital telemetry in the UHF band by radio links and recorded at Budapest in magnetic bubble memories. The central computer synchronizes the data acquisition and determines the parameters of events.

The Hungarian seismic station network will be reorganized in this and in the next year. Based on the research and experiments of several years a new digital telemetering system has been planned for seismological use. The stations will be built and this system will work just like an array. The full array will become operational in 1984, although continuous recordings on the first telemetry station - in FM analog method - have been available since 1977. The main purpose of the STN is to record the fine structure in the frequency-wavenumber domain with large dynamic range and high resolution within a spectral range between 0,2 s and 20 s. Digital data acquisition and processing, however, are the appropriate concept for these purposes.

The present paper describes the main technical elements of the network installation and operation in close connection with the data flow. The planned Hungarian STN consist of four field stations (outstations) with the centre in Budapest. At first every station will be equipped by short-period vertical seismographs. Since the central station is Budapest, where is a high population density, industry, and traffic, noise level is rather high, the seismograph will be set up in a 200 metres deep borehole.

Each outstation contains the seismometer als well as the analog and digital electronic facilities for data acquisition and transmission. The analog electronic set includes a high quality anti-aliasing filter and a gain ranging amplifier. The 3 dB point of the 5 pole antialiasing filter is at 5 Hz. The gain-ranging amplifier consist of 3 cascaded DC-amplifiers. The concept of gain-ranging used in the data acquisition system permits to record the seismic signals with high dynamic range and high resolution. The gain-ranging and the multiplexing are controlled by the software. The digital electronic modules consist of a microcomputer, analog-to-digital converter, a control

1) Institute of Seismology of the Hungarian Academy of Sciences, 1112 Budapest, Meredek u. 18, Hungary

DOI: https://doi.org/10.2312/zipe.1983.078

unit for seismometer calibration and modems. Controlled by the operating system the analog signals are digitized every 50 ms (20 Hz). A 12-bit A/D converter is used and the program provides the conversion of the 12 bit words into 16 bit floating point data format. Digitized words are then converted to serial form and coded for data transmission. The coding consist of two parts: compacting by method predictive code (from 12 bit to 8 bit) and the error correcting code. The data transmission form the outstations to the data center is performed in blocks of 10 s, using synchronous transmission mode of 3600 bits per second. The modems also contain a same bit rate channel in the opposite direction. This is used for transmission of various command codes for system control.

There are several technical possibilities for digital data transmission, but in our case it seemed to be the most reliable way to use radio links in the UHF band. We have got only one duplex frequency for the full radio network, so that we can use the time-dividing transmission method. The synchronous modems and also some of the electronic equipments were developed and contructed in the electronics laboratory at Institute of Communication of Technical University in Budapest.

All components used for data decoding, recording, monitoring, system control are combined in the data center. A minicomputer VT 20 - made in Hungary, firm VIDEOTON - controls the various components. Four synchronous modems are used for telemetric stations, naturally the acquisition instrument in the centre is joined by direct interfaces.

The central computer synchronizes the data acquisition. Selfmonitoring functions in the operating programs are able to detect failures. But the main function of the central computer is: when an event is detected, the data processing begins automatically. The computer can also write magnetic data tapes which are suitable for complex analysing in a computing centre as well as for international data exchange. For simultaneous monitoring the information is converted to analog form and is recorded by ink-pen drum recorders.

A receiver for radio time signals (DCF 77) and the time of day clock provide the center with accurate time pulses. The clock provides BCD data to the minicomputer taken as reference signals for synchronizing the full network.

DOI: https://doi.org/10.2312/zipe.1983.078

Seismic Data Collection in Denmark

by

L. HJELME [1]

Since 1927 seismograph stations have been operated near Copenhagen in Denmark and in Ivigtut and Scoresbysund in Greenland. However digital recording has been introduced only rather recently. A few years ago a dense network of seismometers was implemented in Southern Sweden. This network was extented into Denmark in a co-operation between FOA, Stockholm and Geodetic Institute. All signal were sent to Stockholm for digital recording. Special care have been taken in selection of the situation of the seismometers in Denmark. In a special study two nearby places were compared as regard to local and distant events. Copy tapes of interesting sequences were mailed from Stockholm to Copenhagen for further studies. First the data has been used for locating Danish earthquakes. 13 events were detected during the first 3 years. Danish teleseismic stations were modernized in the sixties with the WWSSN equipment, which was of the classical type. One of these stations (Godhavn, GDH) was upgraded last year to digital recording (DWWSS). But it is too premature to report on the performance.

Seismic Data Teletransmission in Romanian Network

by

F. IONICA, A. GRIGORE [2]

The general configuration of the telemetered seismic network and of the data acquisition is presented. Romania has now an 18 station short-period seismic network. Data from the remote stations are telemetered via UHF data links to central station Bucharest-Măgurele and to secondary center Cheia-Red Mountain, where they are recorded on visual recorders. The station in Măgurele includes also a computer-based data processing and analysis facility which consists of a Digital Equipment Corporation PDP 11/34 with peripherals and software programs. The software programs which are being provided by Teledyne-Geotech automatically process the seismic data and allow to our institute to be most responsive to the scientific needs of the country.

---

1) Geodaetisk Institute, Gamlehave alle 22, DK-2920 Charlottenlund, Denmark

2) Central Institute of Physics, Center of Earth Physics and Seismology, P.O. Box MG-2, Bucharest-Măgurele, Romania

DOI: https://doi.org/10.2312/zipe.1983.078

Direct Measurement of Seismic Forces Using Multi-Pendular Seismometers

by

B.K. KARAPETIAN [1)]

In this paper the instrumental determination of peak seismic forces in structures is presented using the spectral method by A.G. NAZAROV (1959) subsequently developed in cooperation with the author (KARAPETIAN, 1963; NAZAROV and KARAPETIAN, 1973; KARAPETIAN and KARAPETIAN, 1978). The method consists in directly integrating of the equations of seismically produced ground displacements using a multi-pendular seismometer, which is a set of damped horizontal and vertical linear oscillators of differing periods to simulate structures in a wide range of periods and decrements of oscillation. The vertical and horizontal component of the multipendular seismometer is shown in Fig. 1.

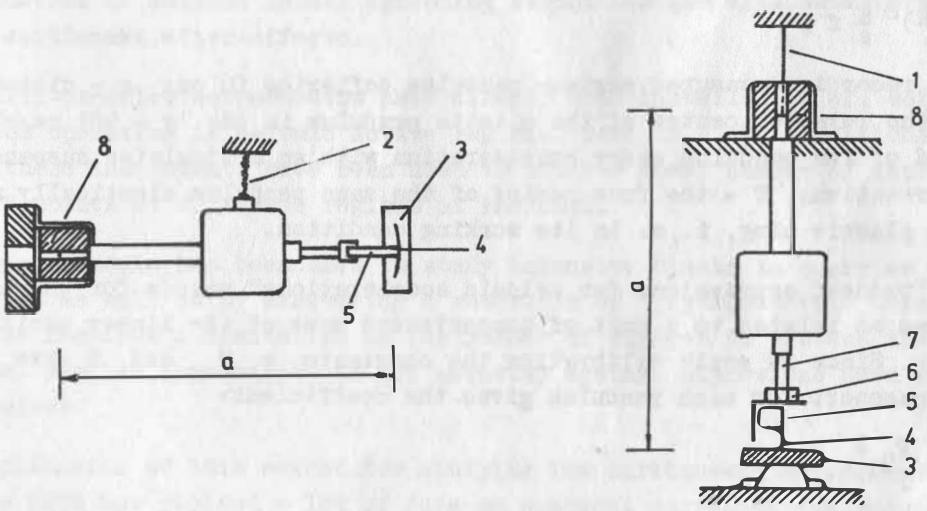

Fig. 1. Schematic principle of the horizontal and vertical pendulums of the seismometer

Both are mounted on a string suspension 1 or spiral ring, respectively, unloading the dampers (rubber or plastic cylinders 8) in the neutral position of the pendulum. The oscillations of the vertical and horizontal pendulums are recorded on smoked glass plates in cassettes using a corundum stylus 4. The stylus is fixed with permaloy plates 5 to the nut 6 which by tightening on the pendulum pin provides the needed pressure of the stylus on the glass. If the pendulums swings, the stylus scratches the smoked surface primed by a thin layer of bone grease for an enduring hold of soot and a reduced stylus-to-glass friction.

---

1) Polytechnical Institute of Yerevan, Terjana 105, Yerevan 375009, USSR

DOI: https://doi.org/10.2312/zipe.1983.078

The vertical-pendulum cassettes are inserted into slots of a displacable table. Insertion of the cassette causes that the stylus traces one of the axes on the glass (in parallel to the cassette guides). The other perpendicular axis appears after the recording of the oscillatory process by displacing the table with cassettes up to the position when the stylus leaves the glass surface. The crossing of these axes gives the zero calculating point to process the recordings. A similar preliminary and recording procedure takes place with the horizontal pendulums although with a substantially reduced complexity of hardware. The instrument sensitivity is 3 to 4 points on the scale.

In operating condition the instrument is enclosed in a case for protection against dust, contamination, and so on. Installation is carried out by using a water level for a precise horizontal position either in a mural recess or on a special concrete slab in a basement or a well. The instrument dimensions are 808 x 480 x 643 mm.

Both the recordings and maximum deflexions of the pendulums yield the reduced expressions for seismic accelerations defined by the following simplified formula:

$$\tau = \left(\frac{T_o}{T}\right)^2 \frac{g}{a} f ,$$

where f - the recording-measured maximum pendulum deflexion in cm; a - distance from stylus tip to the rotation centre of the elastic pendulum in cm; g - 981 cm/s^2; T_o - the free period of the pendulum under consideration with an articulated suspension at the centre of rotation; T - the free period of the same pendulum elastically mounted in a rubber or plastic plug, i. e. in its working condition.

The phrase "reduced expressions for seismic accelerations" stands for the maximum seismic stresses as related to a unit of concentrated mass of the linear oscillator for a given damping. Since in scale calibration the constants a, T_o and T are determined directly, the passport for each pendulum gives the coefficient:

$$K = \frac{g}{a} \left(\frac{T_o}{T}\right)^2 .$$

Thus, the maximum reduced seismic acceleration is determined by the formula:

$$\tau = K f .$$

The values obtained for seismic accelerations are used for plotting the spectral curves. On the abscissae are the free periods for the elastic pendulums T while the ordinates show the reduced seismic accelerations τ. The diagrams of reduced seismic accelerations characterize the seismic stress at a given point. As exemple a spectral curve $\tau(T)$ is shown in Fig. 2.

Indicating stability is controlled by semi-anual checks of the free periods of pendulums as well as of their damping decrements. An insignificant deviation of the free period of the order of $\pm$ 10 per cent can be corrected by re-calculating the value of K given in the passport. More substantial changes will require pendulum replacements.

Thus, direct instrumental measurements of seismic forces using multi-pendular seismometers yield feasible data clarifying certain engineering aspects of earthquakes. This facilitates the formulation of scientifically based definitions as well as the

DOI: https://doi.org/10.2312/zipe.1983.078

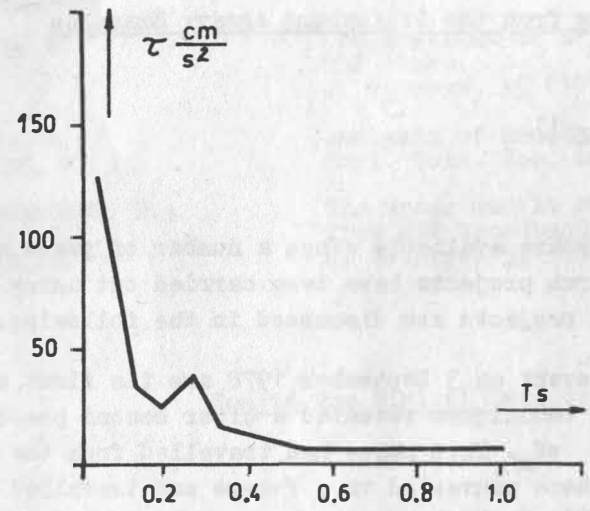

Fig. 2. Reduced seismic acceleration curve

standardization of seismic forces affecting structures and eliminates prejudiced assessments of earthquake after-effects.

The multi-pendular seismometers have already been installed on all seismic stations in the USSR operating in seismic active regions. Both in field conditions and at seismic stations these instruments have been used to study a great number of earthquakes measuring 3 to 8 points at different regions of the USSR.

These instruments has been used to study intensive blasts in quarries and by highway construction as well as by excavating a reservoir of a hydroelectric power plant. The latter case requires a limitation on the number of charges to protect the power plant structures. Similar investigations for security against explosions have also been done on other sites.

The application of this method for studying the earthquakes and powerful explosions within the USSR has yielded a lot of data on spectral curves of the reduced seismic accelerations. These data have become a basis for carrying out a number of jobs on the design calculations of structures and for performing seismic zonation and microzonation of different areas.

References

NAZAROV, A.G. — A method of engineering analysis of seismic forces. Yerevan, Academy of Sciences, Arm. SSR (1959)

KARAPETIAN, B.K. — Multi-pendular Seismometers and the results of their application in engineering seismology. Yerevan, Haipetrat (1963)

NAZAROV, A.G.; KARAPETIAN, B.K. — The results of a complex study of the earthquake of Zangezur. Yerevan, Academy of Sciences, Arm. SSR (1973)

KARAPETIAN, B.K.; KARAPETIAN, N.K. — Effects of seismic forces on buildings and structures. Nauka (1978)

DOI: https://doi.org/10.2312/zipe.1983.078

Interpretation of Broad-Band Seismograms from the Gräfenberg Array: Examples

by

R. KIND [1)]

Broad-band data from the Gräfenberg Array are available since a number of years and an increasing number of seismological research projects have been carried out using these data. Experiences from a few of these projects are discussed in the following.

The Gräfenberg data from the Swabian Alb event on 3 September 1978 are the first example (KIND, 1979). Digital data processing techniques revealed a clear second phase between the P_n and the P_g phases, called sP_n. This phase has travelled from the source to the free surface as S-wave, was there converted to a P-wave and travelled the remaining path as P_n-wave. Theoretical seismograms have been used for the identification of this phase. This phase was also detected at a number of other events from the Swabian Alb. Depth phases like sP_n or pP_n have also been detected in the meantime in records of earthquakes from Northern Italy. The interpretation of these phases represents a great improvement in the accuracy of the source depth determination. Also in GRF earthquake records from the Swabian Alb and from Northern Italy was discovered a splitting of the P_g phase into two phases travelling with different velocities. This observation has not yet been interpreted.

The second example is the interpretation of phases in the P-wave group of events from the Chile-Peru area (KIND and SEIDL, 1982). Practically all GRF records of the largest events from the west coast of sourth Amerika have clear pP and sP phases, allowing a very accurate depth determination. The GRF broad-band data enable the detection of these phases in many more cases than they are reported in bulletins. An unidentified additional phase is also often discovered in GRF records from earthquakes of this region. Complete theoretical seismograms of a homogeneous earthmodel do not predict this phase. There are indications that this phase is related to the descending plate.

The third example are GRF records from Greek earthquakes. Most of these records have clearly two phases at the beginning, travelling with different velocities (RADEMACHER et al. 1983). The second phase was interpreted as reflection from the 400 km discontinuity. A new upper mantle model for South-East Europe is derived with the aid of theoretical seismograms. Again it was found that bulletin data, like epicenter co-ordinates and origin time, must be corrected for studies of this type. It is interesting that the amplitude of the reflection from the 400 km discontinuity is very weak in the northern part of the array for events from the Hellenic Arc. It is supposed that lateral inhomogeneities like the deep roots of the Alps could be responsible for that.

All these examples have shown that three main properties of the GRF data (digital, broad-band and array) greatly improve the information about the earth, which can be obtained from earthquake records.

---

1) Seismologisches Zentralobservatorium, Krankenhausstr. 1-3, D-8520 Erlangen, FRG

DOI: https://doi.org/10.2312/zipe.1983.078

References

KIND, R. — Observations of sP_n from the Swabian Alb earthquake at the GRF Array. J. Geophys. 45 (1979), 337-340

KIND, R.; SEIDL, D. — Analysis of broadband seismograms from the Chile-Peru Area. Bull. Seis. Soc. Am. 72 (1982), 2131-2145

RADEMACHER, H.; ODOM, R.I.; KIND, R. — The upper mantle structure under South-East Europe derived from GRF broadband records of Greek earthquakes. J. Geophys. 52 (1983), 7-17

How to Use Digital Data for Seismological Interpretation?

by

N. V. KONDORSKAYA [1)]

No summary received.

Acquisition and Storage of Digital Seismic Data at the Seismological Observatory Moxa/Jena

by

K. D. KLINGE [2)]

Summary

The signals of the 16 channels of the acquisition system at the seismological observatory Moxa/Jena are sampled with a rate of 20 cps. Data acquisition for each channel is carried out and all data are stored on magnetic disk for half an hour. Selected earthquakes are recorded on magnetic tape. The system records in multiplexed form with 20 samples per second three components of short- and intermediate-periode instruments and also two single vertical short-period components of a small array. The duration of the record is about 10 minutes. Additional intermediate-and long-period signals are stored with 1 sample per second for two hours.

1) Institute of Physics of the Earth of the Academy of Sciences of the USSR, B. Gruzinskaya 10, D-242 Moscow, USSR

2) Central Institute for Physics of the Earth of the Academy of Sciences of the GDR, DDR-69 Jena, Burgweg 11

DOI: https://doi.org/10.2312/zipe.1983.078

1. Introduction

In this paper we present the seismic data acquisition system of the station Moxa/Jena available today as well as existing software for digital data processing. First some common remarks to the recording of seismic events. Generally the bandwidth of seismic signals is small and the dynamic range is wide (140 dB). Usually seismic records are split into separate frequency bands obtained at different sensitivities. These frequency bands are choosen in that way to reduce the influence of seismic background noise and to optimize the conditions for signal recording. Three different types of seismological recording are presently used at the station Moxa, known as short-period, long-period and intermediate-period or broad-band recording. Techniques utilized for recording of seismological data are: visual recording on paper or photographic sheets, analog magnetic tape recording, and digital recording on magnetic tape. The dynamic range of the analog recording is only of the order of 40 dB. Thus, a photographic or analog magnetic tape record can cover only a small part of the whole range of the seismic signals. Analog-to-digital conversion systems with a dynamic range up to 120 dB are available today. For seismological purposes in countries with a low natural seismicity like the GDR, systems with a range of 96 dB or 16 bits can effectively be used. Our available dynamic range for short-period and intermediate-period digital data recording is shown at Fig. 1. The ground displacement in dependence of the frequency for analog recording is also shown. The most convenient way to record digital data is a computer compatible format on magnetic tape so that the data can be analysed on a digital computer. It is an actual disadvantage that different computers or data centres write tapes in a different format and with different data packing densities. More informations about this topic are given in the following paper.

2. Hardware for digital data acquisition

Now I will present a brief summary of the hardware of the digital data acquisition system. You have heared a more detailed discussion to this topic in the paper of TEUPSER. The whole system consists of the 4 different parts (Fig. 2):

1. The Seismological Station Moxa with its different seismometers and the equipment for analog-to-frequency conversion.
2. Two remote stations with one by one vertical short-period seismometer in seismic active regions at Posterstein and Plauen. The distance of each station to Moxa is about 50 km.
3. The 24 channel telephon system for data transmission. Frequency-modulated signals are continuously transmitted to the data recording centre in Jena.
4. The data collection and analysis facilities. The frequency-modulated signals are converted by frequency-to-digital converters into binary form. The word size is 16 bit integer format. The sampling rate of 20 samples/s is controlled by an electronic clock. Moreover, the clock delivers the time signals for the on-line data acquisition with the computer PRS 4000. Analog recording is possible, too. The on-line computer possesses a 32 K word core memory, three disk storages, two magnetic tape units for digital recording and the necessary peripherical equipment.

DOI: https://doi.org/10.2312/zipe.1983.078

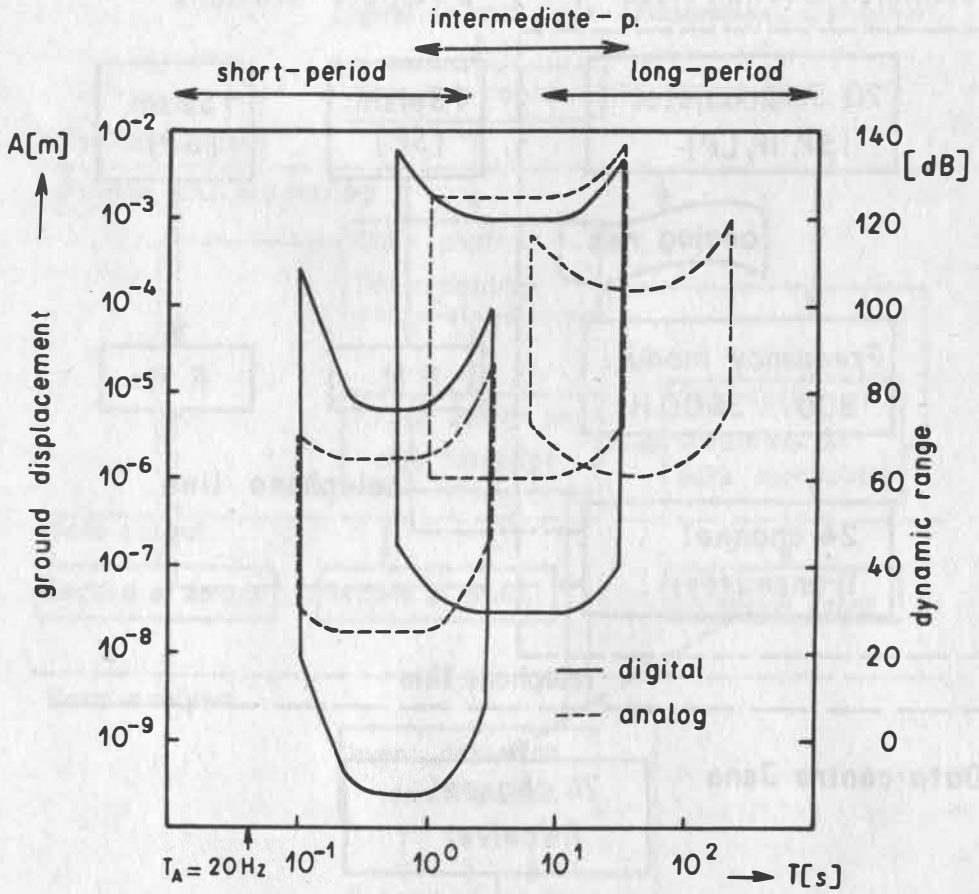

Fig. 1. Available dynamic range for the analog and digital recording of short-, intermediate- and long-period seismic data at the Seismological Station Moxa

3. Software for digital data acquisition

At present the computer is connected with 16 seismic channels. The used sampling rate of 20 samples/s implies all together a data flow of 320 samples/s. A special order for the operation of the computer is necessary to avoid loss of data. The priority of the separate routines is the following (Fig. 3):

1. The receiving of digital data from the frequency-to-digital converter.
2. The on-line data processing of primary data. That means:
   - Data control, dimensioning and reduction,
   - Watching the breakdowns of channels,
   - Continuous time control.
3. Building trace buffers for every channel on the disk storage for half an hour.
4. Data output with records of seismic data, errors and dimension constants.

DOI: https://doi.org/10.2312/zipe.1983.078

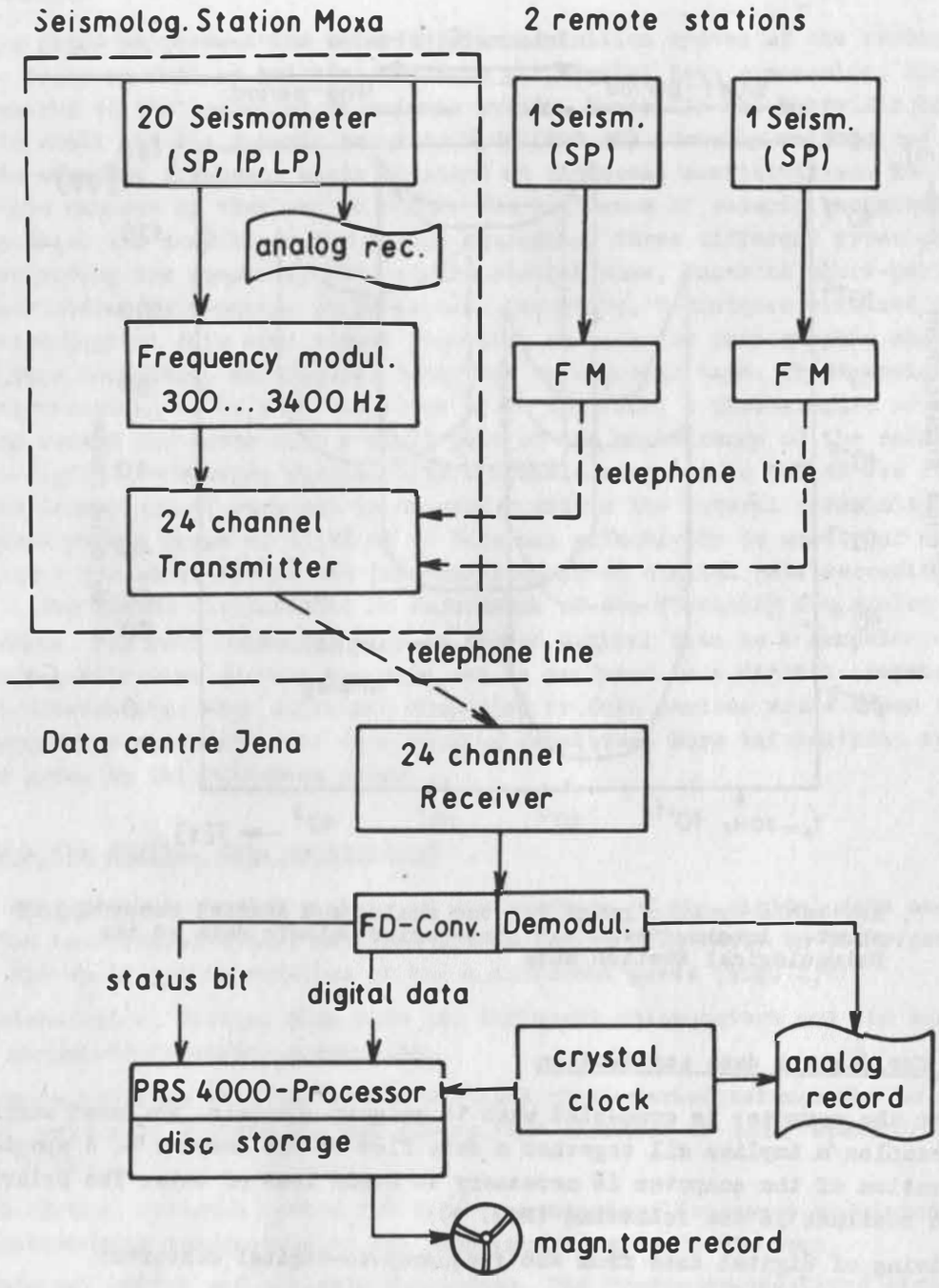

Fig. 2. Digital data acquisition system of the Seismological Observatory Moxa/Jena. The whole system consists of the 4 parts: 1. the Seismological Station Moxa, 2. two remote stations, 3. the data transmission system and 4. the data collection and analysis facilities

DOI: https://doi.org/10.2312/zipe.1983.078

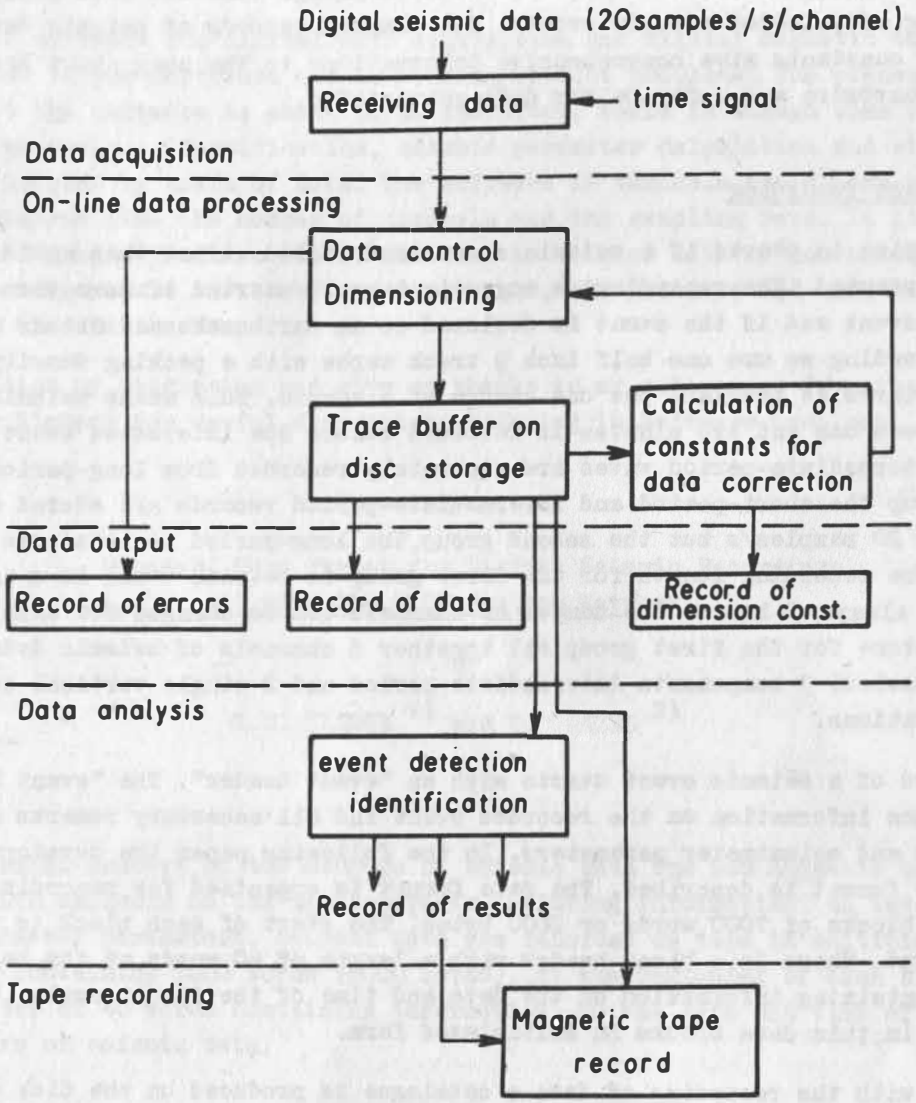

Fig. 3. Digital data acquisition and on-line data processing with the computer PRS 4000 at Jena

5. Data analysis with the separate tasks:
   - Event detection,
   - Event identification,
   - Calculation of the seismic parameters like magnitude and so on and
   - Deciding for event recording on magnetic tape
6. Recording of selected seismic data on tape.
7. Off-line data analysis.
8. Programme test.

The most important task for the on-line work of the processor is the digital data acquisition. Data can be lost if there is a delay in operation. As after receiving all

DOI: https://doi.org/10.2312/zipe.1983.078

data are stored on disk for half an hour, there is enough time for data analysis and tape recording of selected seismic events. The printed records of seismic data, errors and dimension constants give comprehensive informations to the user about the function of the whole hardware and software for data acquisition.

4. Magnetic tape recording

The onset time is stored if a seismic event is detected. After that an identification procedure is started. The recording on magnetic tape is started if more than one station triggers the event and if the event is declared as an earthquake and not as near explosion. For recording we use one half inch 9 track tapes with a packing density of 800 bpi. Each record starts at the last but one change of a minute. This means seismic noise with a length between one and two minutes is recorded before the interested event. Short-period and intermediate-period waves are separately recorded from long-period ones. As the first group the short-period and intermediate-period records are stored with a sampling rate of 20 samples/s but the second group,the long-period records, are stored with 1 sample/s. The recording length for the first group is between 4 and 22 s and for the second group always 2 hours. The number of channels can be changed for each group. Recently we store for the first group all together 8 channels of seismic data - 3 components short-period, 3 components intermediate-period and 2 single vertical components of the remote stations.

Each record of a seismic event starts with an "event header". The "event header" contains common information on the recorded event and all necessary remarks about the used stations and seismometer parameters. In the following paper the development of this standard tape format is described. The data format is organized for recording on tape in fixed-length blocks of 1000 words or 2000 bytes. The start of each block is signalized by an interrupt. There is a block header with a length of 40 words at the beginning of each block containing information on the date and time of the first sample. Seismic data are arranged in this data blocks in multiplexed form.

Connected with the recording of data a catalogue is produced on the disk storage. This catalogue contains the date and time of the beginning of the record, the file number and the number of blocks. Additional informations belonging to the event like localization, magnitude, depth of the seismic source and so on can be stored later. The number of records storeable on one tape is about 150. That means it is possible to store data of a few weeks on one tape. The digital data processing system is exclusively used for scientific purposes. For this reason only about 1/3 of all recorded seismic events is stored on tape. The start point for tape recording was in June 1982.

We have independently developed the necessary programme system for magnetic tape recording. Programmes exist for short- and long-period recordings, for data transfer to a second tape, programmes for tape reading and tape handling.

DOI: https://doi.org/10.2312/zipe.1983.078

5. Conclusion

The whole software for digital data acquisition and digital magnetic tape recording was developed in our institute and is working without problems. The processing time of this part of the software is about 30 %. Therefore, there is enough time for such tasks like event detection, identification, seismic parameter calculation and other tasks desired to process by users of data. The software is variable and allows to change different parameters like the number of channels and the sampling rate. It is possible to receive data of more than two remote stations as well as data of non-seismic measuring points like temperature in the seismometer vault, air pressure and wind velocity in the vicinity of the station Moxa.

Now I finish my discussion and give my thanks to my colleagues from the Geomagnetic Observatory Niemegk for useful discussions refering to software problems.

Standard Tape Format for Digital Seismic Recordings with the CIPE Station Network

by

K.D. KLINGE [1] and H. GÜNZEL [2]

Summary

After a brief summary of the storage of seismic data the GDR magnetic tape format is discussed with emphasis on the various parts including information on the stations and their seismometer parameters. Seismic data are recorded on tape in multiplexed form in data blocks containing 1000 words (2000 bytes). At the beginning of each block there is a block header of 40 words containing information on the date and time of the record and on errors of seismic data.

1. Introduction

A lot of high quality seismic data are produced by the seismological stations or arrays especially in Europa and North-America. Most of them are recorded in analogue form on photographic sheets or paper. For this kind of record there is a high degree of standardization. Nowadays, the use of digital measuring and data processing techniques is rapidly expanding in seismology and it is common to store seismic data on computer tape. But it is not trivial to use data from other institutions due to different tape and data formats. To simplify data exchange, it is necessary to have a common standard. Existing data formats differ from institute to institute due to different requirements with respect to the number and type of the data acquisition instruments

1) Central Institute for Physics of the Earth of the Academy of Sciences of the GDR, DDR-69 Jena, Burgweg 11

2) Central Institute for Physics of the Earth of the Academy of Sciences of the GDR, DDR-1500 Potsdam, Telegrafenberg

DOI: https://doi.org/10.2312/zipe.1983.078

and the special interest of the institutitions regarding local, regional or teleseismic events. This results in different sampling rates between 100 samples/s and 1 sample/s. The format of the data word and the dynamic range is different, too. Some selected digital recording stations are shown in the first table. Most of the stations have short-period and long-period and in two cases intermediate-period recordings. Broad-band recording is used as well. Long-period and broad-band digital data are common recorded continuously, but the short-period digital data are recorded only for triggered events. After a few years magnetic tapes are erased, and only recorded seismic events of common interest are stored.

2. Description of the tape format

For the CIPE station network a flexible standard magnetic tape format for digital seismic recordings was developed which easily accomodates certain differences in digital data acquisition at the central recording facility at Potsdam on the one hand and for the Moxa/Jena subsystem which is connected with the main seismological observatory on the other hand. Due to certain differences in the tasks to be performed by the centralized system and the subsystem the number of channels, sampling rate, time code and the type of computers used differ. Therefore, it is not practicable to standardize the digital data record itself, but rather the tape format and the "event header". This fully guarantees the mutual exchange and use of the digital data within the whole system.

It was not our aim to produce a completely new format but rather to follow the basic lines of internationally well proven concepts such as the "network day tape" or "GRF tape" format. Our format is a generalized one. It satisfies many demands with respect to different primary instruments, station arrays and so on. In detail it enables:

1. the continuous recording of seismic signals
2. the recording of selected events
3. the recording from a single station with different components
4. the recording from several stations or arrays over telemetry equipments on one tape
5. the recording of different sampling rates for short-period and long-period signals
6. to store all necessary annotations from all stations recorded on the tape. The tape does not require any accompanying information except the basic description of its format.
7. to marke datas with wrong samples.

In the following we will discuss our common tape format with emphasis on the various parts included in the tape (Fig. 1).

The first recording on every tape is a descriptive tape header with general information and the catalogue listing of the events recorded on the previous tape. The "event header" is located at the beginning of every new event and contains specific information on that particular seismic event and recording parameters (Tab. 2). It contains the number of the tape and of the event on tape as well as a descriptor for the type of the record. That means an identification mark for short-period or long-period recording. It follows the date and time of the first sample on the record. After that the "event header" contains a description of the data record including the number of words in the

DOI: https://doi.org/10.2312/zipe.1983.078

Table 1: Selected digital data recording stations

Station network	Dyn.range [dB]	Tape recording	Period	Sample/s	Recording	
SRO + ASRO	126	digital 1600 bpi	SP	20	event triggered	"network day tape"
			LP	1	continuously	
DWWSSN	96	digital 1600 bpi	SP	20	event triggered	
			IP	10	event triggered	
			LP	1	continuously	
IFZ Moskva/OBN	60	digital 800 bpi	SP	40	continuously → event selected	
PUL/OBN	60	digital 800 bpi	LP	5	continuously → event selected	
NOTSSJ/Bulg.	ca.100	digital 800 bpi	SP	50	event triggered	
ROMSNET/Romania	ca.100	digital 1600 bpi	SP	50	event triggered	
GRF-Array	132	digital 800 bpi	BB	20	continuously	
NORSAR	100	digital 1600 bpi	SP	20	continuously → event selected	
			LP	1(0,5)	continuously	
HAGFORS	120	digital	SP	20	event triggered	
			LP	4	continuously	
SLEN (SKJ)	120	digital	SP	60	event triggered	
FIN SEIS. ARRAY	72	digital 1600 bpi	SP	25	continuously → event selected	
GJ Praha	80	FM → dig.800 bpi	BB			
IPG Strasbourg	60	digital	SP	90		
	80	digital	BB	1	continuously	
CIPE MOXA/JENA	ca.120	digital 800 bpi	SP	20	event triggered	
			IP	20	event triggered	
			LP	1	event triggered	

Table 2: Format of "event header"

Word	Content	Format
1	Tape number	I = Integer
2	Number of event on tape	I
3	Identification: SP ⇒ 1, LP ⇒ 2	I
4 - 9	Start of the record - date and time	I
10, 11	unused	
12	Words per block	I
13	Words per block header	I
14	Number of seismometer	I
15	Number of data samples per seismometer per block	
16	Sampling rate (20 Hz resp. 1 Hz)	I
17 - 49	Order of seismometer data stored in the data block (word 17 contains number of 1st seismometer)	I
50 - 51	Station code of 1st seismometer	ASC II
52	Component 1st seismometer	ASC II
53 - 57	Latitude, longitude, elevation 1st seismometer	I
58 - 131	Nominal parameter 1st seismometer	I
50+(k-1)x82	1st word station code kth seismometer	ASC II

DOI: https://doi.org/10.2312/zipe.1983.078

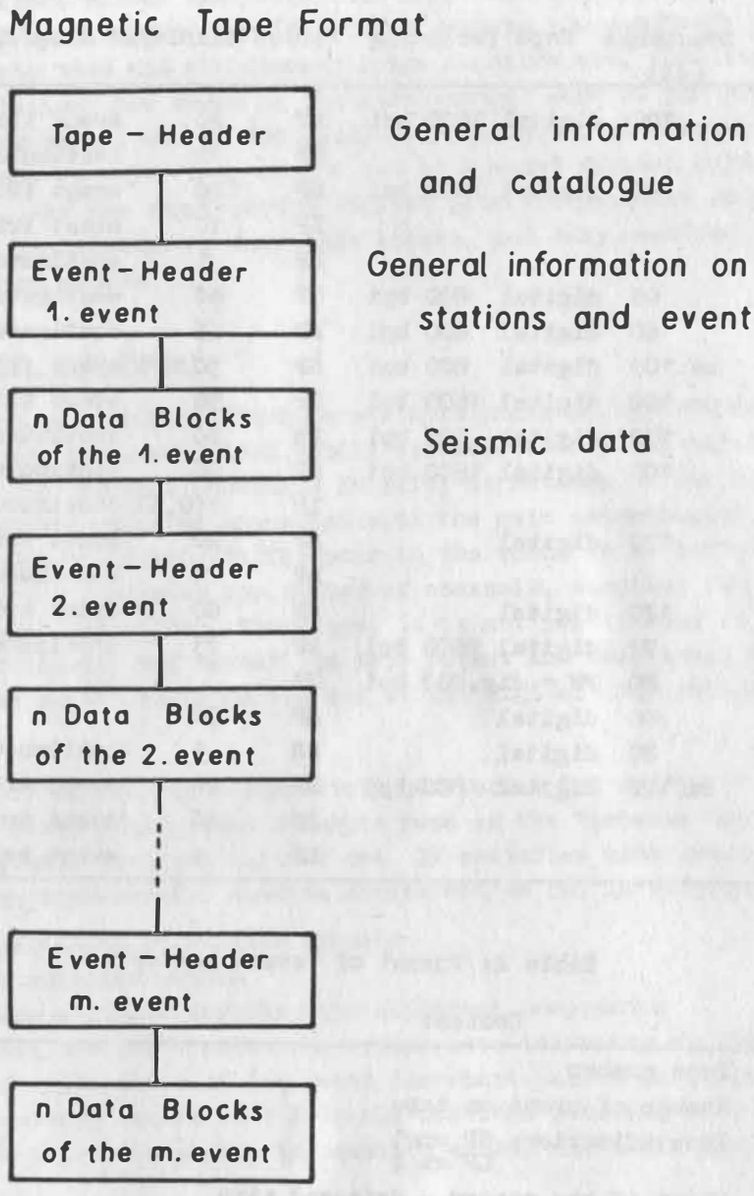

Fig. 1. Common magnetic tape format for digital seismic recordings with the CIPE station network

following data blocks and in the data block header, the number of seismometer, sampling rate, and the order of seismometer data stored in the data block. The station code of the first seismometer stored in the data blocks is written on word 50. It follows the seismometer-component, and the coordinate and elevation of the first seismometer. Calibration data for each channel are followed by detailed information on the complex transfer functions. This includes a listing of all the complex poles and zeros, both real and imaginary. After that the parameters of all other seismometer stored in the data block follow.

DOI: https://doi.org/10.2312/zipe.1983.078

Seismic data are recorded in data blocks. n data blocks for one event are data block. Seismic data are recorded in data blocks. n data blocks for one event are arranged one after another behind the "event header". The block length at the subsystem Moxa/Jena is 1000 words or 2000 bytes. The first 40 words of every block contain header information. Fig. 2 is a listing of the specific data contained in each "block header" word. Word 1 through 3 contain the number of event, the number of the actual block and a flag to identify between short-period and long-period recording. Word 4 through 9 contain the exact date and time for the start of the record. Word 10 through 40 contain error information or loss of data for each of the channel. At present only 8 channels are connected and consequently only word 10 through 17 is used. 960 words contain multiplexed seismic data. The first data word is arranged at word 41. On the understanding of an 8 channel recording each block contains 6 s of data for short-period recording with a sampling rate 20 sample/s and 2 min of data for long-period recording with 1 sample/s. The number n of blocks depends on the recording-length for the seismic event. Data blocks on tapes of the centralized CIPE network are different. They contain no block header. The block length is 1024 words and data are stored from 7 channels.

3. Conclusion

We have developed a generalized standard tape format for digital seismic data recording. We followed the basic lines of internationally well proven concepts. This standard tape format realizes fundamental demands:

1. Multiplexed seismic data are stored continuously or event triggered in fixed length data blocks with sampling rates of 20 samples/s for short-period and 1 sample/s for long-period recording.
2. The dynamic range encloses with its maximum value of 96 dB the occuring ground displacement.
3. An "event header" is recorded at the beginning of every new event. It contains specific information on that particular seismic event and the seismometer and recording parameters. The "event header" is standardized.
4. For tape recording we use 1/2 inch 9 track magnetic tapes with a packing density of 800 bpi.

References

PLEŠINGER, A. — Report on the analysis of EDSNET questionnaires. Paper held at the 17th Assembly of the ESC, Budapest (1980)

HOFFMAN, J.P. — The global digital seismograph network-day-tape. U.S. Geol. Survey Open-File Rept. (1980), 80-289

HARJES, H.-P.; SEIDEL, D. — Digital recording and analysis of broad-band seismic data at the Graefenberg (GRF)-array. J. Geophys. 44 (1978), 511-523

DOI: https://doi.org/10.2312/zipe.1983.078

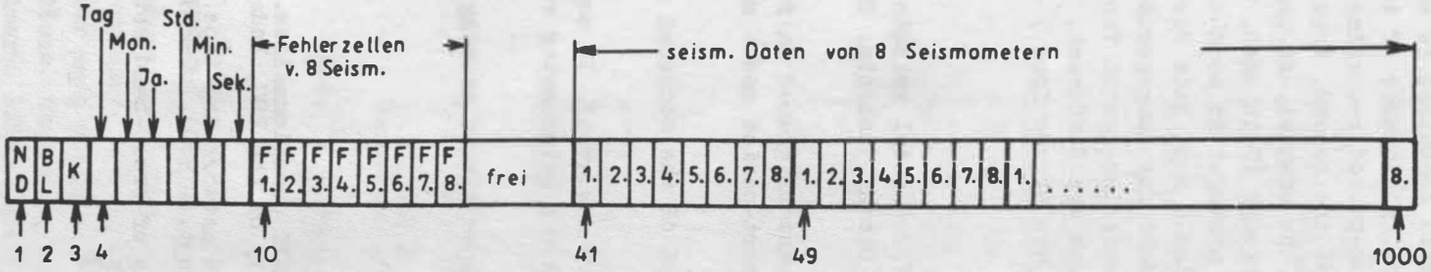

Blockaufbau Magnetbanddatei

1 Block = 1000 Worte

8 Meßstellen, Registrierzeit = 6 s

ND = Nummer der Datei

BL = Blocknummer

K = Kennzahl: kurz.- u. mittelperiod. Seism. = 1

langperiod. Seism. = 2

Fig. 2. Listing of the specific data contained in each block

DOI: https://doi.org/10.2312/zipe.1983.078

Erfahrungen mit einem seismischen Datenfernübertragungs- und Interface-System

von

S. KÜHNERT [1)]

Summary

A report is given on experience with the hardware of that seismic data transmission and acquisition system represented in a paper in Nov. 1977 at Liblice (Czechoslovakia). The remote data transmission with the aid of telephone channel equipped with carrier frequency systems is connected with confinements in the dynamic range of seismic events due to the distortion of sinusoidal waveform. It is under discussion, how to overcome these difficulties.

1. Prinzip des Systems

Die gesamte Einrichtung wurde bereits auf dem Symposium im Nov. 1977 in Liblice/ČSSR vorgestellt. Die in der Station Moxa anfallenden seismischen Daten werden in Form einer Niederfrequenz geliefert, die gerade einen Telefoniekanal (300...3400 Hz) besetzt. Diese Frequenz ist dem Ausschlag des Seismographen proportional (vorzeichenbehaftet). Durch Auszählen ganzer Perioden in einem vorgegebenen Zeitintervall (40 ms) mit einer hohen Frequenz (3,75 MHz) und anschließender Division (f = 1/T) wird im Interface ein 16-Bit-Wort generiert, das in einem Prozeßrechner PR 4000 verarbeitet wird. Die Anlage ist 1980 in Betrieb gesetzt worden.

2. Ergebnisse

Ein Test der Interface-Einrichtung mit Hilfe eines Präzisions-Niederfrequenzgenerators zeigte die erwarteten Ergebnisse, insbesondere die verlangte Auflösung mit einer Genauigkeit $\leq 10^{-4}$, wobei die Temperatur des Basis-Quarz-Generators in einem Thermostat stabilisiert wurde. Störungen durch Einflüsse der Netzfrequenz wurden erwartungsgemäß wegen der Nullstellen in der Übertragung von 25 Hz und vielfachem davon nicht beobachtet.

Der Anschluß des Interface an die Übertragungsstrecke brachte jedoch selbst bei arretiertem Seismographen eine nicht zu vernachlässigende langperiodische Störung. Diese wird im postalischen Übertragungssystem erzeugt, wenn dabei Trägerfrequenzeinrichtungen beteiligt sind, deren Muttergeneratoren für Modulation und Demodulation nicht synchronisiert sind. Die übliche Umsetzung der Niederfrequenz f_o mit einer Trägerfrequenz f_c erzeugt eine Frequenz f_T

$$(1) \quad f_T = f_c + f_o \,.$$

Nach der Rück-Umsetzung mit einer Trägerfrequenz $f_c \pm \Delta f_c$ ergibt sich eine Niederfrequenz f_o':

[1)] Zentralinstitut für Kernforschung Rossendorf, DDR-8051 Dresden, PF 19

DOI: https://doi.org/10.2312/zipe.1983.078

(2) $f_o' = f_c - (f_c \pm \Delta f_c) = f_o \pm \Delta f_c$.

Dieser additive Frequenzversatz verursacht jedoch außer einer geringen Nullpunktverschiebung keine bemerkenswerten Störungen; jedoch eine Anwendung der Formeln (1) und (2) auf Oberwellen $K \cdot f_o$, die einmal durch den nicht idealen Sinus der Modulationsschaltung des Seismographen, andererseits durch Verzerrungen im Übertragungskanal selbst vorhanden sind, ergibt:

(3) $K \cdot f_o' = K \cdot f_o \pm \Delta f_c$, $\quad K = 2, 3, \ldots$,

$\neq K (f_o \pm \Delta f_c)$.

Es zeigt sich also, daß die "Oberwellen" nach der Demodulation keine harmonischen (ganzzahlige Vielfache) Frequenzen der Grundfrequenz sind und somit einen Phasenjitter verursachen, der als virtuelle Bodenbewegung erscheint, weil die Schwankung Δf_c durchaus im Frequenzbereich seismischer Ereignisse liegt.

3. Folgerungen

Um die Anlage in der geplanten Weise betreiben zu können, müßten folgende Bedingungen erfüllt werden:

- extrem verzerrungsarmen Sinus vom Modulator des Seismographen einspeisen,
- extrem geringe nichtlineare Verzerrungen des postalischen Übertragungssystems durch Eingabe möglichst niedriger Pegel.

Da gegenwärtig noch keine endgültigen Ergebnisse vorliegen, wie am Modulator des Seismographen ein Sinus erzeugt werden kann, der den Forderungen genügt, wurde so verfahren, daß Oberwellen automatisch in den Sperrbereich des Übertragungsweges fallen. Das heißt, daß für die Übertragung nur die obere Hälfte des Frequenzbandes eines Fernsprechkanals ausgenutzt werden kann. Damit werden der mögliche Frequenzhub und der Dynamikbereich halbiert.

Sobald ein genügend verzerrungsfreier Modulator zur Verfügung steht, werden neue Versuche zur vollen Ausnutzung des Dynamikbereiches durchgeführt. Der Übertragungspegel ist dann so zu wählen, daß einerseits ein ausreichender Abstand zum Störpegel des Kanals eingehalten wird, andererseits die Verzerrungen des Kanals keine Fehler verursachen.

DOI: https://doi.org/10.2312/zipe.1983.078

Maximum Likelihood Localization of Near Seismic Events

by

R. MAAZ and H. NEUNHÖFER [1)]

Inspite of many qualified solutions of the old and important problem to find focal co-ordinates and time seismologists seak still today for new and better solutions. There are no fundamental difficulties to solve this inverse problem. The main task consists in choosing an algorithm due to the special kind of data, due to the available earth model, due to computing facilities, and finally due to some practical requirements, e. g. to find the solution very rapidly or very precisely.

For our problem focal co-ordinates are more interesting than focal time. Therefore, focal time is treated as a parameter and the most probable focal co-ordinates are sought on base of the observations. Assuming that the observations are statistically independent the probability density to meet them is given by the product of the Gaussian distribution functions of the single observations. The product is a function of the focal parameters. It reaches a maximum if the formal parameters get the value of the true ones.

Step by step some routines are written. One of them allows us to locate crustal seismic events by means of time differences Sg-Pg, Sn-Pn, and Sg-Pn using local travel time curves. It was applied to earthquakes occurring at the boundary of the GDR and the ČSSR. A cluster of tectonical interest was found. Assuming that all stations yield observations of the same variance we are able to compute at any point at the earth's surface an error ellipse for a given probability (e. g. 90 %). The resulting ellipses depend on the configuration of the station network, the relative position of the focal point and the confidence level choosen. The major axis reflects the actual cutting of WATATI's circles.

A special routine combines former observations with azimuthal data. Another one demonstrates the use of P-waves observed by 3-dimensional arrays, e. g. in mining districts. Nowaday, a routine was developed for crustal events including azimuthal information, time differences Sg-Pg, Sn-Pn, Sg-Pn, arrival times of Pn, Sn, Pg, Sg, P, PP, S, SS, and for the first approximation the time of Rayleigh wave maximum, too. Travel times are computed by polynomials. Computation of focal depth is not yet included. After computing an error ellipse, all actual time data are checked on base of the result. In case of relatively large deviation the concerned observation is eliminated at least for the next step of computation. Unclear observations can be interpreted otherwise. Originally undefined or later eliminated information is checked, too, with respect to wave groups provided within the programme.

---

1) Central Institute for Physics of the Earth of the Academy of Sciences of the GDR, DDR-69 Jena, Burgweg 11

DOI: https://doi.org/10.2312/zipe.1983.078

Laterally Variable Velocity of Seismic Surface Waves

by

R. MAAZ [1], H. NEUNHÖFER [1], T.B. YANOVSKAYA [2], D. GÜTH [1]

Summary

For investigating the earth's crust and upper mantle the frequency depending field of surface wave velocities is of interest. The first step is to determine phase or group velocity dispersion for different traces. On base of such results the velocity field for the area covered by enough traces is determined using Yanovskaya's method. An example is discussed.

Identification of Seismic Events by Computer

by

H. NEUNHÖFER [1]

Summary

A characteristic vector is defined for every detected event. It characterizes the observed amplitudes, periods and the seismogram pattern at two nearby seismic stations. Then, the classification of the investigated events is carried out by algorithms found heuristically. The accuracy of this procedure is limited to around 75 % but an improvement is possible by the use of mathematical statistics.

The detection described in detail by BURGHARDT (1983) gives information that a signal possibly coming from a seismic event arrives at the sensor. A succeeding step is to decide what kind of source causes the detection. It is realized by the so-called identification which is a classification procedure applied to the detected signal.
The meaning of such work is

- that the identificator is a qualified trigger,
- that it is the alternative to a continuous recording on magnetic tape with event selection "by hand" later on.

The realization of any classification depends

1. on the defined purpose,
2. on the used sensors (and the computer facilities),
3. on the variety of recorded events.

---

1) Central Institute for Physics of the Earth of the Academy of Sciences of the GDR, DDR-69 Jena, Burgweg 11

2) University of Leningrad, Institute of Physics, Stary Petergof, Streat of the First of May, 100

DOI: https://doi.org/10.2312/zipe.1983.078

The purpose which we have in view in our case is to find false detections, to classify into geophysically relevant subsets (for starting automatically reactions), to reduce the data volume by constructing parameter matrices, and to compile listings of events (very simple bulletin).

The sensors used are a three component set of short-period seismographs at the seismic station MOX and a short-period vertical seismograph at the 57 km distant substation PST. The maximum magnification is choosen to 100 000 for each sensor. Events which can bring out detection are earthquakes, blastings, calibration pulses, instrumental caused interference, and strong noise.

The view of the paper is to classify a set of detected signals into 10 subsets. We have to distinguish between physical and algorithmical classification. The physical one corresponds to the real source of each event and the second one reflects its approximative realization by certain rules. The final intention should be to make equal algorithmical and physical classification. Classification is realized by rules found in the process of discrimination. Most rules used up to now by us are designed ad hoc taking into account the experience of seismologists. For improving it will be necessary to overcome it by introducing statistical discrimination. In Fig. 1 the used classification tree is shown. It consists of two parts, the description of the condition of the sensors and the proper classification. The condition part is described at top. If classification is possible, that means at least one sensor works well, we decide at first between small and large events, calibration pulses and interference pulses. Then, from small events false detections caused by strong microseisms are ruled out and the rest of it is classified together with the large events into the sets earthquakes, quarry blasts, events near MOX, and near PST. Some events are typical ones, they are to classify by additional rules as earthquakes and quarry blasts. It is worth to mention that by using simple rules further subsets can be defined as demonstrated for events near MOX.

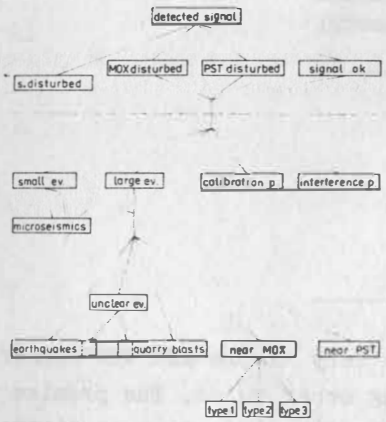

Fig. 1. Used classification tree

The classification bases on the determination of parameters found in two 60 and 64 s long windows covering noise and the signal, respectively. They are positioned relative to the detection time. The noise window begins 3 minutes before it and the signal window 20 s before detection time. Most of the used classification parameters are determined in both windows for short-period vertical seismographs at MOX and PST. In detail they are

AMAX - the maximum amplitude
TMAX - the adjacent period
ZEIT - time of AMAX
AMIT - mean of the absolute values of the five largest negative and five largest positive amplitudes in each window $(0.1 \sum_{i=1}^{10} A_i)$
TMIT - mean of the adjacent periods
LEX - time rank number of AMAX in A_i

DOI: https://doi.org/10.2312/zipe.1983.078

TBER - time range defined by the position of A_i in time
ABER - amplitude range defined by values A_i
MAFFI - metric affinity in comparison with a simple model
AZ - azimuth
P_i - estimation of the power spectrum

As example a first approximation of the discrimination rules between earthquakes and blasts are discussed. They are defined in the plane spanned by TMIT and $|TBER_{mox} - TBER_{pst}|$. The first decision is: if

(1) $TMIT_{mox} \leq 0.8$ s or $TMIT_{pst} \leq 0.8$ s

than the source of the event is a blasting. Another decision says, if

(2) $TMIT_{mox} \geq 1.4$ s or $TMIT_{pst} \geq 1.4$ s

than the source is an earthquake. Events in the intermediate range need the further rule

(3) $|TBER_{pst} - TBER_{mox}| > 100$

as the condition for a blast. The power of these rules is demonstrated for different epicentral distances Δ in the following table:

Table 1

epicentral range	percentage of successful classification
$\Delta =$ 0 - 5°	0
5 - 10°	22.2
10 - 20°	71.4
20 - 50°	75.0
60 - 100°	82.4
130 - 162°	96.5

It is necessary to note that the discrimination rules are very simple and the author feels that it is possible to improve the success by adding other rules. The premise is a collection of a number of events great enough to apply discrimination statistics.

Another example demonstrates how different sources can be classified in the plane (AMAX, AMIT). As we see in this plane monitored in Fig. 2 the events of the class "near MOX" form three chains defined by the conditions 1 to 3. Each chain contains events from one quarry only. This result should be interpreted as the possibility to classify series of events with approximately equal foci.

The program system developed for classification is given in Fig. 3. Classification is started by the detector routine SMEL, it follows the calculation of the parameters (NVM) and the azimuth (AHK). The real classification is carried out by NK which starts the estimation of the power spectrum (PS) and the output of the classification results (NKAU). A second branch contains service routines like NKEB, which allows us to indicate the number of classifications at the current day, NTLI for printing the daily classifi-

DOI: https://doi.org/10.2312/zipe.1983.078

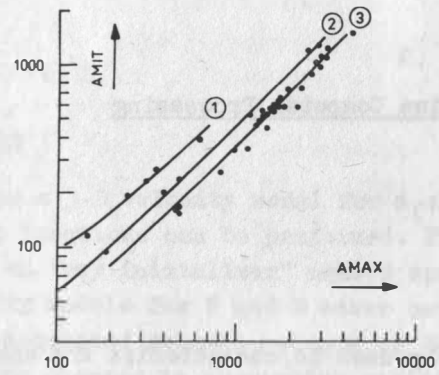

Fig. 2. Subclassification of the class "near MOX"

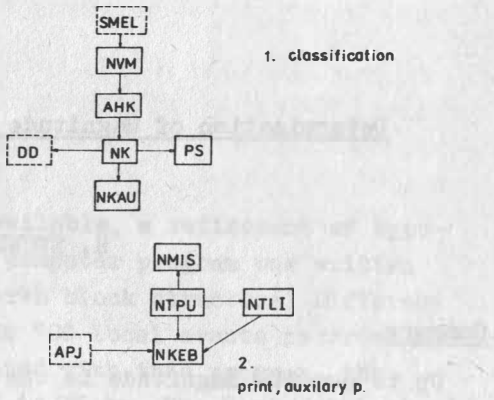

Fig. 3. Program system for classification

cation list as simple bulletin and NTPU which prints the matrices of each event. A last routine NMIS describes in a simple manner the microseismic status for each day.

The success of the classification procedure shows Table 2. Vertically the computer decision is given, horizontally the man made decision. Therefore, the diagonal terms gives the successful classification numbers and other terms gives the numbers of misclassifications. When we exclude nonserious misclassification like blast-near MOX and blasts-near PST the confidence we may put into the ad hoc discrimination results is 73 %. This seems to be near the upper bound of the ad hoc discrimination and for improving statistic discrimination must be introduced in future.

Table 2

computer cl.	seismological class. 1.	2.	3.	4.	5.	6.	7.	9.
1. earthquake	32	43	1	-	10	5	2	9
2. blast	23	224	12	1	4	4	9	6
3. near MOX	-	-	22	-	-	-	-	-
4. near PST	-	-	-	5	-	-	-	-
5. calibr. p.	-	11	-	-	17	-	-	-
6. interference	-	-	2	-	-	14	-	-
7. noise	-	-	-	-	-	1	-	-
8. not classif.	-	2	-	-	-	-	1	-
9. calibr. fr.								
10. undefined								

DOI: https://doi.org/10.2312/zipe.1983.078

Reference

BURGHARDT, TH. Real-time detection of seismic signals. (1983), this volume

Determination of Magnitude by Means of Real-Time Computer Processing

by

H. NEUNHÖFER, J. STELZNER [1)]

Summary

Up to now the magnitude is that number most oftenly used to characterize the energy released by an earthquake. Outstanding steps in developing the magnitude definition are the definition as a matter of fact by GUTENBERG (1956), the improvement of the calibration function by VANĚK and STELZNER (1960), and the introduction of the homogeneous magnitude system by CHRISTOSKOV et al. (1979).

The magnitude is defined by the Manual of Seismological Observatory Practice (1979). That definition is especially useful for the seismological interpreter which reads analog seismic records. For the determination applicable to a real-time computer other more adapted procedures must by developed. Therefore, the so-called maximum and the mean magnitude are defined. The maximum magnitude is calculated from the maximum amplitude observed in a 64-s-long window after the onset and the adjacent period, the mean magnitude follows from the absolute values of the five largest positive and five largest negative amplitudes which occur in the window and from the adjacent mean period.

Classical and here defined magnitude are compared for two nearby stations (MOX and the substation PST). It was found, that in the mean classical and maximum magnitude are equal and that the mean magnitude differs from the maximum one by an almost constant level.

A special investigation deals with the comparison of the mean magnitude of MOX and PST for a set of earthquakes. It can be shown that the accuracy of the mean magnitude is improved significantly compared with the classical magnitude, so that the difference between the mean magnitudes for MOX and PST show clearly distant dependent effects in the epicentral range where core phases of P-waves occur. A detailed paper will be published later on in Gerlands Beiträge zur Geophysik.

References

GUTENBERG, B.; RICHTER. C.F. Magnitude and energy of earthquakes. Annali di Geofisica 9 (1956) 1, 1-15

VANĚK, J.; STELZNER, J. Einheitliche Bestimmung von Erdbebenmagnituden für mitteleuropäische Stationen. Travaux Inst. Geophys. Acad. Tchecosl. Sci., Geofyzikalni sbornik 136 (1960), 299-399

CHRISTOSKOV, L.; KONDORSKAYA, N.V.; VANEK, J. Homogeneous magnitude system of the Eurasian Continent: P waves. World Data Centre A for Solid Earth Geophysics, Report SE-18 (1979)

1) Central Institute for Physics of the Earth of the Academy of Sciences of the GDR, DDR-69 Jena, Burgweg 11

DOI: https://doi.org/10.2312/zipe.1983.078

Hypocenter Location of Local Events in 3-D Structures. Application to Vrancea Seismic Region

by

M. C. ONCESCU [1)]

Summary

Once a 3-D velocity model for a seismic region is available, a refinement of hypocenter locations can be performed. For this purpose, a computer program was written based on "ray initializer" method applied for a flat-earth block structure. Different velocity models for P and S waves can be used. More than 100 local events recorded by the telemetered seismic network of Romania were re-located with this program, the absolute changes in hypocenter positions varying from 5 to 25 km. The horizontal standard errors decreased by a factor of 2 and the depth standard errors by a factor of 10. The overall reduction in station delays is also of a factor of 10. The very little more effort in computations is thus justified by the accuracy of locations.

1. Introduction

By far the oldest inverse problem in seismology, the hypocenter location is now routinely performed in many seismological centers all over the world. The hypocenter location problem get again the attention of seismologists, once 3-D velocity models for certain seismic regions became available and, thus, the refinement of the 4 hypocenter parameters became possible. Accurate hypocenter locations are important not only for monitoring crustal active faults, but also for tectonics of deep structures.

A simple method to routinely locate local events in a 3-D flat-earth block structure will be presented, together with an application to 119 earthquakes occured inside a 10-telemetered seismic station network surrounding Vrancea region.

2. Method

To solve the non-linear inverse problem for hypocenter parameters, the standard Geiger method is used. Written in matrix form, the first order Taylor expansion of the arrival time will be

$$A\Delta x = \Delta T \qquad (1)$$

where ΔT is the $(N \times 1)$ vector with the $(O - C)$ residuals, Δx is the (4×1) vector with the changes in hypocenter parameters, A is the $(N \times 4)$ condition matrix with partial derivatives of travel time with respect to the 4 hypocenter parameters and N is the total number of observations.

Usually, the system (1) is overdetermined, its solution being computed by a least-squares procedure

$$\Delta x = H\Delta T = (A^T A)^{-1} A^T \Delta T \; . \qquad (2)$$

---

1) Central Institute of Physics, Center of Earth Physics and Seismology, P.O. Box MG-2, Bucharest-Măgurele, Romania

DOI: https://doi.org/10.2312/zipe.1983.078

Several iterations are required to converge to the "correct" solution, which is obtained when the squared sum of residuals is less than a prespecified minimum or when the changes in hypocenter parameters are less than prespecified values.

To take into account the lateral velocity variations, the "ray initializer" method is used (THURBER and ELLSWORTH, 1980). The ray tracing is performed in one-dimensional structure (flat-lying layers of constant velocity) and the partial derivatives are computed for this ray path. The travel time is then accumulated on this approximate path, but using a three-dimensional block velocity structure. Fermat's principle impliing this will give second order error in travel time calculation and first order error in partial derivative evaluation; the latter is expected to be a small effect (SPENCER and GUBBINS, 1980).

The procedure was programmed in FORTRAN IV language in program HYPO3 (ONCESCU and SMALBERGHER, 1982). This program can use different P- and S-wave velocity models, both one-dimensional and three-dimensional. Also, different phases (such as P, P_n, P_g, etc.; S, S_n, S_g, etc.) can be used together. If not specified, the first arrival phase is used. Moreover, different weights can be assigned to each phase. If not specified, P phases have 1.0 weight and S phases 0.5 weight. If, accidentally, at any iteration, the normal equation matrix A^TA is algorithmically singular, a damped least-squares procedure is used; this was introduced because, from the outset, the program must be run routinely.

Diagonal elements of covariance (C) and resolution (R) matrix are computed from

$$C = \sigma^2 HH^T ; \quad R = HA$$

where

$$\sigma^2 = \frac{1}{N-4} \sum_{i=1}^{N} (\Delta T_i)^2 .$$

An indication of classic least-squares procedure at the last iteration will be $R = HA = (A^TA)^{-1}A^TA = I$.

3. Application to Vrancea seismic region

A set of 119 events recorded at least at 6 stations was selected for this application; the accuracy in arrival time reading is better than 0.1 s. A map of epicenters resulted from 1-D routine locations is presented in Fig. 1, where open circles correspond to shallow events and full circles to intermediate ones.

For the 3-D velocity structure case, the P-wave and S-wave block velocity models determined by ONCESCU (1983) were used. The models have 7 layers (with depth boundaries at 0, 20, 40, 70, 100, 130, 170 and 230 km), the horizontal dimensions of each block being 35 km × 30 km.

The epicenter positions resulted from the 3-D models are presented in Fig. 2. One can observe a general translation to NW of intermediate earthquakes and an alignment of shallow events. The initial (1-D) and final (3-D) depths of foci are presented in Fig. 3. It is also interesting to note a remarkable decrease of statistical errors of hypocenter parameters: the average standard error of depth decreased from 7.8 km to

DOI: https://doi.org/10.2312/zipe.1983.078

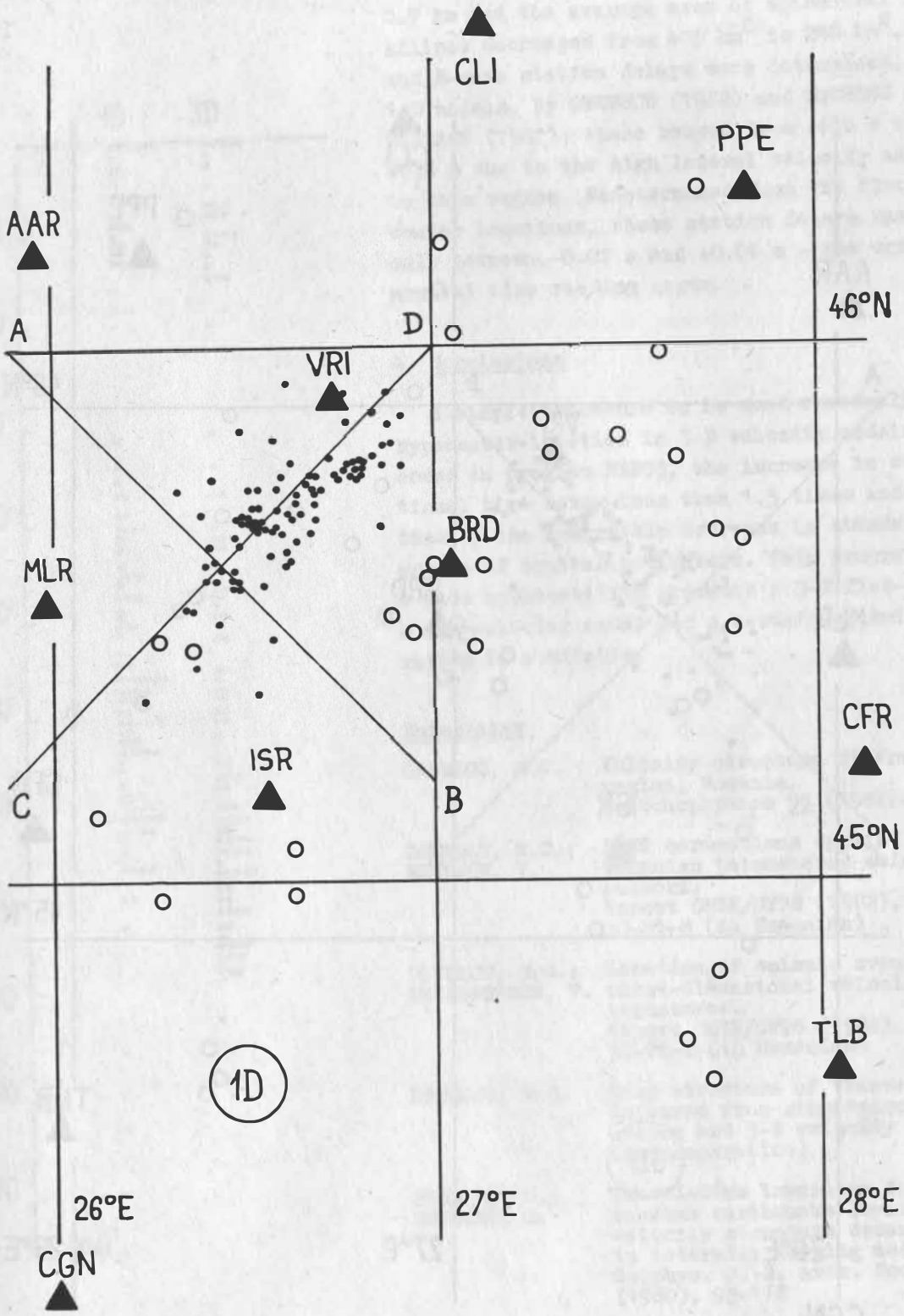

Fig. 1. Initial (1-D) epicenter position

DOI: https://doi.org/10.2312/zipe.1983.078

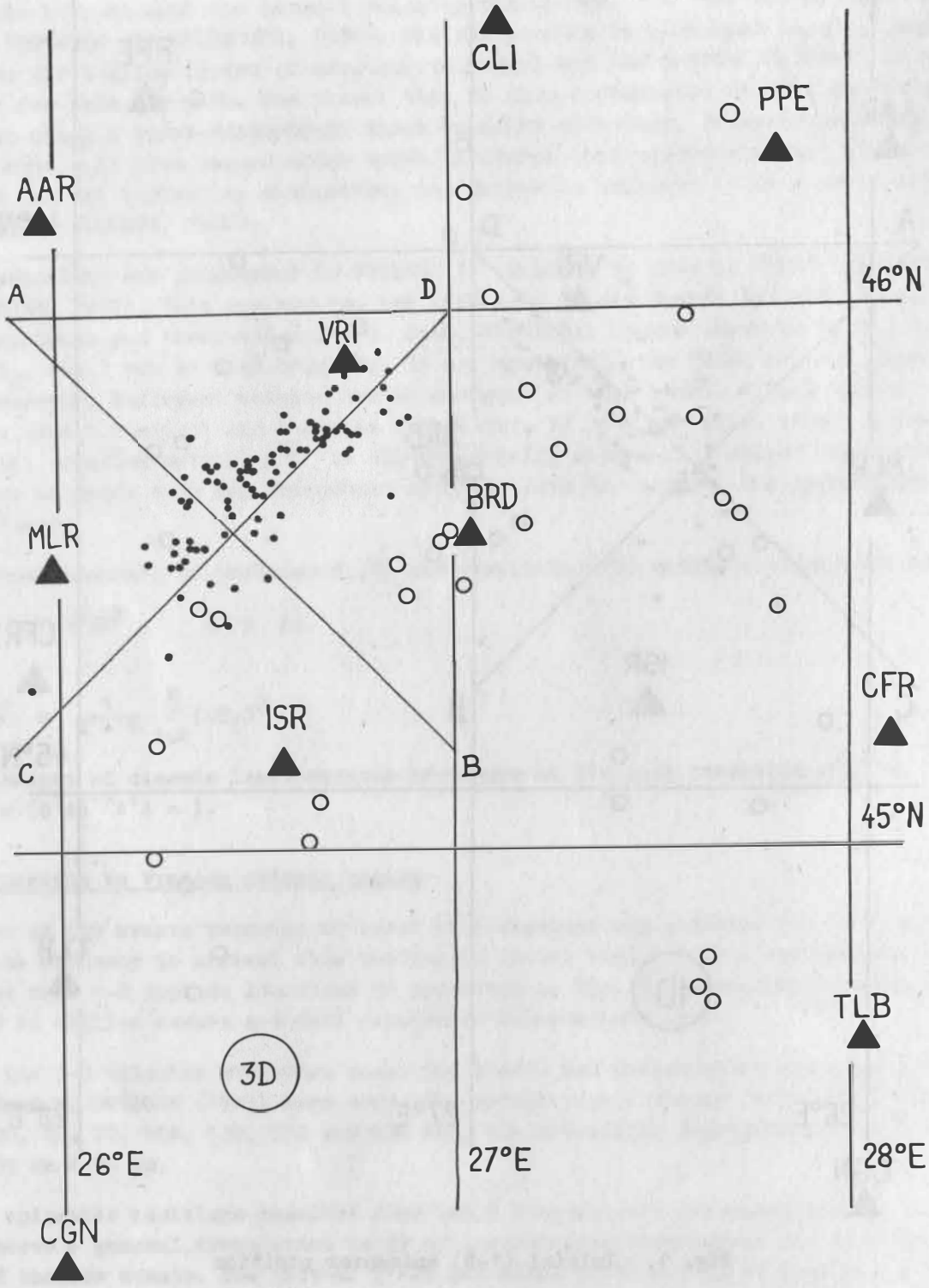

Fig. 2. Final (3-D) epicenter position

DOI: https://doi.org/10.2312/zipe.1983.078

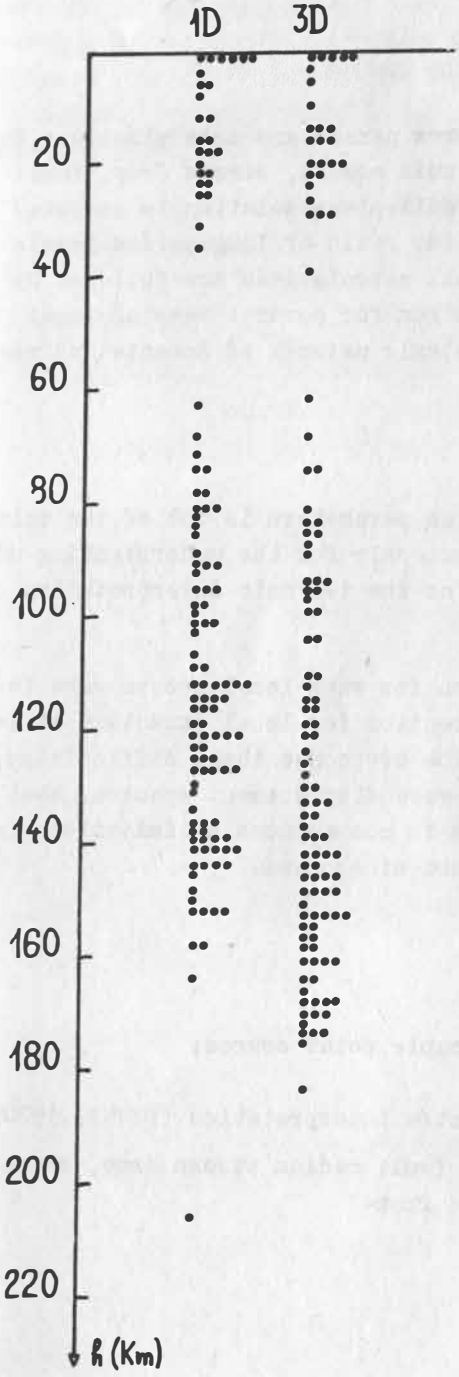

Fig. 3. Comparison between initial (1-D) and final (3-D) focus depths

0.7 km and the average area of epicentral error ellipse decreased from 405 km^2 to 248 km^2. P- and S-wave station delays were determined, for 1-D models, by ONCESCU (1982) and ONCESCU and BURLACU (1982); these ranged from -0.6 s to +0.6 s due to the high lateral velocity anomalies in this region. Redetermined from the final hypocenter locations, these station delays ranged only between -0.07 s and +0.04 s - the order of arrival time reading error.

4. Conclusions

A simple procedure to be used routinely for hypocenter location in 3-D velocity models was coded in program HYPO3, the increase in computational time being less than 1.5 times and justified by the remarkable decrease in standard errors of spatial parameters. This program has a wide applicability provided a 3-D flat-earth block velocity model for a certain seismic region is available.

References

ONCESCU, M.C. Velocity structure of Vrancea region, Romania. Tectonophysics 90 (1982), 117-122

ONCESCU, M.C.; BURLACU, V. SRST corrections applied to the Romanian telemetered seismic network. Report CSEN/CFPS (1982), Contract 30-81-8 (in Romanian)

ONCESCU, M.C.; SMALBERGHER, V. Location of seismic events in three-dimensional velocity structures. Report CSEN/CFPS (1982), Contract 32-81-2 (in Romanian)

ONCESCU, M.C. Deep structure of Vrancea region inferred from simultaneous hypocenter and 3-D velocity inversion (in preparation)

SPENCER, C.; GUBBINS, D. Travel-time inversion for simultaneous earthquake location and velocity structure determination in laterally varying media. Geophys. J. R. astr. Soc. 63 (1980), 95-116

THURBER, C.H.; ELLSWORTH, W.L. Rapid solution of ray tracing problems in heterogeneous media. Bull. Seis. Soc. Am. 70 (1980), 1137-1144

DOI: https://doi.org/10.2312/zipe.1983.078

Automatic Source Parameters Determination for Local Events

by

M. C. ONCESCU [1)]

Summary

A computer program was developed for automatic source parameters determination: fault-plane solution, directions of principal stresses, seismic moment, stress drop, fault radius, and average dislocation of local events. The fault-plane solution is computed using an iterativ least-squares procedure applied on the ratio of long-period levels $(SV/P)_z$ with the first motion polarity associated. All calculations are followed by standard error estimations. The program was routinely run for several tens of local events recorded in digital form by the telemetered seismic network of Romania and remarkable consistent results were obtained.

1. Introduction

The determination of fault-plane solution and source parameters is one of the main tasks of seismology. These parameters are important not only for the understanding of physical properties of the seismic source, but also for the tectonic interpretation of seismic regions.

Studies of individual focal mechanism determination for weak local events were less attempted, especially due to the difficulties in correction for local structure at low periods. In this study a method will be presented which overcomes these difficulties, having as imput data long-period levels of P- and SV-wave displacement spectra, that depends, of course, on having digital waveforms; this is not anymore a limitation since digital recording of seismic data becomes more and more widespread.

2. Theory

The basic assumptions of the proposed method are:

1. The seismic source is represented by the double-couple point source;
2. The P- and SV-waves have the same path;
3. Brune's model is appropriate for displacement spectra interpretation (BRUNE, 1970).

Starting from these assumptions, the seismic moment, fault radius stress drop, seismic energy and average dislocation are respectively found from

$$(1) \quad M_o = \frac{4\pi \varrho_h v_h^2 v_o R\Omega_o}{\mathcal{R}(\varphi_s, \delta, \lambda, \varphi, i_h)} ,$$

$$(2) \quad r = (2.34\, v_h^s)/(2\pi f_o^s) ,$$

$$(3) \quad \Delta\sigma = 7\, M_o/16\, r^3 ,$$

---

1) Central Institute of Physics, Center of Earth Physics and Seismology, P. O. Box MG-2, Bucharest-Măgurele, Romania

DOI: https://doi.org/10.2312/zipe.1983.078

(4) $E_s = (0.454\,\Delta\sigma^2)/(\varrho_h v_h^s v_h^s r^3)$,

(5) $u = M_o/(\pi\varrho_h v_h^s v_h^s r^2)$,

where R is the hypocentral distance, Ω_o is the long-period level of P- or SV-wave spectrum, v is the P- or S-wave seismic velocity (the subscript "h" stands for focus depth), $\mathcal{R}$ is the P- or SV-wave radiation pattern, φ_s, δ, λ are the strike, dip and slip angles, respectively, φ, i_h are the azimuth of the station and the angle of emergence, respectively.

The fault-plane solution (described by φ_s, δ, λ angles) is determined from the ratio of long-period levels Ω_o^{SV}/Ω_o^P, the P-wave first motion sign being associated with Ω_o^P. The use of P-wave polarities not only constrains the solution to be consistent with first motion polarities, but also determines uniquely the slip angle λ.

The starting solution is found from first motion polarities alone, through a search in $\varphi_s - \delta - \lambda$ space on a 10° grid. This solution is then used in a least-squares iterative procedure which minimize the quantity

(6) $$\varepsilon^2 = \sum_{j=1}^{N} \frac{1}{\sigma_j^2}\left[\frac{1}{(\sqrt{3})^3}\left(\frac{\Omega_o^{SV}}{\mathrm{sgn}(p)\Omega_o^P}\right)_j - \left(\frac{|\mathcal{R}^{SV}|}{\mathcal{R}^P}\right)_j\right]^2$$

where σ_j is the standard deviation of the ratio Ω_o^{SV}/Ω_o^P; σ_j is also used to weight (by $1./\sigma_j$) each line of the system

(7) $A\,\Delta x = \Delta b$

where A is the (N × 3) matrix of partial derivatives, Δx is the (3 × 1) vector with the changes in φ_s, δ, λ angles and Δb is the (N × 1) vector with the differences between the observed and calculated ratios of long-period levels. Convergence is obtained in several iterations, when the absolute changes in the three angles are less than prespecified values. Covariances of the three angles are found from $C = \frac{\varepsilon^2}{N-3}(A^T A)^{-1}$.

3. Method

From the onset of P- and SV-waves a time window of 2.56 s is opened. The waveform inside the window is cosine tapered at both ends and Fourier transformed. The obtained spectrum is corrected for the instrument response curve, smoothed and then, in a log-log dependence, fitted with two straight lines, the first horizontal, in a "trial and error" procedure. That combination that gives the minimum total standard deviation is retained. The horizontal line gives the Ω_o level, the intersection of the two lines gives the f_o corner frequency and the slope of the second line is used to compute the Q factor along the ray path. The Ω_o level is then corrected for free surface effect, geometrical spreading and attenuation. Stations with angles of incidence at the free surface between 32° and 36° are skipped from this stage.

The second stage implies the determination of φ_s, δ, λ angles and of the conjugate plane. The third stage is the determination of P, B and T axes, namely their azimuth and plunge. These are obtained from the eigenvectors of the seismic moment tensor for a

DOI: https://doi.org/10.2312/zipe.1983.078

double-couple point source. Let the azimuths and plunges of these axes be a function "F" of φ_s, δ, λ, denoted here by x_i; their covariances will be given by

$$(8) \quad C_{PBT} = \sum_i \sum_j (\partial F/\partial x_i)(\partial F/\partial x_j) C_{ij}$$

where the partial derivatives are numerically evaluated (WARD, 1980).

The fourth stage is the determination of M_o, r, $\Delta\sigma$, E_s and u as averages over station values, using (1) to (5). At the end, one tries to remove the ambiguity in fault-planes by fitting a straight line through

$$(9) \quad \frac{1}{\pi f_{oi}^{p,s}} = \frac{b}{v_r} - \frac{b}{v^{p,s}} \cos\theta_i , \qquad i = 1,\ldots,N$$

where θ_i is the angle between the slip direction and the direction of the ray leaving the focus to station "i". That plane is chosen which gives reasonable values for "b" (fault length, assumed linear) and v_r (rupture velocity) and has the largest linear correlation coefficient.

4. Application to Vrancea earthquakes

The method described above was coded in Fortran IV language. All input data were read from disk files of the Seismic Data Processing System (SDP) developed by Teledyne Geotech, Garland, Texas. The program was routinely run for 56 Vrancea earthquakes occured in the period october 1981 - november 1982 with magnitudes M_L = 2.2 - 4.4. The individual values of M_o, r, $\Delta\sigma$, E_s are not listed, but plotted versus M_L in Fig. 1 to Fig. 4, respectively. The straight line fit was performed not only to obtain useful, but not yet determined, relationships for small Vrancea earthquakes, but also as a check of the robustness of the automatic estimations.

One should note, for example, that the obtained $M_o - M_L$ dependence is quite similar with that of THATCHER and HANKS (1973) for California earthquakes and that $E_s - M_L$ dependence is close to that theoretically predicted ($\log E_s = 2.0\, M_L + 8.1$).

For 9 events (7 events with 4 stations and 2 events with 5 stations) the procedure failed to converge. The fault plane solutions for the rest of 47 events are tabulated in Table 1. Quality "A" stand for fault plane discriminated using (9) and quality "B" stands for fault plane subjective chosen from well known fault plane solutions of Vrancea earthquakes (RADU and ONCESCU, 1980).

5. Discussion

The method of using the ratio of long period levels Ω_o^{sv}/Ω_o^p at several stations to determine the fault plane solution proved effective enough to be used routinely. A minimum number of 5 stations with good azimuthal distribution should be used.

The most time consuming computation is the trial search for the starting solution. It is planned to change this approach with a linear inversion for seismic moment tensor components using the P-wave long-period level (with the signs of the first motions) for a three-couple model without volume change (see e. g. STERLITZ, 1978). A few numerical experiments indicated that this is perhaps the best and fastest starting solution one

DOI: https://doi.org/10.2312/zipe.1983.078

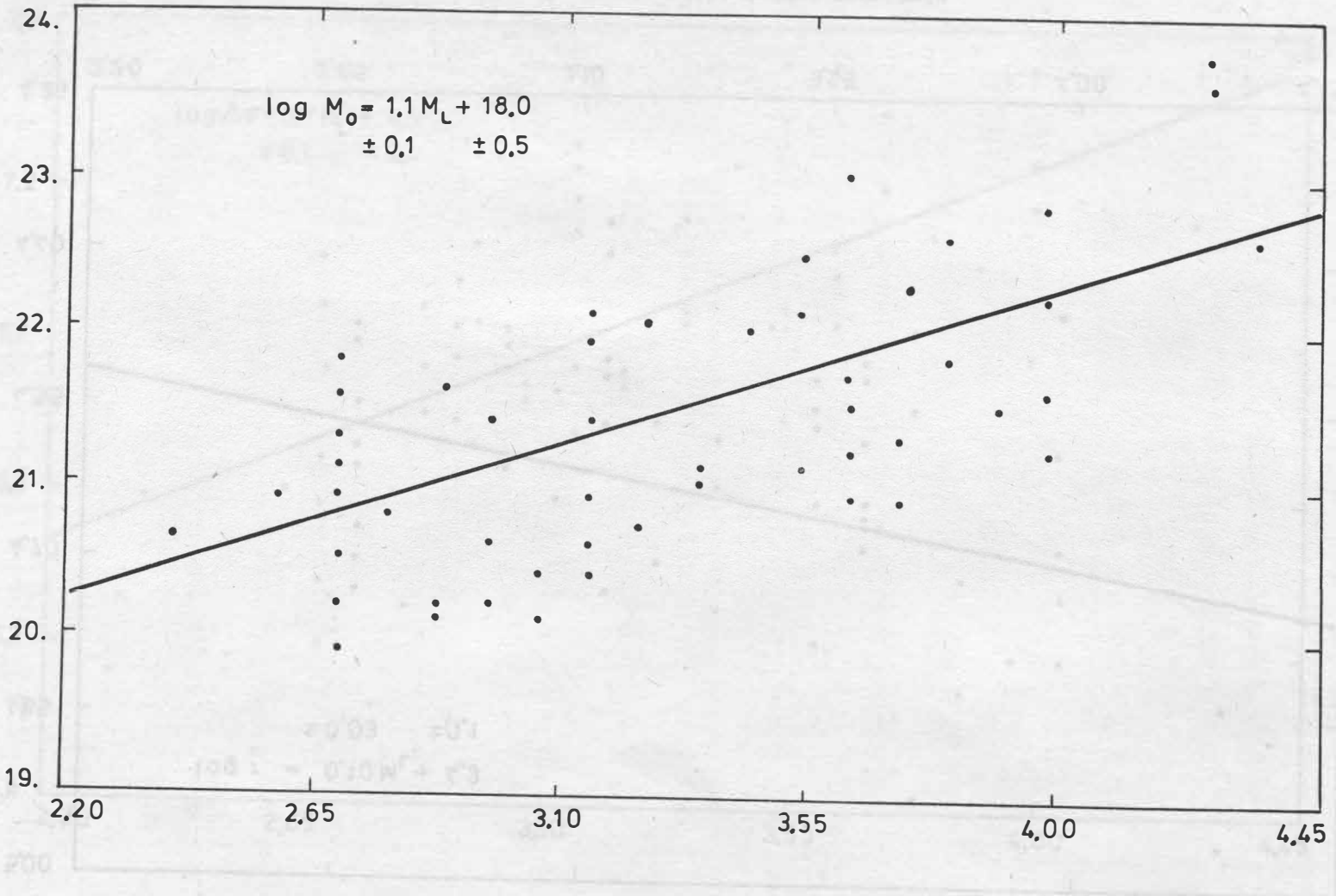

Fig. 1. Seismic moment versus magnitude

DOI: https://doi.org/10.2312/zipe.1983.078

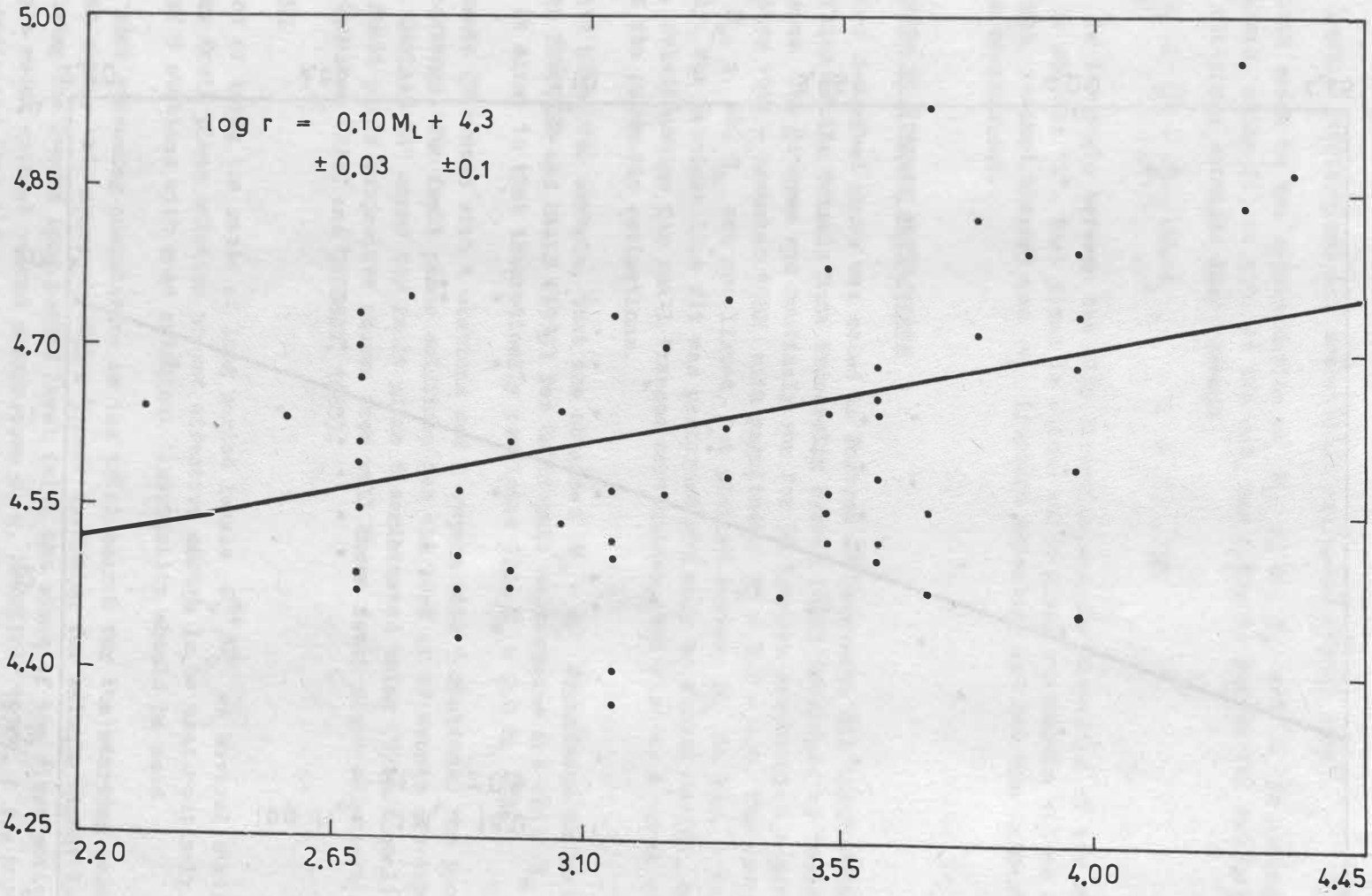

Fig. 2. Fault radius versus magnitude

DOI: https://doi.org/10.2312/zipe.1983.078

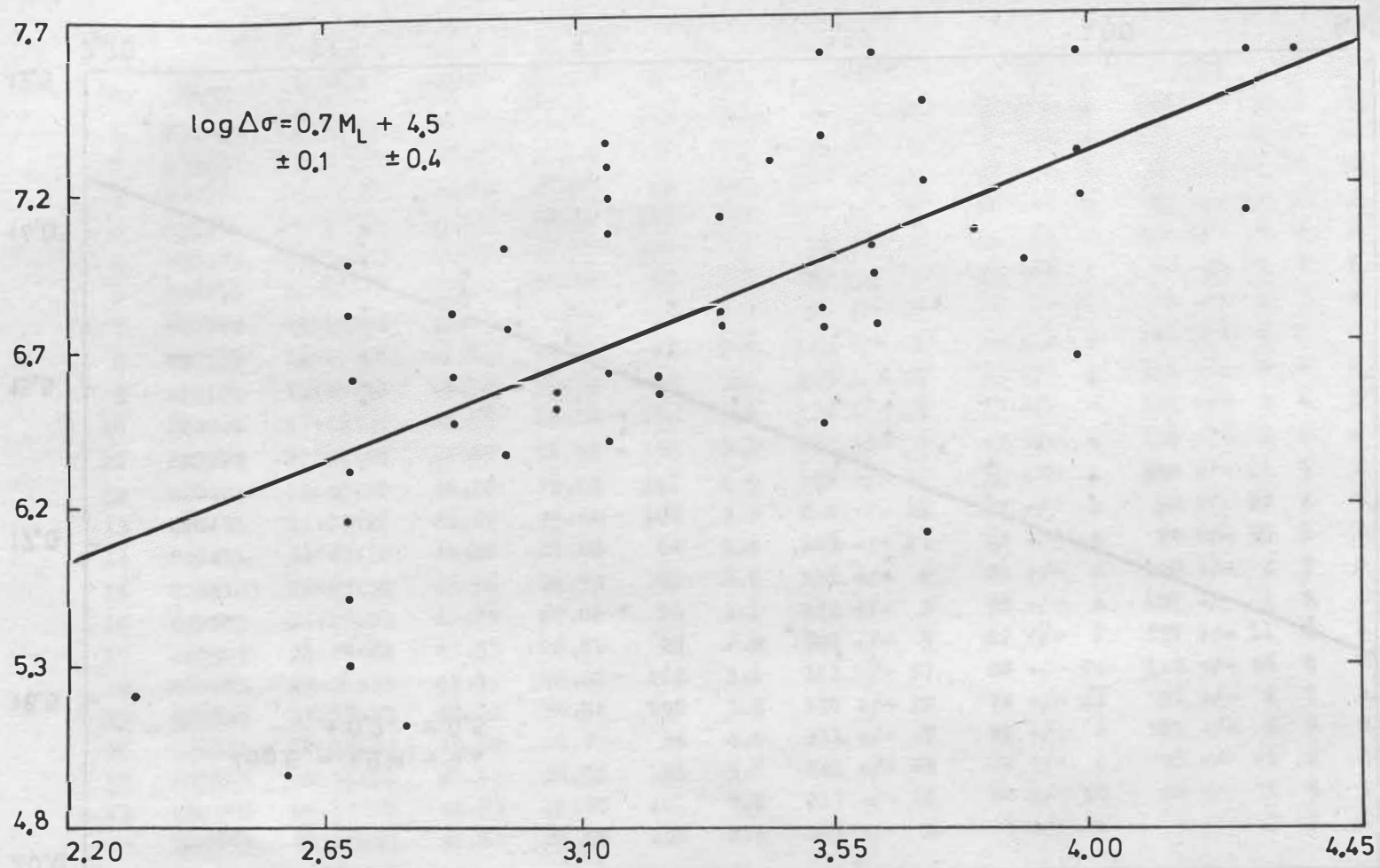

Fig. 3. Stress drop versus magnitude

DOI: https://doi.org/10.2312/zipe.1983.078

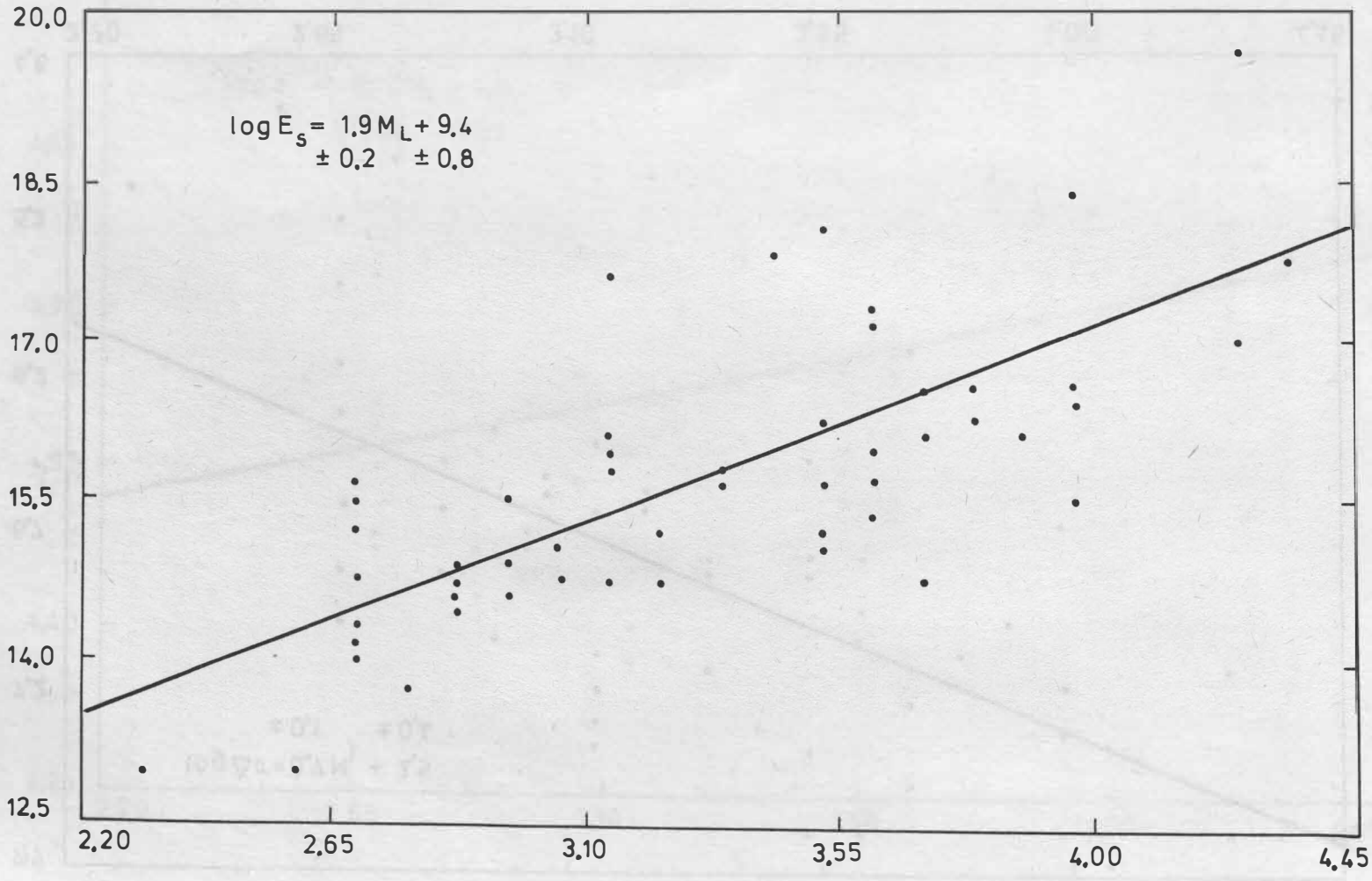

Fig. 4. Seismic energy versus magnitude

DOI: https://doi.org/10.2312/zipe.1983.078

Table 1. List of fault-plane solutions of Vrancea earthquakes

No.	Date	H-Time	Lat.N	Lon.E	h	M_L	Strike	Dip	Slip	N	Q
1	811018	01:14:20	45.67	26.64	143	3.0	16 +/- 21	74 +/- 22	144 +/- 9	7	A
2	811020	04:36:52	46.01	27.06	30	3.2	30 +/- 2	66 +/- 4	172 +/- 6	7	B
3	820101	06:31:39	45.73	26.89	79	4.0	172 +/- 13	65 +/- 8	93 +/- 11	5	B
4	820101	08:32:19	45.65	26.60	114	2.8	191 +/- 33	70 +/- 4	98 +/- 14	6	A
5	820102	14:54:29	45.60	26.63	127	3.6	24 +/- 8	64 +/- 5	181 +/- 9	8	B
6	820113	12:02:27	45.70	26.70	91	3.1	86 +/- 3	86 +/- 3	90 +/- 32	8	A
7	820118	14:49:04	45.72	26.78	117	2.9	87 +/- 18	87 +/- 18	57 +/- 4	7	A
8	820122	14:47:06	45.73	26.67	87	2.6	195 +/- 5	88 +/- 4	118 +/- 6	7	B
9	820131	11:46:34	45.73	26.75	82	3.5	215 +/- 12	83 +/- 4	314 +/- 8	8	B
10	820201	17:15:34	45.69	26.68	100	3.6	134 +/- 15	33 +/- 4	132 +/- 3	6	B
11	820224	11:21:54	45.67	26.52	150	3.6	260 +/- 6	62 +/- 4	138 +/- 5	6	A
12	820404	18:40:38	45.70	26.67	141	2.6	162 +/- 11	10 +/- 1	258 +/- 11	5	B
13	820411	12:05:26	45.67	26.68	107	3.5	206 +/- 29	75 +/- 1	92 +/- 22	4	B
14	820411	14:43:32	45.86	26.86	64	2.6	269 +/- 63	12 +/- 4	94 +/- 55	5	B
15	820418	01:45:30	45.66	26.53	91	2.6	186 +/- 8	28 +/- 1	128 +/- 4	7	A
16	820501	21:29:51	45.55	27.01	24	3.1	271 +/- 3	90 +/- 1	187 +/- 1	8	B
17	820502	22:05:49	45.53	26.99	22	2.9	304 +/- 5	82 +/- 6	337 +/- 11	8	B
18	820505	12:22:32	45.76	26.82	112	3.6	161 +/- 57	80 +/- 24	118 +/- 46	6	B
19	820505	17:23:13	45.70	26.52	150	3.8	110 +/- 32	74 +/- 22	26 +/- 6	7	A
20	820506	01:49:40	45.72	26.73	94	4.0	311 +/- 7	87 +/- 3	101 +/- 5	5	B
21	820507	06:41:04	45.62	26.52	151	3.6	241 +/- 69	84 +/- 1	95 +/- 49	6	A
22	820508	09:21:02	45.63	26.50	101	2.6	217 +/- 10	83 +/- 10	98 +/- 71	5	A
23	820510	08:08:53	45.60	26.68	120	2.6	112 +/- 4	89 +/- 20	6 +/- 3	5	B

DOI: https://doi.org/10.2312/zipe.1983.078

Table 1. (continued)

24	820511	02:00:24	45.56	26.58	126	3.9	252 +/- 21	47 +/- 16	141 +/- 15	4	B
25	820517	05:57:33	45.37	26.55	24	2.6	306 +/- 73	72 +/- 8	3 +/- 45	5	B
26	820523	16:09:31	45.73	26.78	126	3.2	238 +/- 7	78 +/- 4	106 +/- 5	6	A
27	820524	19:14:38	45.72	26.68	127	3.1	212 +/- 4	86 +/- 4	133 +/- 2	5	A
28	820526	09:13:13	45.04	26.46	28	3.1	297 +/- 1	78 +/- 1	88 +/- 1	5	B
29	820529	16:37:25	45.69	26.57	113	3.8	240 +/- 1	89 +/- 1	115 +/- 7	6	B
30	820531	19:37:01	45.71	26.55	75	2.9	214 +/- 4	70 +/- 7	163 +/- 28	5	A
31	820603	18:58:08	45.76	27.64	1	2.6	199 +/- 50	45 +/- 10	107 +/- 17	6	A
32	820605	11:56:03	45.62	26.45	157	4.4	145 +/- 24	69 +/- 14	127 +/- 13	6	B
33	820605	18:54:09	44.80	27.73	2	2.8	148 +/- 12	77 +/- 15	0 +/- 37	7	A
34	820606	15:32:14	45.62	26.66	119	3.5	242 +/- 10	61 +/- 4	125 +/- 7	9	A
35	820611	23:10:52	45.68	26.61	125	2.8	203 +/- 21	87 +/- 4	136 +/- 20	5	A
36	820612	06:58:28	45.66	26.51	142	4.0	205 +/- 15	47 +/- 5	46 +/- 8	7	A
37	820615	20:38:04	45.72	26.79	122	3.1	200 +/- 80	80 +/- 37	96 +/- 70	5	A
38	820619	01:43:43	45.60	27.82	18	3.7	99 +/- 15	85 +/- 5	221 +/- 11	7	B
39	820623	17:51:36	45.46	26.88	19	3.3	270 +/- 5	87 +/- 4	103 +/- 13	8	B
40	820630	21:38:48	45.40	26.34	19	3.5	330 +/- 2	71 +/- 4	203 +/- 11	7	A
41	820702	01:38:19	45.02	26.62	1	3.5	113 +/- 5	84 +/- 2	6 +/- 16	5	A
42	820704	14:57:46	45.40	27.10	1	3.0	176 +/- 6	77 +/- 1	176 +/- 4	7	B
43	820826	21:11:26	45.65	26.37	152	3.3	238 +/- 15	55 +/- 12	169 +/- 7	6	B
44	820828	12:02:08	45.87	26.74	90	3.3	150 +/- 5	80 +/- 11	38 +/- 3	6	A
45	820904	23:39:45	45.44	27.80	1	3.4	159 +/- 4	86 +/- 1	0 +/- 2	5	A
46	821009	06:57:57	45.64	26.51	141	3.7	192 +/- 2	49 +/- 7	25 +/- 10	5	B
47	821113	10:03:02	45.67	26.83	131	4.0	174 +/- 41	16 +/- 3	115 +/- 34	6	A

DOI: https://doi.org/10.2312/zipe.1983.078

could automatically use. With some minor simplifications, the procedure described could be programmed on a microprocessor for real-time source parameter determination.

The interpretation of obtained fault plane solutions and source parameters in terms of the tectonics of Vrancea region will be left for a future study.

Reference

BRUNE, J.N. — Tectonic stress and the spectra of seismic shear waves from earthquakes. J. Geophys. Res., 75 (1970), 4997-5009

RADU, C.; ONCESCU, M.C. — Fault-plane solution catalogue of Romanian earthquakes occured in the period 1929-1980. Report CSEN/CFPS, (1980), Contract 30-78-3 (in Romanian)

STERLITZ, R.A. — Moment tensor inversions and source models. Geophys. J. R. astr. Soc., 52 (1978), 359-364

THATCHER, W.; HANKS, T.C. — Source parameters of Southern California earthquakes. J. Geophys. Res., 78 (1973), 8547-8576

WARD, S.N. — A technique for the recovery of the seismic moment tensor applied to the Oaxaca, Mexico earthquake of November 1978. Bull. Seis. Soc. Am., 70 (1980), 717-734

Source-Station Corrections Applied to the Romanian Telemetered Seismic Network

by

M.C. ONCESCU and V. BURLACU [1)]

Summary

In order to reduce the errors of the hypocentral parameter determination source region/station time (SRST) corrections for the Romanian telemetered seismic network were computed. SRST corrections were defined as: $SRST_j = K_j + L_jX + M_jY + N_jW$ where "j" denotes the seismic station and W is Z, X^2 or Y^2; X, Y, Z represents the focal co-ordinates. Using 95 seismic events the K_j, L_j, M_j and N_j coefficients were determined from a least-squares fit to the jth station's residuals from all events. By comparing the errors of the hypocentral parameters before and after the corrections were applied a sensible difference of these errors was observed.

1. Introduction

One of the most important aspects in using the seismicity data is the accuracy of the earthquake parameters determination. Precise location of the seismic event hypocenters which is very helpful in the regional tectonic feature definition depends on the number and spatial distribution of the seismic stations, the accuracy of the seismic phase readings, the velocity model used, etc.

1) Central Institute of Physics, Center of Earth Physics and Seismology, P. O. Box MG-2, Bucharest-Măgurele, Romania

DOI: https://doi.org/10.2312/zipe.1983.078

The difference between the specific crust and upper mantle velocity structure under a region and the velocity model used causes systematic deviations of the travel times. Simple mathematical expressions for these deviations make possible to remove them from the arrival data and to obtain accurate hypocenter estimates.

2. Source region/station time corrections

The travel-time residual from the ith hypocenter to the jth station may be expressed (VEITH, 1975):

$$(1)\quad \delta t_{ij} = dt_i + (d\theta_i \cos Z_{ij} - d\phi_i \sin\hat{\theta}_i \sin Z_{ij}) \frac{\partial t}{\partial \Delta_{ij}} + dh_i \frac{\partial t}{\partial h_{ij}} + dB_i \frac{\partial t}{\partial \Delta_{ij}} + dC_i \cos Z_{ij} + dD_i \sin Z_{ij} + A_j + B_j \frac{\partial t}{\partial \Delta_{ij}} + C_j \cos Z_{ij} + D_j \sin Z_{ji} + \varepsilon_{ij},$$

where: dt - change in origin time, $d\theta$ - change in colatitude, $d\phi$ - change in east longitude, dh - change in depth, $\hat{\theta}$ - current colatitude estimate, Z_{ij} - azimuth from hypocenter i to station j, $\frac{\partial t}{\partial \Delta}$ - distance derivative, $\frac{\partial t}{\partial h}$ - depth derivative, dB_i - change in source distance-dependent (slope) correction, dC_i - change in cosine term of azimuthal source correction, dD_i - change in sine term of azimuthal source correction, A_j - station correction constant, B_j - station slope correction term, C_j - station azimuthal correction cosine term, D_j - station azimuthal correction sine term, Z_{ji} - azimuth from station j to hypocenter i, ε_{ij} - arrival time error. This equation has some instabilities which can be removed applying source region/station time (SRST) corrections. In a simple manner these corrections can be defined:

$$(2)\quad SRST_j = K_j + L_j X + M_j Y + N_j W$$

where "j" denotes the seismic station and W is Z, X^2 or Y^2; X, Y, Z represents the focal co-ordinates. The co-ordinate system in which the focus is represented was chosen with the origin at 45°N and 26°E and was rotated with 45° to east so the axes have the following directions: X - N 45°E, Y - S 45°E and Z - down.

The K_j, L_j, M_j and N_j coefficients were determined from a least-squares fit to the jth station's residuals from all events.

3. Data and discussion

SRST coefficients are determined based on equation (2) from the residuals of 95 seismic events recorded at least at 6 seismic stations. In Table 1 the coefficients for P and S waves are listed. For each seismic station there is the possibility to adopt for P and S waves a weight value. We have chosen for all the seismic stations the value 1 for the P waves and 0.5 for the S waves.

The next step consists in comparing the errors of the hypocentral parameters before and after the corrections were applied. We used two sets of data: the first, of 22 seismic events whose residuals were not used in the coefficients computation and the second of 95 seismic events. The two sets of data were chosen in order to emphasize the efficiency of applying the SRST corrections.

DOI: https://doi.org/10.2312/zipe.1983.078

Table 1. The SRST coefficients for P and S waves

Station	P wave						S wave					
	K	L	M	N	IND	N_{ev}	K	L	M	N	IND	N_{ev}
VRI	-0.5011	-10.29	10.02	0.0032	1	89	-0.6137	-14.46	13.58	0.0056	1	66
BRD	1.1020	19.93	-18.37	-1.6110	3	35	0.9895	-14.47	15.30	-0.8229	3	26
PPE	1.8510	58.32	-58.12	-0.0082	1	80	-0.5585	-27.50	27.90	-0.5941	2	69
CLI	0.1588	15.53	-16.22	0.6885	3	86	-0.6811	-19.62	19.14	0.5365	3	66
CGN	-1.1100	-26.98	27.13	0.0046	1	26	-0.6393	- 7.33	1.78	5.8450	2	22
TLB	0.1761	15.98	-16.10	-0.0864	3	88	-0.5351	-15.06	12.97	1.915	3	72
CFR	0.1166	22.10	-22.45	0.5018	3	91	0.7024	24.98	-25.12	-0.0053	1	77
ISR	-0.4156	-48.94	48.81	0.0036	1	78	1.7100	81.46	-81.30	-0.0058	1	50
MLR	-0.3802	-19.33	20.11	-0.9077	2	91	-0.5787	-28.37	27.88	0.3574	3	65

N_{ev} - number of events recorded at each station for each phase

$SRSR_j = K_j + L_jX + M_jY + N_jW$ with $W = Z, X^2$, or Y^2 for IND = 1, 2, or 3

The comparative results are listed in Table 2 and Table 3 and consists in:
- standard deviation (SD)
- depth error (DERR)
- area of ellipse of 95 % confidence reliabilit (EAERR)
- origin time error (OTERR).

The results listed in Table 2 and Table 3 represents mean values of the errors of the hypocentral parameters from the two data sets.

Table 2. Errors of hypocentral parameters for the 22 events data set

	With corrections	Without corrections
SC	0.85	1.00
DERR	10.99	12.73
EAERR	482.96	535.73
OTERR	1.67	1.74

Table 3. Errors of hypocentral parameters for the 95 events data set

	With corrections	Without corrections
SD	0.58	0.78
DERR	14.61	15.66
EAERR	344.31	508.69
OTERR	1.73	1.88

DOI: https://doi.org/10.2312/zipe.1983.078

4. Conclusions

Although the equation (2) form is quite simple it represents a good method of correcting station arrival times for systematic source and station effects.

The values listed in Table 2 and Table 3 show a sensible diminution of the errors of the hypocentral parameters after the corrections were applied.

References

VEITH, K.F. Refined hypocenters and accurate reliability estimates. Bull. Seis. Soc. Am., 65 (1975), 1199-1222

Cepstral Analysis and Homomorphic Deconvolution of Teleseismic Body Waves

by

A. PLEŠINGER [1] and R. VICH [2]

Summary

A promising way of determining an earthquake source model from body wave data is the comparison of observed P and/or S wave pulses with theoretical far-field body wave shapes for different source models. The actual shapes of body-wave pulses radiated by shallow finite sources tend, however, to be masked by the interaction of the free surface at the source, and by the filtering effect of the seismograph. An attempt is, therefore, made quantitatively to study the convenience of the cepstral analysis and homomorphic deconvolution of broad-band records of teleseismic body waves for the purpose outlined above. On the basis of observed ground displacement pulses, radiated by deep sources and recorded by broad-band instruments (passband 0.3 - 300 s), synthetic multiple wavelets are constructed, and different methods of enhancing the resolution of the cepstral analysis are tested. An optimum decimation of the signal and its low-pass filtering by an optimum linear-phase finite impulse response (FIR) filter are proved to be much more effective for resolution enhancement than the conventional methods of hamming or exponential weighting. This was found for complex as well as real cepstra. The limits of the practical applicability of homomorphic deconvolution are studied on the basis of synthetic and observed P wave groups of shallow events. Examples are demonstrated and discussed.

---

[1] Geophysical Institute of the Czechoslovak Academy of Sciences, Bočni II/1401, 141 31 Praha 4, ČSSR

[2] Institute of Radio Engineering & Electronics of the Czechoslovak Academy of Sciences, Lumumbova 1, 182 51 Praha, ČSSR

DOI: https://doi.org/10.2312/zipe.1983.078

1. Introduction

A method which has been widely used among seismologists studying the nature of earthquake sources is the estimation of empirical source parameters (seismic moment, fault dimensions, rupture velocity) for different kinematic dislocation models from far-field body wave spectra. The correctness of this approach is, however, deteriorated by several factors: (i) in the case of shallow earthquakes, by arrivals of the deep phases (pP, sP or pS, sS) which produce prominent spectral minima and maxima, (ii) for certain epicentral distances, by further interfering phases (PcP, PcS, PS, SKS etc.) producing the same effect, (iii) by the subjective truncation of a wave group the corresponding true ground motion of which is not known (band-pass filtering effect of the seismograph), and (iv) by the strong accentuation of spurious signal components (i. e. of components generated by non-linearities of the seismograph, by imperfect zero-level restoration, by the truncation, and, in the case of analog graphic records, by unavoidable digitizing errors) in the process of correction of the spectrum for the transfer function of the seismograph. All these phenomena leave a considerable arbitrariness to the interpreter of the resulting disturbed logarithmic spectrum and make the estimation of the spectral parameters - i. e. of the d. c. level, the corner frequency(-ies), and the high-frequency decay(-s) - unreliable (see Figures 1 and 2). The applicability of the more correct method consisting in the restoration of the true ground motion by deconvolution, selection of the wave group, and computation of the Fourier spectrum is mostly impracticable because of the heavy distortion or even instability of the deconvolved signal caused, besides (iv), by the limited dynamic range of standard-class analog seismograms.

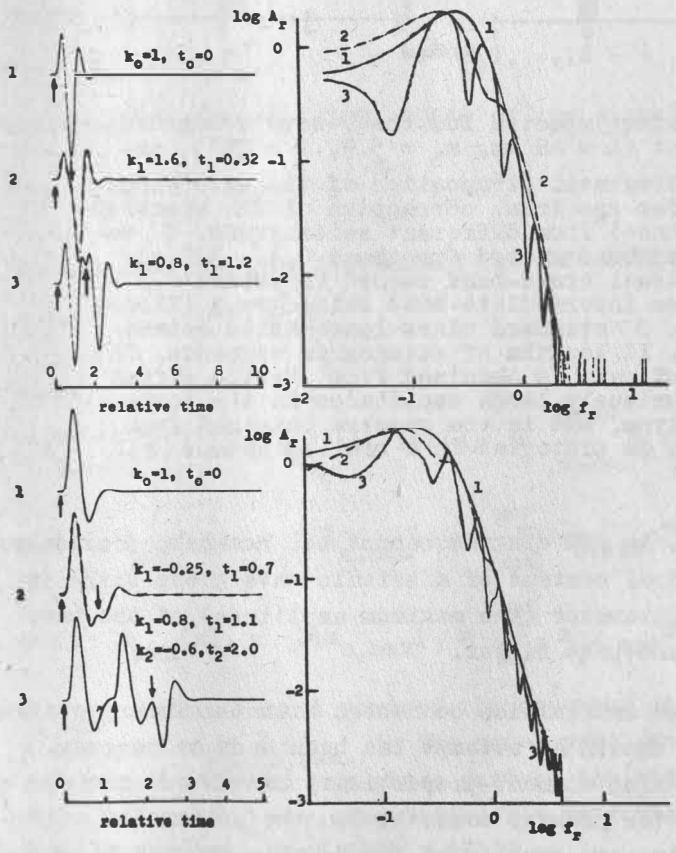

The major discrepancies among earthquake parameters determined by different authors or agencies for the same earthquake aroused a comparative study of the spectral properties of teleseismic body waves obtained from amplitude-periodband (APB) diagrams and from conventional spectral analysis of broad-band seismograms (SITARAM et al., 1980; ROGLINOV et al., 1978/79; PLEŠINGER et al., 1983). APB diagrams, as opposed to Fourier spectra, are relatively insensitive to spurious signal components and characterized by decreasing

Fig. 1. Basis (1) and composite (2, 3) wavelets and their logarithmic spectra. $k_{0,1,2}$ relative amplitudes, $t_{0,1,2}$ relative onset times. The effect of echoes is to produce spurious spectral maxima which are shifted in frequency in comparison with the genuine maximum of the basic wavelet

DOI: https://doi.org/10.2312/zipe.1983.078

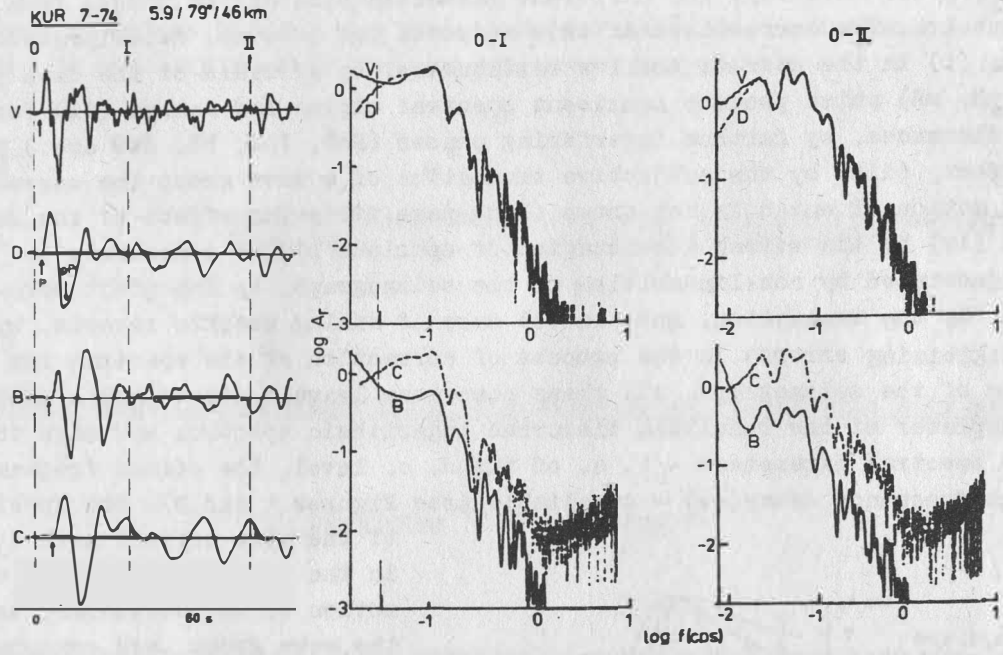

Fig. 2. Vertical ground displacement spectra for the P-wave group of a shallow Kurile Isl. event (h = 46 km, m_b = 5.9, D = 79°), obtained by conventional treatment (truncation of the wave group, computation of the Fourier spectrum, correction of the spectrum for the instrument response) from different seismograms. V velocity-proportional broad-band record (passband 0.3 - 300 s), D displacement-proportional broad-band record (passband 0.3 - 300 s), B standard class intermediate-band seismograph (Kirnos SVK, passband 1 - 15 s), C standard class long-period seismograph (Kirnos SVK-D); I, II lengths of seismogram segments. The most correct spectral estimate is obtained from D; the effect of B is to produce spuriously large amplitudes in the long-period part of the spectrum, and in the spectra obtained from C the short-period part is distorted in a similar manner

amplitudes for low-frequency passbands. An APB diagram cannot be, however, considered as a representation of the actual spectral content of a seismic wave group since it represents the dependence of only one parameter (the maximum amplitude) of the wave group on the center frequency of the band-pass filter.

In order to avoid the above mentioned ambiguities connected with the interpretation of observed waveforms in the frequency domain an attempt has been made to recover "pure" far-field body wave pulses from displacement-proportional broad-band records by means of homomorphic deconvolution. In the present contribution the principles of the employed method are explained and preliminary results of homomorphic processing of both synthetic and observed P-wave groups of shallow earthquakes are presented.

DOI: https://doi.org/10.2312/zipe.1983.078

2. Principles of employed signal processing procedures

In comparison with predictive decomposition the homomorphic deconvolution of multiple signals has two substantial advantages: (i) no "a priori" knowledge of the shape of the basic wavelet, nor of the number of echoes is required, (ii) results of homomorphic processing are relatively insensitive to minor differences between the shape of the basic wavelet and that of the echoes. For source studies both these advantages are of fundamental importance: the radiated waveforms depend on the type and depth of the source, on the fault plane orientation, and on the rupture direction relative to the receiver and the shapes of later phases may be modified by frequency dependent phase shifts accompanying overcritical reflection or caustics passing refraction.

The object of our study is to recover the basic wavelet, corresponding to the source function, from a broad-band recorded teleseismic wave group. In the following sections we briefly sum up the procedures used for this purpose.

2.1. Computation of the complex cepstrum

Let $\{f_n\}$, n integer, be a discrete signal (digitized seismogram). The signal segment $\{x_n\}$ (wave group) to be processed is obtained by applying a window $\{w_n\}$ of length N,

$$(1) \quad x_n = w_n f_n , \qquad n = 0,1,\ldots,N-1 .$$

For the Z-transform (VICH, 1964) of the signal segment holds

$$(2) \quad X(z) = Z\{x_n\} = \sum_{n=0}^{N-1} x_n z^{-n} .$$

The complex cepstrum (OPPENHEIM and SCHAEFER, 1975) is defined by

$$(3) \quad \hat{x}_n = Z^{-1}\{\hat{X}(z)\} ,$$

where

$$(4a) \quad \hat{X}(z) = Z\{\hat{x}_n\} = \ln X(z) = \sum_{n=-\infty}^{n=+\infty} \hat{x}_n z^{-n} = \hat{X}_{min}(z) + \hat{X}_{max}(z) ,$$

$$(4b) \quad \hat{X}_{min}(z) = Z\{\hat{x}_{n,min}\} = \sum_{n=0}^{+\infty} \hat{x}_{n,min} z^{-n} ,$$

$$(4c) \quad \hat{X}_{max}(z) = Z\{\hat{x}_{n,max}\} = \sum_{n=1}^{+\infty} \hat{x}_{-n,max} z^{n} ;$$

$\hat{x}_{n,min}$ is the causal part of the cepstrum corresponding to the minimum-phase part of the signal and $\hat{x}_{n,max}$ is the non-causal (anticipative) part of the cepstrum corresponding to the maximum-phase part of the signal. Usually the procedures defined by Eqs. (2) and (3) are computationally performed by means of the discrete Fourier transform (TRIBOLET and QUATIERI, 1979)

$$(5a) \quad X_k = DFT\{x_n\} = X(z)\Big|_{z=e^{j\frac{2\pi}{N}k}} = \sum_{n=0}^{N-1} x_n e^{-j\frac{2\pi}{N}kn} ,$$

DOI: https://doi.org/10.2312/zipe.1983.078

$$(5b) \qquad \hat{X}_k = \ln \dot{X}_k = \ln|X_k| e^{j \arg X_k} = \ln|X_k| + j \arg X_k ,$$

$$(5c) \qquad \hat{x}_n = \frac{1}{N} \sum_{k=0}^{N-1} \hat{X}_k e^{j \frac{2\pi}{N} nk} .$$

In (5a) it is assumed that $\arg X_k$ is an "unwrapped" continuous phase curve from which the linear-phase component must be subtracted.

Another method of cepstrum computation consists in the factorization of (2) by the solution of the equation $X(z) = 0$ (STEIGLITZ and DICKINSON, 1977; VICH, 1983). In this case $X(z)$ is obtained in the form

$$(6) \qquad X_{(z)} = x_0 \prod_{r=1}^{R} (1 - a_r z^{-1}) \prod_{s=1}^{S} (1 - b_s z^{-1})$$

where R is the number of zeros $|a_r| < 1$, S is the number of zeros $|b_s| > 1$, and $R + S = N - 1$. The complex cepstrum, $\{\hat{x}_n\}$, is given by (4a) with

$$(7a) \qquad \hat{x}_n = - \sum_{r=1}^{R} \frac{a_r^n}{n} \qquad \text{for} \qquad n > 0 ,$$

$$(7b) \qquad \hat{x}_n = \sum_{s=1}^{S} \frac{b_s^n}{n} \qquad \text{for} \qquad n < 0 ,$$

$$(7c) \qquad \hat{x}_0 = \ln(|x_0| \prod_{s=1}^{S} |b_s|) .$$

The linear phase component is given by the number of zeros outside the unit circle, i. e. by S. The procedure does not require phase unwrapping, avoids cepstrum aliasing, and enables to compute selected portions of the cepstrum. Since the polynomial equation (6) currently is of 200th to 300th degree, its solution seems to be questionable. With the aid of a proper strategy a reliable solution is, however, possible. We have solved equations up to the 275th degree in double precision arithmetic (64-bit-words) with a relative root accuracy of 0.5×10^{-6}.

Cepstral analysis by the latter method was experienced to be successful even in case when the former method via DFT failed because of instabilities in the procedure of phase unwrapping. Although the factorization requires more computation time than cepstrum analysis by means of the FFT, it yields - besides the mentioned advantages - a more profound insight into the problem. It was, e. g., experienced that a minimum phase system may have a non-minimum phase impulse response.

2.2. Approximations in cepstral analysis

The computation of the complex cepstrum of seismic signals is connected with some unavoidable approximations. One of them is the choice of the parameters (type, onset, length) of the window used to extract from the seismogram the wave group which we wish to process. On the basis of previous experience with spectral analyses of teleseismic signals we use hanning for this purpose. The choice of the optimum onset and length of the window depends on the seismological knowledge of the analyst/interpreter. Helpful in cases of complicated wave interferences is the polarization analysis of the respective part of the seismogram (PLEŠINGER and HORALEK, 1976).

DOI: https://doi.org/10.2312/zipe.1983.078

In a decisive manner is the success of cepstral analysis influenced by the signal-to-noise ratio and by the relative bandwidths of signal and noise. Therefore, it is necessary carefully to choose an optimum sampling frequency, and to reduce the noise by smoothing. In other words, for a given sampled signal a data dependent optimum combination of interpolation, filtering, and decimation must be found to achieve maximum cepstral resolution.

The discrete Fourier transform (5a) is usually performed by the FFT algorithm. In order to reduce cepstrum aliasing, a large number of zero samples must be appended to the signal segment. Unwrapping of the transform phase must be performed and the linear trend of the phase must be removed. Although efficient procedures were developed, they are not always successful especially if the spectrum exhibits zeros which obstruct the unwrapping. In such a case exponential weighting must be applied at the price of distortion of the cepstrum.

In the case of multiple mixed-phase reflections many peaks appear in the cepstrum as a consequence of the logarithm in its definition. These peaks may obstruct the interpretation of the cepstrum and considerably deteriorate the result of homomorphic deconvolution. A judicious exponential weighting must, therefore, sometimes be used to transform a mixed-phase signal into a minimum or maximum phase signal. In this case the factorization of the Z-transform of the signal combined with a classification of the zeros according to their modulus is helpful for the optimum choice of the exponential weighting.

2.3. Homomorphic deconvolution

Homomorphic deconvolution is based on windowing (liftering) of the complex cepstrum and on the inverse cepstral transformation

$$(8a) \quad y_n = Z^{-1}\{Y(z)\}$$

where

$$(8b) \quad Y(z) = e^{Z\{\hat{w}_n \hat{x}_n\}} .$$

The sequence $\hat{w}_n$ represents the cepstral window which is used for the suppression of certain parts of the cepstrum according to the aim of homomorphic processing - wavelet (source function) extraction, or reflection (impulse trace) extraction. The relations (8) are computationally performed using the discrete Fourier transform.

The process of homomorphic deconvolution again contains several approximations, the most delicate of these is the choice of the cepstral window in relation to exponential weighting. The problem of optimization of this choice is discussed in Section 3.

3. Results of homomorphic processing of teleseismic signals

For the present study data from the magnetic tape library of the FBV Broad-band Seismograph System operating at the KHC Seismic Station (Kašperské Hory in South Bohemia) were used. The FBV System has a flat-velocity response in the period range $0.3 < T < 300$ s. The individual components (Z, N, E) are recorded with an overall dynamic range of 80 dB on FM magnetic tape. Pre-processing of the data was performed

DOI: https://doi.org/10.2312/zipe.1983.078

by the ADT 4300 Mincomputer-Controlled Hybrid Data Processing System of the Geophysical Institute (PLEŠINGER, 1980). For the homomorphic processing a HP 45 (Institute of Radio Engineering and Electronics) and an EC 1040 computer (Computer Centre of the CS.A.S.) were employed.

On the basis of teleseismic body waves of deep earthquakes, obtained by intergration of FBV broad-band records, theoretical composite ground displacement signals for shallow earthquakes were constructed. The theoretical signals were used to study the influence of the approximations (see Section 2.2) on the resolution of the cepstral analysis and on the accuracy of the wavelet reconstruction. The results can be summarized as follows: (i) most instructive for the optimum choice of interpolation, filtering, and decimation is the shape of the high-frequency part of the logarithmic amplitude spectrum and the complexity of the power cepstrum, (ii) if the power cepstrum exhibits an unreasonably complicated form even in the case of optimum interpolation, filtering, and decimation exponential weighting must be applied, (iii) the most reliable wavelet reconstruction is obtained if the exponential weighting parameter α is chosen so that those of the zeros b_s in (6) which correspond to reflections (echoes) are shifted tightly inside the unit circle, (iv) the most convenient liftering procedure for wavelet reconstruction is logical windowing and smoothing of the complex cepstrum.

Examples of homomorphic treatment of theoretical and observed composite teleseismic P-wave signals are shown in Figures 3 to 6. Fig. 3 demonstrates the influence of exponential weighting on the reconstruction of both wavelet and impulse trace of an optimally filtered and decimated theoretical mixed-phase signal. For $\alpha = 0.958$ the signal is still of mixed-phase type (see cepstrum (d)), the reconstructed impulse trace contains many spurious peaks and the reconstructed wavelet appears in a position corresponding to that of the echo with the largest amplitude (= -1.5; the basic wavelet and the 2nd echo have amplitudes of +1.0 and +0.8 respectively). For $\alpha = 0.95$ the complex cepstrum (plot (f)) contains no maximum-phase echo peaks, the wavelet appears in its actual position and the impulse trace indicates the echo onsets correctly in time, polarity, and amplitude (plot (e)). The low peaks and the weak signal near the end of plot (e) are noise components enhanced by exponential de-weighting.

By homomorphic deconvolution of actual broad-band recorded teleseismic signals without the application of exponential weighting we obtained results like those shown in Fig. 4. In almost all cases the observed signals were of mixed-phase type (plot (d) and (f)). As a consequence of the presence of seismic noise and of many unsuppressed reflections the impulse trace was very complicated (plot (c)), and the reconstructed wavelet had a rather unrealistic shape (plot (e)). Optimum exponential weighting yielded results two typical examples of which are given in Figs. 5 and 6. The impulse trace of signal 1131 (Fig. 5) reveals the existence of three prominent onsets within the first period of the signal, and the reconstructed wavelet resembles in its shape that of far-field displacement pulses for simple kinematic dislocation models (AKI and RICHARDS, 1980). The signals near the ends of the plots (c), (e), and (f) are caused - as already mentioned - by the exponential de-weighting. The last example (Fig. 6) demonstrates how the wavelet reconstruction is influenced by the length of the short-pass liftering window in a particular case.

DOI: https://doi.org/10.2312/zipe.1983.078

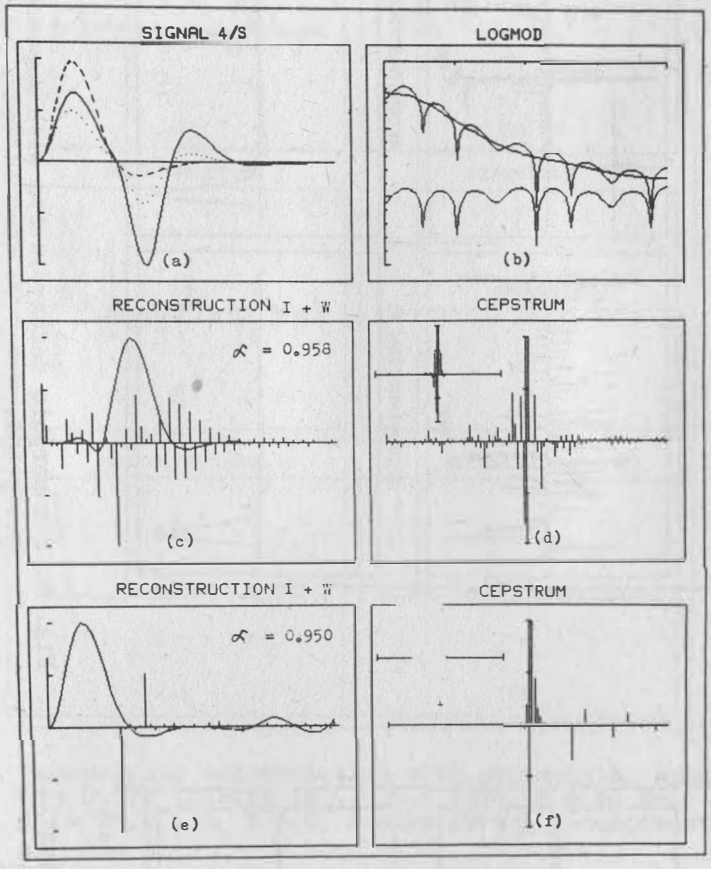

Fig. 3. Homomorphic deconvolution of a theoretical composite mixed-phase Berlage-type signal $(f(t)) = \sum_{i=0}^{2} k_i f_o(t-\tau_i)$, $f_o(t) = t^{\gamma} e^{-\beta t} \sin\omega t$, $\gamma = 2$, $\beta = 10$, $\omega = 2\pi$; $k_o = 1$, $\tau_o = 0$; $k_1 = -1.5$, $\tau_1 = 0.45$; $k_2 = 0.8$, $\tau_2 = 0.6$). (a) basic wavelet f_o (dashed), composite signal f (full), and signal f exponentially weighted with $\alpha = 0.985$ (dotted), (b) logarithmic spectra of exponentially weighted composite signal (upper curve), of reconstructed wavelet (upper smoothed curve), and of reconstructed impulse trace (lower curve), (c) reconstructed wavelet and impulse trace for $\alpha = 0.985$, (d) corresponding complex cepstrum; upper left plot: windowed and smoothed (liftered) cepstrum used for wavelet reconstruction, (e) and (f) reconstructions and cepstra for $\alpha = 0.95$

DOI: https://doi.org/10.2312/zipe.1983.078

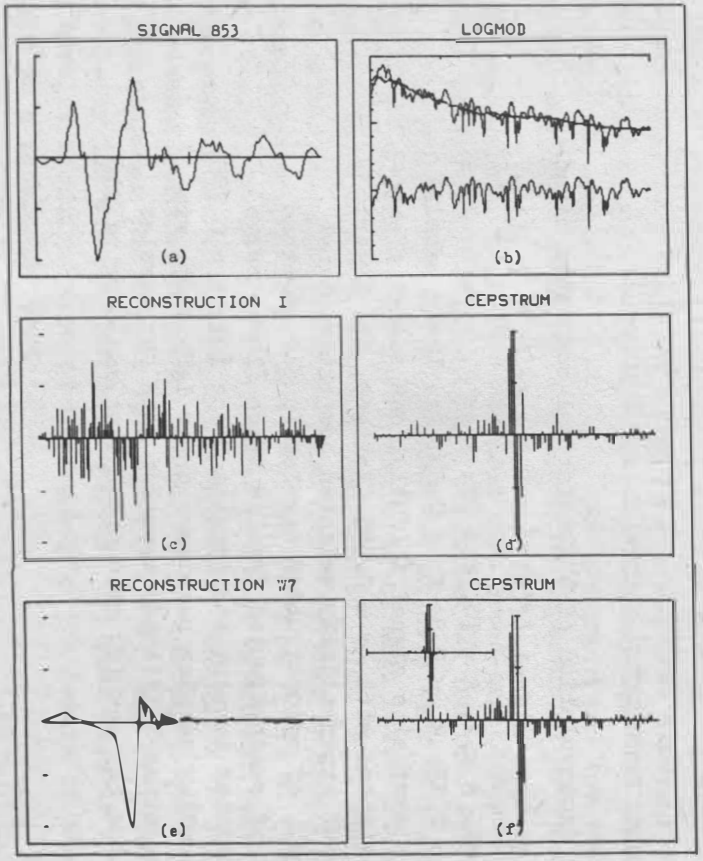

Fig. 4. Homomorphic deconvolution without exponential weighting (Kurile Isl., 22.6.1975, depth h = = 21 km, epicentral distance D_c = 80.1°, magnitude m_b = 5.7, P-wave group, vertical Z component). (a) observed signal, (b) logarithmic amplitude spectra, (c) reconstructed impulse trace, (d) cepstrum of composite signal, (e) reconstructed wavelet, (f) upper left plot: liftered cepstrum used for wavelet reconstruction

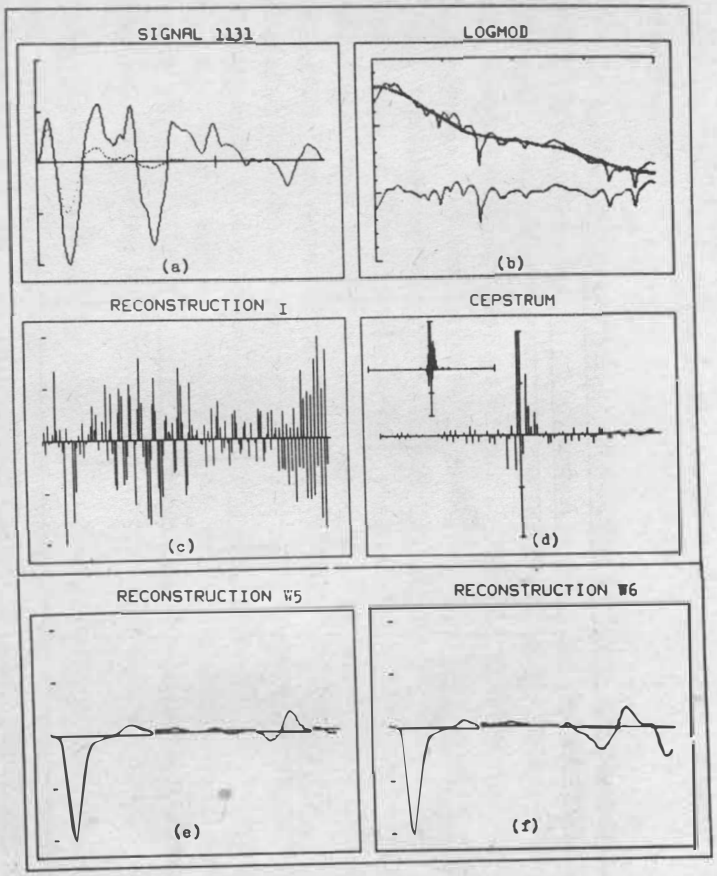

Fig. 5. Homomorphic deconvolution with exponential weighting, α = 0.96 (Kurile Isl., 13.6.1975, h = 72 km, D_c = 79.4°, m_b = 5.9, P-wave group, Z-component). (a) signal (full), weighted signal (dotted); (b), (c), (d) see Fig. 4; (e), (f) reconstructed wavelets

DOI: https://doi.org/10.2312/zipe.1983.078

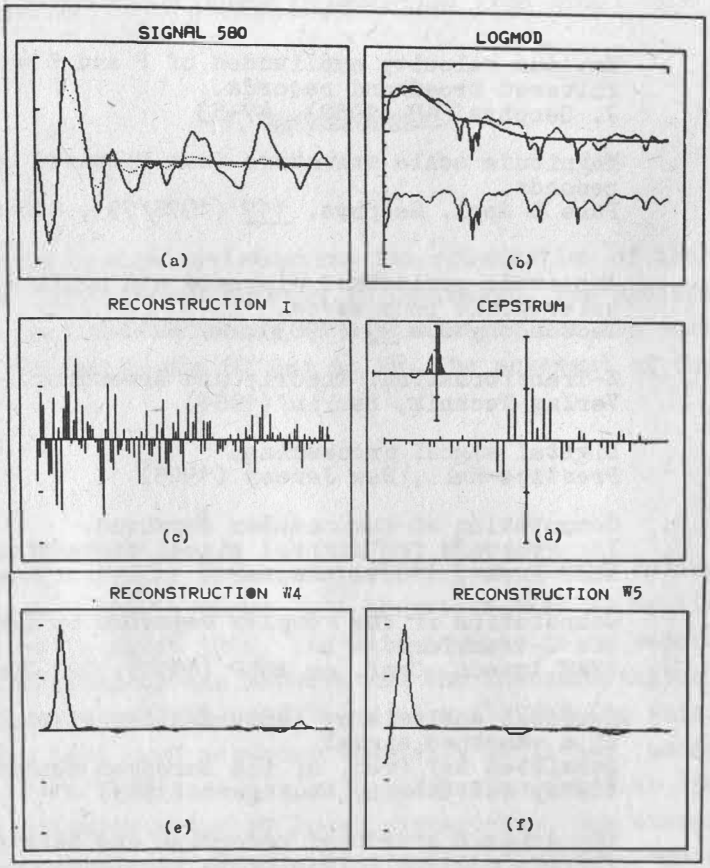

Fig. 6. Homomorphic deconvolution with exponential weighting, $\alpha = 0.975$ (Kurile Isl., 29.7.1974, h = 46 km, $D_c = 78.8°$, $m_b = 6.0$, P-wave group, Z-component)

4. Conclusion

The obtained results of homomorphic deconvolution of both theoretical and observed composite teleseismic body wave signals are, in our opinion, encouraging enough to substantiate a continuation of the work. According to our experience both an optimum choice of the critical approximation parameters and a profound knowledge of the seismological background are decisive for a successive realistic application of homomorphic deconvolution to the problem of recovery of source functions from broad-band seismograms. The developed procedures are intended to be employed in investigations into source mechanism differences for selected seismoactive regions with known source geometries.

Acknowledgement. The authors express their hearty thanks to Ellen Vichová who wrote the programs and performed the extensive computational work connected with this study.

DOI: https://doi.org/10.2312/zipe.1983.078

References

SITARAM, M.V.D.; PLEŠINGER, A.; VANĚK, J. — Maximum velocity amplitudes of P and S waves from filtered broadband records. J. Geophys. 48 (1980), 47-53

ROGLINOV, A.; HORÁLEK, J.; PLEŠINGER, A.; VANĚK, J. — Magnitude scale structure from filtered broadband P-wave records. Pure & Appl. Geophys. 117 (1978/79), 816-826

PLEŠINGER, A.; VANĚK, J.; SOBOTOVA, C. — Amplitude-periodband diagrams and amplitude spectra of teleseismic body waves. Tectonophysics 93 (1983), 277-288

VÍCH, R. — Z-Transformation. Theorie und Anwendung. Verlag Technik, Berlin (1964)

OPPENHEIM, A.V.; SCHAEFER, R.W. — Digital signal processing. Prentice-Hall, New Jersey (1975)

TRIBOLET, J.M.; QUATIERI, T.F. — Computation of the complex cepstrum. In: Programs for digital signal processing. IEEE Press, (1979) chapter 7

STEIGLITZ, K.; DICKINSON, B. — Computation of the complex cepstrum by factorization of the Z-transform. IEEE Intern. Conf. on ASSP (1977), 723-726

VÍCH. R. — Cepstral analysis by factorization of the Z-transform of a smoothed signal. Submitted to: Proc. of the European conference on circuit theory and design, Stuttgart (1983)

PLEŠINGER, A.; HORÁLEK, J. — The seismic broadband recording and data processing system FBV/DPS and its seismological applications. J. Geophys. 42 (1976), 201-217

PLEŠINGER, A. — Interactive hybrid processing of seismic brcadband data. Proc. of the 17th Assembly of the ESC, Budapest (1980), 17-22

AKI, K.; RICHARDS, P.G. — Quantitative seismology. Theory and methods. Vol. II, W.H. Freeman & Comp., (1980) chapter 14.1.

Digital Data Transmission

by

H.-J. PÖHL [1)]

Summary

The necessity of digital data transmission in seismic networks will be explained. The instrumentations of a substation of a seismic network for data acquisition and teletransmission controlled by microprocessor will be shown. First results of digital data transmission by telephone lines will be presented.

1) Central Institute for Physics of the Earth of the Academy of Sciences of the GDR, DDR-1500 Potsdam, Telegrafenberg

DOI: https://doi.org/10.2312/zipe.1983.078

Estimation of the Fault Plane Orientation from Broad-band Array Data

by

H. RADEMACHER [1)]

Summary

With the aid of theoretical seismograms the orientation of the fault plane of a deep focus earthquake in the Bavarian molasse is estimated. The synthetics are compared with digital recordings from the GRF array. The parameters for the earthquake on May 17, 1982 are: Strike N 20 deg E, dip 60 deg to NW. The movement of the fault was a reversed normal faulting.

1. Introduction

The GRF broad-band array in the southeastern part of the Federal Republic of Germany has been set up since 1976. It began full operation with 13 vertical and 6 horizontal WIELANDT seismometers in March 1980. Its main purpose is to record teleseismic events. For a detailed description of the network and the instrumentation see SEIDL and KIND (1982), WIELANDT and STRECKEISEN (1982) and also AICHELE (in this volume). Several thousand earthquakes have been recorded digitally until now, among them are a lot of local shocks. This data base combined with refraction profiles opens new possibilities especially for the interpretation of local earthquakes. One example for the use of GRF-data to determine the focal depth of a local quake was given by KIND (1979a). He studied the Swabian Jura event of September 3, 1978. Another aim to use array data in the field of local earthquakes could be the estimation of the orientation of the fault plane.

2. The data

In their determination of the seismic zones in the Federal Republic of Germany AHORNER et al. (1970) defined the Molasse basin north of the Alps as an independent seismic active area. Especially, the region around Lake Constance in the western part of the basin was shaken by stronger quakes in historic times. Two other subregions could be identified within the Molasse Basin: One near Saulgau in Upper Swabia, the other near Peissenberg in the Bavarian part of the Molasse. Another prominent active seismic region defined by AHORNER et al. is the Swabian and Franconian Jura. One characteristic feature of all events occuring in these regions is that in general the source depth does not exceed 15 km.

So it was a surprise that an earthquake with a deep focus occured near Günzburg at the border of the two seismic zones on May 17, 1982. Calculations carried out by SCHMEDES (1982, personal communication) showed that this earthquake occured at a depth between 20 and 30 km. Thus, this shock is one of the deepest earthquakes ever recorded

1) Seismologisches Zentralobservatorium, Krankenhausstr. 1-3, D-8520 Erlangen

DOI: https://doi.org/10.2312/zipe.1983.078

in Germany. The parameters of the quake are:

Origin Time: 17:30:06.6, Epicenter: 48.55 N, 10.25 E, Ml: 3.6.

The Graefenberg-Array operated with ten vertical broad-band stations at the time the earthquake occured. Fig. 1 shows a map with the epicenter and the locations of the stations. The GRF array covers an epicentral range between 107 and 160 km and an azimuthal range of 39 deg for that earthquake. One can also see a refraction profile in Fig. 1. It was recorded in 1970. The shot point was located in a quarry near the

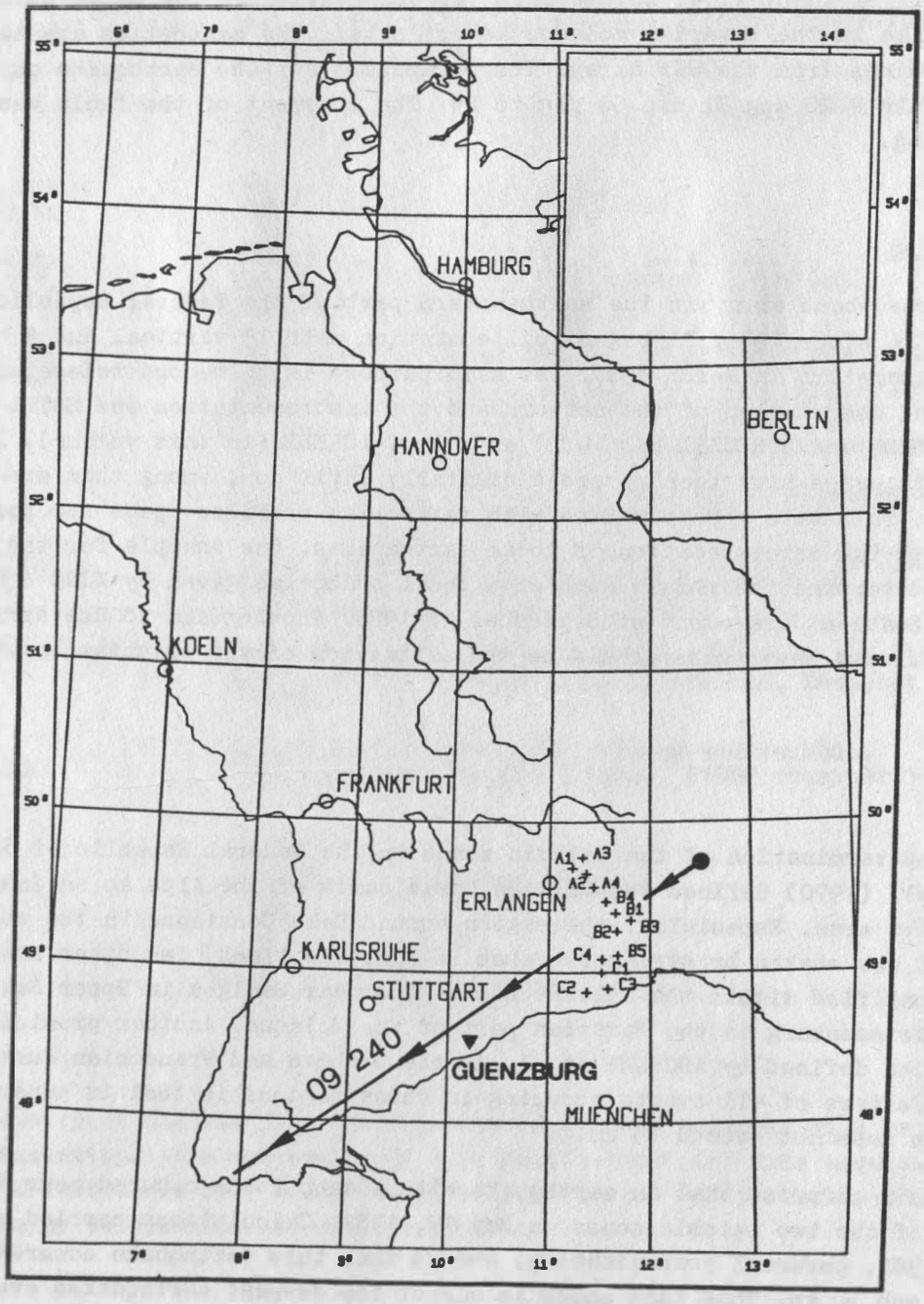

Fig. 1. Map showing the GRF array, the epicenter, and a refraction profile shot in 1970

DOI: https://doi.org/10.2312/zipe.1983.078

village of Böhmischbruck. The profile named 09 240 covered about 400 km and reached nearly to the city of Basel. It crossed the array area and also passed the epicenter within a range of about 30 km.

The recordings of the deep earthquake are shown in the seismogram sections in Figs. 2 and 3. The different tracks are shifted, so that they line up along a travel time curve with the slope of 8.4 km/s. The traces in the two figures are ordered with increasing distance. Fig. 2 shows the unfiltered broad-band data, which are proportional to the ground velocity. The Pn onset is clearly to be seen. A slower second phase marked P2 can also be detected. Fig.3 shows the seismograms proportional to ground displacement. The second phase can be seen much clearer now. Its first appearance is at the station C4, 110 km away from the epicenter. This phase has an apparent velocity of approximately 7.5 km/s.

The most interesting observation in both figures, however, is the change in the sign of the Pn phase between the stations B2 and A4, that means between the azimuths of 42 and 50 deg, determined against north. This feature, which has not been observed in the GRF data until now, makes it possible to estimate the orientation of the source by interpreting the array data with the aid of theoretical seismograms.

3. Computation of synthetic seismograms

With the reflectivity method described by KIND (1978, 1979b) theoretical seismograms have been computed for several models of the crust in the region between the epicenter and GRF. The reflectivity method was originally derived to deduce crustal models from seismogram sections gained in refraction profiles. So before one can attempt to get informations about the source, an identification of the phases in the data is necessary.

Fig. 4 shows synthetics for a very simple velocity-depth model consisting of a homogeneous crust (v_p = 6 km/s) and upper mantle (v_p = 8.4 km/s). The layer is separated from the halfspace by a Moho in a depth of 30 km. We used a simple explosive point source as an input-signal for the computation. The source depth in this and all further calculations was set at 19 km. At least three phases are clearly to distinguish: A weak Pn-phase, a Pg- or PmP-phase with most of the energy, and finally the first multiple marked MULT in Fig. 4. The last two phases are splitted into two phases each, due to P-reflections at the free surface. A weak pPn-Phase can be seen at around 10 s reduced traveltime.

As the data the theoretical seismogram section is also reduced with 8.4 km/s and covers the same epicentral range. That applies to all further synthetic sections. The dominant second phase of the data cannot be found in the synthetics. Therefore, such a simple model is unsatisfactory.

EMTER (1971) derived a velocity-depth model for the profile 09 240. It is shown in Fig. 5 (solid line). The main feature is a big jump in the P-wave velocity from 6.2 km/s to 6.9 km/s at a depth of 20 km. The theoretical seismograms computed for this model are shown in Fig. 6. We used a point source with a double couple characteristic of an arbitrary chosen orientation for this computation. At least four phases can be clearly indentified and will be

DOI: https://doi.org/10.2312/zipe.1983.078

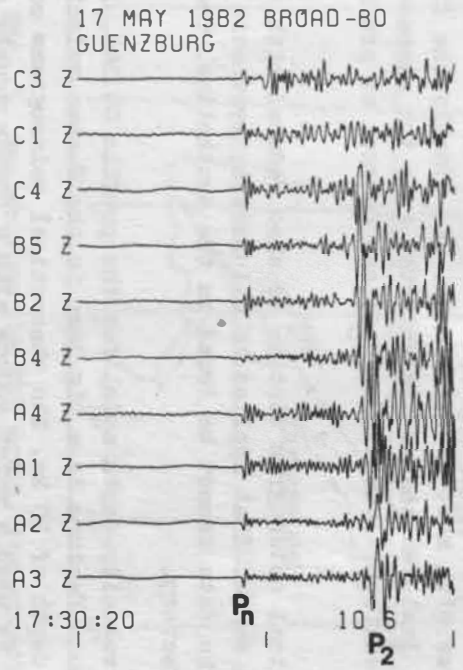

Fig. 2. Unfiltered broadband data of ten vertical stations. The tracks are shifted so that a phase with a velocity of 8.4 km/s would line up. The phase P2 has a velocity of 7.5 km/s

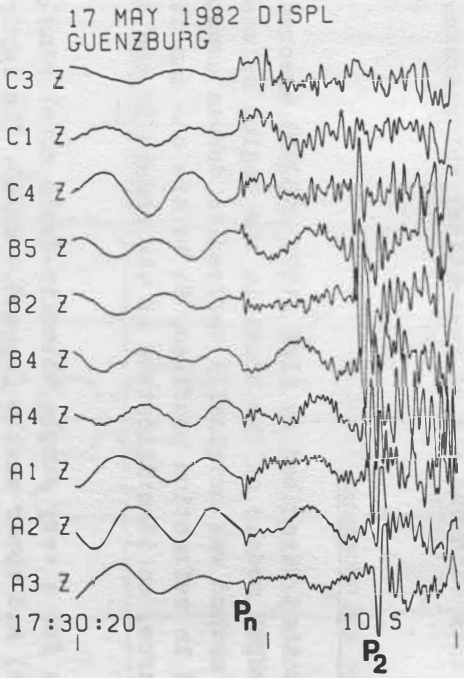

Fig. 3. The same as in Fig. 2, but the data are shown proportional to displacement

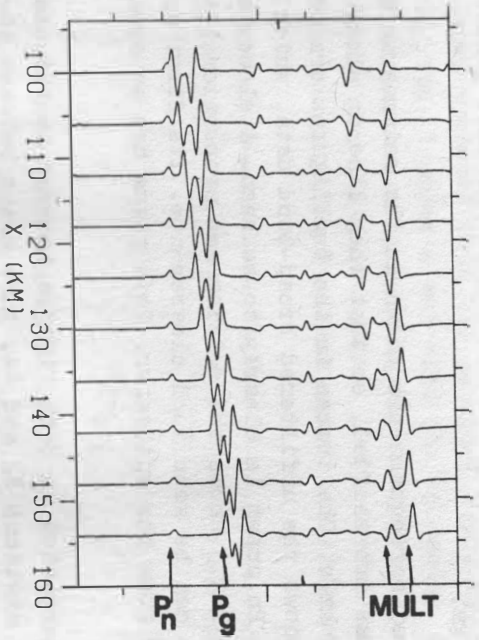

Fig. 4. Theoretical seismograms for a simple model (homogeneous crust over homogeneous halfspace). Four phases can be seen. The section is reduced with 8.4 km/s and covers a distance range between 100 and 160 km

DOI: https://doi.org/10.2312/zipe.1983.078

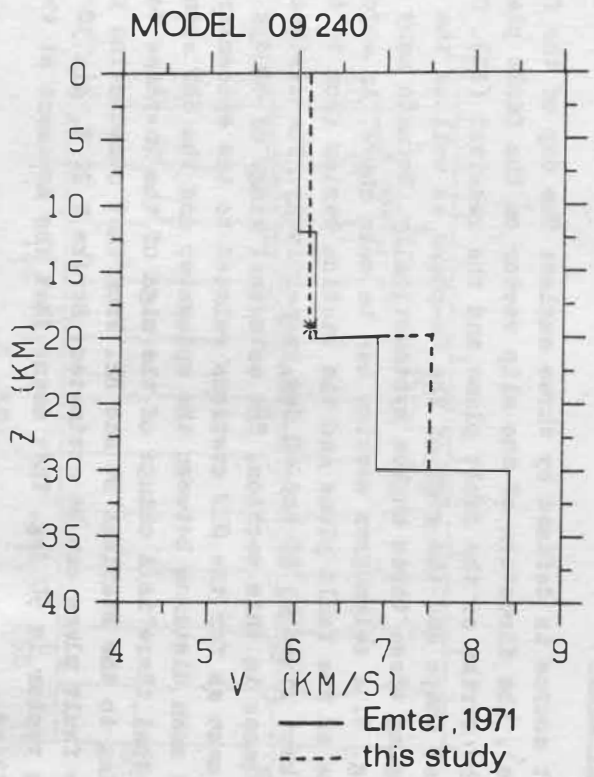

Fig. 5. The velocity depth model derived by EMTER (1971) is shown with the solid line. The dashed line represents the model derived here

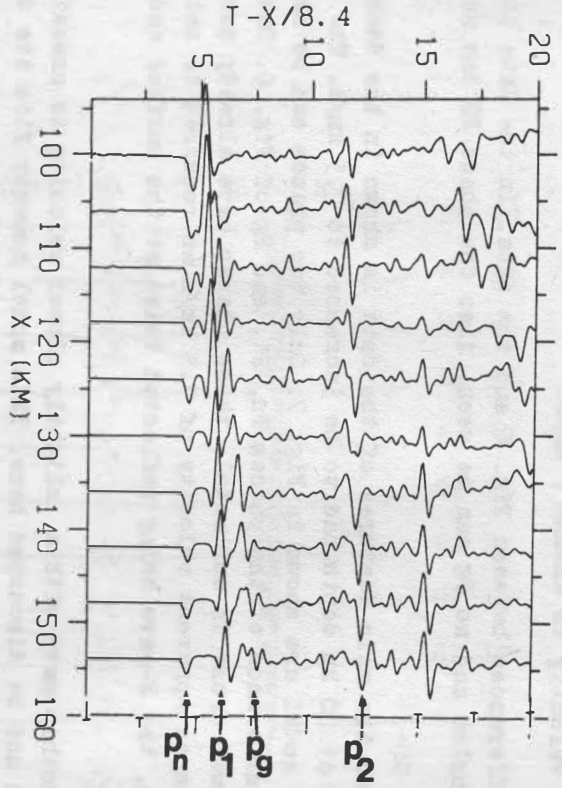

Fig. 6. Theoretical seismograms computed for the model of EMTER (1971)

DOI: https://doi.org/10.2312/zipe.1983.078

discussed here. The first arrival is a Pn-phase with a velocity of 8.4 km/s, followed directly by a phase marked P1. This is the wave which is refracted at the discontinuity in a depth of 20 km. It has an apparent velocity of 6.9 km/s. The next phase with a velocity of 6.1 km/s is the Pg- or PmP-wave, respectively. The phase marked P2 arriving later in the seismogram is a wave reflected twice: First at the free surface and then at the discontinuity. Its velocity is around 7 km/s.

There are two major differences between Fig. 6 and the data. In the data the Pn wave structure is much simpler and no Pg can be seen. Also the phase P2 has more energy and a higher velocity.

A model, which satisfies the main features of the data is shown in the dashed line Fig. 5. The velocity jump at 20 km depth had to be increased to 7.5 km/s. The theoretical seismograms for that model are shown in Fig. 7. Only two phases can be seen. The phase marked Pn is an interference of the phases Pn, P1, and Pg of Fig. 6. Due to the higher velocity of the lower crust in our model, these phases have already merged together. The phase P2 has an apparent velocity of 7.5 km/s as required to satisfy the data. It is, as in Fig. 6, the P-wave being reflected twice at the surface and at the discontinuity.

It can be seen that another wave with a slightly slower velocity is crossing the phase P2. Its origin will not be discussed here. This model however fits the data qualitatively well, especially the amplitude ratio P2/Pn, the arrival times, and the velocities. The frequency content of the synthetic section is lower than in the data. It can be increased but this would require more computing time.

4. Orientation of the fault plane

The double couple point source is defined by three angles: The dip of the fault plane (abbreviated NH here), the direction of the slip vector on the fault plane (DV), and the azimuth between the strike of the fault plane and the receiver (AZ). One should be able to match the signal shape and the sign of the Pn-phase as well as the amplitude ratio in the data by changing these three angles systematically. We made many attempts and finally came up to Fig. 8. A seismogram section can be seen there, in which the azimuth between the strike of the fault plane and the station varies from 10 to 50 deg. The angles DV and NH are kept fixed at 90 and 60 deg, respectively. The distance is also fixed at 130 km for all traces in this section. The azimuthal range of 40 deg has been chosen because it is the same as for the GRF stations related to the epicenter. The distance of 130 km is the mean distance between the epicenter and the GRF array. It can be seen in Fig. 8 that there is a change of the sign of the Pn-phase between 20 and 25 deg corresponding to the stations B4 and B2. From that computation the following orientation of the fault plane can be estimated: Strike N 20 E, dip 30 to NW. The direction of the slip vector is 90 deg. That means that the movement at the fault is a reversed normal faulting.

Strike and dip agree fairly well with a classical fault plane solution derived by SCHMEERS (1983, personal communication), but there is a great discrepancy in the direction of the slip vector.

DOI: https://doi.org/10.2312/zipe.1983.078

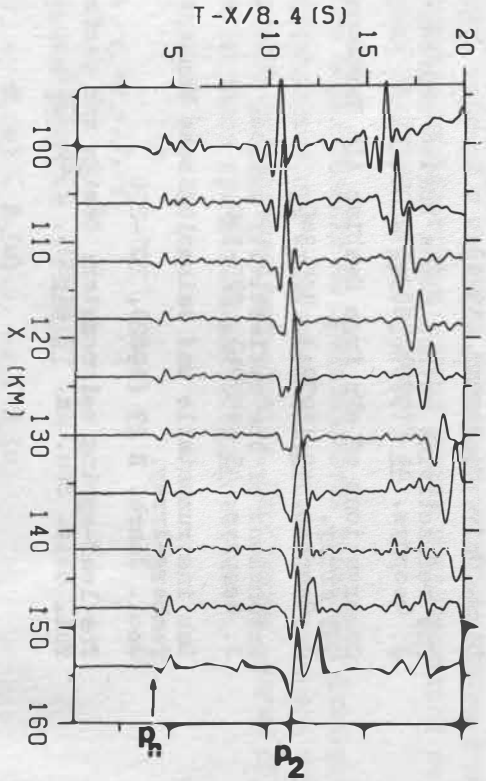

Fig. 7. Synthetics computed for the model derived in this paper

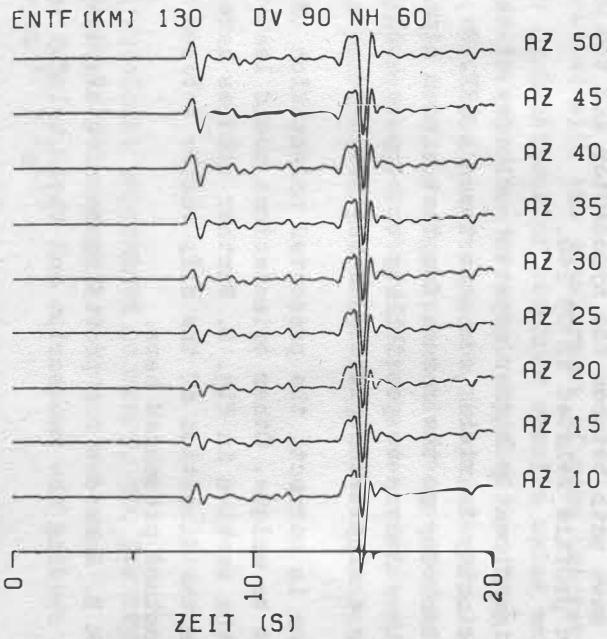

Fig. 8. Seismogram section showing synthetics for the same distance and different azimuths. The two other angles defining the double couple source are kept fixed

DOI: https://doi.org/10.2312/zipe.1983.078

5. Discussion

Before any conclusions about the source can be drawn from the theoretical seismograms, a velocity depth model had to be found which fits the onset times and the apparent velocities in the data. Our model with that big velocity jump at 20 km depth has not been seen in any refraction profile in southern Germany, especially not in the model of EMTER (1971). The wave path between the hypocenter and the GRF stations can be considered as a reversed profile related to 09 240.

It could lead to a significantly higher apparent velocity of the second phase when the plane of the discontinuity is rising somewhat towards GRF. We consider either this effect or a velocity anisotropy as the reason for that extrem high velocity in our model. The reflectivity method leaves no possibility to compute such lateral variations, so our model can only be a simplified picture of the reality.

If this interpretation is correct, the presented orientation of the fault plane is possible but it must not be unique. Other orientations could lead to the same theoretical seismograms as in the section in Fig. 8. Further studies have to be carried out to clear the discrepancy in the direction of the slip vector between the classical fault plane solution and the method presented here.

I would like to thank E. Schmedes for providing me with his computations and H. Aichele and R. Kind for reading the manuscript and their helpful suggestions.

References

AHORNER, L.; MURAWSKI, H.; SCHNEIDER, G.
Die Verbreitung von schadenverursachenden Erdbeben auf dem Gebiet der Bundesrepublik Deutschland.
J. Geophys. 36 (1970), 313-343

EMTER, D.
Ergebnis seismischer Untersuchungen der Erdkruste und des oberen Erdmantels in Südwestdeutschland.
Diss. Univ. Stuttgart, (1971)

KIND, R.
The reflectivity method for a buried source.
J. Geophys. 44 (1978), 603-612

KIND, R.
Observations of sPn from Swabian Alb Earthquakes at the GRF array.
J. Geophys. 45 (1979a), 337-340

KIND, R.
Extensions of the reflectivity method.
J. Geophys. 45 (1979b), 373-380

SEIDL, D.; KIND, R.
Das instrumentelle und seismologische Konzept des Gräfenberg-Array.
Geol. Jahrb. E 23 (1982), 207-220

WIELANDT, E.; STRECKEISEN, G.
The leaf-spring seismometer: Design and performance.
Bul. Seis. Soc. Am. 72 (1982), 2346-2367

DOI: https://doi.org/10.2312/zipe.1983.078

Спектральная структура очагового импульса с точки зрения гомоморфного анализа

М.В. РОЖКОВ, Н.Т. ТАРАСОВ и Г.Л. ШПИЛЬКЕР [1)]

Summary

The paper is concerned with the development of some theoretical propositions of homomorphic analysis and applications of obtained results using methods of digital seismic data processing. The determination of origin impulse spectral structure is carried out for a 6-station set. Obtained results permit, in particular, to identify seismic events with high precision and show the significant advantage of this kind of processing compared with widely held methods. Furthermore, the described approach to the problem of homomorphic analysis based on polynom algebra permits to enlarge significantly its application.

Как правило, при обработке информации полагают, что регистрируемый сигнал является аддитивной функцией своих составляющих, и что

$$f_{reg}(t) = f_{pol}(t) + f_m(t)$$

а преобразование фурье такого сигнала будет

$$F(_{reg}(t)) = F(f_{pol}(t)) + F(f_m(t))$$

где $f_{reg}(t)$ - регистрируемый сигнал, $f_{pol}(t)$ - полезный сигнал, $f_m(t)$ - сигнал помехи (БАЛАКРИШНАН, и др., 1972; ДЖЕНКИНС и ВАТТС, 1971; ЛЕННИНГ и БЭТТИН, 1958).

Однако во многих областях исследований, также, например, как в исследовании речи, гидролокации, морской и наземной сейсмологии, исследовании и обнаружении сейсмических явлений, электроэнцефалографии сигнал должен моделироваться не как аддитивная функция, а как свертка (ЧАЙЛДЕРС и др., 1977).

При таком моделировании не представляется восможной фильтрация сигналов теми методами, которые используются при аддитивном представлении полезного сигнала и помехи вследствие мультипликативности составляющих-образов. Необходимо, таким образом, разработать метод фильтрации сигналов представленных в виде свертки.

Пусть

$$f = f_1 * f_2 * \ldots * f_n$$

Преобразование фурье от f есть

$$F(f) = F_1(\omega) \cdot F_2(\omega) \cdot \ldots \cdot F_n(\omega)$$

---

1) Институт Физики Земли, АН СССР, Москва Д-242, Грузинская 10

DOI: https://doi.org/10.2312/zipe.1983.078

Обозначим нормированный спектр $|F_k(\omega)|$ через $G_k(\omega)$. Тогда

$$\prod_{k=1}^{n} G_k(\omega) \equiv L(\omega) , \quad G_k(\omega) = |F_k(\omega)| , \quad G_k(\omega) \in (0,1) . \quad \omega \in \Omega$$

$$\ln L(\omega) = \sum_{k=1}^{n} \ln G_k(\omega)$$

Обозначим $G_k(\omega)$ через $1 - Z_k(\omega)$. Тогда, т. к.

$$\ln G_k(\omega) = \ln(1-(1 - G_k(\omega))) = \ln(1 - Z_k(\omega)) = - \sum_{j=1}^{m} \frac{Z_k^j(\omega)}{j}$$

то

$$\ln L(\omega) = - \sum_{j=1}^{m} \sum_{k=1}^{n} \frac{Z_k^j(\omega)}{j}$$

Ограничимся рассмотрением того случая, когда $m = n$.

$$\ln L(\omega) = - \sum_{j=1}^{n} \frac{1}{j} \sum_{k=1}^{n} Z_k^j(\omega) ,$$

где $\sum_{k=1}^{n} Z_k^j(\omega) \equiv S_j$, причем S можно рассматривать как симметрические функции корней алгебраического уравнения

$$f(Z(\omega)) = a_o Z^n(\omega) + a_1 Z^{n-1}(\omega) + \dots + a_{n-1} Z(\omega) + a_n = 0 .$$

Между корнями, коэффициентами и симметрическими функциями такого уравнения существуют следующие соотношения:

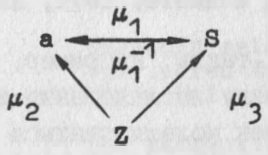

$$\mu_1: \quad S_j = (-\frac{1}{a_o})^j \begin{vmatrix} a_1 & a_o & 0 & \dots & 0 \\ 2a_2 & a_1 & a_o & 0 & \dots & 0 \\ 3a_3 & a_2 & a_1 & a_o & 0 & \dots & 0 \\ \dots & \dots & \dots & \dots & \dots & \dots & \dots \\ ja_j & a_{j-1} & \dots & \dots & \dots & a_1 \end{vmatrix} , \quad j = 1,2,\dots,n$$

$$\mu_1^{-1}: \quad \frac{a_j}{a_o} = \frac{(-1)^j}{j!} \begin{vmatrix} S_1 & 1 & 0 & \dots & 0 \\ S_2 & S_1 & 2 & 0 & \dots & 0 \\ S_3 & S_2 & S_1 & 3 & \dots & 0 \\ \dots & \dots & \dots & \dots & \dots & \dots \\ S_j & S_{j-1} & \dots & \dots & \dots & S_1 \end{vmatrix} , \quad j = 1,2,\dots,n$$

DOI: https://doi.org/10.2312/zipe.1983.078

$$\mu_2: \quad -\frac{a_1}{a_0} = S_1, \quad \frac{a_2}{a_0} = S_2, \ldots, (-1)^{n-1}\frac{a_{n-1}}{a_0} = S_{n-1}, \quad (-1)^n\frac{a_n}{a_0} = S_n$$

$$S_1 \equiv \sum_{k=1}^{n} z_k, \quad S_2 \equiv z_1z_2 + z_1z_3 + \ldots, \quad S_3 \equiv z_1z_2z_3 + z_1z_2z_4 + \ldots,$$

$$S_n \equiv z_1z_2z_3 \ldots z_n$$

$$\mu_3: \quad S_j \equiv \sum_{k=1}^{n} z_k^j .$$

Непосредственно $S_j (j = 1,2\ldots)$ выражается через S_j по I-ой формуле Варинга:

$$S_j = j \sum (-1)^{2\lambda_1+3\lambda_2+\ldots+(n+1)\lambda_n} \frac{(\lambda_1 + \ldots + \lambda_{n-1})!\, S_1^{\lambda_1} \ldots S_n^{\lambda_n}}{\lambda_1! \ldots \lambda_n!}$$

где суммирование распространяется на все наборы неотрицательных чисел $\lambda_1, \lambda_2, \ldots \lambda_n$ со свойством:

$$\lambda_1 + 2\lambda_2 + \ldots + n\lambda_n = j$$

Обратно, элементарные симметрические функции выражаются через степенные суммы по 2-ой формуле Варинга:

$$S_j = \sum \frac{(-1)^{\lambda_1+\lambda_2+\ldots+\lambda_j+j}}{1^{\lambda_1}2^{\lambda_2} \ldots j^{\lambda_j}\lambda_1!\, \lambda_2! \ldots \lambda_j!} S_1^{\lambda_1} \ldots S_j^{\lambda_j}$$

где суммирование распостаняется на те же наборы чисел λ, что и в первой формуле Варинга. Из рассмотренной диаграммы следует, что S_j и a_j являются в общем случае функциями частоты ω.

Таким образом получаем:

$$\ln L(\omega) = -\sum_{j=1}^{n} \frac{1}{j} S_j = -\left(S_1 + \frac{S_2}{2} + \ldots + \frac{S_n}{n}\right)$$

т. е. свёрточная система $f = f_1 * f_2 * \ldots * f_n$ свелась к аддитивной системе независимых энергитических параметров, удовлетворяющих условию $Z_k(\omega) \in (0,1)$.

Следовательно, возможным будет дальнейшее применение фурье-анализа по следующему алгоритму $P(\xi) = F(\ln L(\omega))$ - прямое преобразование фурье (ПФ) от $\ln L(\omega)$; $h = h(\xi)$ - линейная фильтрация (сглаживание) $P(\xi)$:

$$P(\xi) \xrightarrow{h} P_h(\xi)$$

$\ln L(\omega) = \check{P}_h(\xi)$ - обратное преобразование фурье (ОПФ) сглаженной функции $P_h(\xi)$.

Исходя из предположения, что свойства очага не зависят от пространственного расположения точки регистрации, при анализе наблюдений по группе станций для данной модели следует ожидать, что каждая запись будет содержать общую часть, соответствующую очаговому импульсу.

DOI: https://doi.org/10.2312/zipe.1983.078

Практические результаты подтверждают описанный подход к проблеме выделения очагового импульса. Были проведены вычисления для группы станций Гармского полигона. Алгоритм обработки цифровых массивов информации был следующий:

1. $F(\omega) = F(x_1, x_2, \ldots x_n)$ - БПФ исходного цифрового массива.
2. $\Phi(\omega) = F^2(\omega)$ - вычисление спектра мощности сигнала.
3. $L(\omega) = \ln \Phi(\omega)$ - вычисление логарифма спектра мощности.
4. $P(\xi) = F(L(\omega))$ - ПФ $L(\omega)$.
5. $h = h(\xi)$, $P(\xi) \xrightarrow{h} P_h(\xi)$ - линейное сглаживание.
6. $L_h(\omega) = \check{P}_h(\xi)$ - ОПФ $P(\xi)$.
7. $\Phi_h(\omega) = \exp L_h(\omega)$

Прилагаемый иллюстративный материал состоит из двух серий. Первая: записанный сигнал и его спектр до обработки; приводятся результаты наблюдений по 6-ти станциям. Вторая: спектр логарифма спектра мощности исходного сигнала, сглаженный спектр и восстановленный сигнал. Выбор формы сглаживающей функции определяется формой спектра логарифма спектра мощности. Основная доля энергии приходится на низкочастотную область; остальная часть приходится на высокочастотные низкоэнергетические составляющие. Следовательно, оптимальной сглаживающей функцией будет функция $\Pi(t)$ - прямоугольный импульс.

Как видно из представленного материала, задача идентификации событий существенно облегчается. Если сравнить сглаженные спектры по различным станциям, то наблюдается идентичная часть для всех кривых в определенном диапазоне частот, соответствующая очаговому импульсу. Незначительные отклонени заметны в высокочастотной области спектра, которые, видимо, вызваны воздействием передающей среды. Таким образом, данным методом можно пользоваться и при определении спектральной структуры среды.

Литература

БАЛАКРИШНАН, А.В.; Карлил, Дж.В.; РУТ, В.Л.; ХЕЛСТРОМ, К.В.; СОЛОМОН, Г. — Теория связи. Москва: Связь (1972)

ДЖЕНКИНС, Т.; ВАТТС, Д. — Спектральный анализ и его применение.

ЛЕННИНГ, Дж.Х.; БЕТТИН, Р.Г. — Случайные процессы в задачах автоматического управления. Москва: Иностранная литература (1958)

ЧАЙЛДЕРС, Дж.; СКИННЕР, Д.П.; КЕМЕРЕИТ, Р.Ч. — Кепстр и его применение при обработке данных. Обзор ТИИЭР 65 (1977) 10, 5-23

DOI: https://doi.org/10.2312/zipe.1983.078

DOI: https://doi.org/10.2312/zipe.1983.078

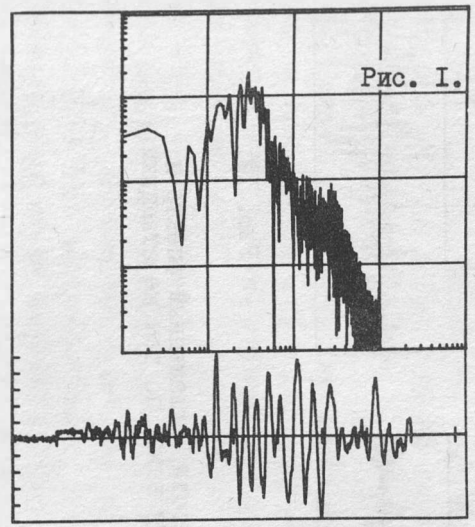

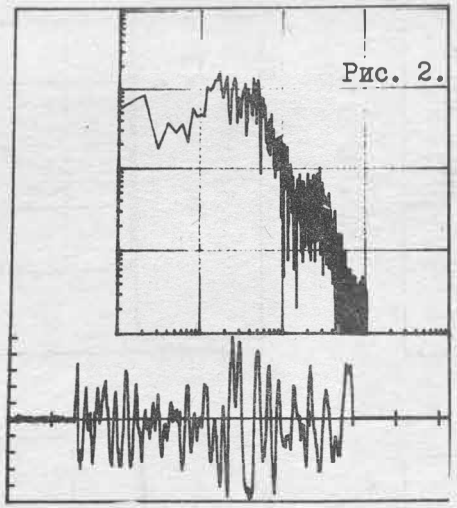

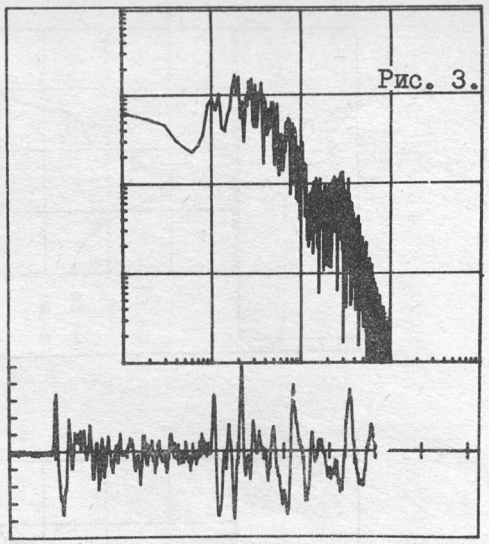

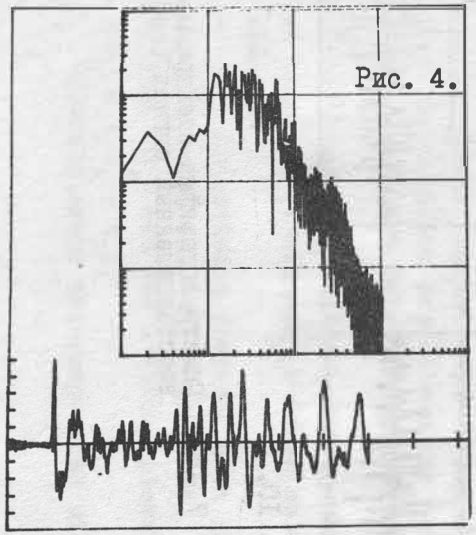

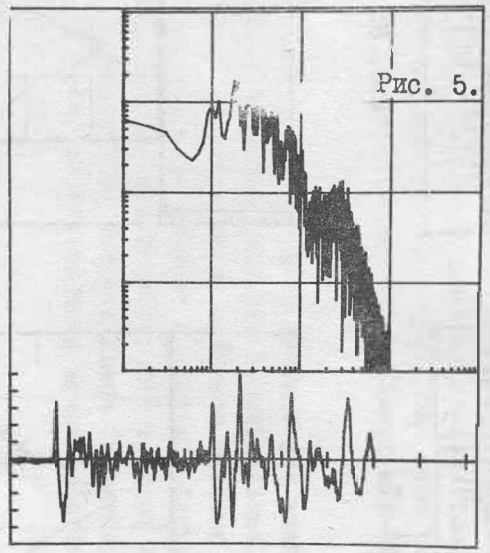

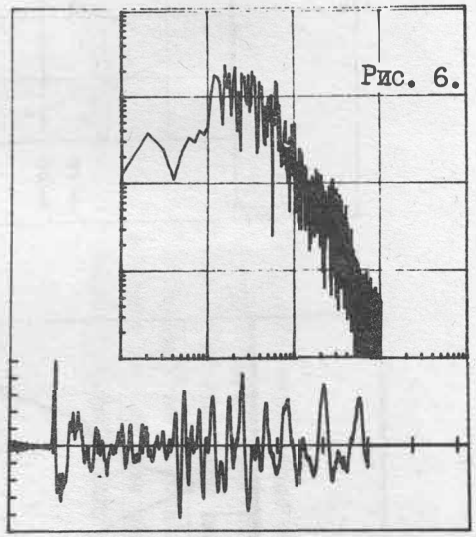

Рис. I.- 6. Записи сейсмических сигналов и их спектры (соответственно нижние и верхние части рисунков) по 6-ти различным станциям Гармского полигона

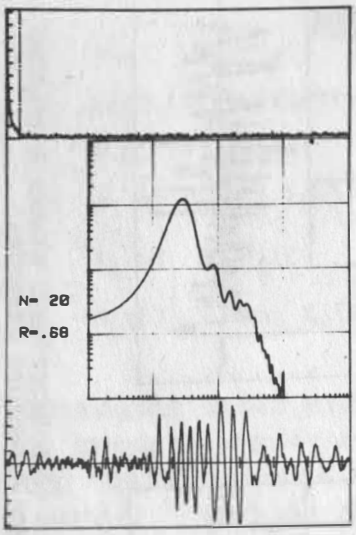

Рис. 7.

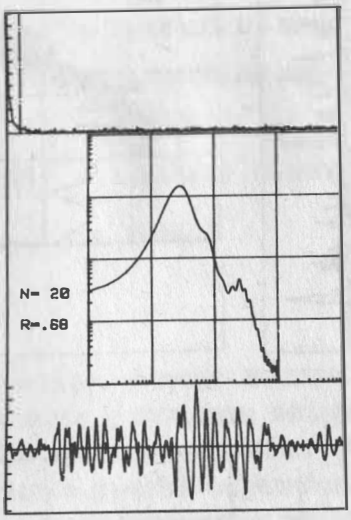

Рис. 8.

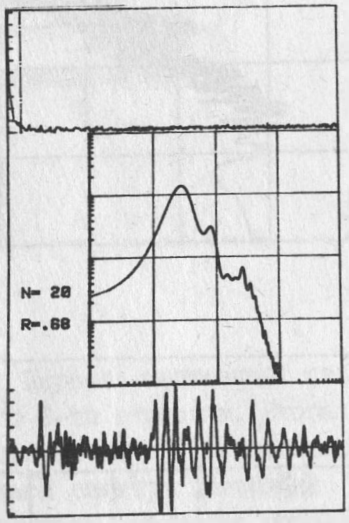

Рис. 9.

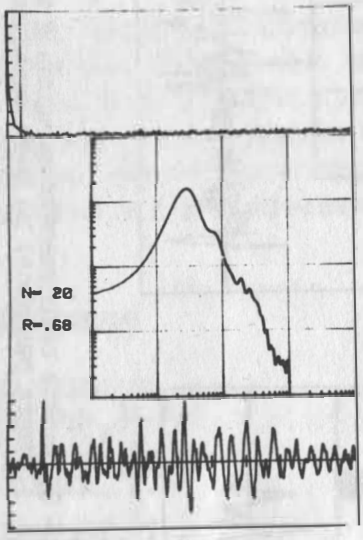

Рис. I0.

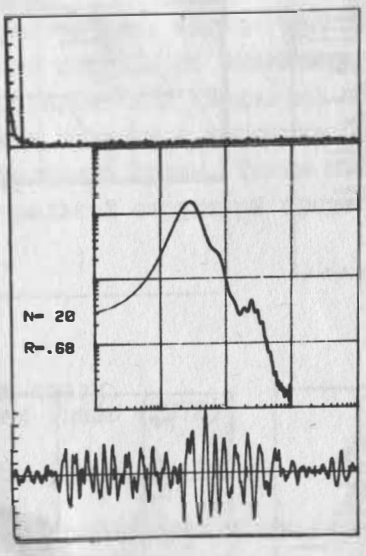

Рис. II.

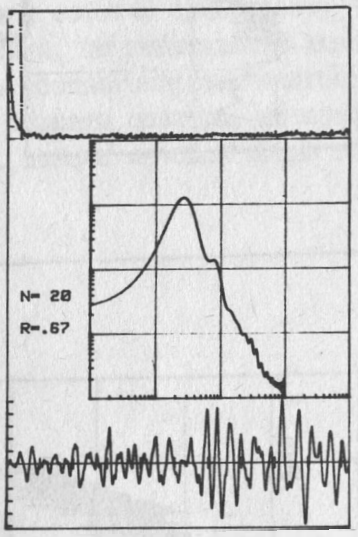

Рис. I2.

Рис. 7.-I2. Спектр логарифма спектра мощности, сглаженный спектр и восстановленный сигнал (сверху вниз) по тем же станциям

DOI: https://doi.org/10.2312/zipe.1983.078

Localization of Regional and Local Earthquakes with the CIPE Network

by

W. STRAUCH [1)]

Summary

Preliminary epicentre and magnitude data of seismic events are determined at the Potsdam centre of the CIPE network and reported daily to co-operating observatories in the GDR and abroad. Due to the weak natural seismicity of the GDR territory mainly small events have to be recorded and evaluated. The accuracy of localization strongly depends on the position of the focus with respect to the station network and on the phase readings available. The use of later arrivals is essential to ensure satisfactory localization results.

1. The routine localization process

The centralized digital recording network of the Central Institute for Physics of the Earth (CIPE) is developing to the standard basis for seismological observations in the GDR (technical description see BRIBACH, STRAUCH, and GÜNZEL, 1983). The main task of the network is the detection and localization of seismic events at the territory of the GDR and nearby.

Normally the local natural earthquakes recorded by the CIPE network are weak and it is often difficult to get the necessary information for reliable localizations. The basic material for the off-line processing are the records of a direct writing oscillograph with a paper speed of 1 mms^{-1}. Stronger events trigger a digital playback unit and high speed records up to 20 mms^{-1} are additionally available. The reading accuracy should be usually 0.1 s. The real error of the measured arrival times is hardly to determine but it is at least 2 or 3 times greater. At the highest speed records the times can be measured with an accuracy of 0.01 s.

The evaluation is carried out in the Potsdam centre of the CIPE network by an operator controlled by a scientist. After the interpretation of phases using local or regional travel time curves the times are put in a desk computer. The localization routine was written in the special language of the computer and allows the localization and magnitude estimation of near, regional as well as teleseismic events.

The routine for the epicentre determination of near and regional earthquakes was specially designed to regard the problems of possible divergence or false solutions in the case of only few and perhaps bad informations:

- the input of $n + 1$ (or more) onset times t_i is strictly demanded when n stations are used, i. e. at least one station has to give more than one onset time,
- this enables the calculation of the origin time t_o and the station-epicentre distances r_s solving the equations $r_s + v_i t_o = v_i t_i - v_i T_i$ $i = 1, m$; $m > n$; s-station index; v_i, T_i velocity resp. intercept time of the i-th phase as proposed by WAHLSTRÖM (1975),

---

1) Central Institute for Physics of the Earth of the Academy of Sciences of the GDR, DDR-1500 Potsdam, Telegrafenberg

DOI: https://doi.org/10.2312/zipe.1983.078

- a stepwise search for a minimum of the sum of squared residuals along a circle r_{min} around the station nearest to the epicentre finds a good starting point for the final,
- damped Gauss-Newton iteration which gives the epicentre.

The teleseismic events are localized with the well-known technique of the determination of azimuth and apparent velocity of P-waves crossing the network. Azimuth and distance (from apparent velocity) give the epicentre accurate enough for preliminary information. Systematical deviations were investigated by BORMANN and WYLEGALLA (1980) and can be considered. Later onsets are used if available to get a higher distance accuracy.

In the case of unsure interpretation the advantage of interactive work at the computer plays a great role. Often the trial and error method has to be used - including weak, unsure phases, changing their interpretation or taking them away - to get finally the best solution.

Therefore, the experience of the operator is very important. It must be considered that the residuals resp. the mean of squared residuals are no good controls for the quality of the solution when only few phases are used. There is even a chance to get very small residuals in the case of complete misinterpretation. Checking the results with independent information, comparison with master records, and repeated computations with various combinations of phases help to avoid bad mislocalizations.

The routine interpretation and localization takes about 2 - 3 hours per day for the operator. The results are printed for internal use in the CIPE and a paper tape is produced to report the epicentres to the three seismic observatories in the GDR (MOX, CLL, BRG) and to co-operating observatories in Czechoslovakia and Poland. The epicentre determinations are checked and eventually relocated when the reports from other stations are available receiving via Telex or WMO/GTS some days later.

2. An example: The localization of the 1982, Feb. 20 earthquake near Leipzig

An example for the localization of a comparatively strong local earthquake with the CIPE net might be the processing of an event which occured on 1982, Feb. 20 beneath the city of Leipzig. The magnitude 2.5 event was felt by some thousands of Leipzig inhabitants. The macroseismic investigation gave the localization 51.33 N, 12.46 E (GRÜNTHAL, GROSSER, GRÄSSL, 1983). By localizing using the records of the CIPE net a focus at 51.345 N, 12.427 E was computed.

3. Estimation of expected random localization errors for events at GDR territory

For the relocalization of seismic events and for studies about the localization capability of networks a computer program was developed which allows optionally
- single event localization,
- master event localization,
- modeling of random and systematic errors which can be expected for the localization with a given network configuration in a certain region.

DOI: https://doi.org/10.2312/zipe.1983.078

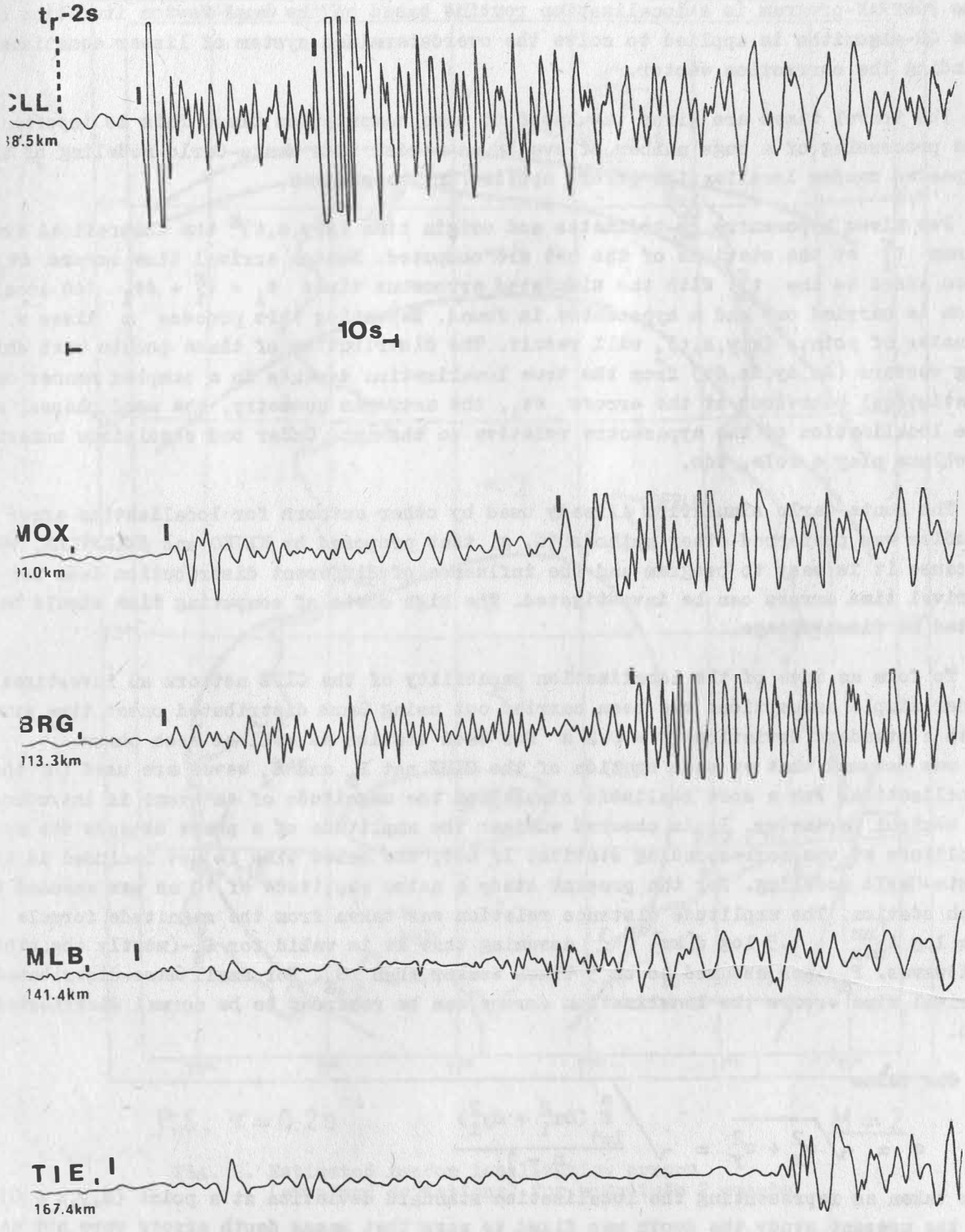

Fig. 1. Records of the Leipzig event

DOI: https://doi.org/10.2312/zipe.1983.078

This program can be used to process near and distant earthquakes recorded by local, regional, and global networks and to study their localization capabilities. The core of the FORTRAN-program is a localization routine based on the Gauss-Newton iteration scheme. The QR-algorithm is applied to solve the overdetermined system of linear equations for finding the correction vector.

The travel times are given tabulated to save computation time. This is important for the processing of a huge number of events as needed in a Monte-Carlo modeling of the expected random localization errors applied in the program.

For given hypocentre co-ordinates and origin time $(x,y,z,t)^g$ the theoretical arrival times t_i^g at the stations of the net are computed. Random arrival time errors Δt_i are then added to the t_i^g. With the simulated erroneous times $t_i = t_i^g + \Delta t_i$ the localization is carried out and a hypocentre is found. Repeating this process n times a cluster of points $(x,y,z,t)_j$ will result. The distribution of these points with shifting vectors $(\Delta x,\Delta y,\Delta z,\Delta t)$ from the true localization depends in a complex manner on the statistical behaviour of the errors Δt_i, the networks geometry, the used phases, and the localization of the hypocentre relative to the net. Under bad conditions numerical problems play a role, too.

The Monte-Carlo simulation already used by other authors for localization error studies was preferred other methods (e. g. that proposed by KIJKO and SELLEVOLL, 1982) because it is easy to program and the influence of different distribution laws for the arrival time errors can be investigated. The high costs of computing time should be noted as disadvantage.

To form an idea of the localization capability of the CIPE network an investigation under simple assumptions has been carried out using Gauss distributed onset time errors with a standard deviation $\tau = 0.2$ s for each station as well as each phase.
It was assumed that at each station of the CIPE net P_g and S_g waves are used for the localization. For a more realistic simulation the magnitude of an event is introduced as control parameter. It is checked whether the amplitude of a phase exceeds the noise amplitude at the corresponding station. If not, the onset time is not included in the Monte-Carlo modeling. For the present study a noise amplitude of 10 nm was assumed for each station. The amplitude distance relation was taken from the magnitude formula $M = \log A_{max}^{[nm]} + 1.5 \log d[km]^{-0.3}$ assuming that it is valid for S_g-(mostly the strongest)waves. P_g was assumed to be 5 times weaker than S_g. For small Gauss-distributed arrival time errors the localization errors can be regarded to be normal distributed, too.

The value

$$\sigma = \sqrt{\sigma_x^2 + \sigma_y^2} = \sqrt{\frac{\sum_{i=1}^{n} (\Delta x_i^2 + \Delta y_i^2)}{n-1}}$$

was taken as representing the localization standard deviation at a point $(x,y,z = 0)$. In the present study the depth was fixed to zero that means depth errors were not calculated. The calculations were carried out for a grid covering the whole GDR territory. The results are plotted as isolines in Fig. 2 for magnitude $M = 2$ and in Fig. 3 for $M = 3$, respectively. The localization errors σ (in km) are denoted and the stations are drawn as full circles.

DOI: https://doi.org/10.2312/zipe.1983.078

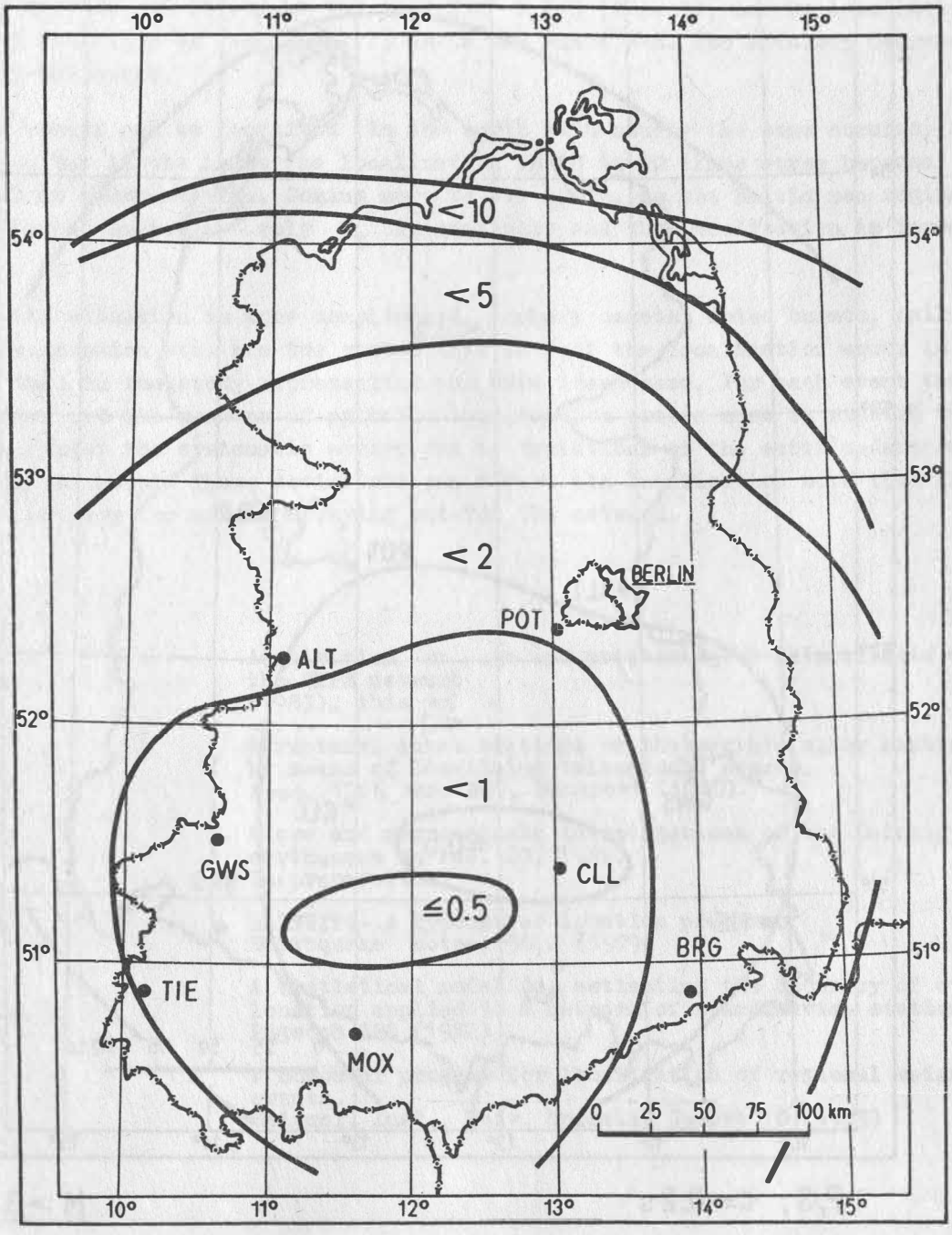

Fig. 2. Estimated random localization errors (standard deviations) for magnitude 2 events

DOI: https://doi.org/10.2312/zipe.1983.078

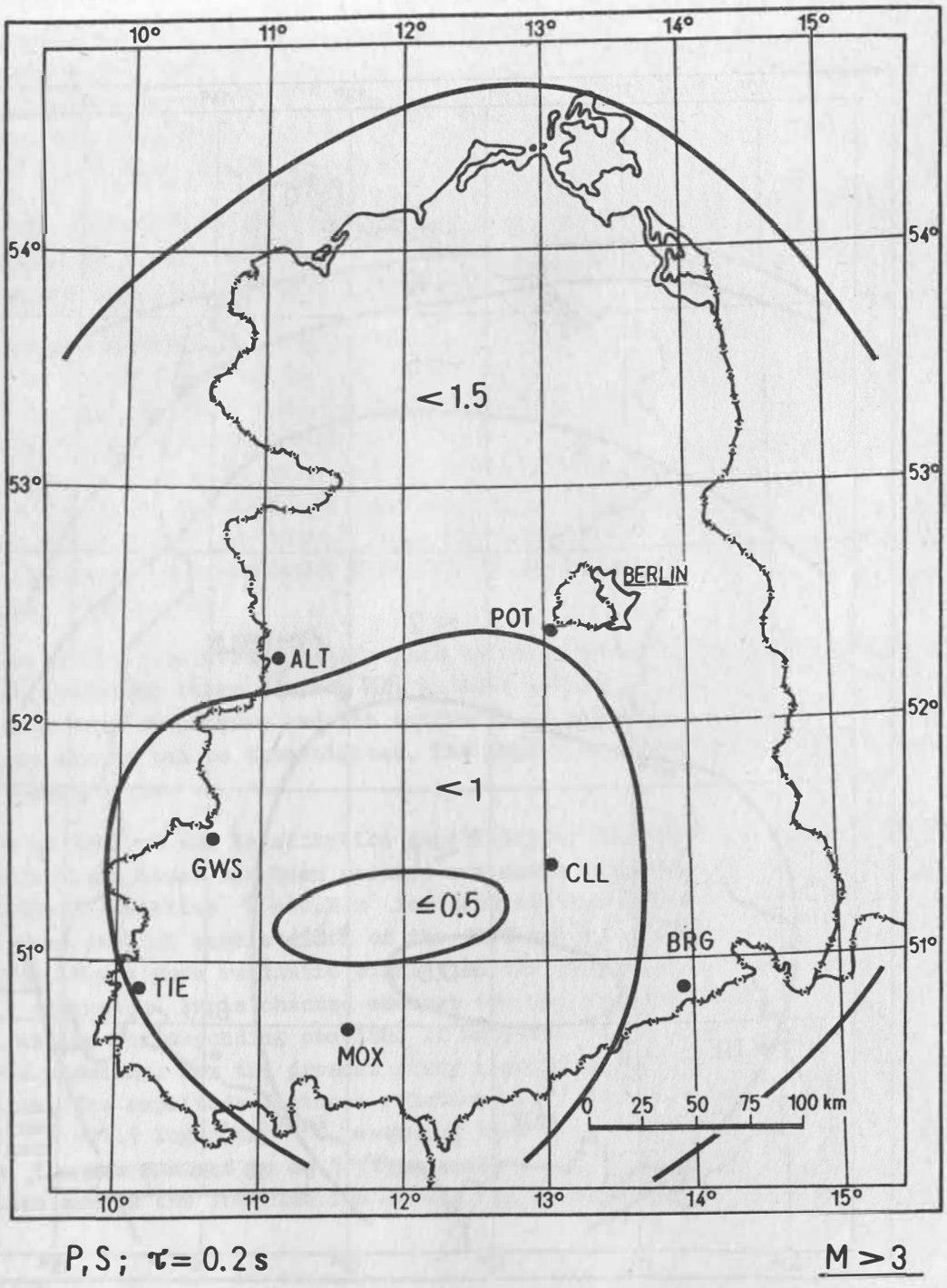

Fig. 3. Estimated random localization errors (standard deviations) for magnitude 3 events

DOI: https://doi.org/10.2312/zipe.1983.078

Due to the rather simple model the results give only a rough impression about the localization capability of the net. A well redorded event with P_g and S_g times determined at every station, as it may be the case for $M > 3$ (Fig. 3), can be localizated with a standard deviation of less than 1.5 km in the whole GDR. The accuracy decreases not too much to the north.

Magnitude 2 events can be localized in the south with nearly the same accuracy like those of $M > 3$. But in the north the localization is 10 to 20 times worse because P_g is not recorded at every station. Coming more to the north, to the Baltic sea region, the solutions become unstable - only S_g is available and the localization is impossible.

In reality the situation is more complicated. Unsharp onsets, noise bursts, failures in the data transmission etc. are the reason that in fact the localization error is surely higher than in the study representing the more ideal case. For each event the situation differs and the reasons of probable localization errors must be studied in detail, not to forget the systematic errors due to variations of the earth underground not included in the model. These deviations can affect the localization more than the reading errors primary for events occuring outside the network.

References

BRIBACH, J.; STRAUCH, W.; GÜNZEL, H. — Acquisition, st[illegible]ge and processing of seismic data with the CIPE network (1983), this vo[illegible]me

BORMANN, P.; WYLEGALLA, K. — Structural inves[illegible]igations of the earth's upper mantle by means of localizing teleseismic events. Proc. 17th Ass. ESC, Budapest (1980)

GRÄSSL, S.; GROSSER, H.; GRÜNTHAL, G. — Micro and macroseismic investigations of the Leipzig earthquake on Feb. 20, 1982. In preparation

HERRMANN, R.B. — FASTHYPO- A Hypocenter location program. Earthquake notes, 50,2 (1979)

KIJKO, A.; SELLEVOLL, M.A. — A statistical model for estimating the accuracy of event location applied to a network of scandinavian stations. Pageoph 120 (1982)

WAHLSTRÖM, R. — A computer program for localization of regional seismic events. Seismol. Inst., Univ. Uppsala, Report 10 (1975)

DOI: https://doi.org/10.2312/zipe.1983.078

Instrumentation and Calibration of the Digital Processing System Moxa - Jena

by

Ch. TEUPSER [1)]

Summary

The equipment used for the data transmission between Moxa and Jena is described. The transfer function of the 16 seismological channels is given as parameterized model. The signals are transmitted on telephone lines after frequency modulation with direct sampling in 16-bit computer compatibel word. The channels are calibrated by a low-frequency generator.

At first there are detailed information about the equipment used for the digital data acquisition of the seismological observatory Moxa-Jena. As outlined in the paper of BORMANN et al. the important seismographs of the station Moxa are linked with a real-time computer in Jena by a 24-channel carrier telephone system. The hardware configuration of the complete system is shown schematically in Fig. 1.

The seismographs operating in this system are the long- and short-period electromagnetic systems SSJ-I and SSJ-II and the new electronic seismograph EDS 1 all developed in our institute. The last ones delivers already a frequency modulated signal in the range from 300 to 3,400 Hz suitable for transmission in the telephone band. The signals of the seismographs with electromagnetic transducers are amplified and converted in a frequency modulated one in the same range. In Moxa as well as in Jena at the terminal of the carrier system there are demodulators in order to obtain analogue records for monitoring the seismographs and the transmission system or other seismological purposes.

The read-in of the seismic signals into the computer is carried out by an input-output device called "ursadat" after the direct sampling of frequency modulated signals. The converter delivers a 16-bit word with a sampling rate of 50 ms. An advantage of the conversion principle used is an additional filtering with zeros at multiples of 25 Hz. The converter enables a sampling rate of 100 per second under diminishing of word size, too. Besides, a read-in of analogue signals received after demodulation and filtering or other handling is also possible using a 10-bit analogue-to-digital converter.

Though, the acquisition of seismological data are the main task of the computer input device other informations like temperature, air pressure, and wind velocity are necessary for monitoring the functions of seismographs and identification of records caused by nonseismic sources. As the variations of such signals are generally slower than the seismic ones a slower sampling rate can be used. A carrier-current system, therefore, is provided to transmit these datas and will be set in operation next time. This system engages only one channel of the carrier telephone system and can be used for the transmission of other control signals between Moxa and Jena in both directions. The maximum sampling rate of each of the 24 channels is 50 samples per second.

---

1) Central Institute for Physics of the Earth of the Academy of Sciences of the GDR, DDR-69 Jena, Burgweg 11

DOI: https://doi.org/10.2312/zipe.1983.078

The periphery of the computer is shown in the lower part of Fig. 1. The main devices are the three exchangeable disc stores in order to extend the capacity of the storage. All data red-in are transferred to the exchangeable disc stores and kept for half an hour. During this time the data have got to be processed. Earthquake data may transferred to magnetic tape and stored for later off-line processing.

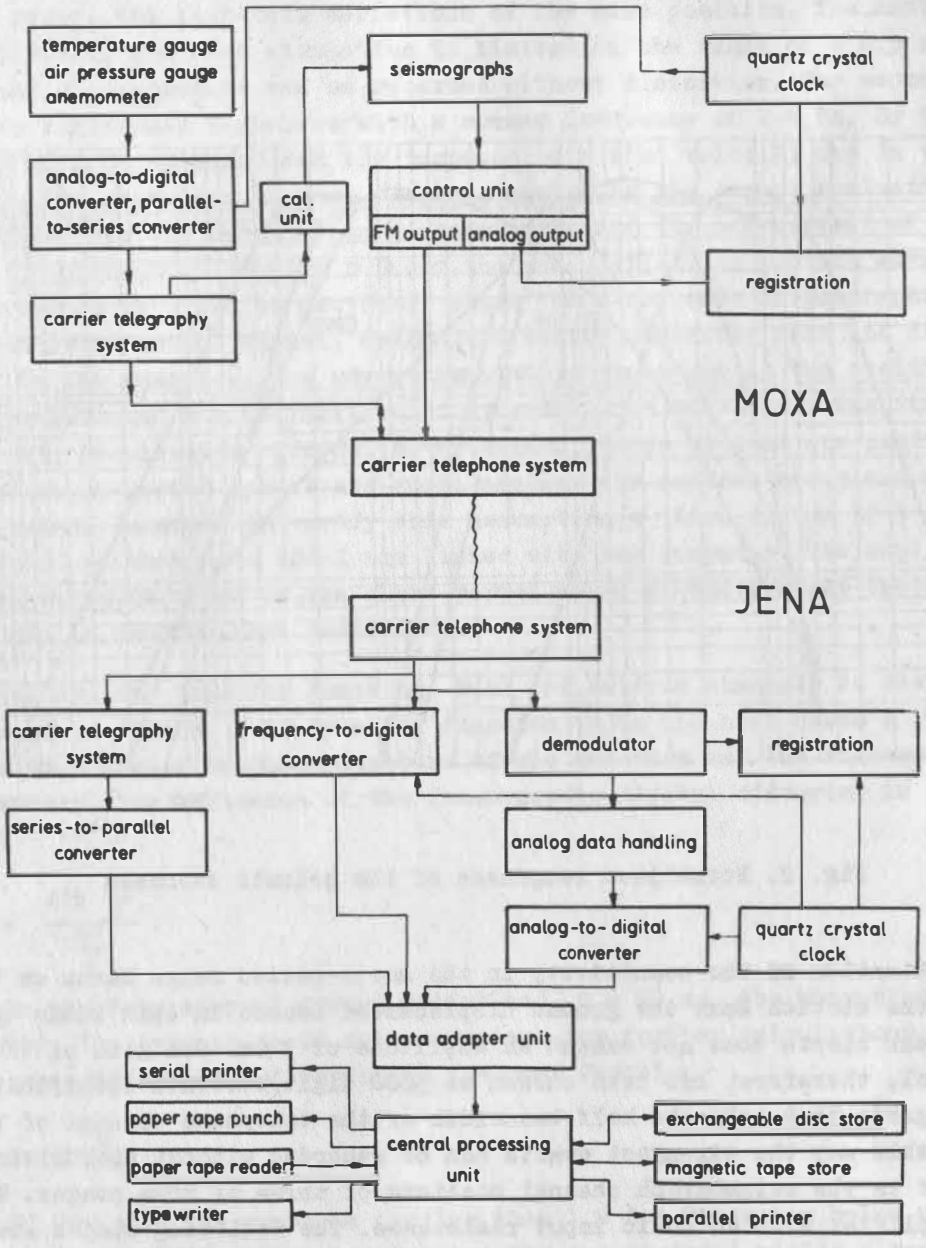

Fig. 1. Configuration of the acquisition system Moxa-Jena

DOI: https://doi.org/10.2312/zipe.1983.078

The response curves of the seismographs provided for transmission are given Fig. 2. The short-period types, essentially, are a three component set like the standard type A IV of the socialist countries. Two especially tuned vertical seismographs are additionally in operation. One of them has its maximum sensitivity at 1 s. This peak is adopted to the noise at Moxa. The other one has a maximum sensitivity in the range from 5 to 10 Hz, which is very suitable for the detection of near earthquakes and quarry blasts. Both types proved a success during last years because they enable a fast discrimination between near and distant events (TEUPSER, 1975).

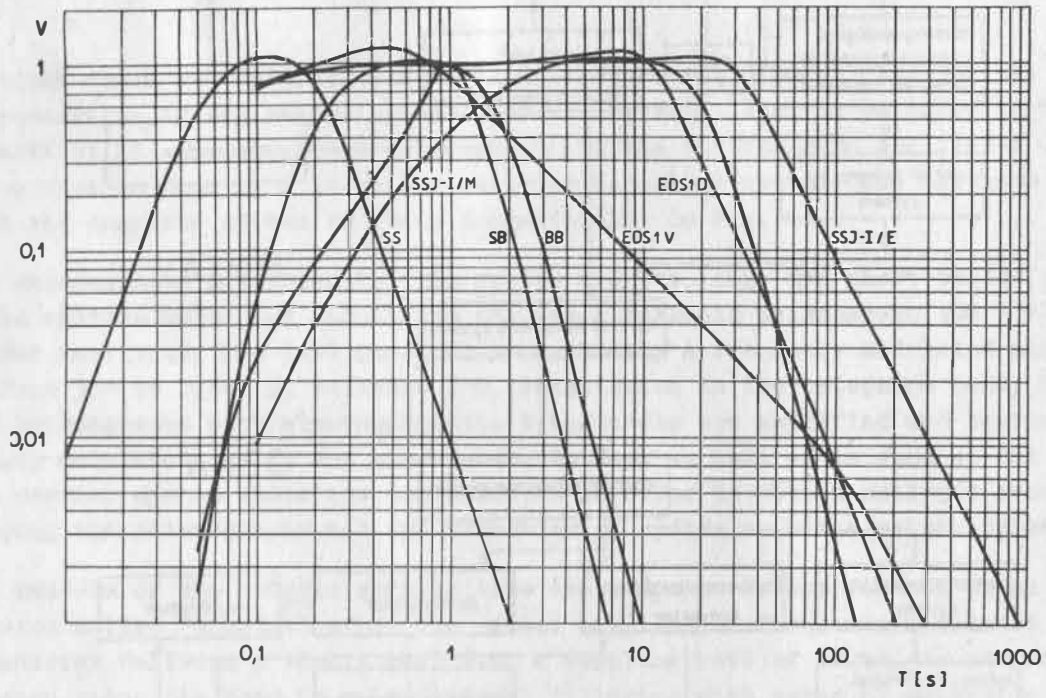

Fig. 2. Normalized responses of the seismic channels

The determination of the sensitivity in the short-period range bases on the following aspects. At the station Moxa the ground displacement caused in this range by earthquake as well as near blasts does not exceed an amplitude of 3 μm. The gain of the short-period channel, therefore, has been chosen as 5000 digit/μm. This specification, additionally, regards that only the half bandwidth of the telephone channel of 1700 Hz can be used. By this way the strongest events can be recorded without overdriving. The amplifier built in the seismograph channel consists of three or more stages. The first is a voltage amplifier with an ohmic input resistance. The following stages are second-order active RC networks with low-pass or band-pass transfer function. In the most cases the first low-pass simulates the properties of the galvanometer so that nearly the demanded responses corresponding the standard electromagnetic types has been obtained. The last stage is a band-pass in order to eliminate long-time drifts and noises outside of the registered range. As the response of the standard seismograph A IV does not drop enough at the Nyquist frequency of 10 Hz corresponding to the sampling rate of 50 ms an

DOI: https://doi.org/10.2312/zipe.1983.078

additional low-pass with a corner frequency of 5 Hz has been built in. The response of the whole channel shows Fig. 2. The same responses have the short-period seismographs at the station Posterstein and Plauen. The first one operates at this time and the second one will be linked with the computer this year.

The acquisition of long-period seismic signals is carried out by the triaxial feedback-controlled seismograph EDS 1 and the modified seismographs SSJ-I. The first system called EDS 1 D has only a high-pass with a corner period of 1000 s in the feedback loop in order to reduce the long-term variations of the mass position. The maximum sensitivity is 35 digit/μm. The boom elongation is limited in the range of $\pm$ 0.5 mm and only smaller ground displacements can be recorded without distortion. The second system EDS 1V has an additional high-pass with a corner frequency of 2.4 Hz. By this way a high damping will be obtained and the response is a flat velocity one in the range from 0.5 to 140 s. The advantage of such a velocitymeter is the direct evaluation of the ratio A/T needed for the calculation of magnitudes and the measurement of large ground displacement. As the high damping reduces the mass deflection surface wave amplitudes can be recorded up to 5 mm. As mentioned above the electronic seismographs produces a frequency-modulated output signal, which is directly converted into the digital input signal feed in the computer. The advantage of this procedure is the avoiding of demodulator distortions and the realization of dynamic range of 16 bit. The disadvantage is the possibility of aliasing effects. Nevertheless, these systems are used because the amplitude of short-period onsets are small against the surface waves and no influence will be expected. In order to verify this assumption a third system of 3 componentes of the long-period seismographs SSJ-I are linked with the computer. The amplifier response of these seismographs drops at the short-period waves at the Nyquist frequency (Fig. 2) so that it can be used without hesitation.

In general use the transfer function $W(s)$ of seismic channels is described in the Laplace transform domain. This transfer function is in the most cases a ratio of two polynomials in s depend on the parameters of the pendulum and the filters in the electronic circuitry. The influence of the frequency-to-digital converter is determined by the formula

$$U_w = \frac{\sin \frac{\omega\tau}{2}}{\frac{\omega\tau}{2}},$$

where ω is the frequency of ground motion and $\tau = 40$ ms the measuring intervall of the converter. The expression is not convenient for further calculations. Nevertheless, it can be approximated by a first-order low-pass function

$$\bar{U}_w = \frac{\omega_w}{s + \omega_w}.$$

For $\omega_w = 77.786\ s^{-1}$ the error is smaller than 1 % for frequency below the Nyquist frequency of 10 Hz. With this approximation the system model yields a transfer function

$$W(s) = \frac{DAs^2(s - n_1) \cdots (s - n_m)}{(s - p_1) \cdots (s - p_n)}.$$

The response of the seismograph reaches nearly its maximum at the frequency ω_n. The normalizing factor A is chosen so that

DOI: https://doi.org/10.2312/zipe.1983.078

$$|W(\omega_n)| \approx D .$$

Therefore, D is nearly the maximum sensitivity of the channel. m are the numbers of complex zeros and n the number of the complex poles. The term s^2 proceeds from the ground acceleration as the cause of the pendulum deflection. In our case of short-period seismographs there are only two zeros ($n_1 = n_2 = 0$) caused by the electromagnetic transducer and the output bend pass of the amplifier. In the case of feedback-controlled seismographs there are not vanishing zeros caused by the filters in the feedback loop. All these parameters will be written in the header of the magnetic tape records as described in the paper of KLINGE (this volume).

Controlling the response calculated by use of the parameters of the channel the calibration is carried out by a sine-wave generator. Up till now only the short-period channels are carefully calibrated. The agreement with the calculated response has been in the limits of 1 - 2 %. As the seismographs does not own two separate magnet coil assemblies and the windings of the calibration and signal coil are in one assembly the mutual inductance between these coils influences the calibration for frequencies higher than 3 Hz. The calibration, therefore, can be carried out only till this limit with demanded precision. But former calibrations of our short-period instruments using shaking table has been shown that the response are in good agreement with the theory of the seismographs taking in account only one degree of freedom up to frequencies of 40 Hz. The operation of the system has been started in 1980. In some other papers of this Symposium it will reportet about the first results of the on-line processing of seismological data with this hardware.

References

BORMANN, P.; HURTIG, E.; KOWALLE, G.; TEUPSER, Ch.
The system for acquisition and processing seismological data in the GDR. (1983), this volume

TEUPSER, Ch.
The Seismological Station of Moxa. Veröff. Zentralinst. Physik der Erde 31 (1975) T.2, 377-5 4

UNTERREITMEIER, E.; TEUPSER, Ch.; BUDER, H.
Der elektronische Seismograph EDS 1. Gerlands Beitr. Geophys. 87 (1978), 441-454

TEUPSER, Ch.; KLINGE, K.-D.
Die seismologische Datenerfassungsanlage Moxa-Jena. Gerlands Beitr. Geophys. 90 (1981), 507-513

TEUPSER, Ch.
Der Einsatz elektronischer Seismographen an seismologischen Stationen. Freiberger Forschungshefte C356 (1980), 63-73

TEUPSER, Ch.; BOHL, W.
Breitbandige Aufzeichnung der Bodengeschwindigkeit mit den Seismographen EDS 1. Gerlands Beitr. Geophys. 92 (1983), 327-330

KLINGE, K.-D.
Acquisition and storage of digital seismic data at the seismological observatory Moxa-Jena. (1983), this volume

DOI: https://doi.org/10.2312/zipe.1983.078

Joint Seismological Bulletin of GDR Stations and Further Use of Stored Data

by

S. WENDT [1)]

During one year about 3000 seismic events are recorded and evaluated at each of the three basic seismological stations in GDR. Since many years the kinematic results of evaluation and corresponding focal data are published as seismological bulletins in typewritten form. These bulletins contain many details of station data not published by the ISC (for instance periods and amplitudes, different time accuracy of onsets, various magnitudes, special phase denotations). Up to the 1st quarter of 1976 a conventional form of preparation of the bulletin in the shape of a typewritten manuscript was used at Collm station. But this method had the disadvantage that there was no possibility of direct use of published data with the help of a computer. That was the proper cause for me to develop a new treatment to store all information published as bulletin in a computer compatible form.

Basing on Collm station bulletin a computer programme of more than 4000 FORTRAN-statements was developed to compile a joint seismological bulletin of the stations BRG, CLL and MOX using single station files.

The following main aspects are to be taken into account:

- the printing of a clearly arranged joint bulletin without essential restrictions in comparison with the previous version and considering all of the experience gathered during many years,
- the storage of all published informations on punched cards and magnetic tapes to use it for further seismological investigations,
- the use of duplicates of cards sent to ISC
- the continuation of Moxa and Collm station bulletins and occuring for the first time a final form of Berggießhübel station data.

All three single station files can be used separately to test punched cards and also for special investigations. The data sets belonging to individual seismic events are very inhomogeneous with respect to structure and volume. There are differences as to number and type of the distinguishable phases, measurable periods and amplitudes, and possibilities to determine distance, depth, and magnitudes. To minimize the number of cards per event by avoiding a too complicated code, we use different types of cards with special formats. Focal data are punched in a special shape on one card; ISC-data on another one. The other supplements occur in an irregular manner. Therefore, we use some special types of format. The data input is arranged in such a way that the loss of information is as small as possible in comparison with the conventional technique. All supplementary information concerning station data can but must not be given. The mean number of punched cards per event is a little more than two. Short-period P-wave magnitude MPV and surface wave magnitudes MLH/MLV can be calculated automatically if periods and amplitudes of corresponding onsets are available.

---

1) Karl-Marx-Universität Leipzig, Geophysikalisches Observatorium Collm, DDR-7261 Collm

DOI: https://doi.org/10.2312/zipe.1983.078

The arrangement of station data concerning a special seismic event is done automatically in general. The sequence of stations depends on epicentral distance if focal data are available. Otherwise, the sequence depends on time of first onset. For special cases there is the possibility to determine the arrangement manually by the help of punched cards with event numbers. The single stations are responsible for the content of their own station files. Only the last called manipulation concerning arrangement can be done by myself manually.

The subroutine for arrangement of station data is the central part of the new programme. The single station files are stored on three separate magnetic tapes and are red event by event. If focal data are available, it is tested whether red origin times differ less than a given limit. In principle it is enough if only one station gives the focal data. The actual events of other stations are collected if the times of first onsets differ less than a given limit. The lot of possibilities of arrangements is one cause of the large volume of the programme and of the difficulties to arrange a joint bulletin. There are variants using one, two or all three stations for a special event. A comparison of the resulting output list shows that many inconsistencies in station files can be seen only in the joint version.

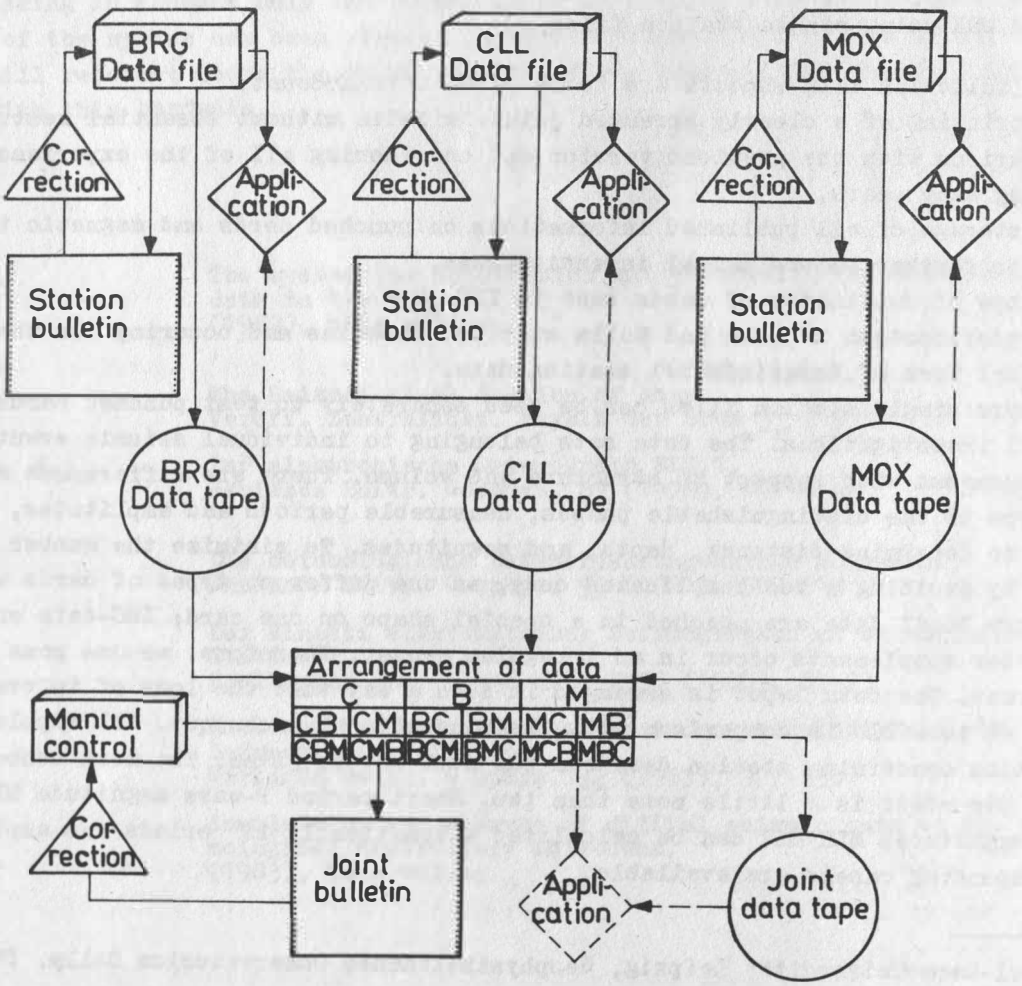

Fig. 1. Main steps to be done in preparation of joint bulletin on the basis of single station data files

DOI: https://doi.org/10.2312/zipe.1983.078

additional low-pass with a corner frequency of 5 Hz has been built in. The response of the whole channel shows Fig. 2. The same responses have the short-period seismographs at the station Posterstein and Plauen. The first one operates at this time and the second one will be linked with the computer this year.

The acquisition of long-period seismic signals is carried out by the triaxial feedback-controlled seismograph EDS 1 and the modified seismographs SSJ-I. The first system called EDS 1 D has only a high-pass with a corner period of 1000 s in the feedback loop in order to reduce the long-term variations of the mass position. The maximum sensitivity is 35 digit/μm. The boom elongation is limited in the range of $\pm$ 0.5 mm and only smaller ground displacements can be recorded without distortion. The second system EDS 1V has an additional high-pass with a corner frequency of 2.4 Hz. By this way a high damping will be obtained and the response is a flat velocity one in the range from 0.5 to 140 s. The advantage of such a velocitymeter is the direct evaluation of the ratio A/T needed for the calculation of magnitudes and the measurement of large ground displacement. As the high damping reduces the mass deflection surface wave amplitudes can be recorded up to 5 mm. As mentioned above the electronic seismographs produces a frequency-modulated output signal, which is directly converted into the digital input signal feed in the computer. The advantage of this procedure is the avoiding of demodulator distortions and the realization of dynamic range of 16 bit. The disadvantage is the possibility of aliasing effects. Nevertheless, these systems are used because the amplitude of short-period onsets are small against the surface waves and no influence will be expected. In order to verify this assumption a third system of 3 componentes of the long-period seismographs SSJ-I are linked with the computer. The amplifier response of these seismographs drops at the short-period waves at the Nyquist frequency (Fig. 2) so that it can be used without hesitation.

In general use the transfer function $W(s)$ of seismic channels is described in the Laplace transform domain. This transfer function is in the most cases a ratio of two polynomials in s depend on the parameters of the pendulum and the filters in the electronic circuitry. The influence of the frequency-to-digital converter is determined by the formula

$$U_w = \frac{\sin \frac{\omega\tau}{2}}{\frac{\omega\tau}{2}},$$

where ω is the frequency of ground motion and $\tau = 40$ ms the measuring intervall of the converter. The expression is not convenient for further calculations. Nevertheless, it can be approximated by a first-order low-pass function

$$\bar{U}_w = \frac{\omega_w}{s + \omega_w}.$$

For $\omega_w = 77.786\ s^{-1}$ the error is smaller than 1 % for frequency below the Nyquist frequency of 10 Hz. With this approximation the system model yields a transfer function

$$W(s) = \frac{DAs^2(s - n_1) \cdots (s - n_m)}{(s - p_1) \cdots (s - p_n)}.$$

The response of the seismograph reaches nearly its maximum at the frequency ω_n. The normalizing factor A is chosen so that

DOI: https://doi.org/10.2312/zipe.1983.078

$$|W(\omega_n)| \approx D .$$

Therefore, D is nearly the maximum sensitivity of the channel. m are the numbers of complex zeros and n the number of the complex poles. The term s^2 proceeds from the ground acceleration as the cause of the pendulum deflection. In our case of short-period seismographs there are only two zeros ($n_1 = n_2 = 0$) caused by the electromagnetic transducer and the output band pass of the amplifier. In the case of feedback-controlled seismographs there are not vanishing zeros caused by the filters in the feedback loop. All these parameters will be written in the header of the magnetic tape records as described in the paper of KLINGE (this volume).

Controlling the response calculated by use of the parameters of the channel the calibration is carried out by a sine-wave generator. Up till now only the short-period channels are carefully calibrated. The agreement with the calculated response has been in the limits of 1 - 2 %. As the seismographs does not own two separate magnet coil assemblies and the windings of the calibration and signal coil are in one assembly the mutual inductance between these coils influences the calibration for frequencies higher than 3 Hz. The calibration, therefore, can be carried out only till this limit with demanded precision. But former calibrations of our short-period instruments using shaking table has been shown that the response are in good agreement with the theory of the seismographs taking in account only one degree of freedom up to frequencies of 40 Hz. The operation of the system has been started in 1980. In some other papers of this Symposium it will reportet about the first results of the on-line processing of seismological data with this hardware.

References

BORMANN, P.; HURTIG, E.; KOWALLE, G.; TEUPSER, Ch.
The system for acquisition and processing seismological data in the GDR. (1983), this volume

TEUPSER, Ch.
The Seismological Station of Moxa. Veröff. Zentralinst. Physik der Erde 31 (1975) T.2, 577-584

UNTERREITMEIER, E.; TEUPSER, Ch.; BUDER, H.
Der elektronische Seismograph EDS 1. Gerlands Beitr. Geophys. 87 (1978), 441-454

TEUPSER, Ch.; KLINGE, K.-D.
Die seismologische Datenerfassungsanlage Moxa-Jena. Gerlands Beitr. Geophys. 90 (1981), 507-513

TEUPSER, Ch.
Der Einsatz elektronischer Seismographen an seismologischen Stationen. Freiberger Forschungshefte C356 (1980), 63-73

TEUPSER, Ch.; BOHL, W.
Breitbandige Aufzeichnung der Bodengeschwindigkeit mit den Seismographen EDS 1. Gerlands Beitr. Geophys. 92 (1983), 327-330

KLINGE, K.-D.
Acquisition and storage of digital seismic data at the seismological observatory Moxa-Jena. (1983), this volume

DOI: https://doi.org/10.2312/zipe.1983.078

Joint Seismological Bulletin of GDR Stations and Further Use of Stored Data

by

S. WENDT [1)]

During one year about 3000 seismic events are recorded and evaluated at each of the three basic seismological stations in GDR. Since many years the kinematic results of evaluation and corresponding focal data are published as seismological bulletins in typewritten form. These bulletins contain many details of station data not published by the ISC (for instance periods and amplitudes, different time accuracy of onsets, various magnitudes, special phase denotations). Up to the 1st quarter of 1976 a conventional form of preparation of the bulletin in the shape of a typewritten manuscript was used at Collm station. But this method had the disadvantage that there was no possibility of direct use of published data with the help of a computer. That was the proper cause for me to develop a new treatment to store all information published as bulletin in a computer compatible form.

Basing on Collm station bulletin a computer programme of more than 4000 FORTRAN-statements was developed to compile a joint seismological bulletin of the stations BRG, CLL and MOX using single station files.

The following main aspects are to be taken into account:

- the printing of a clearly arranged joint bulletin without essential restrictions in comparison with the previous version and considering all of the experience gathered during many years,
- the storage of all published informations on punched cards and magnetic tapes to use it for further seismological investigations,
- the use of duplicates of cards sent to ISC
- the continuation of Moxa and Collm station bulletins and occuring for the first time a final form of Berggießhübel station data.

All three single station files can be used separately to test punched cards and also for special investigations. The data sets belonging to individual seismic events are very inhomogeneous with respect to structure and volume. There are differences as to number and type of the distinguishable phases, measurable periods and amplitudes, and possibilities to determine distance, depth, and magnitudes. To minimize the number of cards per event by avoiding a too complicated code, we use different types of cards with special formats. Focal data are punched in a special shape on one card; ISC-data on another one. The other supplements occur in an irregular manner. Therefore, we use some special types of format. The data input is arranged in such a way that the loss of information is as small as possible in comparison with the conventional technique. All supplementary information concerning station data can but must not be given. The mean number of punched cards per event is a little more than two. Short-period P-wave magnitude MPV and surface wave magnitudes MLH/MLV can be calculated automatically if periods and amplitudes of corresponding onsets are available.

---

1) Karl-Marx-Universität Leipzig, Geophysikalisches Observatorium Collm, DDR-7261 Collm

DOI: https://doi.org/10.2312/zipe.1983.078

The arrangement of station data concerning a special seismic event is done automatically in general. The sequence of stations depends on epicentral distance if focal data are available. Otherwise, the sequence depends on time of first onset. For special cases there is the possibility to determine the arrangement manually by the help of punched cards with event numbers. The single stations are responsible for the content of their own station files. Only the last called manipulation concerning arrangement can be done by myself manually.

The subroutine for arrangement of station data is the central part of the new programme. The single station files are stored on three separate magnetic tapes and are red event by event. If focal data are available, it is tested whether red origin times differ less than a given limit. In principle it is enough if only one station gives the focal data. The actual events of other stations are collected if the times of first onsets differ less than a given limit. The lot of possibilities of arrangements is one cause of the large volume of the programme and of the difficulties to arrange a joint bulletin. There are variants using one, two or all three stations for a special event. A comparison of the resulting output list shows that many inconsistencies in station files can be seen only in the joint version.

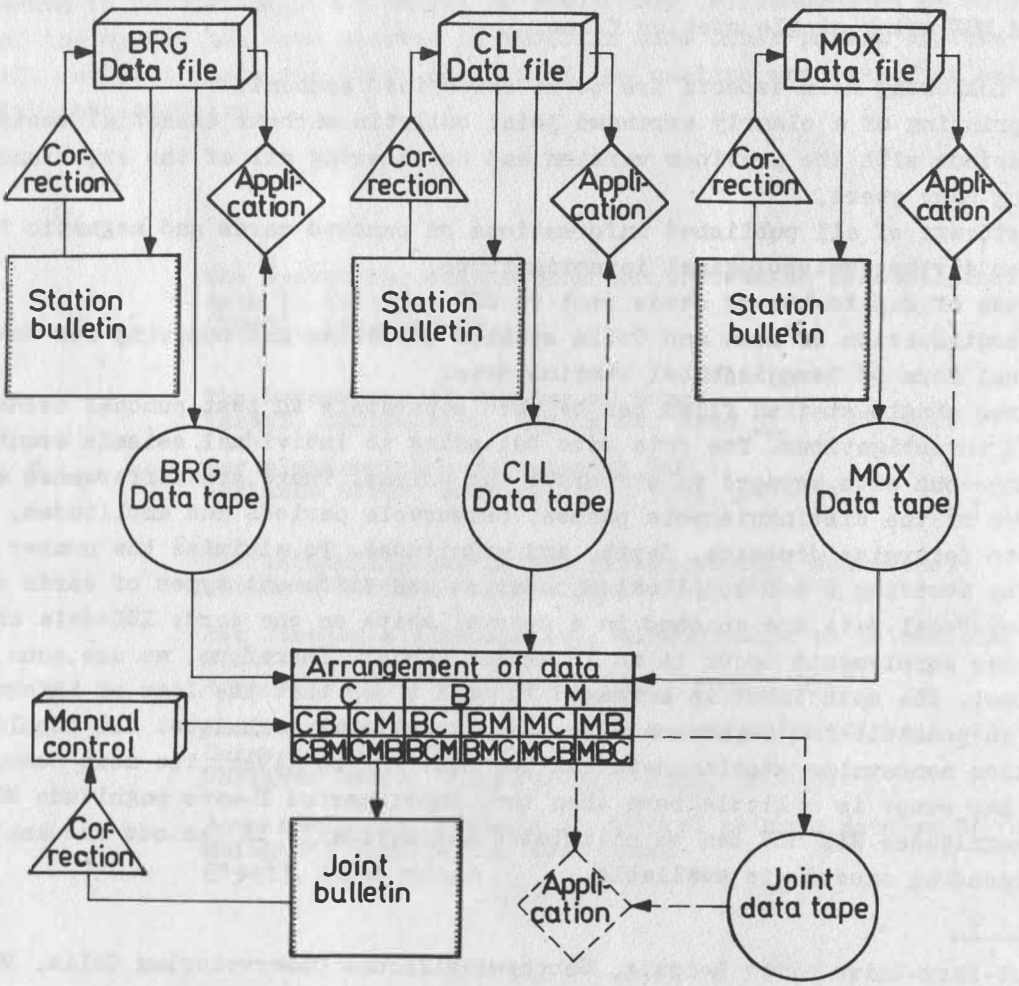

Fig. 1. Main steps to be done in preparation of joint bulletin on the basis of single station data files

DOI: https://doi.org/10.2312/zipe.1983.078

Till now is tested only the basic version of the programme, which is used to prepare bulletin either on line printer or as microfishes with 30 output pages per microfish. The extended version, which exists in main parts already for single station, shall be developed in next time for the joint version. Till now there are subroutines for compilation of travel-time and travel-time difference curves, calculation of residuals of the most important waves, calculation of calibrating functions and of differences between P-magnitudes and an average body wave magnitude given by data centre.

The Emergence of the General-Purpose Seismograph

by

P.L. WILLMORE [1)]

Summary

In the early days of seismometry, the "stable platform" provided by the mass of a long-period pendulum was regarded as the ideal reference against which to measure earth displacement. However, the mass required to deflect high-magnification mechanical or even optical levers, coupled with problems of friction and long-term stability, led to the development of a wide range of specialised instruments. These became subdivided into classes characterised by long and short period, high and low sensitivity, and as portable or observatory types. Now we can recognise the dynamic range in terms of earth acceleration as some 220 dB, with periods ranging from less than 0.01 s up to the free oscillations of the earth. The force-balance accelerometer, whose frequency response needs shaping only to the extent to which we still need a compromise between the acceptance of all input and the limitations of archival storage, has emerged as the single class of instrument which can cover the whole band. It needs to be physically small to avoid problems of internal oscillation, it must be robust enough to survive a passage down a borehole and there are theoretical advantages of operating within an evacuated pressure case which bring, as side benefits, almost total protection against other intrusions of the environment. Several "good" modern systems can now be recognised as approaching "perfection" by these criteria.

1. Introduction

In the days of the idealised "stable platform" the implied target was to set up a system of levers so as to produce a magnified image of earth displacement in the form of recordable motions of an "indicator". For horizontal motions, the very long simple pendulum, or its more compact equivalents of nearly-unstable inverted pendulums and "swinging-gates" were recognised as the available means of providing acceptable approximations to the ideal. For vertical motions, the mass constrained to allow linear motion at the end of a low-rate spring was the obvious equivalent of the simple pendulum, and

1) Department of Cybernetics, University of Reading, England

DOI: https://doi.org/10.2312/zipe.1983.078

its swinging-boom equivalent was brought to near-perfection by the introduction of the La Coste suspension. The significance of damping was partially recognised in this early stage as the means whereby the free oscillations of the mass were prevented from dominating the response, with damping constants in the range of 0.5 and 1 being used to separate the two basic modes of utilisation as the "accelerometer" for earth periods longer than the pendulum period, and the "displacement meter" for earth periods shorter than that of the pendulum. The idea that there was a third useful range in which mass displacement, controlled by high levels of damping, was proportional to earth velocity did not receive much attention until later (WILLMORE, 1961).

Given the fundamental understanding of the inertial reference, the development of seismometry divides naturally between that of the transducing system whereby the relative motions between the mass and its frame are presented as "output", and of the recording system which preserves the output for later consideration. We now ask how far we have advanced along these two lines, and whether we can yet see the end of the road.

2. Detection

Starting with the idea of a simple lever attached to the inertial mass and ending in the recording stylus, we saw the development of beautifully engineered systems of levers and dashpots for smoked-paper recording, but this line came to an end in instruments such as the large Wiechert seismograph, for which the mass was pushed up to 17 tons to overcome frictional resistance at a magnification of 10,000.

The optical lever, in instruments such as the Milne-Shaw and the elegantly simple Wood-Anderson, eliminated much of the friction and lost motion which had been limiting factors in passive smoked-paper systems, but left untouched the problem of zero-drift, which we would now recognise as one of excessive bandwidth (i. e. we just give the system time to drift) in relation to the long-term stability of materials and environmental conditions. This problem was overcome by the use of electromagnetic coupling in which the linkage between the velocity of the seismometer mass and the torque transmitted to the galvanometer coil gave low-frequency rejection of 6 dB/octave in comparison with a direct mechanical linkage. The opportunities for band-shaping could also be used to alleviate the problems of short-period earth vibration, 5-second microseisms and long-period instability of mass position, whilst the large ratio of seismometer mass to galvanometer coil inertia opened up the possibility of developing high magnifications in the classical long-period and short-period instruments.

Electronic amplifiers began to compete seriously with galvanometers in the early 1950 s, initially in conjunction with short-period, moving-coil seismometers to work into hard-stylus paper recorders or magnetic tape. At the long-period end, the galvanometer, reinforced by the photo-cell amplifier, remained as the most sensitive detector of the very small emfs which could be generated by slowly-moving coils. We can now see that the future of wide-band systems must lie with the condenser microphone, whose output surpasses that of practical moving-coil transducers for periods in excess of a few seconds.

DOI: https://doi.org/10.2312/zipe.1983.078

The introduction of electronic amplification re-awakened interest in the fourth-order differential equation which describes the transfer function of two coupled pendulums. In Galitzin's original theory (GALITZIN, 1914) the seismometer and galvanometer were assumed to operate independently of each other, and the "reaction", which arose from the emfs generated by rotations of the galvanometer coil, was neglected. Wenner in America and Kirnos in USSR developed systems in which overdamped galvanometers behaved as though rigidly attached, over a wide range of periods, to the seismometer mass, whilst Grenet and Coulomb in France showed that all of the partial constants of the galvanometer and seismometer could be combined into three independent coefficients of the differential equation, plus scaling factors for normalising time and amplitude (see, for example, WENNER, 1929; COULOMB and GRENET, 1935). When the active systems were introduced, all of the necessary parameters of the equation of motion could be set up by feedback whether or not there was actually a galvanometer in the system (see, for example, WILLMORE, 1961; PLEŠINGER, 1973; BALLARD and WILLMORE, 1980) and external filtering could be superimposed if desired.

A less obvious advantage of feedback in seismometry stems from the fact (largely, in this context, recognised by Fellgett and developed in Reading by Usher and his colleagues) that the Brownian motion of a suspended mass is generated entirely by dissipative elements such as the passage of current through resistors, or mechanical motions in a viscous medium. Controlling response characteristics by feedback rather than by dissipation therefore permits the development of much smaller and lighter seismometers, and the force-balance principle leads to very wide bandwidth and high dynamic range for acceleration input. By 1975 it was possible to demonstrate (USHER et al., 1977) that the essential conditions had been met down to acceleration levels of about 2×10^{-10} ms^{-2} at 20 s period. The American SRO development (PETERSEN et al., 1976, and subsequent papers to GANSE and HUTT, 1982) started concurrently but moved much faster to world-wide deployment. Others (e. g. USHER et al., 1978 and 1979; WIELANDT and STRECKEISEN, 1982) are continuing on this path, and it now seems that all the essential problems of the transducer system have been overcome.

3. Recording

In visual systems, the spiral trace on the rotating drum or wide loop soon achieved ascendancy over the rival narrow-strip or disc recordings, but it is important to remember that this ascendancy depends on the prevalence of situations in which the seismic event is a comparatively short-lived disturbance seen against a background which is normally much quieter. In this way, the system achieves compactness by putting many turns of the spiral within the span of maximum deflection, but the record soon loses legibility if the events become too frequent, if any one event extends over several turns of the spiral, or if the seismic background (as during a microseism storm) rises to the level which approaches the pitch of the spiral. It was this limitation of the drum recorder, coupled with the near-impossibility of reprocessing after primary recording, that made it necessary to limit the data content of any one record. One therefore had divisions growing up between short-period, long-period and wide-band seismometers, several levels of sensitivity for first-class observatories in active regions, and the development of new highly specialised system like the HGLP. Field deployment was limited to a very restricted (normally short-period) range of instrumentation.

DOI: https://doi.org/10.2312/zipe.1983.078

Analogue tape recording entered the field in the 1950s and developed rapidly (notably by the use of frequency modulation) through the sixties. From the start, it offered better dynamic range than the photographic trace, it overcame the problem of trace-overlap on the drum recorder, and it provided the opportunity of optimising frequency band, sensitivity and recording speed on playback for visual interpretation. Unfortunately, operational habits inherited from the interpretation of drum records led the majority of network operators to continue to select the recording characteristics with which they were most familiar. In most cases, the systems had been set up with array processing or first-onset detection in mind and the short-period option was selected. Although some medium-period data can be recovered by integration of longer period on playback, there has been considerable loss of potential content from this 20-year world archive, and there remains a considerable degree of under-utilisation of the medium-band content of the records which have been accumulated.

Digital recording was growing through the 1970s, immediately offering a further increment of dynamic range, but being limited at first by the high cost of hardware, and subsequently by the fact that the bulk and cost of magnetic tape per unit of bandwidth was some ten times higher than that of analogue recording. This latter aspect had a considerable effect on design, notably by rendering it uneconomic to store short-period components of the output and thereby forcing the distinction between short-period triggered systems and long-period continuously-recording ones. There is a further significant distinction between the triggered elements of a sensitive system and the strong-motion seismographs which are typically deployed in earthquake engineering. In the former case, triggering will be frequent, events will be collected from all distances and the need to examine a regular supply of records will go hand-in-hand with proper maintenance. Strong-motion instruments react to a much more limited selection of events and all too often fail during real emergencies because the storage capacity has been exhausted or because the equipment has simply failed to operate. The network superintendent who demands that his new equipment will operate from the lowest to the highest levels of disturbance is asking for much more than a separate set of strong-motion equipment can provide. He is asking for a total record of a situation which may develop from some barely noticeable change in the frequency or character of microtremors, through the crescendo of a great earthquake and into its aftermath. In such circumstances, he may well be thinking of earth displacements ranging from 10^{-11} to 1 metre, accelerations from 10^{-10} to 10 metres s^{-2}, and signal frequencies up to 30 Hz or more. In short, he can be asking for 220 dB at 100 or more samples/second.

In the very last few years, we have seen the breakthrough, firstly in the availability of magnetic cartridge recorders offering storage capacity of some 20 megabytes, then in solid-state stores (now past a megabytes and growing fast), and thirdly in video tape recorders (giving several hundred megabyte on a 3-hour casette, allowing for necessary redundancy). Now we have the digital-optical recorder (DOR) with software available to provide random access for 1,000 megabytes on each side of a disc. If we think of 1 megabyte as half an hour of 3-component recording, we see the complete disc as holding 42 station-days, and its average power consumption (say 10 seconds at 750 watts for each megabyte withdrawn from a solid-state store) as about 4.2 watts per station. Thus we have both the incentive and the means of making the data content of each channel complete in itself, in a station which can easily be made independent of mains power supply.

DOI: https://doi.org/10.2312/zipe.1983.078

4. Band-shaping

On a log-log plot, the transfer function of the simple pendulum, connecting earth velocity with mass displacement is contained within the familiar pattern of two sloping asymptotes and a horizontal tangent. We can shift either of the two corner frequencies or apply sharper filtering either in advance of primary recording or on playback. The bandwidth over which we can apply these processes will be limited only to the extent to which the signals (earth motions) which interest us are detected with adequate linearity, at levels above the internal noise of the system.

Within these options, we have the choice of sharp cut-off "filters" or broad-band "shaping" processors. These have quite different functions, as follows:

4.1. Narrow-band filtering

- Band rejection to reduce the impact of noise peaks (notably ocean microseisms) on neighbouring parts of the spectrum.
- Band-pass, to limit the intake of broad-band noise when only a low level, narrow band of the signal is of interest.

The noise levels in these categories are far below the maximum signal levels for which we must design the new generation of instruments, and the corresponding filters therefore unnecessary in the primary recording stage. They are, indeed, basically unsuitable in relation to our target, in so far as they destroy the universatility of the record.

4.2. Broad-band shaping

Broad-band shaping is used to fit expected maximum signal levels into the dynamic range of the recording format. As the largest peak accelerations (and the easiest options for avoiding background noise) occur at the high-frequency end of the spectral range, one will need to set the sensitivity to input at these frequencies carefully within the constraints (upper and lower limits of count, and sampling frequency) of the record. At the long-period end, we may have large ground amplitudes from surface waves and earth tides and spurious effects from thermal expansion, creep and tilt. Response here must be limited if the short-period signals are not to be measured from an excessively displaced baseline.

Few would now question the proposition that the optimum shape involves a band of high-frequency reduction (say velocity-flat for periods shorter than a few seconds) and of low-frequency reduction with a crossover point not much beyond 100 seconds period. These requirements can be met by adding the effects of the differential and the time integral of the transducer displacement signal to that of the direct input to the feedback coil. The period ranges over which each of the three outputs dominate will be determined by their relative levels (BALLARD and WILLMORE, 1980). We note further from the above publication that the integrated feedback is mathematically equivalent to a mechanical force, which could otherwise be applied to the mass by means of an auxiliary spring or (in the horizontal case) by tilting the frame. Either of these processes, if applied as an isolated step function, would produce a long transient in the shaped output. One of the requirements for a clean response is, therefore, that the mechanical

DOI: https://doi.org/10.2312/zipe.1983.078

input should be available in precisely controlled increments (as from a stepping motor) and offset by an equivalent reduction in the electrical centering force.

5. Dynamic range

We have accepted a target of some 220 dB of dynamic range in the level of earth disturbance. We can detect motions at the lower limit of the input in open-loop operation of our displacement transducer. Now we must apply feedback to reduce signal and noise levels at the input of our seismometer to the point at which the maximum transducer displacements are within working range. An electromagnetic transducer will support the weight of its magnet with a power input of the order of 10 W/kg and we can restrain the motion of our displacement transducer to about 0.25 mm/g if we apply enough feedback to push up the closed-loop frequency to about 32 Hz. So far. so good.

Our problems begin when we start thinking of the feedback loop and the A/D conversion process. If we thought of maximum voltage output as being constrained between limits of $\pm$ 10 volts, which we would apply directly to the force transducer to give maximum support of the mass, we would have to detect 10^{-10} volts at our digitizer input to provide for the minimum signal. We could raise this to a working level by delivering the coil input through a high load resistance, but only at the cost of pushing up the maximum voltage in the same ratio. There will be further problems if we wish to shape the output by integration and differention, because we cannot build passive RC networks which will meet the frequency requirements with available component values. What we can do is to use available microcircuit elements to provide about 110 dB of signal-noise ratio (8-bit mantissa and 4-bit exponent) and accept that as an effective upper limit for the whole system.

Fortunately, there is a way out by gain-ranging. If we set up variable sensitivity in the forward loop (either by changing the transducer drive or the voltage gain in the amplifier chain) and balance this by switching blocks of load resistance in or out of the feedback path, we can set up several ranges without altering the band-pass characteristic or the voltage range at the input to the digitiser. The simplest example is to note that rather severe 5-second microseisms (say 3×10^{-5} ms^{-2}) are near the centre of the decibel range of earth acceleration. The most sensitive range with a threshold of 10^{-10} ms^{-2} would be almost saturated, and the strong-motion range would barely detect them. In such a situation, a range providing 55 dB above and below microseism level could be the working norm.

6. Environmental stability

We have seen above that the key to high performance in small seismometers lies in developing a high "Q" in the open loop, which in practice implies operating in an evacuated container. This requirement simultaneously removes problems of buoyancy and disturbance by convection currents, and can also slow down temperature fluctuations within the enclosure.

The final requirement is to provide coupling to the ground over a sufficiently extended area to smooth out the effects of local inhomogeneities of the base. In a bore-

DOI: https://doi.org/10.2312/zipe.1983.078

hole, the use of a long, rigid pressure capsule meets the requirement. For vault or shallow-pit installations, one sees the advantage of packaging all three components in a single, fairly large container.

7. Conclusions

(1) The basic technical problems for a miniature seismometer capable of covering the full range of amplitudes and periods of significant earth motions had been overcome by 1975. Thereafter, the remaining problems lay in the economics of storing digital data and in the economic and psychological investment which was locked up in older systems.

(2) The problems of digitisation and bulk data storage have been progressively solved by the computer industry and we can now envisage a package of intermediate and long-term storage modules which could meet, at moderate cost, all the requirements for prompt use and archival storage in a first-class observatory or network.

(3) Now that we have the means, we see great advantages in aiming for total coverage within each data track of the first-class system, without excluding the possibility that specialised or auxiliary requirements might continue to be met by less expensive or more portable equipment.

References

BALLARD, G.; WILLMORE, P.L. — Progress report on wide-band accelerometers, in Proceedings of the XVI General Assembly of the European Seismological Commission. Publ. Inst. Geophys. Pol. Acad. Sci. A-9 (135), (1980), 93

COULOMB, J.; GRENET, G. — Nouveaux principes de construction des séismographes électromagnetiques. Annales de Physique 11 (1935), 3, 321

GALITZIN, B. — Vorlesungen über Seismometrie. Deutsche Bearbeitung, Teubner, Leipzig (1914)

GANSE, R.; HUTT, C.R. — Directory of world digital seismic stations. WDC A for Solid Earth Geophysics Report SE-32, (1982) Boulder, Colorado

PETERSEN, J.; BUTLER, H.M.; HOLCOMBE, L.G; HUTT, C.R. — The Seismic Research Observatory. B.S.S.A. 66 (1976), 2049

PLEŠINGER, R. — Synthesis of feedback-controlled broadband modifications of conventional seismograph systems. Zeitschr. f. Geophysik 39 (1973), 573

USHER, M.J.; BUCKNER, I.W.; BURCH, R.F. — A minature wideband horizontal-component feedback seismometer. J. Phys. E. Sci. Instrum. 10 (1977), 1253

USHER, M.J.; BURCH, R.F.; GURALP, C. — Wideband feedback seismometers. Phys. Earth and Planetary Interiors 18 (1979), 38

DOI: https://doi.org/10.2312/zipe.1983.078

USHER, M.J.; GURALP, C.
The design of miniature wideband seismometers.
Geophys. J. R. Astron. Soc. 55 (1978), 605

WENNER, F.
A new seismometer equipped for electromagnetic damping and electromagnetic and optical magnification.
Bur. Stand. J. Res. Wash. 2 (1929), 963

WIELAND, E.; STRECKEISEN, G.
The leaf spring seismometer design and performance.
B.S.S.A. 72 (1982), 2349

WILLMORE, P.L.
Some properties of heavily damped electromagnetic seismographs.
Geophys. J. R. Astron. Soc. 4 (1961), 389

DOI: https://doi.org/10.2312/zipe.1983.078

DOI: https://doi.org/10.2312/zipe.1983.078